X Winter Shool on Theoretical Physics, Dubna 2012

A FIELD-THEORETICAL APPROACH TO THE NEUTRINO OSCILLATION PROBLEM

V. Naumov (BLTP JINR)

Содержание

Часть I

Preface

Neutrino as a keystone of (astro)particle physics

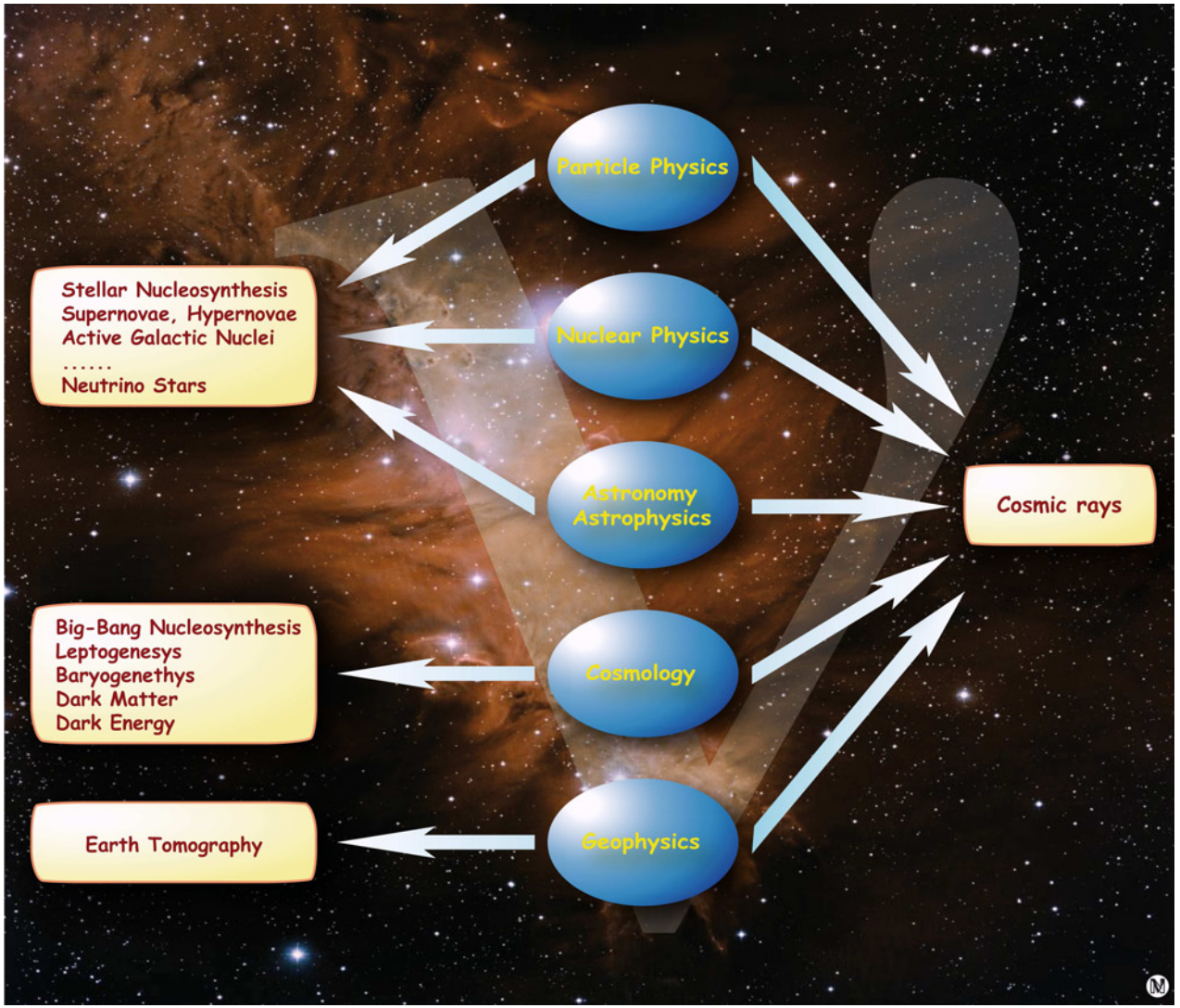

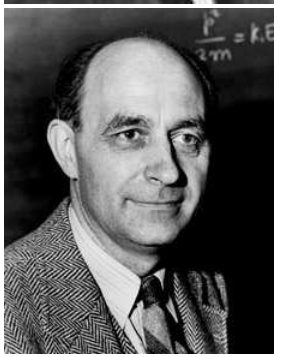

0.1 Neutrinos on the Earth and in the Heavens

Neutrino & antineutrino fluxes on Earth (tentative)

Energy range or average energy (eV)	Source	Local flux ($1/\mathrm{cm}^2\,\mathrm{s}$)
1.7×10^{-4}	Big Bang (relic or CνB)	10^{13}
$10^3 - 10^7$	Sun	6.5×10^{10}
$10^3 - 10^7$	Terrestrial radioactivity	7.5×10^6
$10^3 - 10^7$	Man-made nuclear reactors	7.5×10^6
$10^9 - 10^{12}$	Man-made accelerators	$<10^6$
$>10^8$	Cosmic rays (atmospheric)	$<10^6$
$>10^{12}$	Astrophysical objects (e.g. AGN)	$<10^{-6}$
$>10^{16}$	UHECR+ γ_{CMB} (cosmogenic)	10^{-12}

A tentative representation of the (anti)neutrino fluxes on Earth.

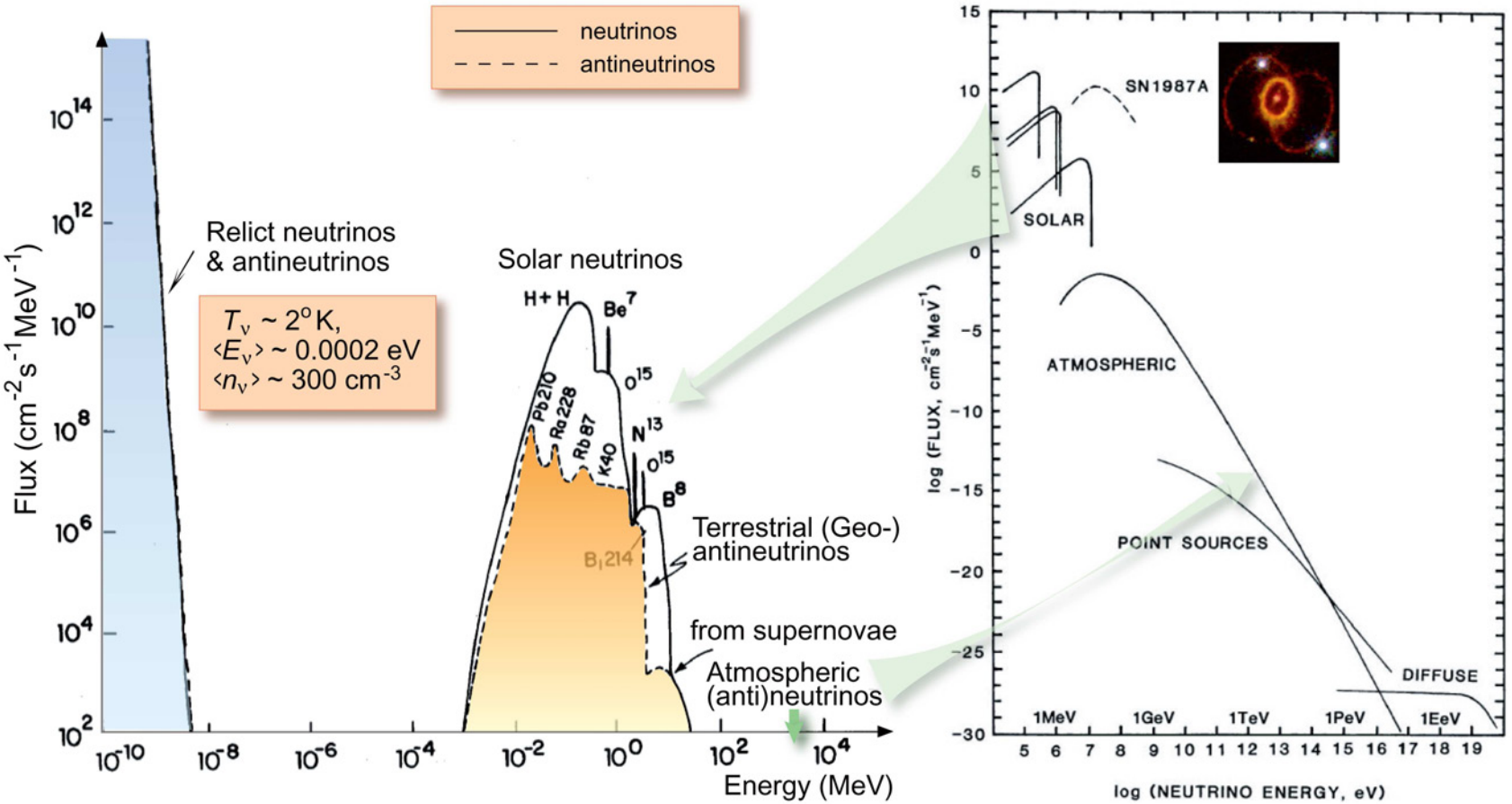

[Constructed from the data of L. M. Krauss, S. L. Glashow, and D. N. Schramm, "Antineutrino astronomy and geophysics", Nature **310** (1984) 191–198 (*left panel*) and A. M. Bakich, "Aspects of neutrino astronomy", Space Sci. Rev. **49** (1989) 259–310 (*right panel*).]

Relic neutrinos ("CνB") compose a small part of invisible (nonluminous) matter in the Universe.

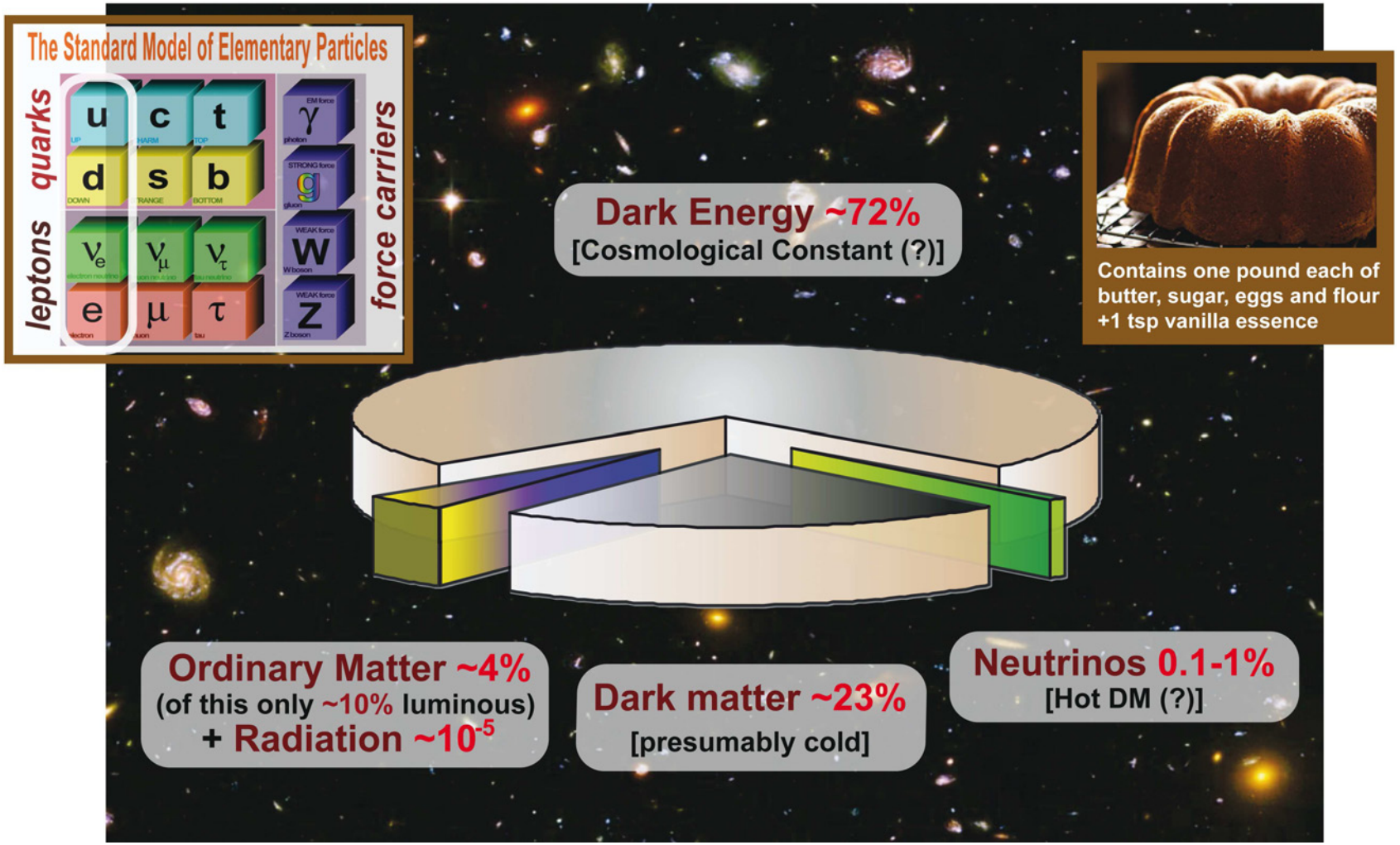

Cosmic Coincidence Problem: why this cake is almost a poundcake today?

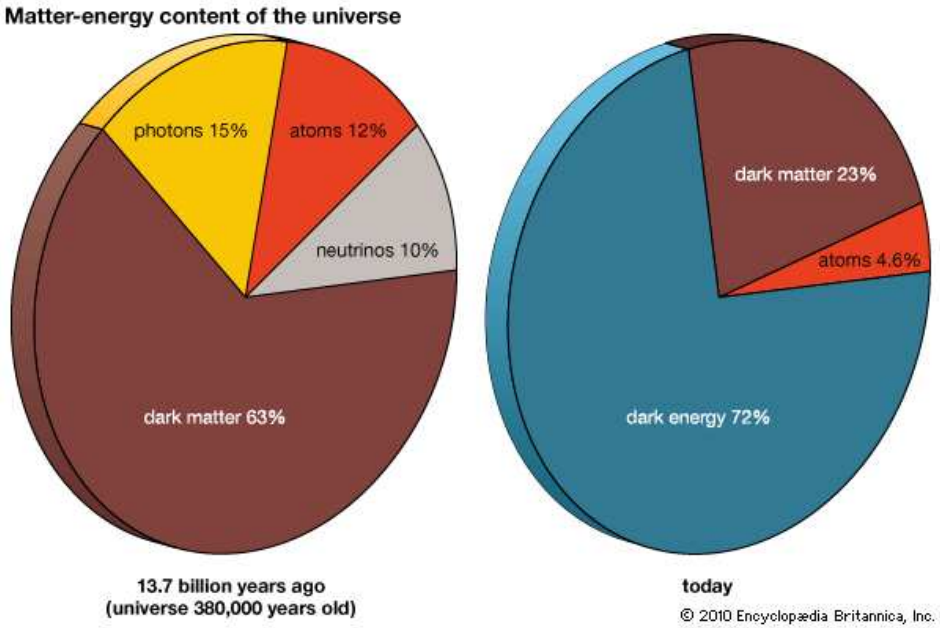

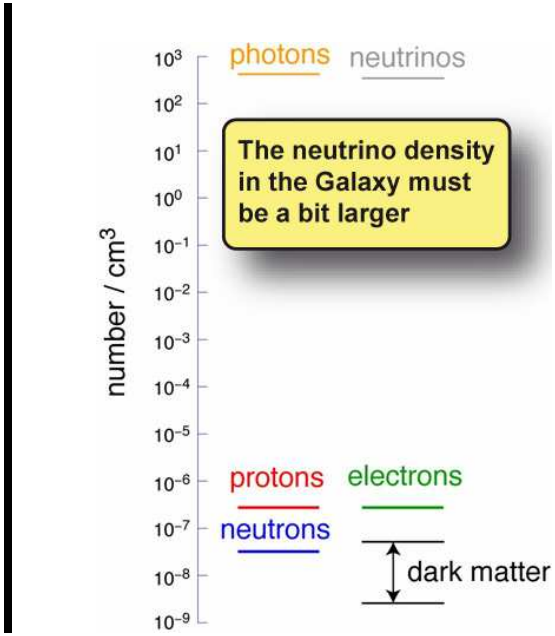

The Standard Models of particle physics and cosmology make a (more or less) robust prediction that the number density of relic neutrinos is $\approx 112\ \text{cm}^{-3}$ per species. This result implies that massive neutrinos constitute the following fraction of the total matter density in the Universe:

$$f_\nu = \frac{\Omega_\nu}{\Omega_m} = \frac{\sum m_\nu}{93\Omega_m h^2\ \text{eV}} \simeq 0.08 \frac{\sum m_\nu}{1\ \text{eV}} \qquad [\Omega_m h^2 = 0.134\ \text{(WMAP-7 best fit)}]$$

Here and below $\Omega_\nu = \rho_\nu/\rho_c$, $\Omega_m = \rho_m/\rho_c$, the today's Hubble expansion rate is parameterized as $H_0 \equiv 100h\,\text{km}\,\text{s}^{-1}\,\text{Mpc}^{-1}$ (h is the normalized Hubble rate) and the critical density is

$$\rho_c = \frac{3H_0^2}{8\pi G} \approx \begin{cases} 1.88 \times 10^{-29} h^2\ \text{g/cm}^3 \approx 0.98 \times 10^{-29}\ \text{g/cm}^3 \\ 1.05 \times 10^{-5} h^2\ \text{GeV/cm}^3 \approx 0.54 \times 10^{-5}\ \text{GeV/cm}^3 \end{cases} \qquad [h = 0.72 \pm 0.08]$$

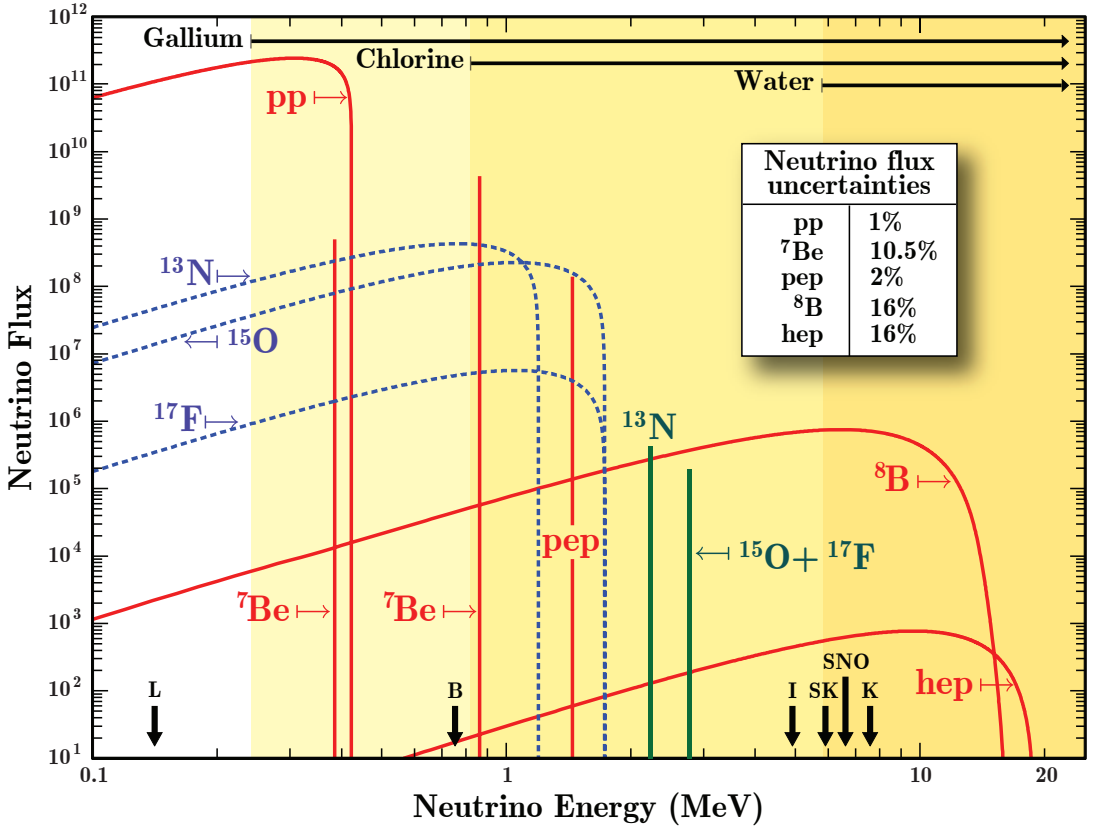

Рис. 1: The predicted solar neutrino energy spectrum at 1 AU. Line fluxes are in $cm^{-2}s^{-1}$ and spectral fluxes are in $cm^{-2}s^{-1}MeV^{-1}$. The vertical arrows point on the energy threshold of the H_2O detectors Kamiokande (K) and Super-Kamiokande (SK), D_2O detector at Sudbury Neutrino Observatory (SNO), liquid-argon detector ICARUS (I), scintillation detector Borexino (B), and Indium-based detector LENS (L).

[VN, Phys. Part. Nucl. Lett. **8** (2011) 683–703. The data are taken from J. N. Bahcall *et al.*, Astrophys. J. **621** ((2005)) L85–L88 and L. C. Stonehill *et al.*, Phys. Rev. C **6** (2004) 015801.]

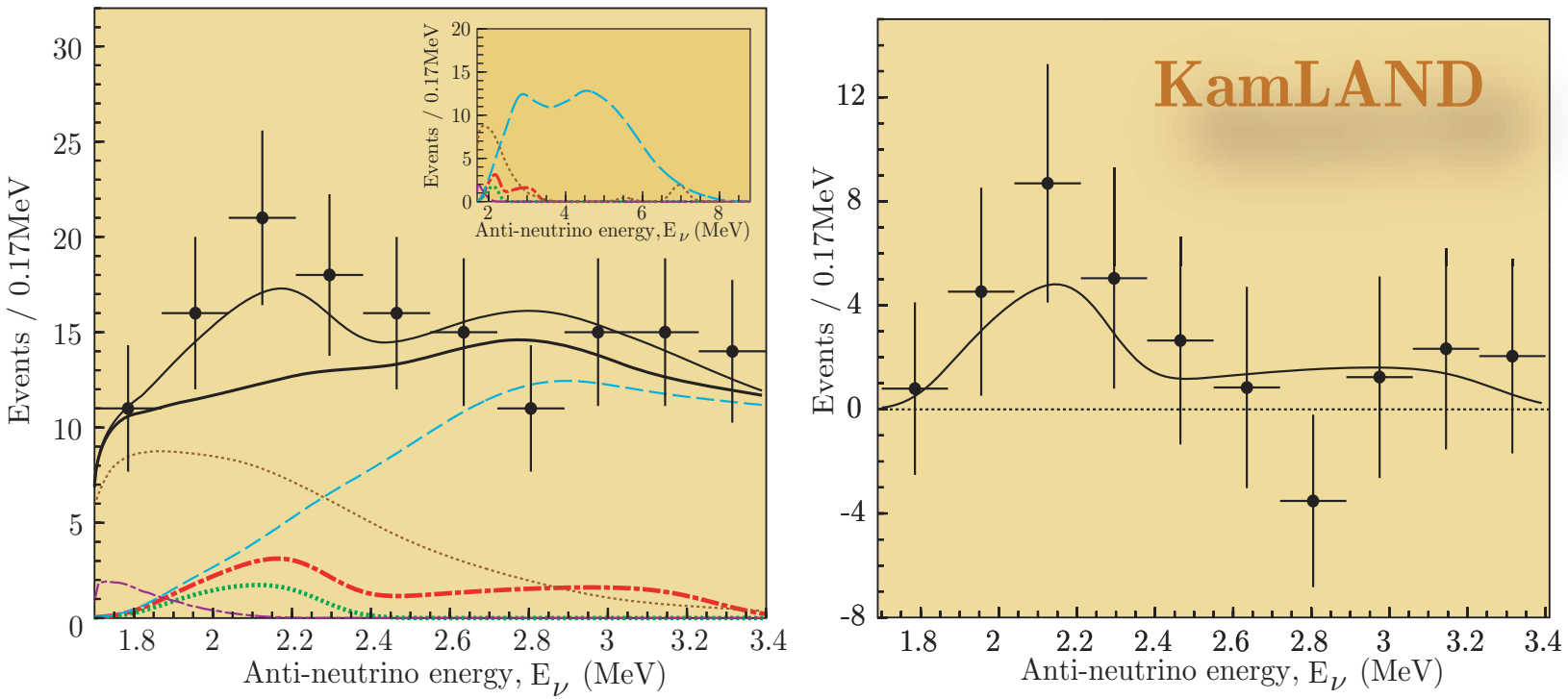

Рис. 2: Left panel: $\overline{\nu}_e$ energy spectra of the candidate events (data), the total expectation (thin solid black line), the total background (thick solid black line), the expected ^{238}U (dot-dashed red line, the expected ^{232}Th (dotted green line), and the backgrounds due to reactor $\overline{\nu}_e$ (dash blue line), $^{13}\mathrm{C}(\alpha, n)^{16}\mathrm{O}$ reactions (dotted brown line) and random coincidences (dot-dashed violet line). The inset shows the expected signal extended to higher energies.
Right panel: $\overline{\nu}_e$ energy spectra of the candidate events substructed by the total backgrounds
[From A. Suzuki (for the KamLAND Coll.), AIP Conf. Proc. **815** (2006) 19–28.]

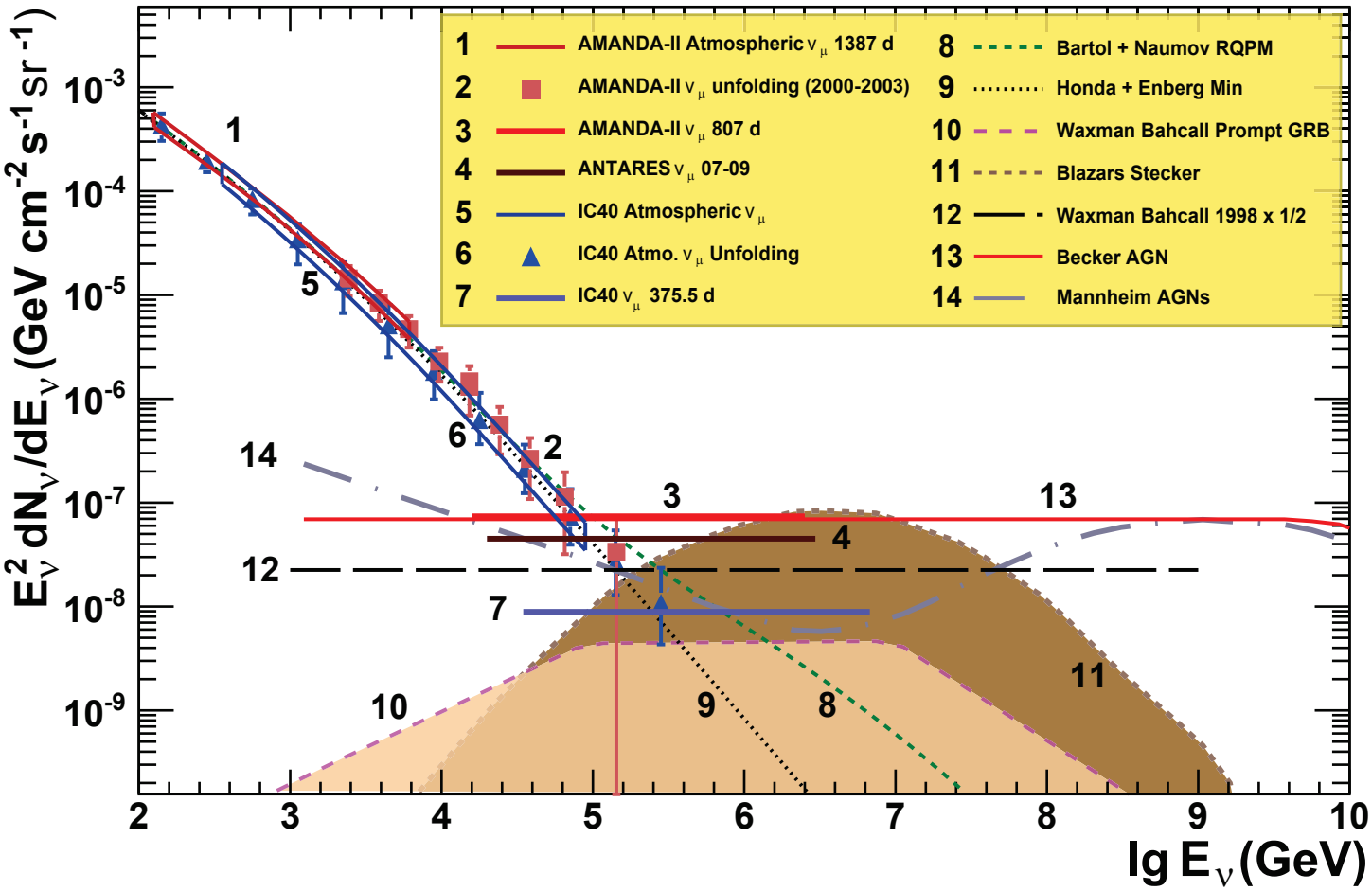

Рис. 3: Upper limits on an astrophysical muon (anti)neutrino flux with an E^2 spectrum along with theoretical model predictions of diffuse astrophysical muon neutrinos from different sources. The atmospheric ν_μ measurements shown are from AMANDA-II, the IceCube 40-string (IC40) unfolding measurement, and IC40 Atmospheric ν_μ.

[From R. Abbasi *et al.* (IceCube Coll.), Phys. Rev. D **84** (2011) 082001 [arXiv:1104.5187 [astro-ph.HE]].]

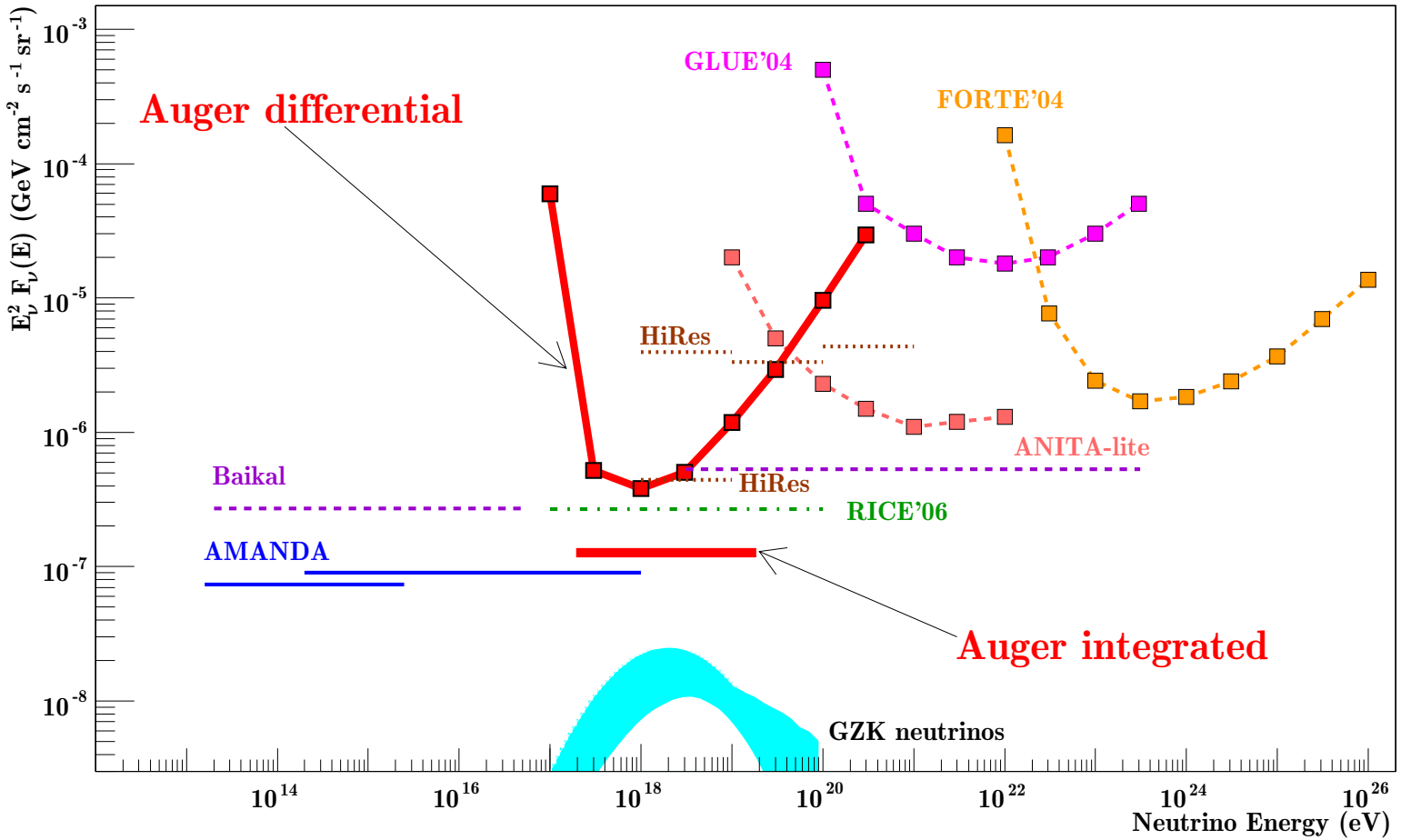

Рис. 4: The 90% CL bounds on diffuse flux of ν_τ from Auger. Bounds from other experiments apply assuming equal proportions of the three ν flavors (horizontal lines assume E^{-2} spectrum). Shaded region indicates possible expectations from GZK neutrinos.

[From E. Roulet (for the Pierre Auger Coll.), arXIv:0809.2210 [astro-ph]]

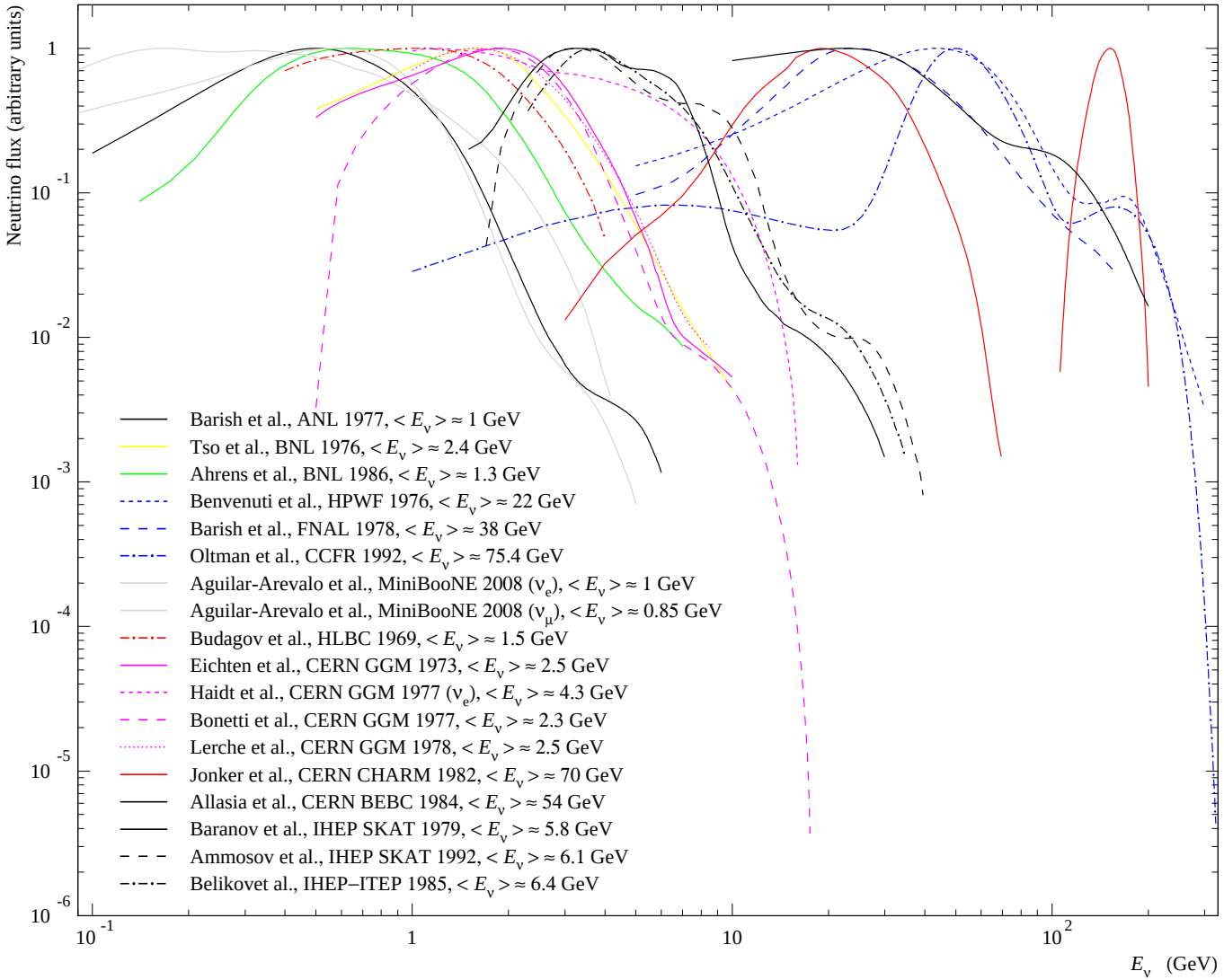

Рис. 5: Muon neutrino energy spectra in several accelerator experiments (a.u.).

[A. Bodek, K. S. Kuzmin & VN (unpublished). The data are collected from many sources.]

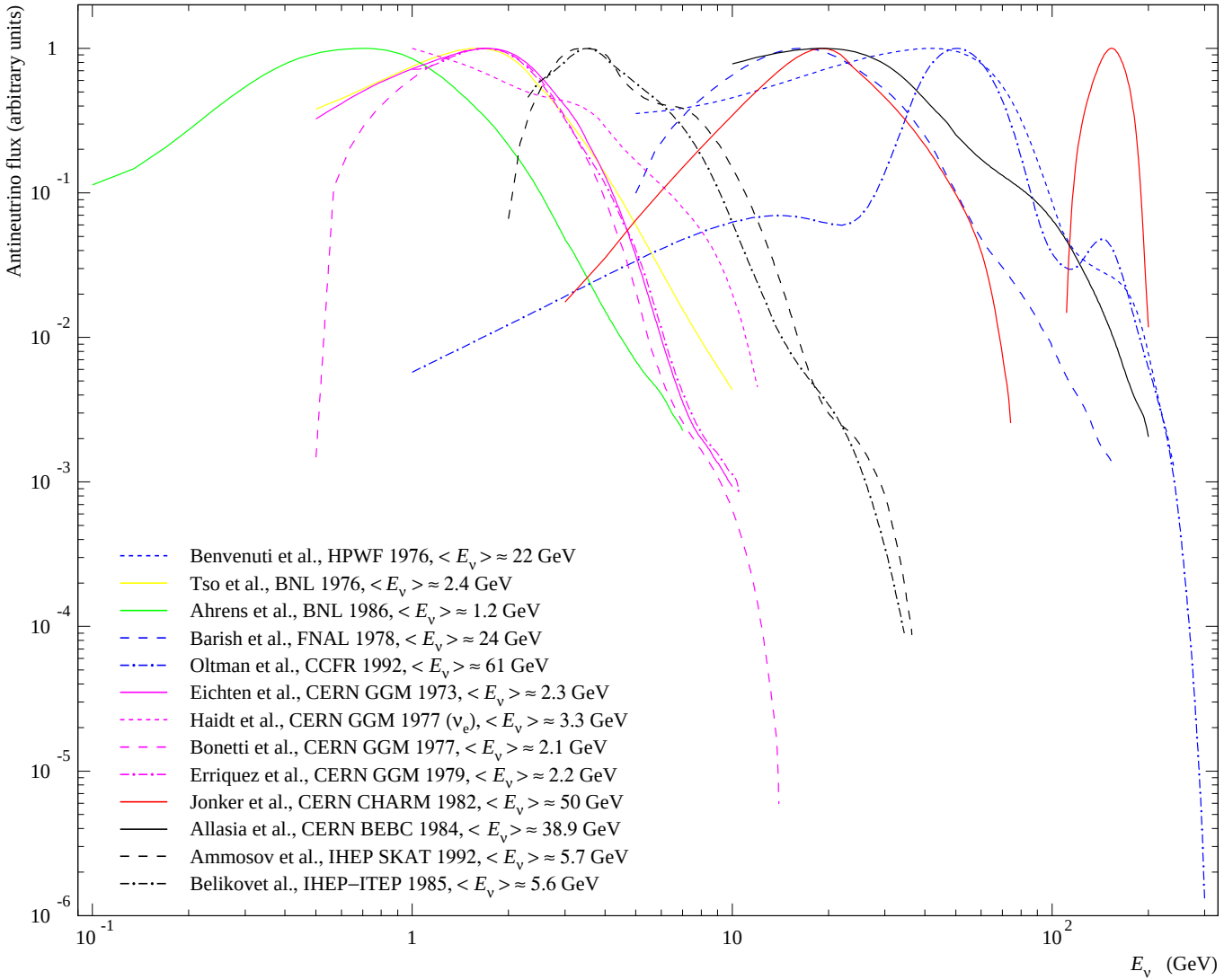

Рис. 6: Muon and electron antineutrino energy spectra in several accelerator experiments (a.u.).
[A. Bodek, K. S. Kuzmin & VN (unpublished). The data are collected from many sources.]

0.2 Neutrino interactions

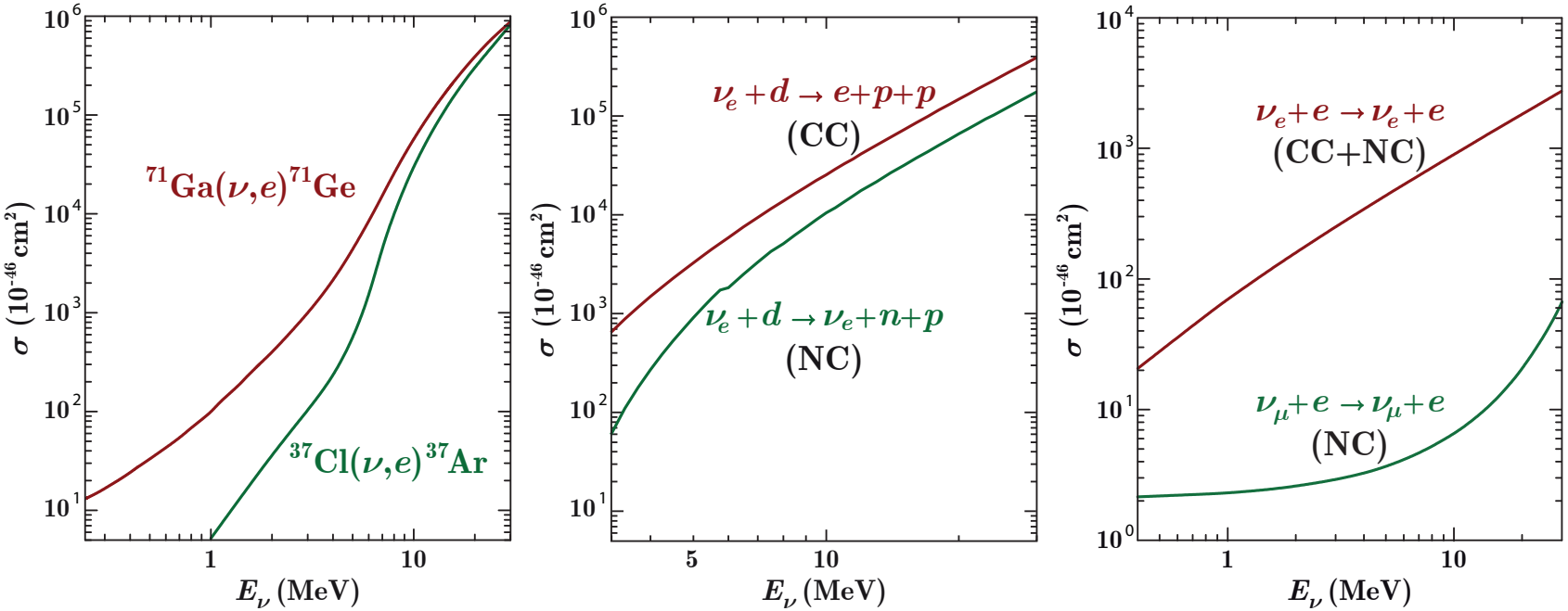

Рис. 7: Low-energy neutrino capture cross sections for gallium and chlorine (left), CC and NC induced neutrino cross sections for deuterium (middle), and neutrino–electron scattering cross sections (right) vs. neutrino energy.

[VN, Phys. Part. Nucl. Lett. **8** (2011) 683–703. The data are taken from J. N. Bahcall *et al.*, Phys. Rev. C **54** (1996) 411–422, J. N. Bahcall, Phys. Rev. C **56** (1997) 3391–3409, S. Ying *et al.*, Phys. Rev. C **45** (1992) 1982–1987, and J. N. Bahcall *et al.*, Phys. Rev. D **51** (1995) 6146–6158.]

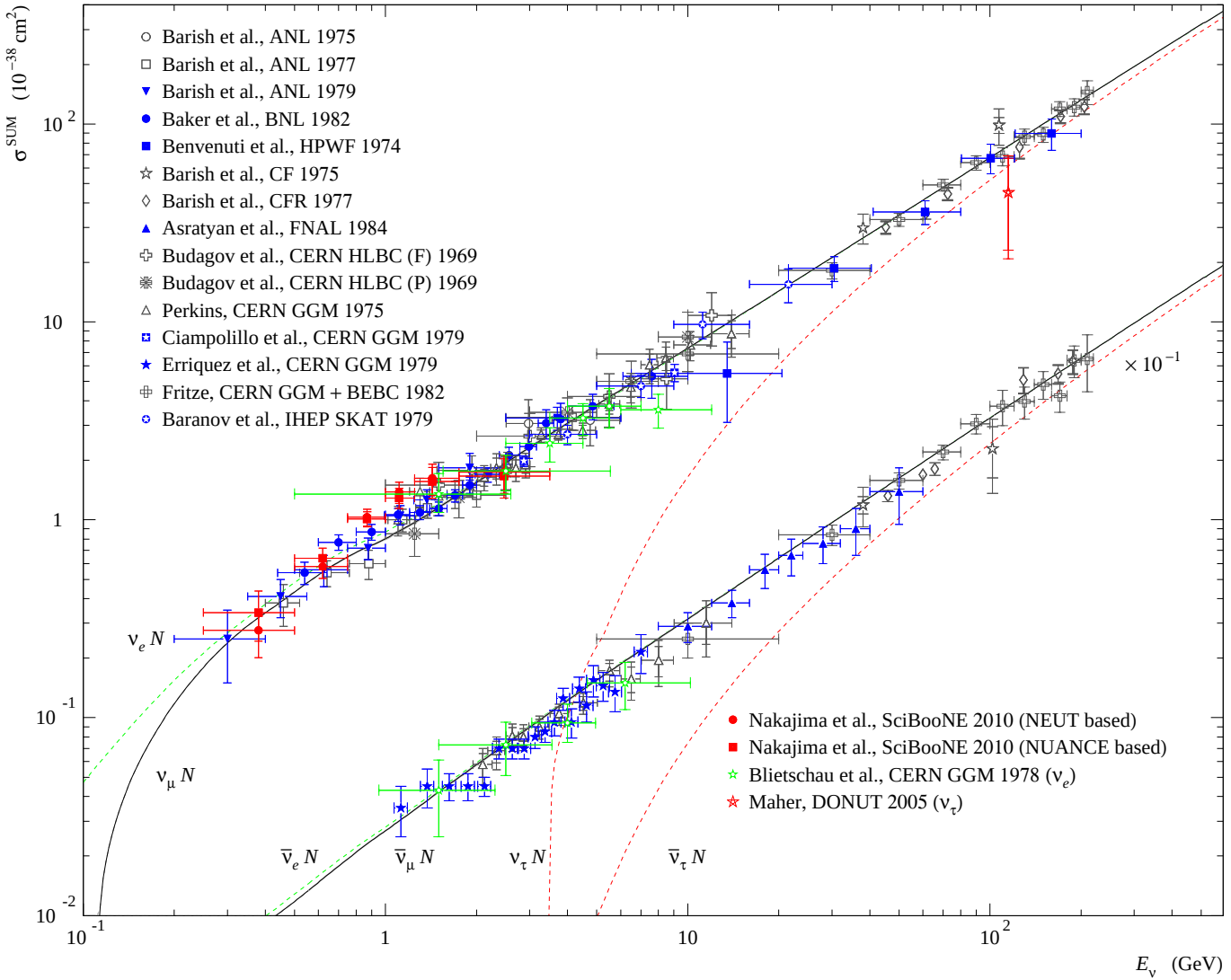

Рис. 8: The total cross sections for $\nu_e N$, $\nu_\mu N$, $\overline{\nu}_e N$, $\overline{\nu}_\mu N$, and $\overline{\nu}_\tau N$ (N = "isoscalar nucleon").
[K. S. Kuzmin & VN (unpublished).]

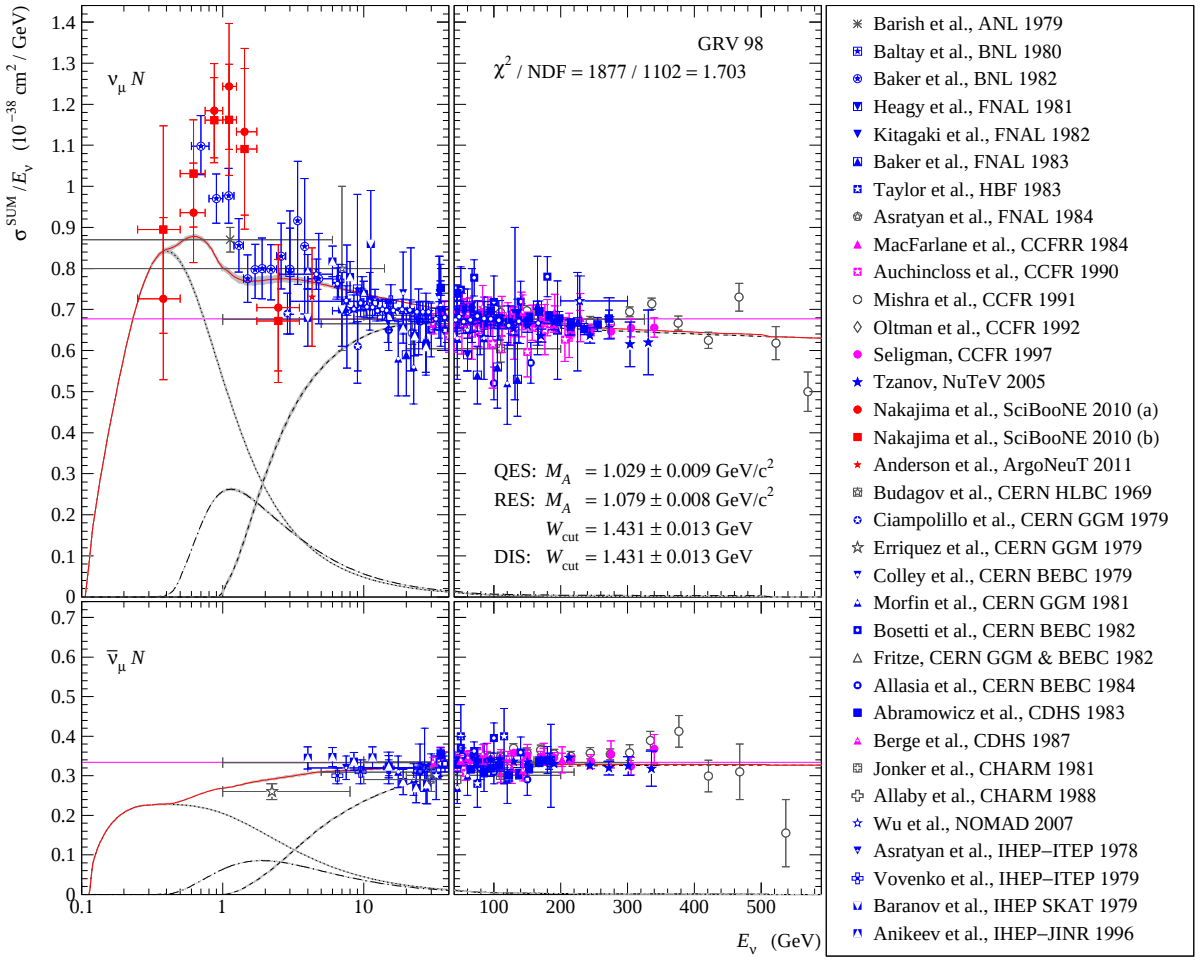

Рис. 9: Measured and calculated slopes of the muon neutrino and antineutrino total cross sections at high energies. Three main contributions and their sums are shown.

[K. S. Kuzmin *et al.*, Phys. Atom. Nucl. **69** (2005) 1857–1871 and hep-ph/0511308 (updated).]

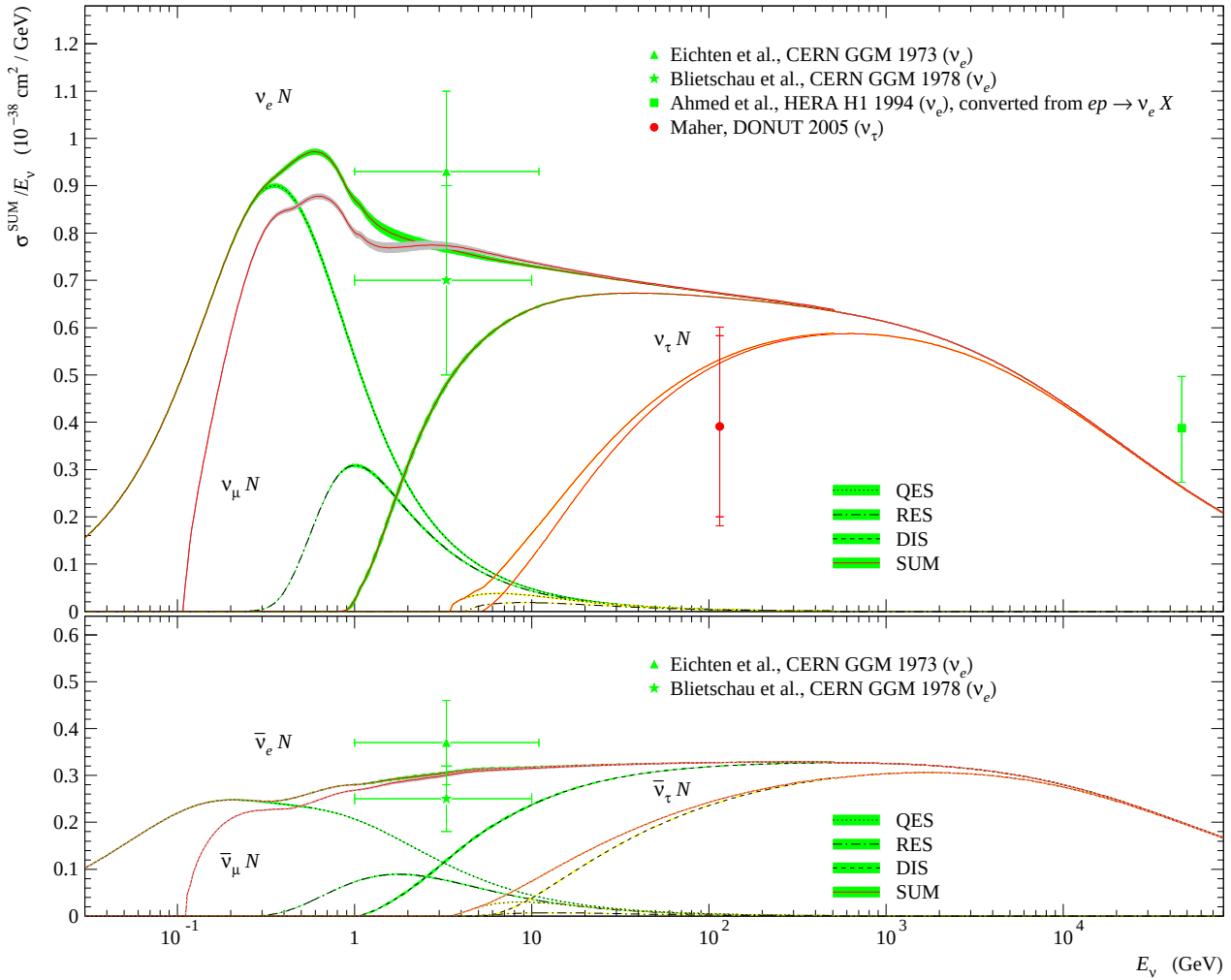

Рис. 10: Comparison of the slopes of the total cross sections for $\nu_e N$, $\nu_\mu N$, and $\nu_\tau N$ (top panel) and $\overline{\nu}_e N$, $\overline{\nu}_\mu N$, and $\overline{\nu}_\tau N$ (bottom panel). The main contributions are also shown.
[K. S. Kuzmin & VN (unpublished).]

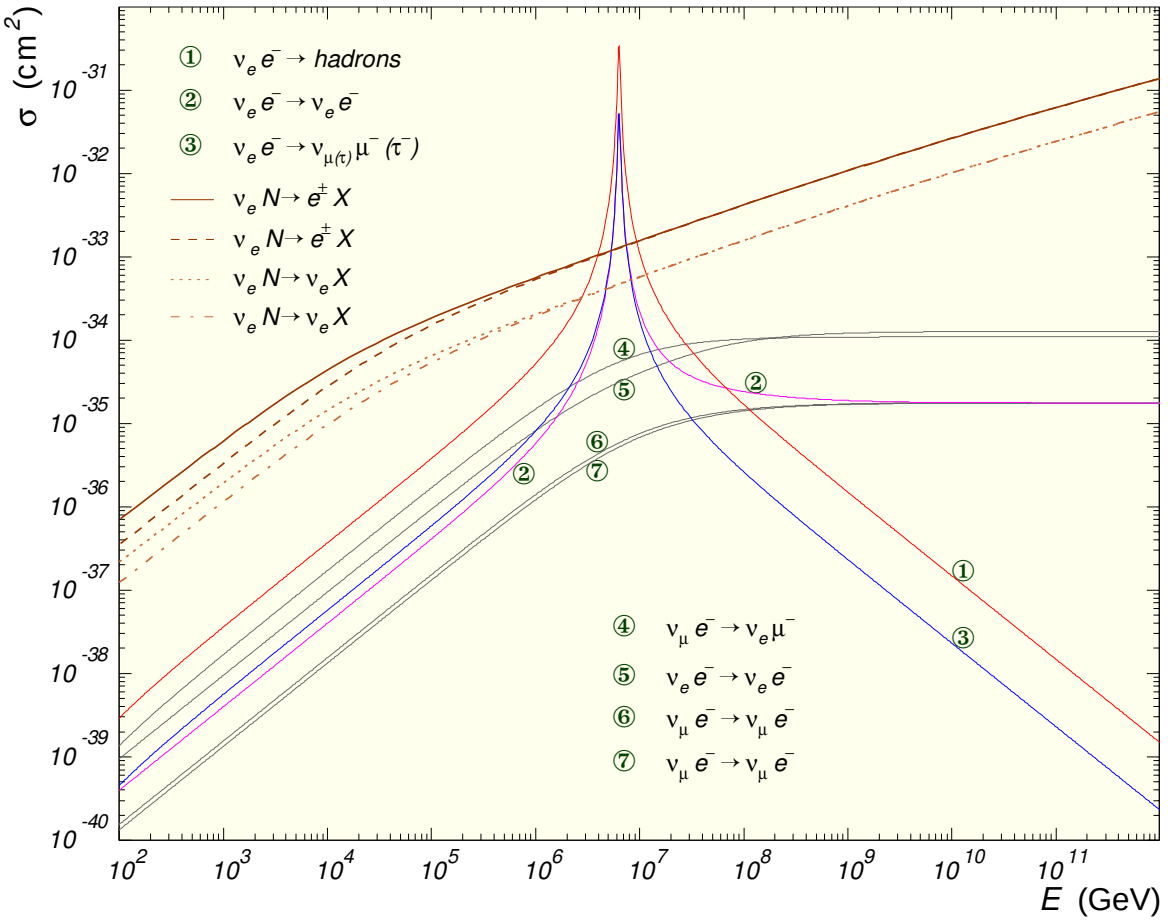

Рис. 11: Comparison of the $\nu_e(\overline{\nu}_e)$ total cross sections on electron and nucleon targets at super-high energies. The picks in reactions 1-3 are due to the W boson resonance formed in the neighborhood of $E_\nu^{\text{res}} = m_W^2/2m_e \approx 6.33$ PeV ("Glashow resonance").

[K. S. Kuzmin *et al.* (for the ANTARES Coll.), "Implementation of tau lepton polarization into ANTARES neutrino generator," ANTARES-Soft/2005-001.]

0.3 Modern neutrino toolkit

- **Accelerator $\nu/\overline{\nu}$s** [ANL, BNL, CERN, FNAL, IHEP, KEK, LAMPF, J-PARC,...]

Examples of the LBL experiments

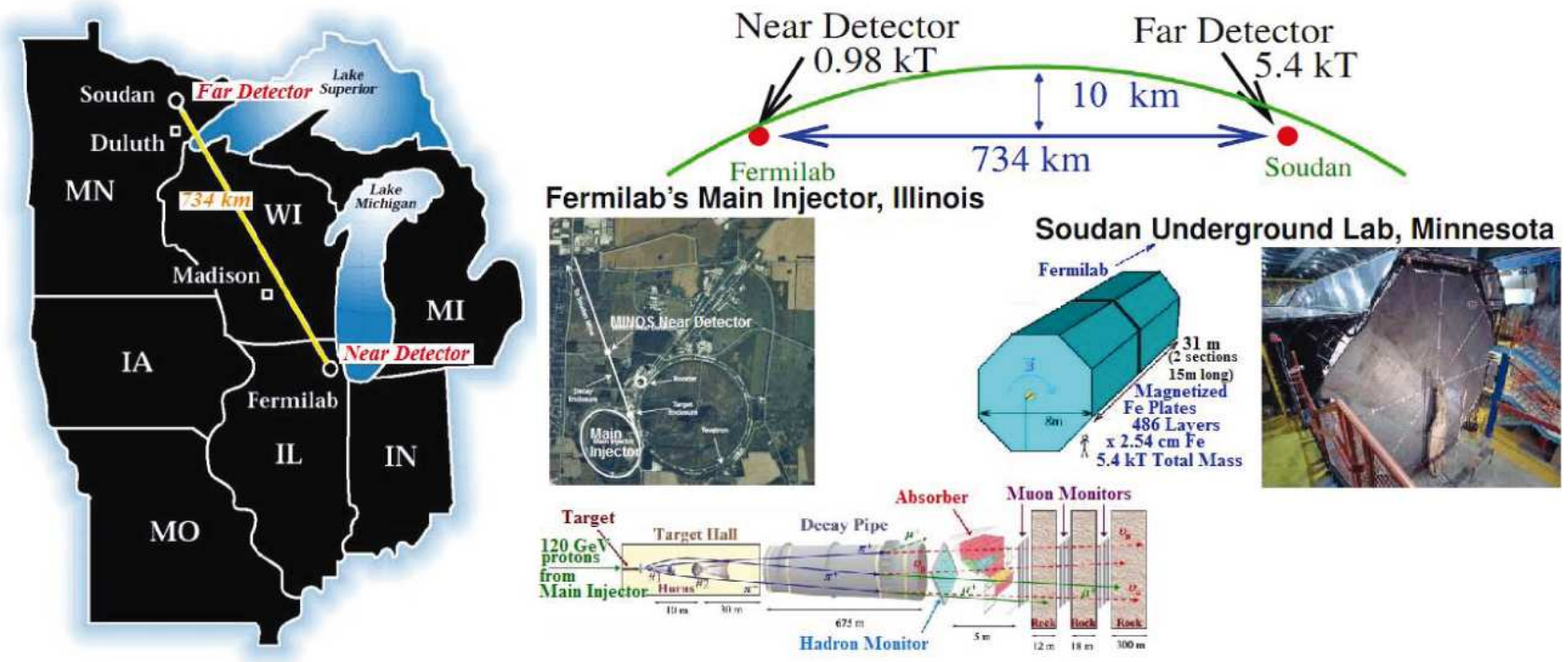

Рис. 12: Schematic layout of the MINOS experiment [FNAL – SOUDAN].

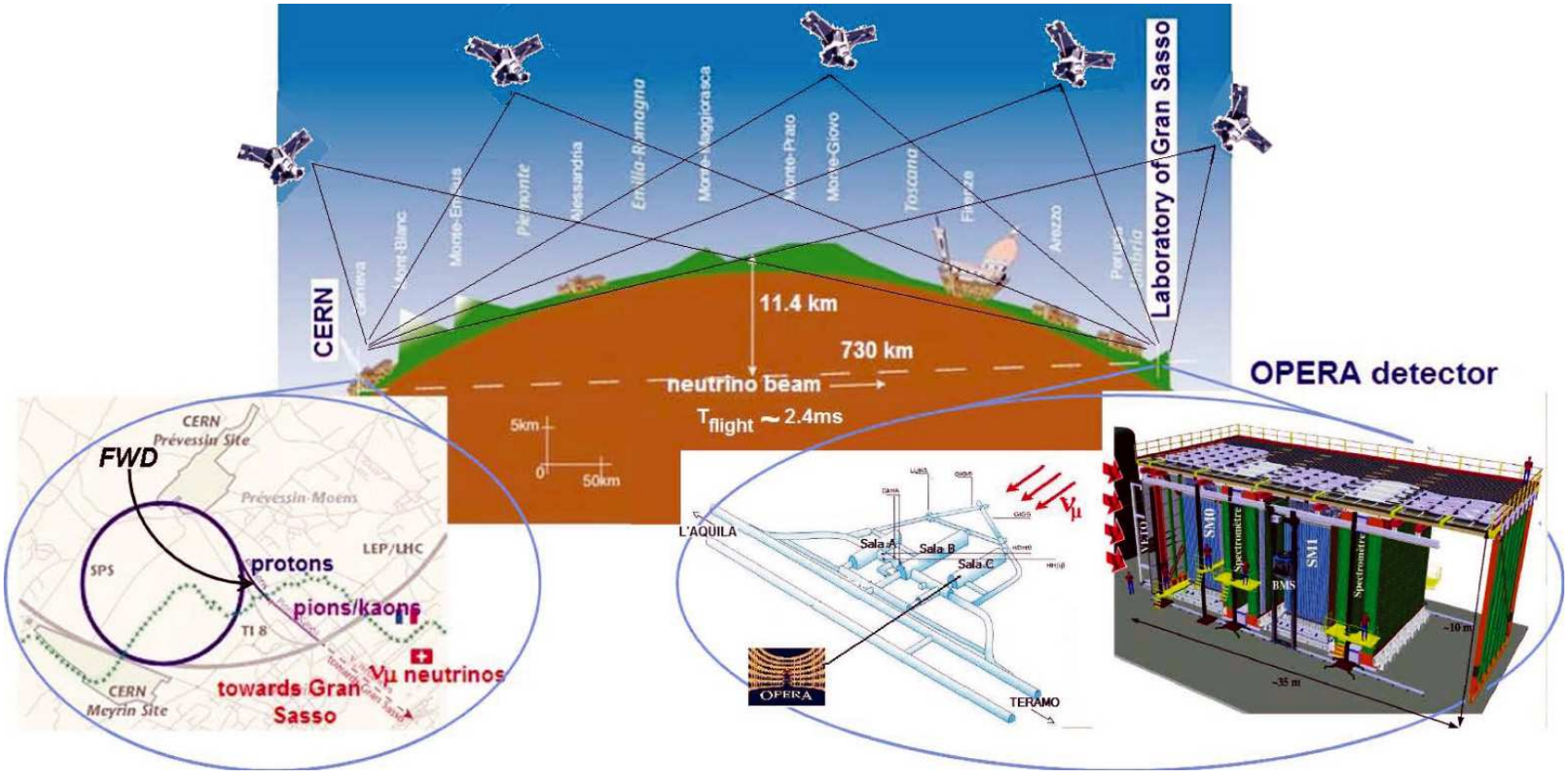

Рис. 13: Schematic layout of the OPERA experiment [CERN – LNGS].

[Figures 12 and 13 are borrowed from G. Brunetti,"Neutrino velocity measurement with the OPERA experiment in the CNGS beam," PhD thesis, in joint supervision of the Université Claude Bernard, Lyon-I and Universitá degli Studi di Bologna (May 2011), N° d'ordre 88-2011, LYCEN–T 2011-10; <http://amsdottorato.cib.unibo.it/3917>, <http://tel.archives-ouvertes.fr/tel-00633424>.]

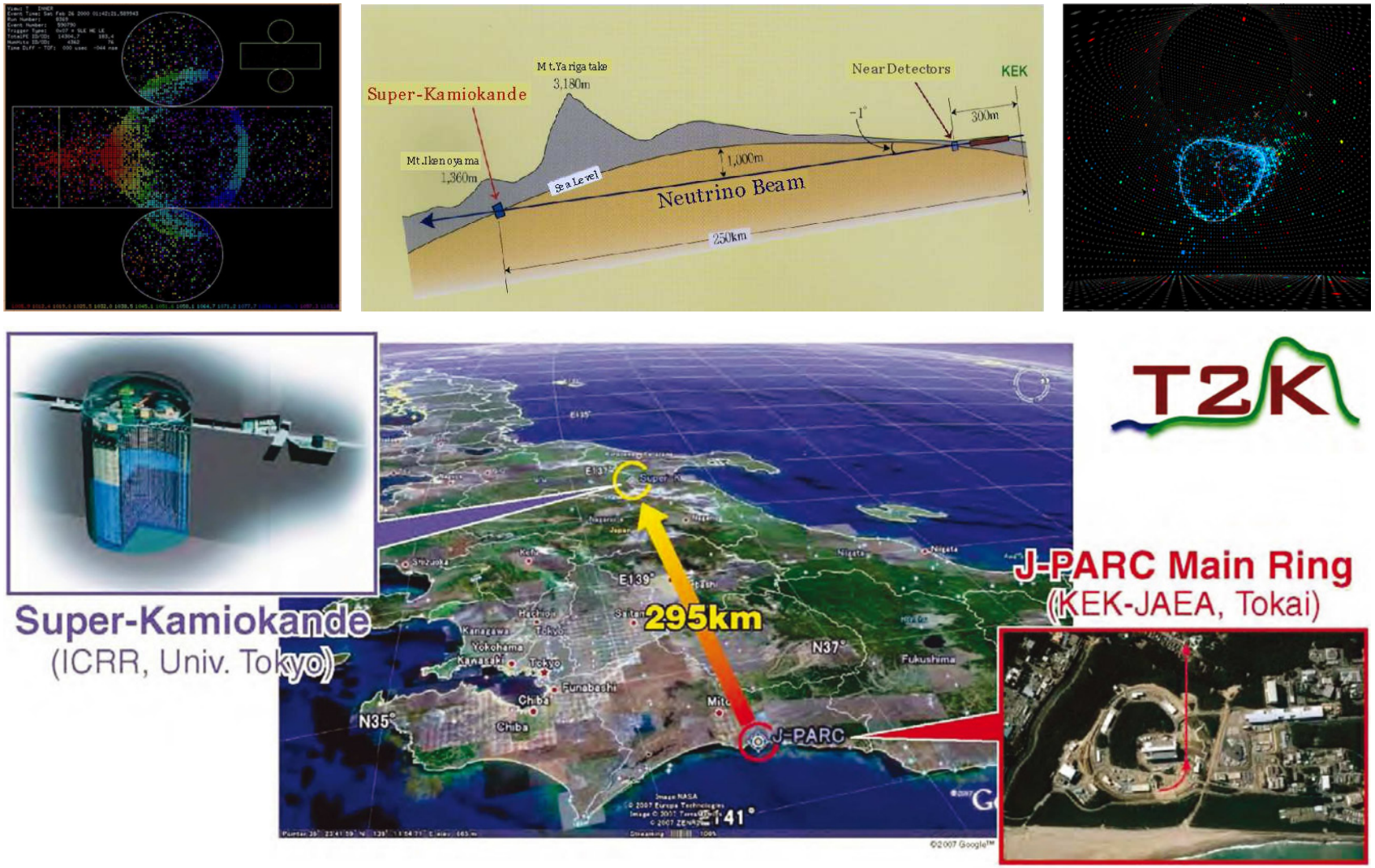

Рис. 14: Schematic layouts of the K2K [KEK (Tsukuba) – Super-Kamiokande] and T2K [J-PARC (Tokai) – Super-Kamiokande] experiments. [From relevant websites].

- **Reactor $\overline{\nu}$s** [Angra, Braidwood, Bugey, CHOOZ & Double CHOOZ, Daya Bay, Gosgen, JOYO, KASKA, KNPP-GEMMA, KamLAND, Krasnoyarsk, Kuo-Sheng, Palo Verde, RENO, Rovno, Savannah River Site, SONGS, TEXONO,...]

Examples of the reactor antineutrino experiments

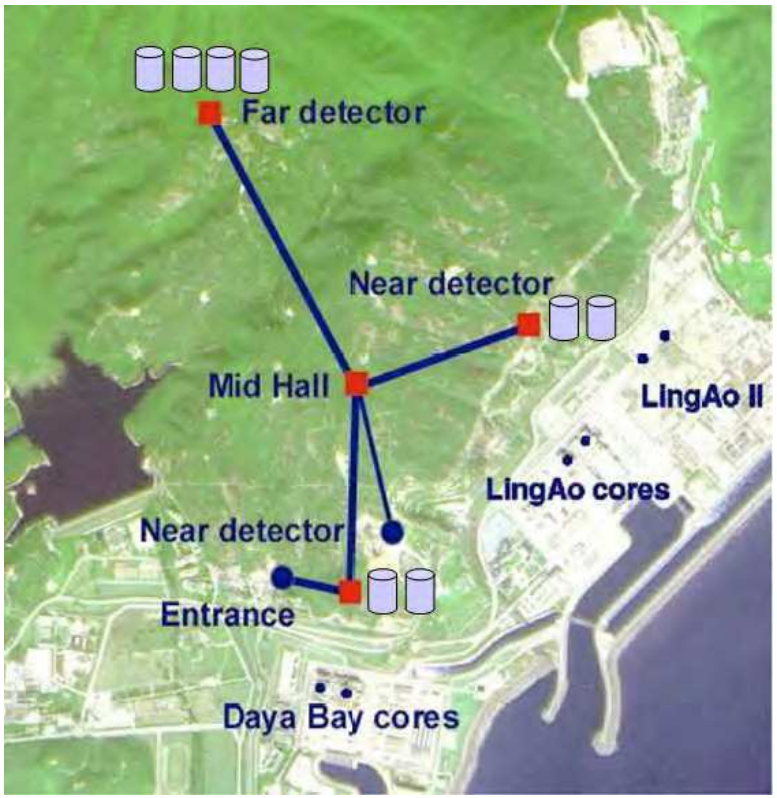

Рис. 15: Default configuration of the Daya Bay experiment (left panel) and the power stations around the KamLAND experiment (right panel). [From Daya Bay & KamLAND Proposals.]

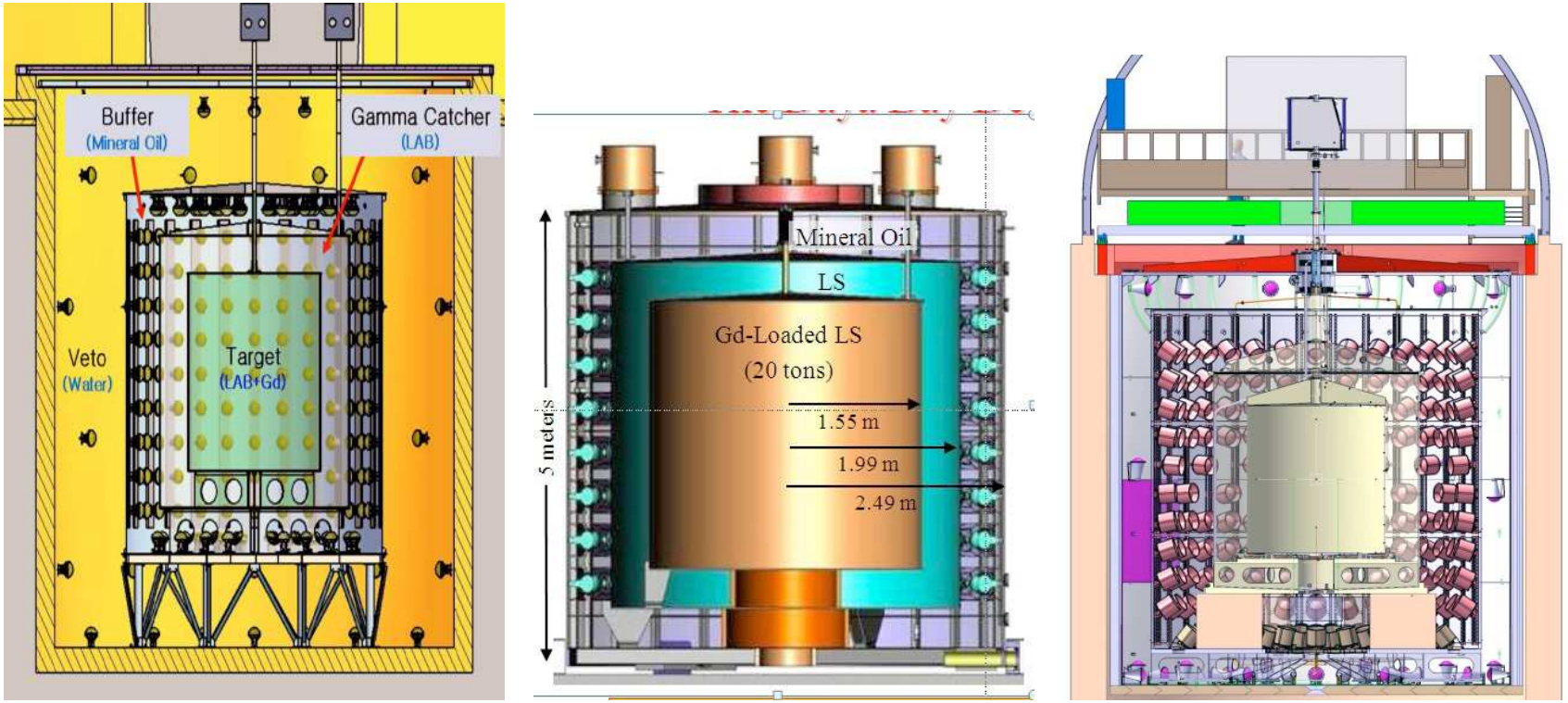

Рис. 16: The Daya Bay (left), Reno (middle), and Double Chooz (right) detector layouts. The common design is an evolution of the CHOOZ detector.

[From T. Lasserre, "Oscillation Parameters with forthcoming Reactor Neutrino Experiments", in: Proceedings of the Workshop 'European Strategy for Future Neutrino Physics', Geneva, Switzerland, October 1–3, 2009, edited by A. Blondel & F. Dufour, CERN-2010-003, pp. 33–40.]

- **Underground Laboratories for terrestrial and extraterrestrial neutrinos**
  [BNO, DUSEL, Homestake, Gran Sasso, Kamioka, KGF, Modane, Mont Blanc, Pyhäsalmi, SOUDAN, SNO,...]

  Examples of the underground experiments

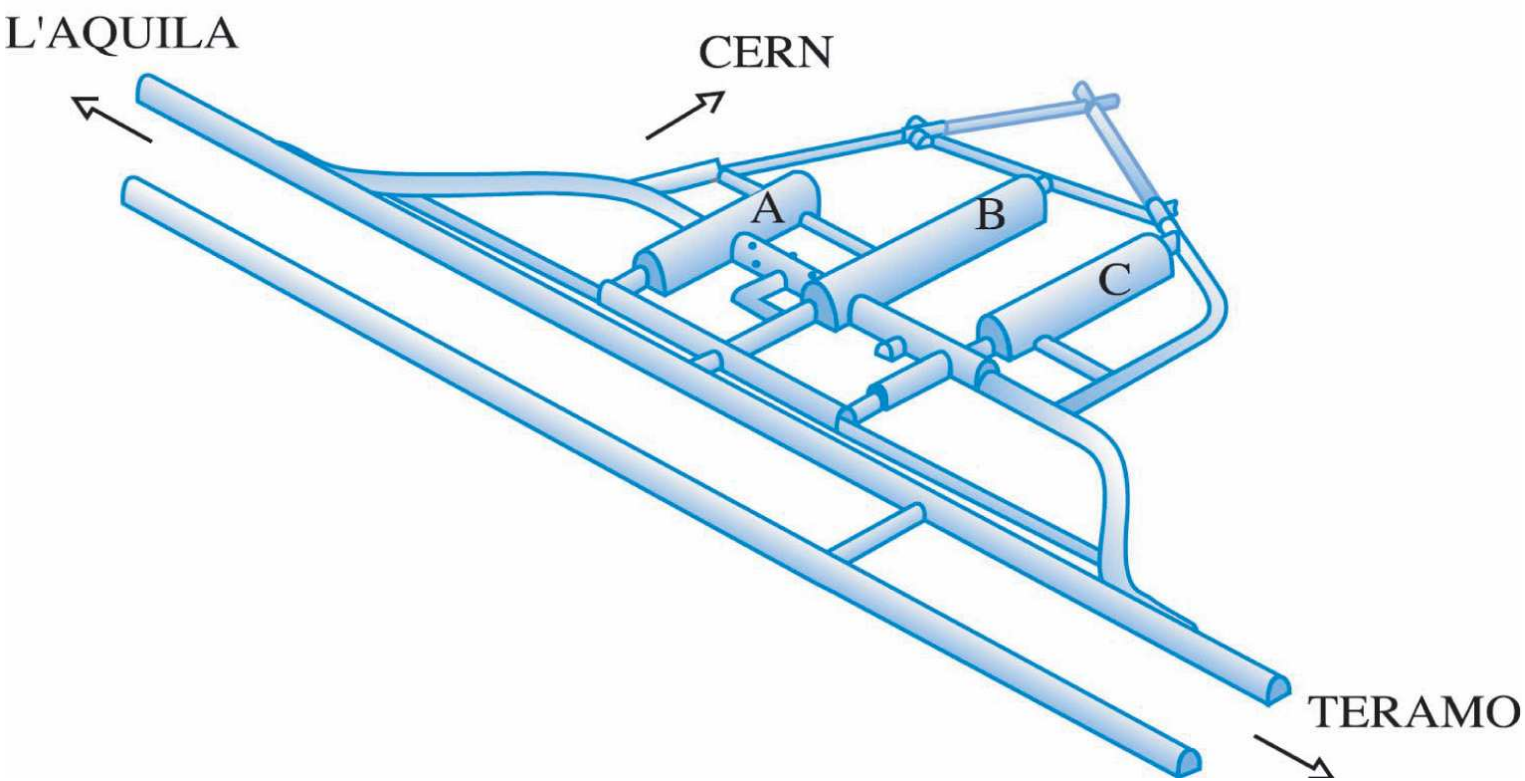

Рис. 17: Gran Sasso underground laboratory (INFN). Most relevant neutrino experiments are Borexino, Icarus, LVD, MACRO, OPERA.

[From <http://www.lngs.infn.it>.]

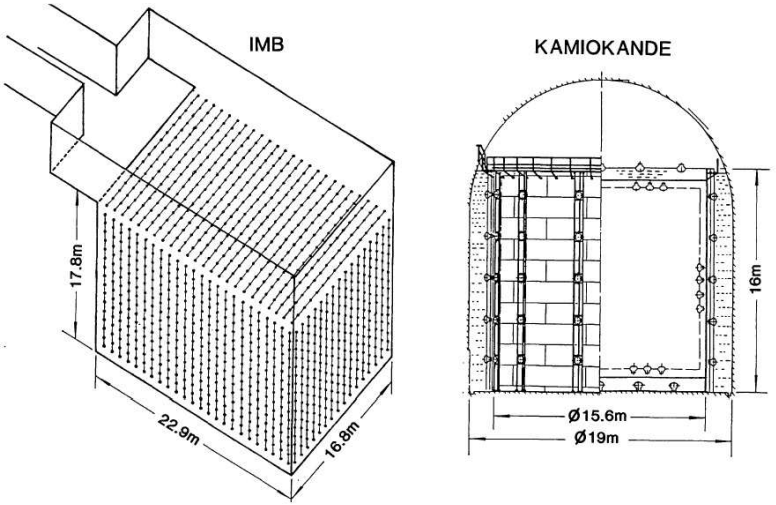

Рис. 18: Water Cherenkov detectors.

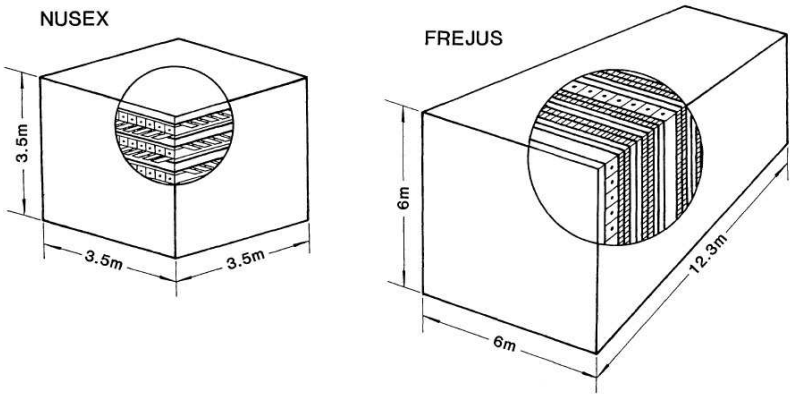

Рис. 19: Tracking calorimeter detectors.

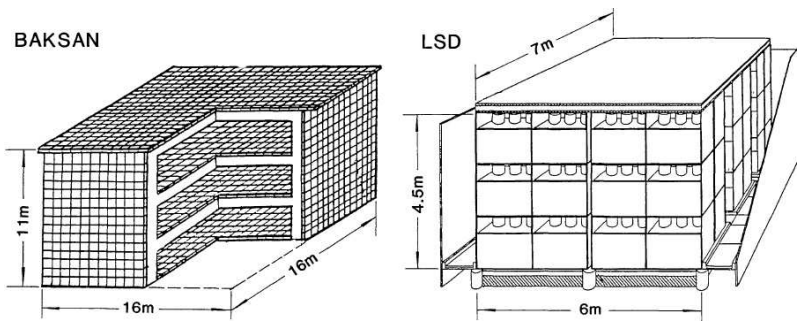

Рис. 20: Liquid scintillator detectors.

Figures 18–20 show the park of underground detectors (as it was on 1989) capable to catch atmospheric neutrinos. Only the Baksan telescope remains in operation till now (2012).

[Borrowed from A. M. Bakich, "Aspects of neutrino astronomy," Space Sci. Rev. **49** (1989) 259–310.]

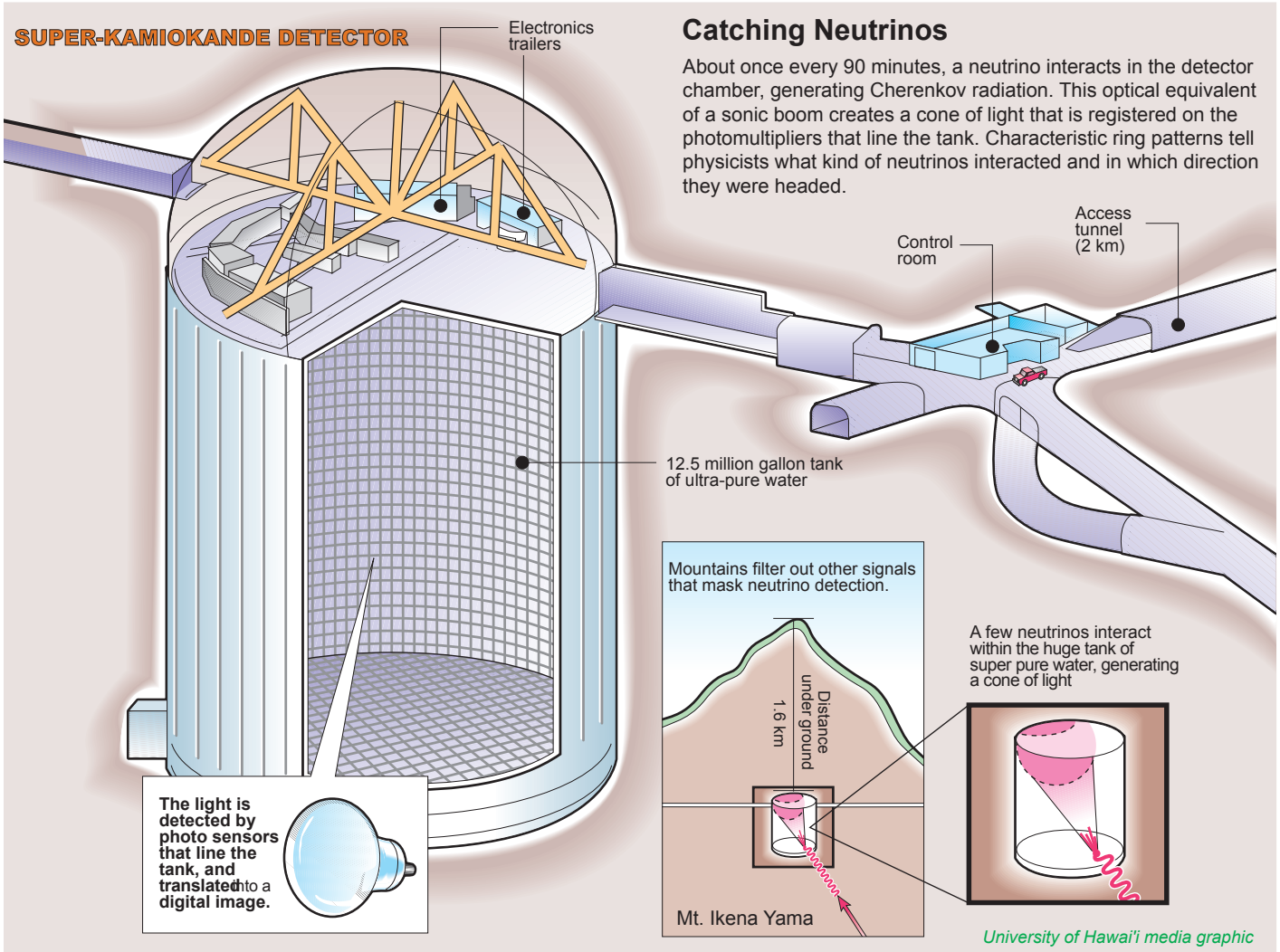

Рис. 21: Super-Kamiokande, the largest ever underground neutrino detector.

[This and next images are borrowed from the Super-Kamiokande website <http://www-sk.icrr.u-tokyo.ac.jp>.]

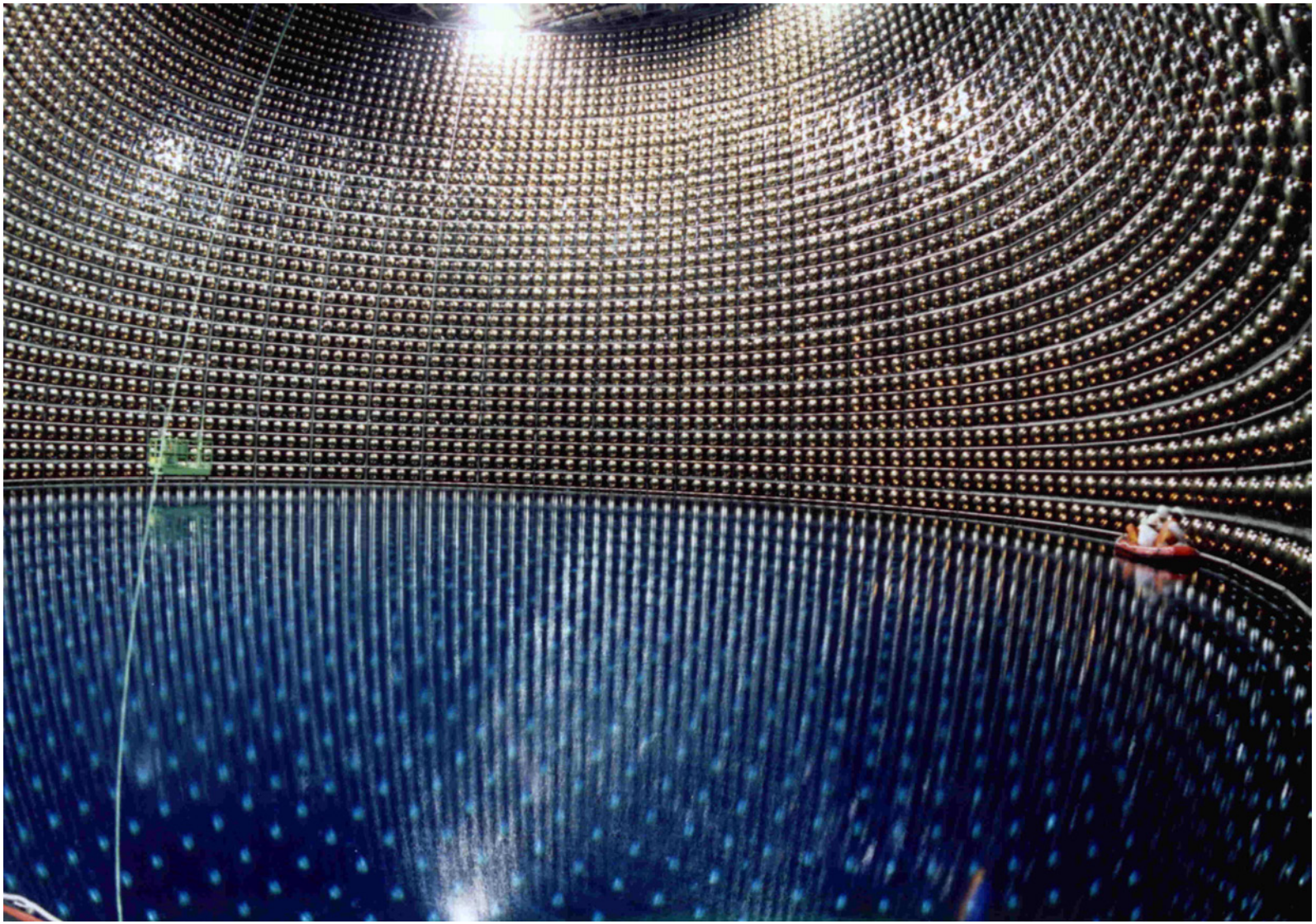

Рис. 22: Inside of the Super-Kamiokande detector during water filling.

Figures 23 and 24 show two real (not Monte Carlo) events recorded in the Super-Kamiokande-I detector.

[From Tomasz Barszczak webpage <http://www.ps.uci.edu/~tomba/sk/tscan/pictures.html> (UC).]

A real multiple ring event (found by Brett Michael Viren, State University of New York at Stony Brook) is shown in Fig. 23. ▷

This event recorded on 24/09/1997, 12:02:48 was one of the close candidates for decay $p \to e^+ + \pi^0$ but did not pass analysis cuts.

The π^0 meson would decay immediately into two gammas which make overlapping fuzzy rings. Positron and π^0 would fly in opposite directions.

Time color scale spans 80 ns.

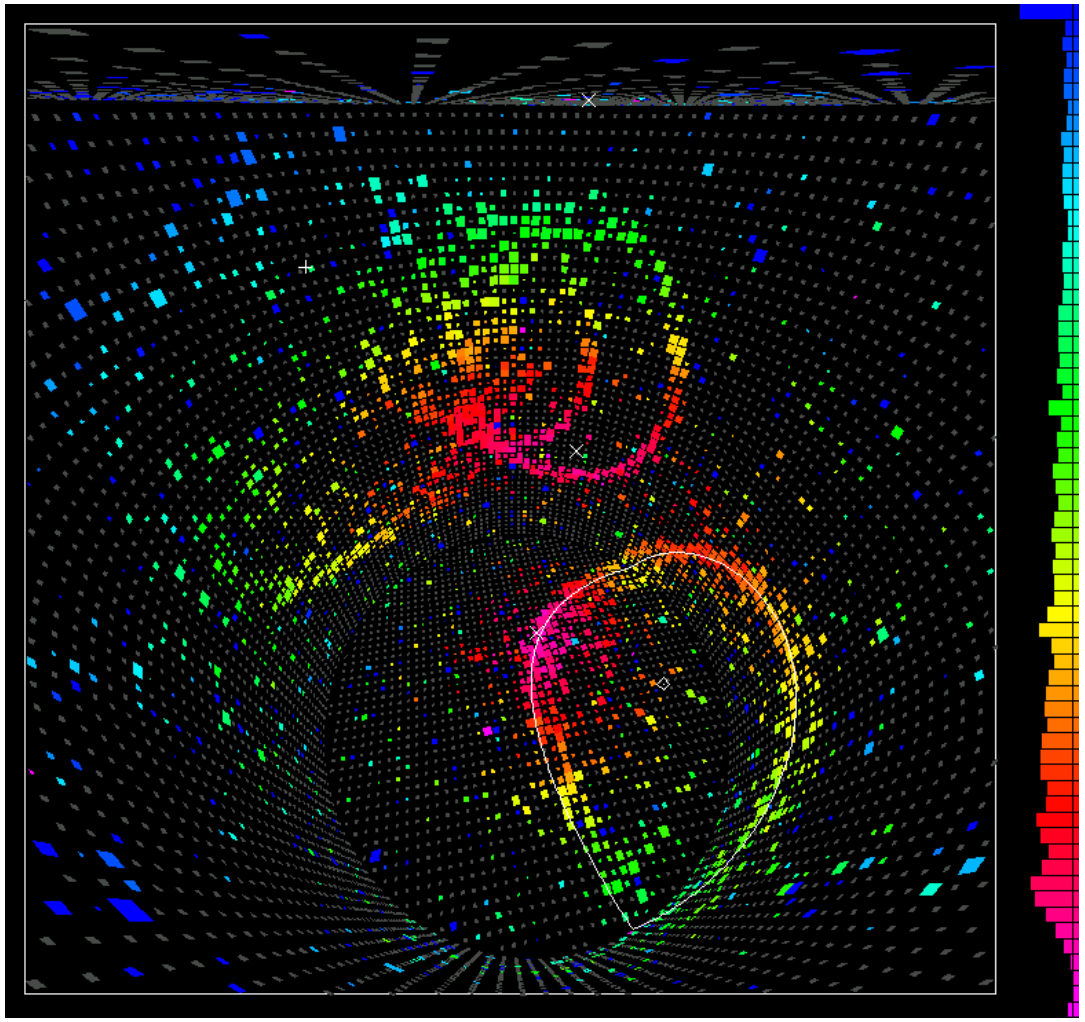

Рис. 23: Multiple ring event recorded in the Super-Kamiokande detector on 24/09/1997, 12:02:48.

In Fig. 24, an upward-going through-going muon event recorded on 30/05/1996, 17:12:56 is shown. ▷

The muon entered through the flat circular part of the detector near the bottom of the picture where purple earliest PMT hits can be seen. It exited through the cylindrical side wall in the middle of the picture.

Time color scale spans 262 ns.

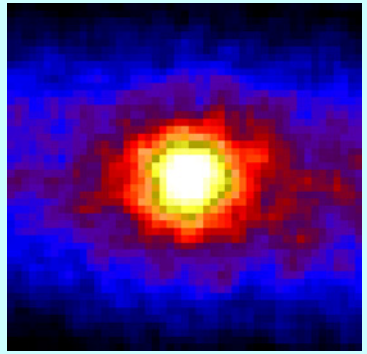

The Sun in neutrino light.

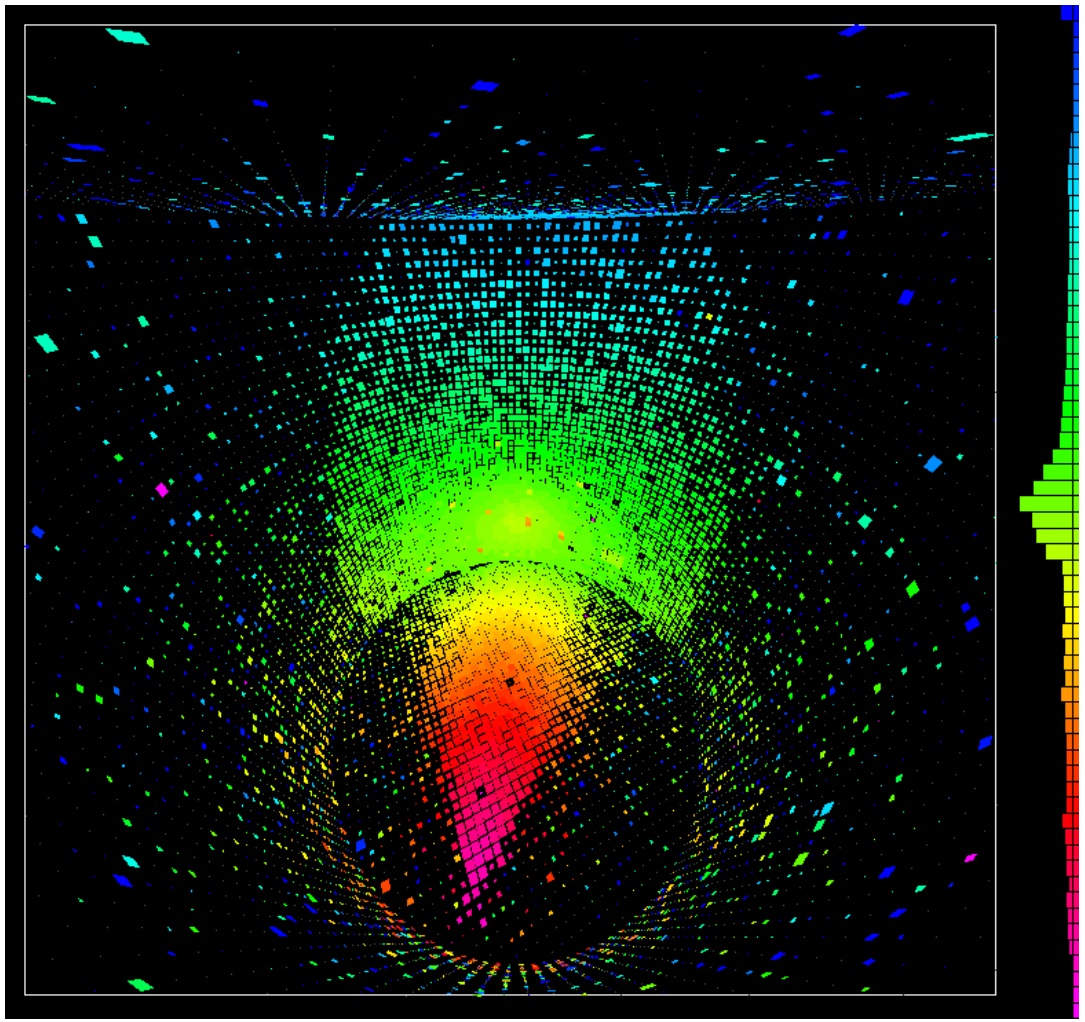

Рис. 24: Through-going muon event recorded in the Super-Kamiokande detector on 30/05/1996, 17:12:56.

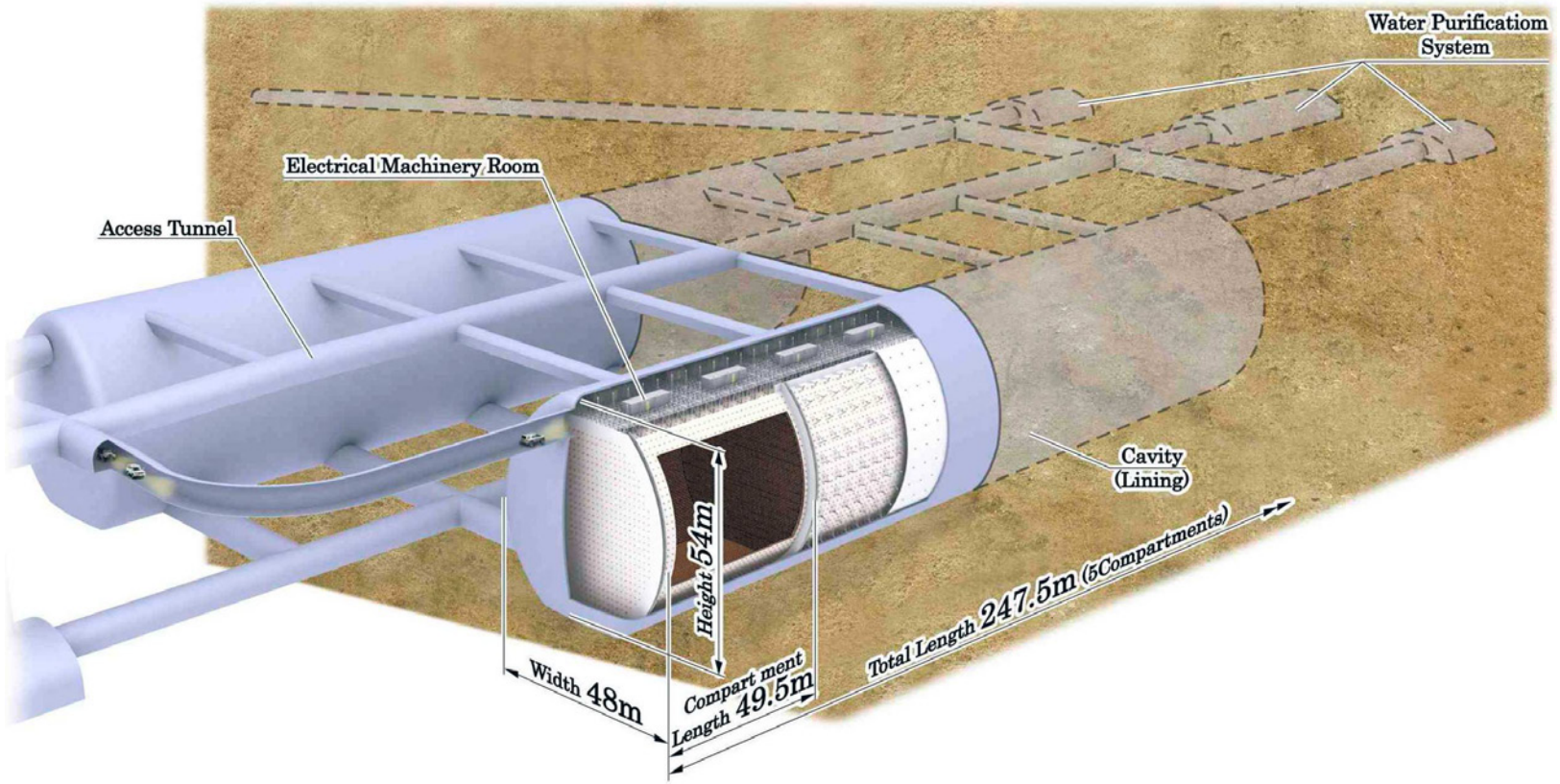

Рис. 25: Schematic view of the Hyper-Kamiokande detector, a megaton water Cherenkov detector, proposed as a successor to Super-Kamiokande; to be located at Tochibora, a few kilometers from the Kamioka site, 648 m rock (1,750 m w.e.) overburden.

[From K. Abe *et al.*, "Letter of Intent: The Hyper-Kamiokande Experiment – Detector Design and Physics Potential", arXiv:1109.3262 [hep-ex].]

Таблица 1: Hyper-Kamiokande detector parameters of the baseline design.

Detector type		Ring-imaging water Cherenkov detector
Candidate site	Address	Tochibora mine, Kamioka town, Gifu, Japan
	Latitude	$36°21'08.928''$ N
	Longitude	$137°18'49.688''$ E
	Altitude	508 m
	Overburden	648 m rock (1,750 m w.e.)
	Cosmic Ray Muon flux	$\sim 2.3 \times 10^{-6}$ sec^{-1}cm^{-2}
	Off-axis angle for the J-PARC ν	$2.5°$ (same as Super-Kamiokande)
	Distance from the J-PARC	295 km (same as Super-Kamiokande)
Detector geometry	Total Volume	0.99 Megaton
	Inner Volume (Fiducial Volume)	0.74 (0.56) Megaton
	Outer Volume	0.2 Megaton
PM tubes	99,000 20-inch ϕ PMTs	
		20% photo-coverage
	Outer detector	25,000 8-inch ϕ PMTs
Water quality	light attenuation length	> 100 m @ 400 nm
	Rn concentration	< 1 mBq/m^3

- **Underwater/ice neutrino telescopes**
  [AMANDA, ANTARES, Baikal, IceCube, NEMO, NESTOR,..., $\longmapsto$ KM3NET]

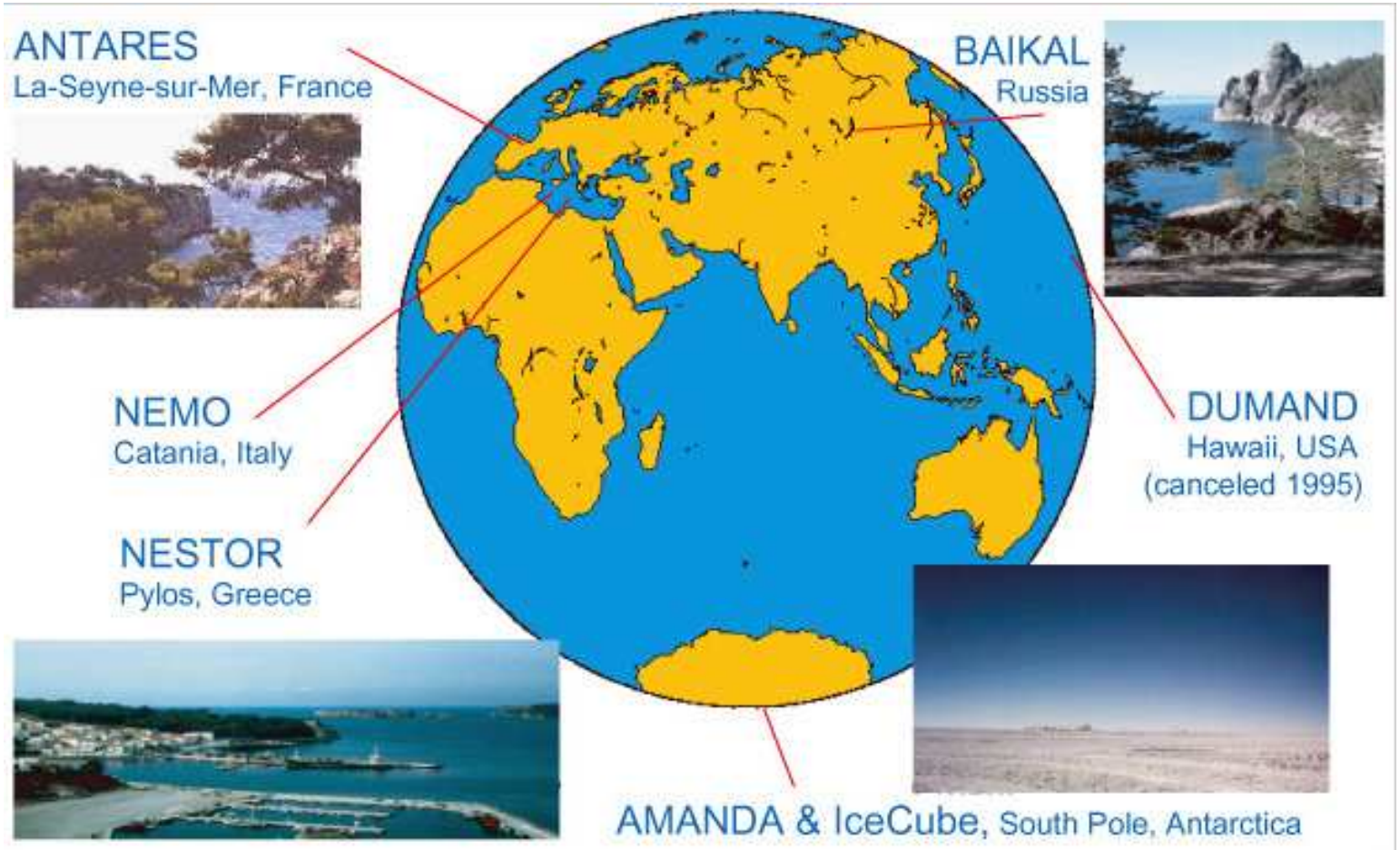

Рис. 26: A map of underwater/ice Cherenkov neutrino telescope projects.
[From Francis Halzen web-page <http://icecube.wisc.edu/~halzen/>].

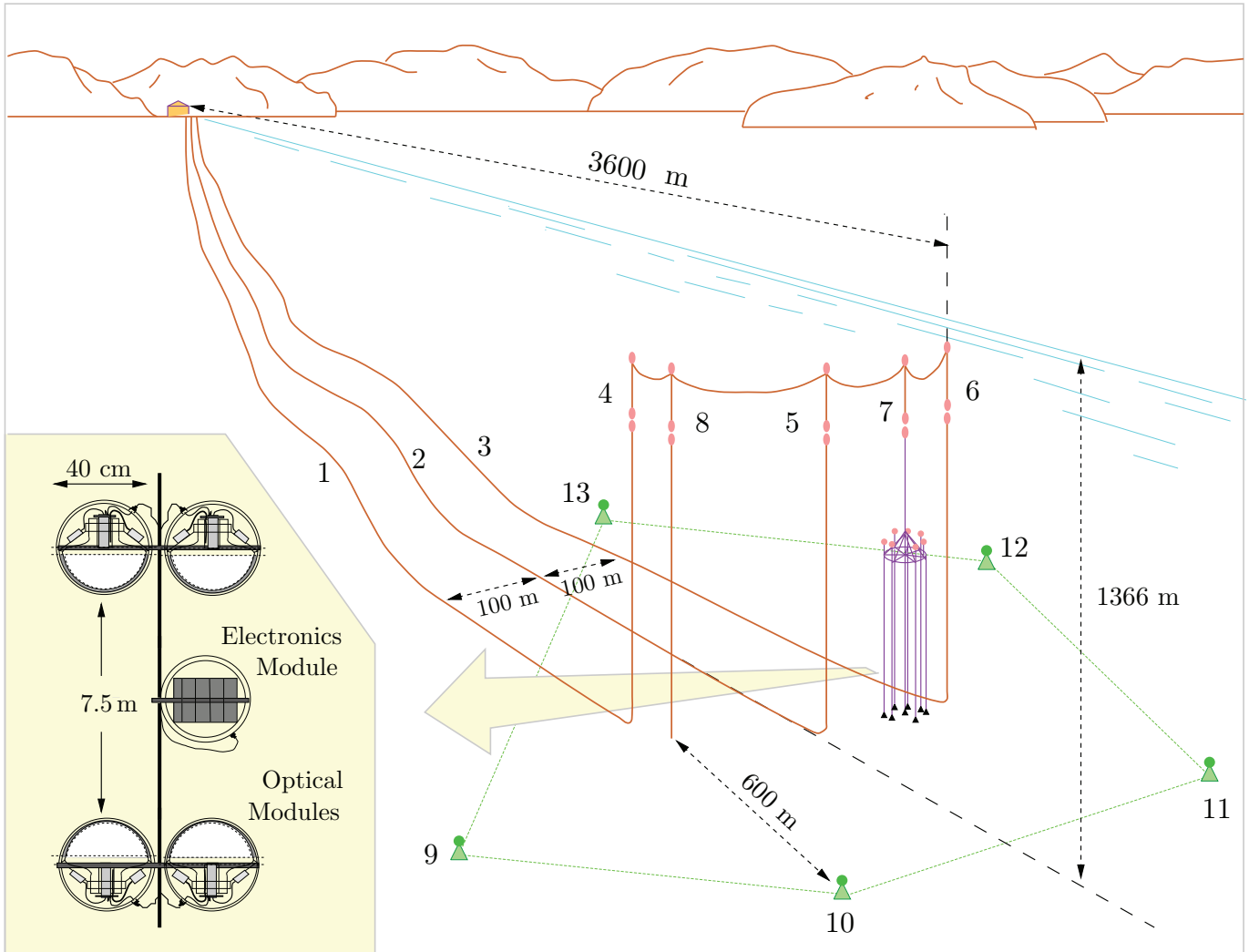

Рис. 27: Overall view of the NT-200 complex in Lake Baikal.

[From V. A. Balkanov *et al.* (Baikal Coll.) Appl. Opt. **33** (1999) 6818–6825 [astro-ph/9903342].]

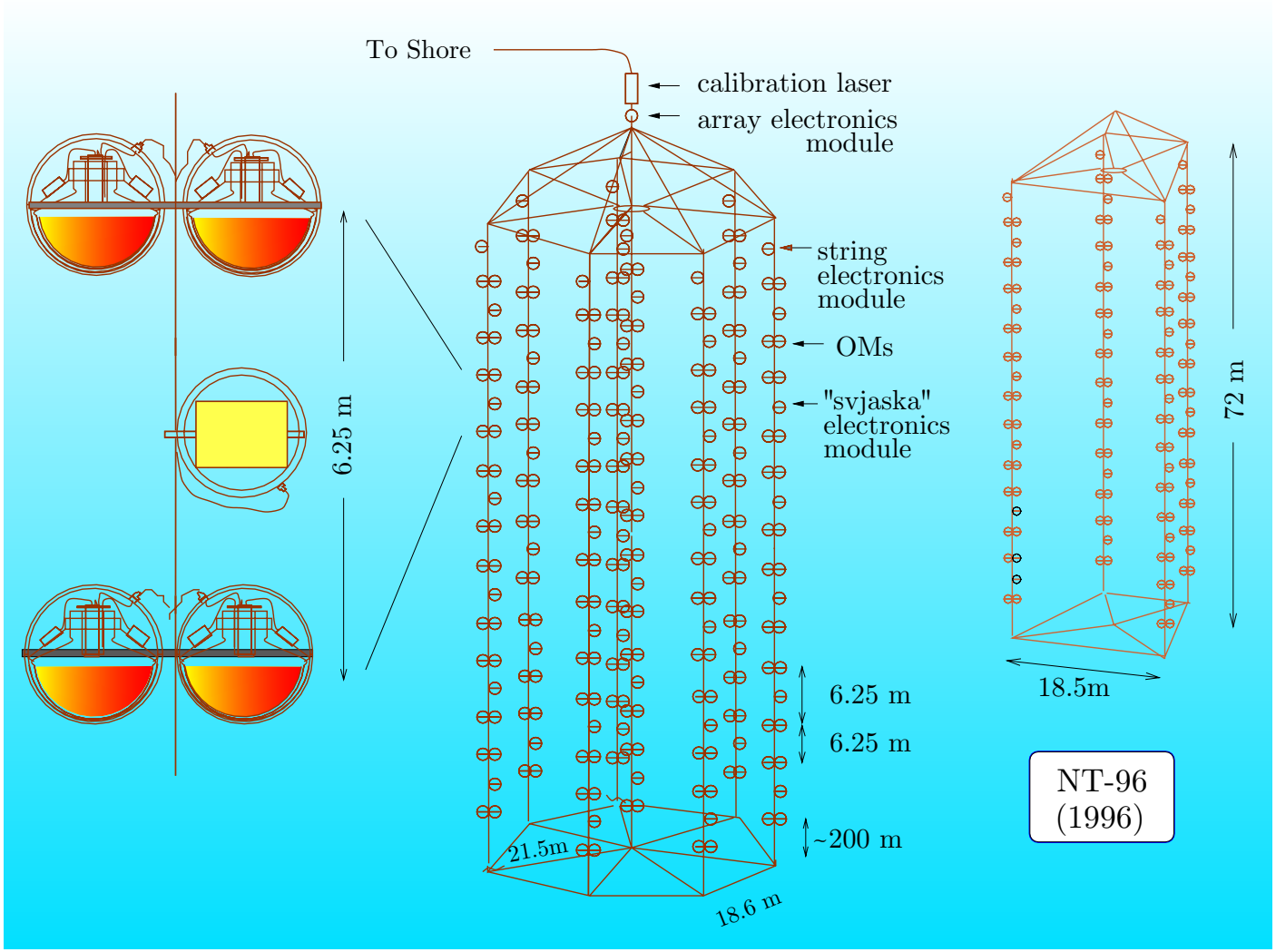

Рис. 28: Baikal NT-200 and NT-96 schematic view.

[From Ch. Spiering *et al.* (Baikal Coll.), Prog. Part. Nucl. Phys. **40** (1998) 391 [astro-ph/9801044].]

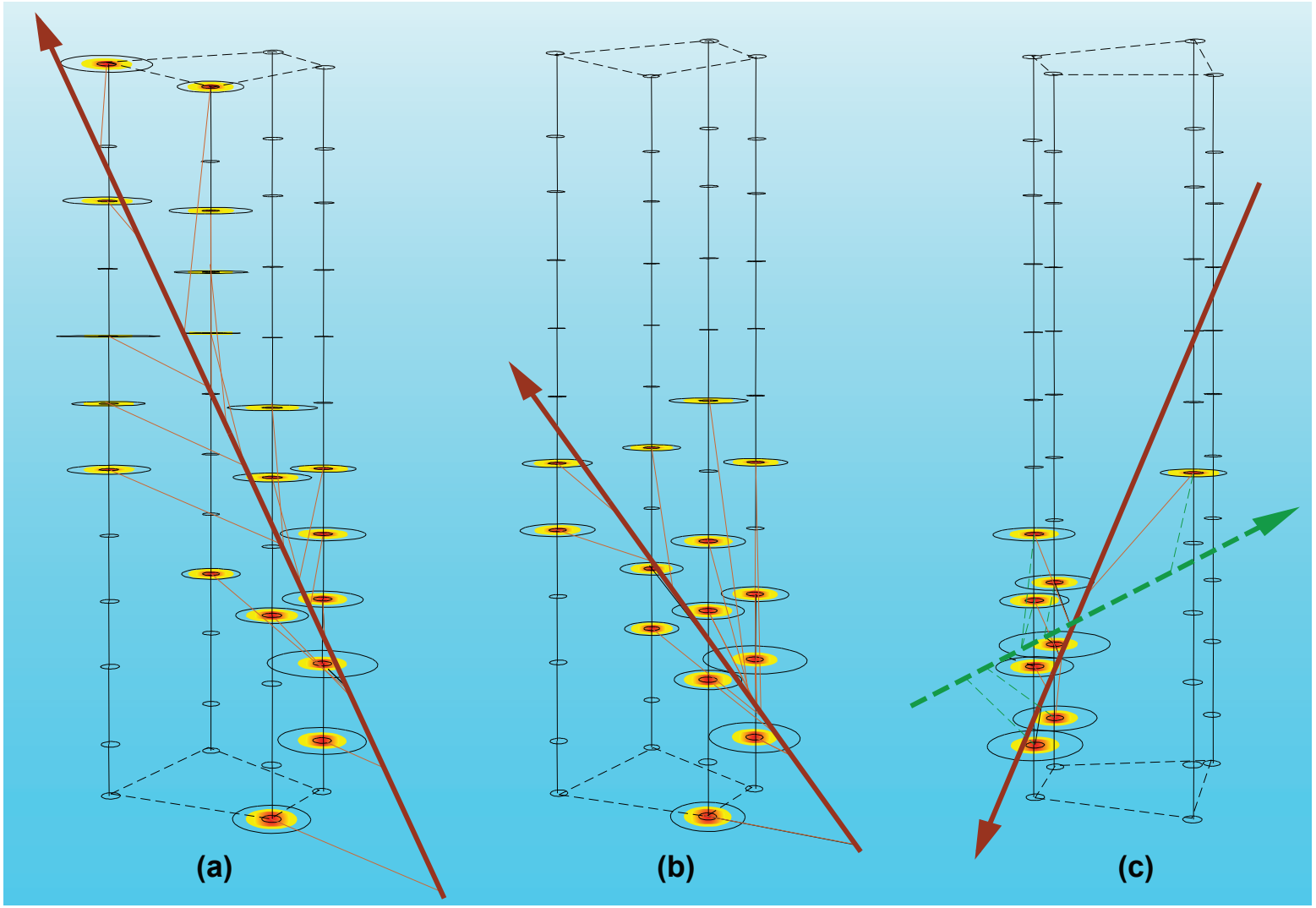

Рис. 29: Three neutrino candidates recorded in NT-96.

[From V. A. Balkanov *et al.* (Baikal Coll.) Yad. Fiz. **63** (2000) 1027–1036 [Phys. Atom. Nucl. **63** (2000) 951–961].]

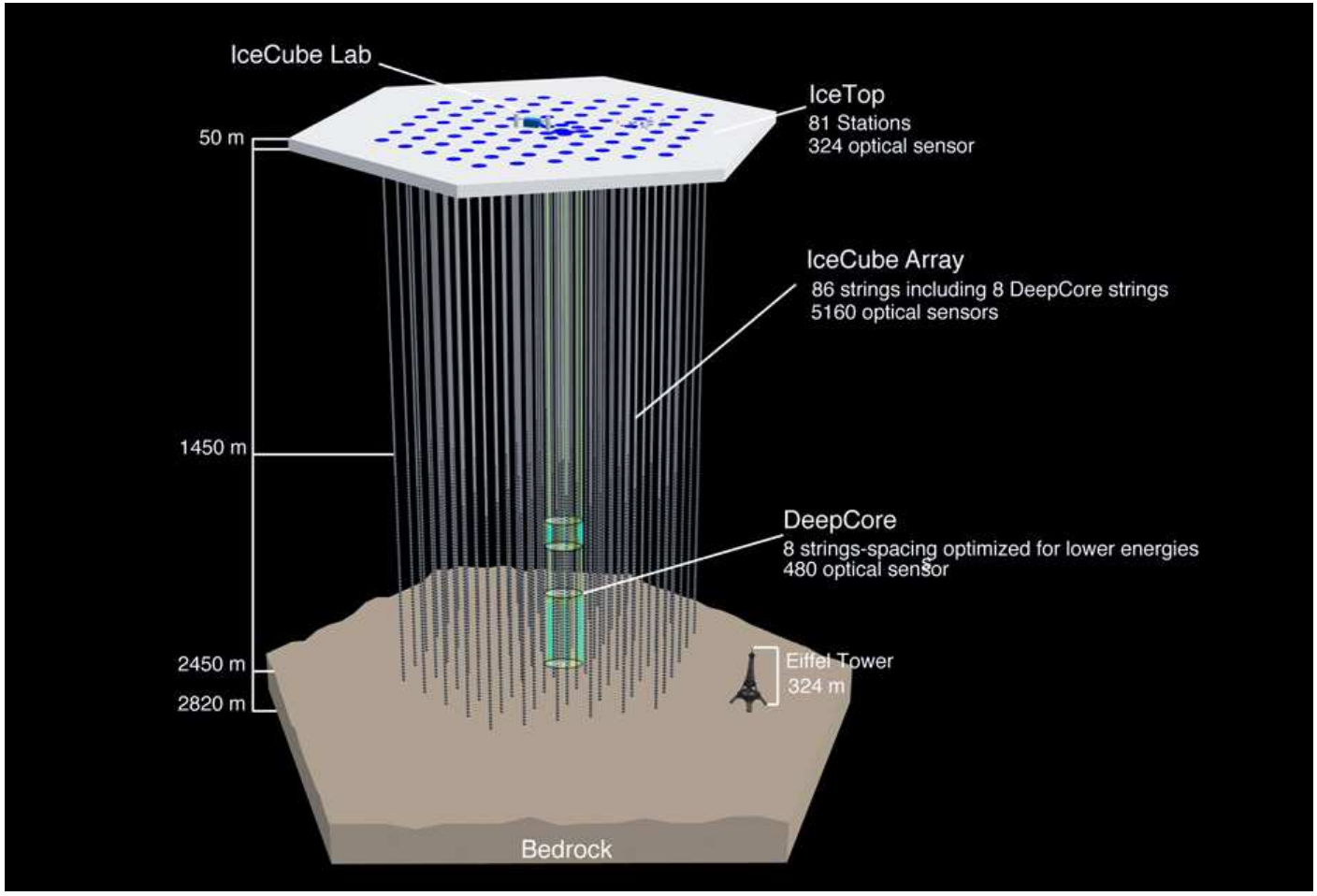

Рис. 30: The IceCube Neutrino Telescope is made up of 86 strings with a total of 5,160 Digital Optical Modules that are used to sense and record neutrino events. Although the telescope is 2,820 meters tall, the average hole is 2,452 meters deep.

[Image by Danielle Vevea & Jamie Yang, taken from the IceCube NO webpage <http://icecube.wisc.edu/>].

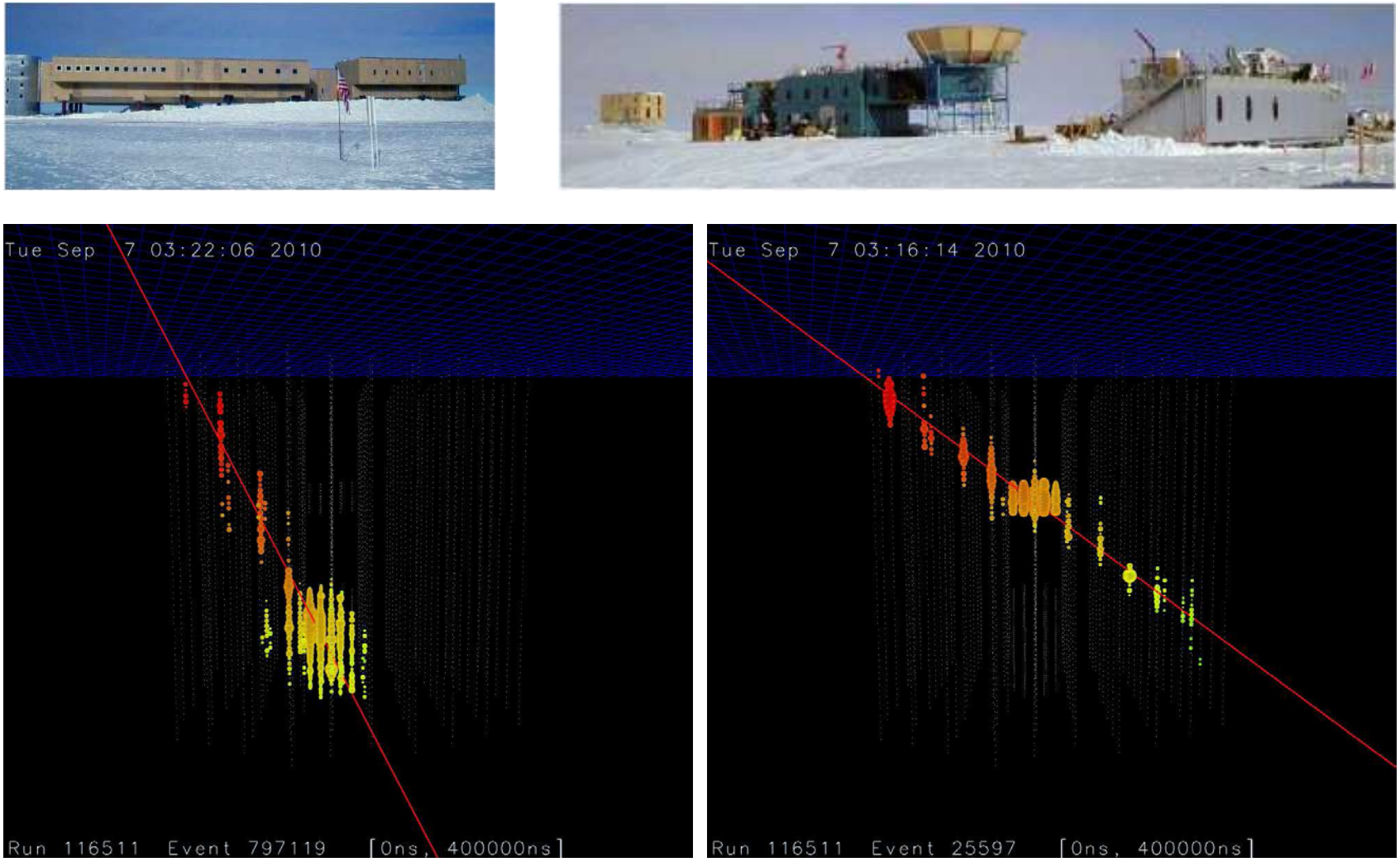

Рис. 31: Two typical neutrino events captured by the IceCube Neutrino Observatory. [From <http://icecube.wisc.edu/>].

- **Arrays and methods for detecting UHE neutrinos**

  - ⋆ **Radio detection**
    [ANITA, AURA-ARA, CODALE-MA, ELVIS, FORTE, GLINT, GLUE, GMRT, Ooty RT, HAS-RA, IceRay, LOFAR, LOPES, LORD, LUNASKA, RESUN, RICE, SalSA, SKA, TREND, WSRT NuMoon,...]

  - ⋆ **Sonic/acoustic detection**
    [ACoRNE, AMADEUS, AUTEC, SAUND, SPATS+HADES,...]

  - ⋆ **Fluorescence detection**
    [JEM-EUSO, S-EUSO, EUNO, OWL, KOSMOTEPETL Project (KLYPVE, TUS),...]

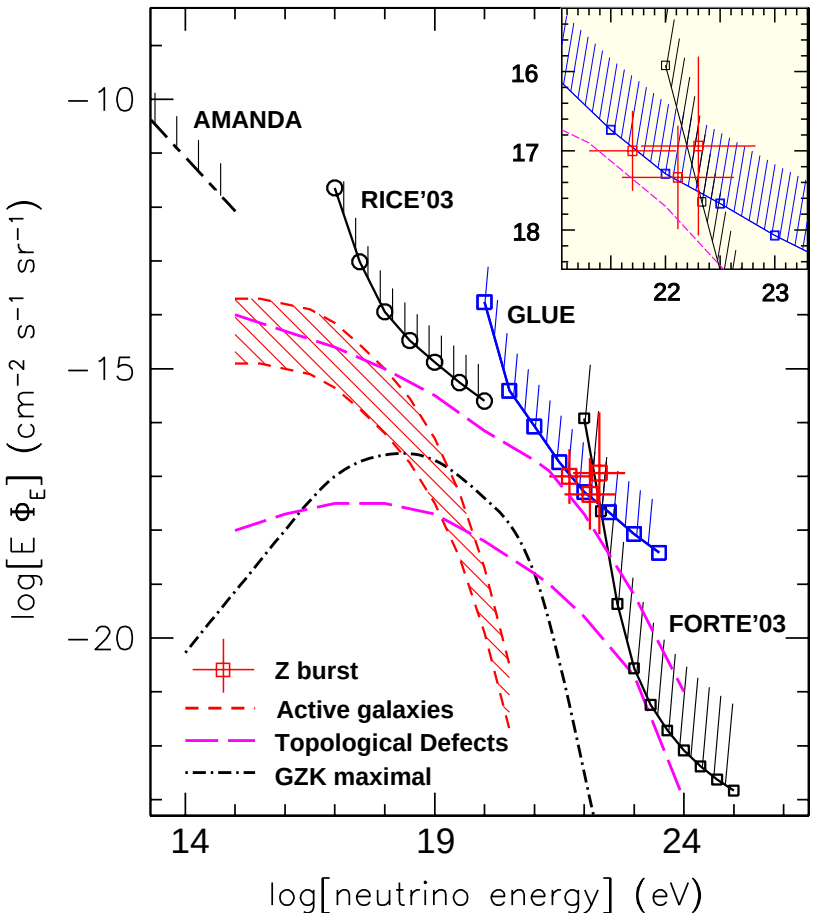

Рис. 32: Model neutrino fluxes & upper limits from experiments AMANDA, RICE, GLUE, and FORTE. [From P. W. Gorham *et al.*, Phys. Rev. Lett. **93** (2004) 041101 [astro-ph/0310232v3].]

Часть II

Neutrino Masses in the Standard Model

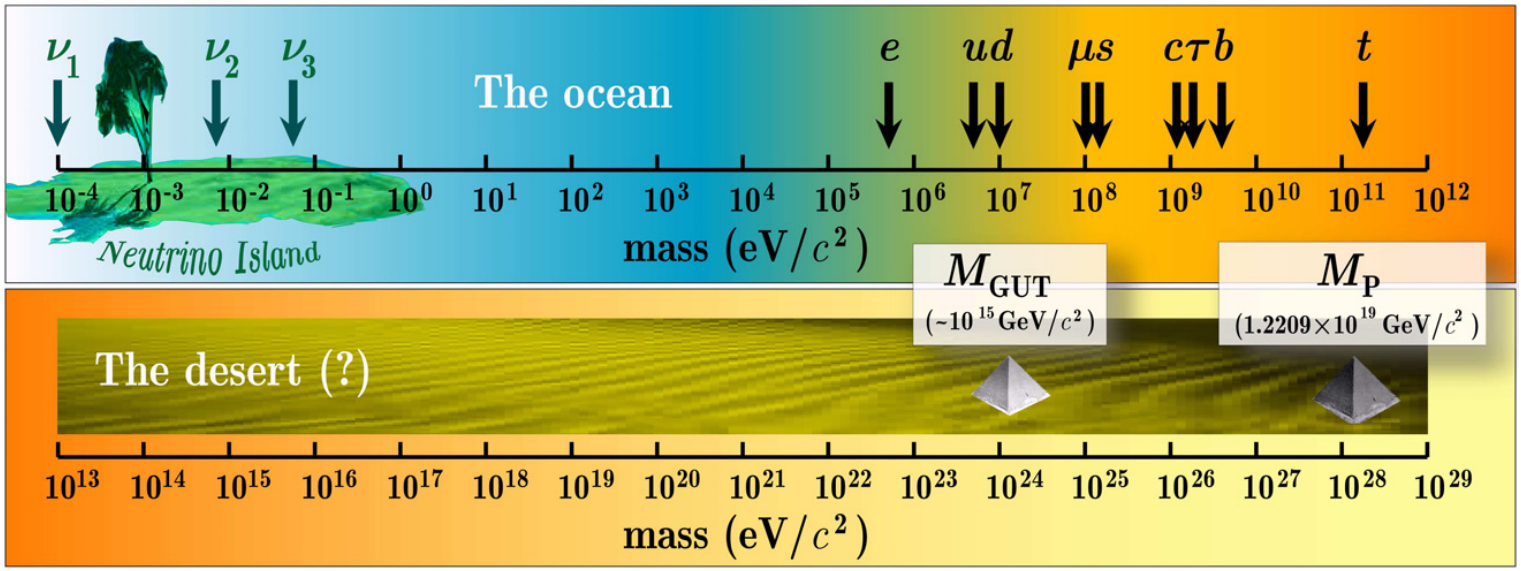

1 Interaction Lagrangian and weak currents

In the Standard Model (SM), the charged and neutral current neutrino interactions are described by the following parts of the full Lagrangian:

$$\mathcal{L}_I^{\mathsf{CC}}(x) = -\frac{g}{2\sqrt{2}} j_\alpha^{\mathsf{CC}}(x) W^\alpha(x) + \mathsf{H.c.} \quad \text{and} \quad \mathcal{L}_I^{\mathsf{NC}}(x) = -\frac{g}{2\cos\theta_{\mathsf{W}}} j_\alpha^{\mathsf{NC}}(x) Z^\alpha(x).$$

Here g is the $SU(2)$ (electro-weak) gauge coupling constant

$$g^2 = 4\sqrt{2} m_W^2 G_F, \quad g \sin\theta_{\mathsf{W}} = |e|$$

and θ_{W} is the weak mixing (Weinberg) angle ($\sin^2\theta_{\mathsf{W}}(M_Z) = 0.23120$).

The leptonic charged current and neutrino neutral current are given by the expressions:

$$j_\alpha^{\mathsf{CC}}(x) = 2 \sum_{\ell=e,\mu,\tau,\ldots} \overline{\nu}_{\ell,L}(x) \gamma_\alpha \ell_L(x) \quad \text{and} \quad j_\alpha^{\mathsf{NC}}(x) = \sum_{\ell=e,\mu,\tau,\ldots} \overline{\nu}_{\ell,L}(x) \gamma_\alpha \nu_{\ell,L}(x).$$

The currents may include (yet unknown) heavy neutrinos and corresponding charged leptons. The left- and right-handed fermion fields are defined as usually:

$$\nu_{\ell,L/R}(x) = \left(\frac{1 \pm \gamma_5}{2}\right) \nu_\ell(x) \quad \text{and} \quad \ell_{L/R}(x) = \left(\frac{1 \pm \gamma_5}{2}\right) \ell(x).$$

Note that the kinetic term of the Lagrangian includes both L and R handed neutrinos and moreover, it can include other sterile neutrinos:

$$\begin{aligned}\mathcal{L}_0 =& \frac{i}{2}\left[\overline{\nu}(x)\gamma^\alpha\partial_\alpha\nu(x) - \partial_\alpha\overline{\nu}(x)\gamma^\alpha\nu(x)\right] \equiv \frac{i}{2}\overline{\nu}(x)\overleftrightarrow{\boldsymbol{\partial}}\nu(x)\\ =& \frac{i}{2}\left[\overline{\nu}_L(x)\overleftrightarrow{\boldsymbol{\partial}}\nu_L(x) + \overline{\nu}_R(x)\overleftrightarrow{\boldsymbol{\partial}}\nu_R(x)\right],\end{aligned}$$

$$\boldsymbol{\nu}(x) = \boldsymbol{\nu}_L(x) + \boldsymbol{\nu}_R(x) = \begin{pmatrix}\nu_e(x)\\ \nu_\mu(x)\\ \nu_\tau(x)\\ .\\ .\\ .\end{pmatrix}, \quad \boldsymbol{\nu}_{L/R}(x) = \begin{pmatrix}\nu_{e,L/R}(x)\\ \nu_{\mu,L/R}(x)\\ \nu_{\tau,L/R}(x)\\ .\\ .\\ .\end{pmatrix} = \frac{1\pm\gamma_5}{2}\begin{pmatrix}\nu_e(x)\\ \nu_\mu(x)\\ \nu_\tau(x)\\ .\\ .\\ .\end{pmatrix}.$$

Neutrino chirality: $\gamma_5\nu_L = -\nu_L$ and $\gamma_5\nu_R = +\nu_R$.

The Lagrangian of the theory with massless neutrinos is invariant with respect to the global gauge transformations

$$\nu_\ell(x) \to e^{i\Lambda_\ell}\nu_\ell(x), \quad \ell(x) \to e^{i\Lambda_\ell}\ell(x) \quad \text{with} \quad \Lambda_\ell = \text{const}.$$

This leads to conservation of the individual lepton flavor numbers L_ℓ (electron, muon, tauon, etc.). It is not the case for massive neutrinos.

There are two types of possible neutrino mass terms: Dirac and Majorana.

2 Dirac neutrinos

The Dirac mass term has the form

$$\mathcal{L}_{\mathsf{D}}(x) = -\overline{\boldsymbol{\nu}}_R(x)\mathbf{M}_{\mathsf{D}}\boldsymbol{\nu}_L(x) + \mathsf{H.c.},$$

where $\mathbf{M}_{\mathsf{D}}$ is a $N \times N$ complex *nondiagonal* matrix. In general, $N \geq 3$ that is the column $\boldsymbol{\nu}_L$ may include the heavy *active* neutrino fields as well as *sterile* neutrino fields which do not enter into the standard charged and neutral currents.

An arbitrary complex matrix can be diagonalized by means of an appropriate *bi-unitary* transformation. One has

$$\mathbf{M}_{\mathsf{D}} = \widetilde{\mathbf{V}}\mathbf{m}\mathbf{V}^{\dagger}, \quad \mathbf{m} = ||m_{kl}|| = ||m_k\delta_{kl}||,$$

where $\mathbf{V}$ and $\widetilde{\mathbf{V}}$ are unitary matrices and $m_k \geq 0$. Therefore

$$\mathcal{L}_{\mathsf{D}}(x) = -\overline{\boldsymbol{\nu}'}_R(x)\mathbf{m}\boldsymbol{\nu}'_L(x) + \mathsf{H.c.} = -\overline{\boldsymbol{\nu}'}(x)\mathbf{m}\boldsymbol{\nu}'(x) = -\sum_{k=1}^{N} m_k\overline{\nu}_k(x)\nu_k(x),$$

where the new fields ν_k are defined by

$$\boldsymbol{\nu}'_L(x) = \mathbf{V}^{\dagger}\boldsymbol{\nu}_L(x), \quad \boldsymbol{\nu}'_R(x) = \widetilde{\mathbf{V}}^{\dagger}\boldsymbol{\nu}_R(x), \quad \boldsymbol{\nu}'(x) = (\nu_1, \nu_2, \ldots, \nu_N)^T.$$

The matrix $\widetilde{\mathbf{V}}$ is out of play...

It is easy to check that the neutrino kinetic term in the Lagrangian is transformed to

$$\mathcal{L}_0 = \frac{i}{2}\,\overline{\boldsymbol{\nu}'}(x)\overleftrightarrow{\boldsymbol{\partial}}\boldsymbol{\nu}'(x) = \frac{i}{2}\sum_k \overline{\nu}_k(x)\overleftrightarrow{\boldsymbol{\partial}}\nu_k(x).$$

Hence, one can conclude that $\nu_k(x)$ is the field of a Dirac neutrino with the mass m_k and the flavor LH neutrino fields $\nu_{\ell,L}(x)$ present in the standard weak lepton currents are linear combinations of the LH components of the fields of neutrinos with definite masses:

$$\boldsymbol{\nu}_L = \mathbf{V}\boldsymbol{\nu}'_L \quad \text{or} \quad \nu_{\ell,L} = \sum_k V_{\ell k}\nu_{k,L}.$$

The matrix $\mathbf{V}$ is sometimes referred to as the Pontecorvo-Maki-Nakagawa-Sakata (PMNS) neutrino (vacuum) mixing matrix.

Quark-lepton complementarity (QLC): Of course the PMNS matrix it is not the same as the CKM (Cabibbo-KobayashiMaskawa) quark mixing matrix. However the PMNS and CKM matrices may be, in a sense, *complementary* to each other.

The QLC means that in the same parametrizations the (small) quark and (large) lepton mixing angles satisfy the *empirical* relations:

$$\theta_{12}^{\mathsf{CKM}} + \theta_{12}^{\mathsf{PMNS}} \simeq \pi/4, \quad \theta_{23}^{\mathsf{CKM}} + \theta_{23}^{\mathsf{PMNS}} \simeq \pi/4.$$

2.1 Parametrization of mixing matrix for Dirac neutrinos

It is well known that a complex $n \times n$ unitary matrix depends on n^2 *real* parameters.

The classical result by Murnagham[a] states that the matrices from the unitary group $U(n)$ are products of a diagonal phase matrix

$$\boldsymbol{\Gamma} = \text{diag}\left(e^{i\alpha_1}, e^{i\alpha_2}, \ldots, e^{i\alpha_n}\right),$$

containing n phases α_k, and $n(n-1)/2$ matrices whose main building blocks have the form

$$\begin{pmatrix} \cos\theta & \sin\theta\, e^{-i\phi} \\ -\sin\theta\, e^{+i\phi} & \cos\theta \end{pmatrix} = \begin{pmatrix} 1 & 0 \\ 0 & e^{+i\phi} \end{pmatrix} \underbrace{\begin{pmatrix} \cos\theta & \sin\theta \\ -\sin\theta & \cos\theta \end{pmatrix}}_{\text{Euler rotation}} \begin{pmatrix} 1 & 0 \\ 0 & e^{-i\phi} \end{pmatrix}.$$

Therefore any $n \times n$ unitary matrix can be parametrized in terms of

$$n(n-1)/2 \text{ “angles” (taking values within } [0, \pi/2])$$

and

$$n(n+1)/2 \text{ “phases” (taking values within } [0, 2\pi)).$$

The usual parametrization of both the CKM and PMNS matrices is of this type.

[a] F. D. Murnagham, “The unitary and rotation groups,” Washington, DC: Sparta Books (1962).

One can reduce the number of the phases further by taking into account that the Lagrangian with the Dirac mass term is invariant with respect to the transformation

$$\ell \mapsto e^{ia_\ell}\ell, \quad \nu_k \mapsto e^{ib_\ell}\nu_k, \quad V_{\ell k} \mapsto e^{i(b_k - a_\ell)}V_{\ell k},$$

and to the global gauge transformation

$$\ell \mapsto e^{i\Lambda}\ell, \quad \nu_k \mapsto e^{i\Lambda}\nu_k, \quad \text{with} \quad \Lambda = \text{const}. \tag{1}$$

Therefore $2N-1$ phases are unphysical and the number of physical (*Dirac*) phases is

$$n_{\mathsf{D}} = \frac{N(N+1)}{2} - (2N-1) = \frac{N^2-3N+2}{2} = \frac{(N-1)(N-2)}{2} \qquad (N \geq 2);$$

$$n_{\mathsf{D}}(2) = 0, \quad n_{\mathsf{D}}(3) = 1, \quad n_{\mathsf{D}}(4) = 3, \ldots$$

- The global symmetry (1) leads to conservation of the lepton charge

$$L = \sum_{\ell = e,\mu,\tau,\ldots} L_\ell$$

common to all charged leptons and all neutrinos ν_k. However

The individual lepton flavor numbers L_ℓ are no longer conserved.

- The nonzero phases lead to the CP and T violation in the neutrino sector.

Three-neutrino case

In the most interesting (today!) case of three lepton generations one defines the orthogonal rotation matrices in the ij-planes which depend upon the mixing angles θ_{ij}:

$$\mathbf{O}_{12} = \underbrace{\begin{pmatrix} c_{12} & s_{12} & 0 \\ -s_{12} & c_{12} & 0 \\ 0 & 0 & 1 \end{pmatrix}}_{\text{Solar matrix}}, \quad \mathbf{O}_{13} = \underbrace{\begin{pmatrix} c_{13} & 0 & s_{13} \\ 0 & 1 & 0 \\ -s_{13} & 0 & c_{13} \end{pmatrix}}_{\text{Reactor matrix}}, \quad \mathbf{O}_{23} = \underbrace{\begin{pmatrix} 1 & 0 & 0 \\ 0 & c_{23} & s_{23} \\ 0 & -s_{23} & c_{23} \end{pmatrix}}_{\text{Atmospheric matrix}},$$

(where $c_{ij} \equiv \cos\theta_{ij}$, $s_{ij} \equiv \sin\theta_{ij}$) and the diagonal matrix with the Dirac phase factor:

$$\boldsymbol{\Gamma}_{\mathsf{D}} = \mathsf{diag}\left(1, 1, e^{i\delta}\right).$$

The parameter δ is commonly referred to as the Dirac CP-violation phase.

Finally, by taking into account the Murnagham theorem, the PMNS mixing matrix for the Dirac neutrinos can be parametrized as[a]

$$\begin{aligned} \mathbf{V}_{(\mathsf{D})} &= \mathbf{O}_{23}\boldsymbol{\Gamma}_{\mathsf{D}}\mathbf{O}_{13}\boldsymbol{\Gamma}_{\mathsf{D}}^{\dagger}\mathbf{O}_{12} \\ &= \begin{pmatrix} c_{12}c_{13} & s_{12}c_{13} & s_{13}e^{-i\delta} \\ -s_{12}c_{23} - c_{12}s_{23}s_{13}e^{i\delta} & c_{12}c_{23} - s_{12}s_{23}s_{13}e^{i\delta} & s_{23}c_{13} \\ s_{12}s_{23} - c_{12}c_{23}s_{13}e^{i\delta} & -c_{12}s_{23} - s_{12}c_{23}s_{13}e^{i\delta} & c_{23}c_{13} \end{pmatrix}. \end{aligned}$$

[a] This is the *Chau–Keung presentation* advocated by the PDG for both CKM and PMNS matrices.

3 Majorana neutrinos

The charge conjugated bispinor field ψ^c is defined by the transformation

$$\psi \longmapsto \psi^c = C\overline{\psi}^T, \quad \overline{\psi} \longmapsto \overline{\psi^c} = -\psi^T C,$$

where C is the charge-conjugation matrix which satisfies the conditions

$$C\gamma_\alpha^T C^\dagger = -\gamma_\alpha, \quad C\gamma_5^T C^\dagger = \gamma_5, \quad C^\dagger = C^{-1} = C, \quad C^T = -C,$$

and thus coincides (up to a phase factor) with the inversion of the axes x^0 and x^2:

$$C = \gamma_0\gamma_2 = \begin{pmatrix} 0 & \sigma_2 \\ \sigma_2 & 0 \end{pmatrix}$$

Reminder. The Pauli matrices:

$$\sigma_0 \equiv 1 = \begin{pmatrix} 1 & 0 \\ 0 & 1 \end{pmatrix}, \quad \sigma_1 = \begin{pmatrix} 0 & 1 \\ 1 & 0 \end{pmatrix}, \quad \sigma_2 = \begin{pmatrix} 0 & -i \\ i & 0 \end{pmatrix}, \quad \sigma_3 = \begin{pmatrix} 1 & 0 \\ 0 & -1 \end{pmatrix}.$$

The Dirac matrices:

$$\gamma^0 = \gamma_0 = \begin{pmatrix} \sigma_0 & 0 \\ 0 & -\sigma_0 \end{pmatrix}, \quad \gamma^k = -\gamma_k = \begin{pmatrix} 0 & \sigma_k \\ -\sigma_k & 0 \end{pmatrix}, \quad k = 1,2,3, \quad \gamma^5 = \gamma_5 = -\begin{pmatrix} 0 & \sigma_0 \\ \sigma_0 & 0 \end{pmatrix}.$$

Clearly a charged fermion field $\psi(x)$ is different from the charge conjugated field $\psi^c(x)$.

But for a *neutral* fermion field $\nu(x)$ the equality

$$\boxed{\nu^c(x) = \nu(x)} \tag{2}$$

(*Majorana condition*) is not forbidden.[a] Everything which is not forbidden is allowed...

Majorana neutrino and antineutrino coincide.

In the chiral representation

$$\nu = \begin{pmatrix} \phi \\ \chi \end{pmatrix}, \quad \nu^c = C\overline{\nu}^T = \begin{pmatrix} -\sigma_2\chi^* \\ +\sigma_2\phi^* \end{pmatrix}.$$

According to the Majorana condition (2)

$$\phi = -\sigma_2\chi^* \quad \text{and} \quad \chi = \sigma_2\phi^* \quad \Longrightarrow \quad \phi + \chi = \sigma_2\,(\phi - \chi)^*.$$

(The Majorana neutrino is two-component, i.e. needs only one chiral projection). Then

$$\nu_L = \left(\frac{1+\gamma_5}{2}\right)\nu = \begin{pmatrix} \phi - \chi \\ \chi - \phi \end{pmatrix} \quad \text{and} \quad \nu_R = \left(\frac{1-\gamma_5}{2}\right)\nu = \begin{pmatrix} \phi + \chi \\ \phi + \chi \end{pmatrix} = \nu_L^c.$$

$$\Downarrow$$

$$\boxed{\nu = \nu_L + \nu_R = \nu_L + \nu_L^c.}$$

[a] The simplest generalization of Eq. (2), $\nu^c(x) = e^{i\varphi}\nu(x)$ ($\varphi = \text{const}$), is not very interesting.

Now we can construct the Majorana mass term in the general N-neutrino case. It is

$$\mathcal{L}_{\mathsf{M}}(x) = -\frac{1}{2}\overline{\boldsymbol{\nu}}^{c}_{L}(x)\mathbf{M}_{\mathsf{M}}\boldsymbol{\nu}_{L}(x) + \mathsf{H.c.},$$

where $\mathbf{M}_{\mathsf{M}}$ is a $N \times N$ complex *nondiagonal* matrix and, in general, $N \geq 3$.

It can be proved that the $\mathbf{M}_{\mathsf{M}}$ should be symmetric, $\mathbf{M}^{T}_{\mathsf{M}} = \mathbf{M}_{\mathsf{M}}$.

If one assume for a simplification that its spectrum is nondegenerated, the mass matrix can be diagonalized by means of the following transformation

$$\mathbf{M}_{\mathsf{M}} = \mathbf{V}^{*}\mathbf{m}\mathbf{V}^{\dagger}, \quad \mathbf{m} = ||m_{kl}|| = ||m_{k}\delta_{kl}||,$$

where $\mathbf{V}$ is a unitary matrix and $m_{k} \geq 0$. Therefore

$$\mathcal{L}_{\mathsf{M}}(x) = -\frac{1}{2}\left[(\overline{\boldsymbol{\nu}'}_{L})^{c}\mathbf{m}\boldsymbol{\nu}'_{L} + \overline{\boldsymbol{\nu}'}_{L}\mathbf{m}(\boldsymbol{\nu}'_{L})^{c}\right] = -\frac{1}{2}\,\overline{\boldsymbol{\nu}'}\mathbf{m}\boldsymbol{\nu}' = -\frac{1}{2}\sum_{k=1}^{N} m_{k}\overline{\nu}_{k}\nu_{k},$$

$$\boldsymbol{\nu}'_{L} = \mathbf{V}^{\dagger}\boldsymbol{\nu}_{L}, \quad (\boldsymbol{\nu}'_{L})^{c} = C\left(\overline{\boldsymbol{\nu}'_{L}}\right)^{T}, \quad \boldsymbol{\nu}' = \boldsymbol{\nu}'_{L} + (\boldsymbol{\nu}'_{L})^{c}.$$

The last equality means that the fields $\nu_{k}(x)$ are Majorana neutrino fields.

Considering that the kinetic term in the neutrino Lagrangian is transformed to

$$\mathcal{L}_{0} = \frac{i}{4}\,\overline{\boldsymbol{\nu}'}(x)\overleftrightarrow{\boldsymbol{\partial}}\boldsymbol{\nu}'(x) = \frac{i}{4}\sum_{k}\overline{\nu}_{k}(x)\overleftrightarrow{\boldsymbol{\partial}}\nu_{k}(x),$$

one can conclude that $\nu_{k}(x)$ is the field with the definite mass m_{k}.

The flavor LH neutrino fields $\nu_{\ell,L}(x)$ present in the standard weak lepton currents are linear combinations of the LH components of the fields of neutrinos with definite masses:

$$\boldsymbol{\nu}_L = \mathbf{V}\boldsymbol{\nu}'_L \quad \text{or} \quad \nu_{\ell,L} = \sum_k V_{\ell k}\nu_{k,L}.$$

Of course neutrino mixing matrix $\mathbf{V}$ is not the same as in the case of Dirac neutrinos.

There is no global gauge transformations under which the Majorana mass term (in its most general form) could be invariant. This implies that there are no conserved lepton charges that could allow us to distinguish Majorana νs and $\overline{\nu}$s. In other words,

Majorana neutrinos are truly neutral fermions.

3.1 Parametrization of mixing matrix for Majorana neutrinos

Since the Majorana neutrinos are not rephasable, there may be a lot of extra phase factors in the mixing matrix. The Lagrangian with the Majorana mass term is invariant with respect to the transformation

$$\ell \mapsto e^{ia_\ell}\ell, \quad V_{\ell k} \mapsto e^{-ia_\ell}V_{\ell k}$$

Therefore N phases are unphysical and the number of the physical phases now is

$$\frac{N(N+1)}{2} - N = \frac{N(N-1)}{2} = \underbrace{\frac{(N-1)(N-2)}{2}}_{\text{Dirac phases}} + \underbrace{(N-1)}_{\text{Majorana phases}} = n_{\mathsf{D}} + n_{\mathsf{M}};$$

$$n_{\mathsf{M}}(2) = 1, \quad n_{\mathsf{M}}(3) = 2, \quad n_{\mathsf{M}}(4) = 3, \ldots$$

In the case of three lepton generations one defines the diagonal matrix with the extra phase factors: $\boldsymbol{\Gamma}_{\mathsf{M}} = \mathrm{diag}\left(e^{i\alpha_1/2}, e^{i\alpha_2/2}, 1\right)$, where $\alpha_{1,2}$ are commonly referred to as the Majorana CP-violation phases. Then the PMNS matrix can be parametrized as

$$\mathbf{V}_{(\mathsf{M})} = \mathbf{O}_{23}\boldsymbol{\Gamma}_{\mathsf{D}}\mathbf{O}_{13}\boldsymbol{\Gamma}_{\mathsf{D}}^{\dagger}\mathbf{O}_{12}\boldsymbol{\Gamma}_{\mathsf{M}} = \mathbf{V}_{(\mathsf{D})}\boldsymbol{\Gamma}_{\mathsf{M}}$$

$$= \begin{pmatrix} c_{12}c_{13} & s_{12}c_{13} & s_{13}e^{-i\delta} \\ -s_{12}c_{23} - c_{12}s_{23}s_{13}e^{i\delta} & c_{12}c_{23} - s_{12}s_{23}s_{13}e^{i\delta} & s_{23}c_{13} \\ s_{12}s_{23} - c_{12}c_{23}s_{13}e^{i\delta} & -c_{12}s_{23} - s_{12}c_{23}s_{13}e^{i\delta} & c_{23}c_{13} \end{pmatrix} \begin{pmatrix} e^{i\alpha_1/2} & 0 & 0 \\ 0 & e^{i\alpha_2/2} & 0 \\ 0 & 0 & 1 \end{pmatrix}.$$

Neither L_ℓ nor $L = \sum_\ell L_\ell$ is conserved allowing a lot of new processes, for example, $\tau^- \to e^+(\mu^+)\pi^-\pi^-$, $\tau^- \to e^+(\mu^+)\pi^- K^-$, $\pi^- \to \mu^+\overline{\nu}_e$, $K^+ \to \pi^-\mu^+e^+$, $K^+ \to \pi^0 e^+\overline{\nu}_e$, $D^+ \to K^-\mu^+\mu^+$, $B^+ \to K^-e^+\mu^+$, $\Xi^- \to p\mu^-\mu^-$, $\Lambda_c^+ \to \Sigma^-\mu^+\mu^+$, etc.

No one was discovered yet but (may be!?) the $(\beta\beta)_{0\nu}$ decay (Heidelberg-Moscow experiment).

4 See-saw mechanism

4.1 Dirac-Majorana mass term for one generation

It is possible to consider mixed models in which both Majorana and Dirac mass terms are present. For simplicity sake we'll start with a toy model for one lepton generation.

Let us consider a theory containing two independent neutrino fields ν_L and ν_R:

$$\begin{cases} \nu_L \text{ would generally represent any active neutrino (e.g., } \nu_L = \nu_{eL}), \\ \nu_R \text{ can represents a right handed field unrelated to any of these or} \\ \quad \text{it can be charge conjugate of any of the active neutrinos (e.g., } \nu_R = (\nu_{\mu L})^c). \end{cases}$$

We can write the following generic mass term between ν_L and ν_R:

$$\mathcal{L}_m = - \underbrace{m_D \, \overline{\nu}_L \nu_R}_{\text{Dirac mass term}} - \underbrace{(1/2) \left[m_L \, \overline{\nu}_L \nu_L^c + m_R \, \overline{\nu}_R^c \nu_R \right]}_{\text{Majorana mass term}} + \text{H.c.} \tag{3}$$

- ⋆ As we know, the Dirac mass term respects L while the Majorana mass term violates it.
- ⋆ The parameter m_D in Eq. (3) is in general complex but we'll assume it to be real (but not necessarily positive).
- ⋆ The parameters m_L, and m_R in Eq. (3) can be chosen real and (by an appropriate rephasing the fields ν_L and ν_R) non-negative, but the latter is not assumed.
- ⋆ Obviously, neither ν_L nor ν_R is a mass eigenstate.

In order to obtain the *mass basis* we can apply the useful identity[a]

$$\overline{\nu}_L \nu_R = (\overline{\nu}_R)^c (\nu_L)^c$$

which allows us to rewrite Eq. (3) as follows

$$\mathcal{L}_m = -\frac{1}{2} (\overline{\nu}_L, (\overline{\nu}_R)^c) \begin{pmatrix} m_L & m_D \\ m_D & m_R \end{pmatrix} \begin{pmatrix} (\nu_L)^c \\ \nu_R \end{pmatrix} + \text{H.c.} \equiv -\frac{1}{2} \overline{\boldsymbol{\nu}}_L \mathbf{M} (\boldsymbol{\nu}_L)^c + \text{H.c.}$$

If (for simplicity) CP conservation is assumed the matrix $\mathbf{M}$ can be diagonalized through the standard orthogonal transformation

$$\mathbf{V} = \begin{pmatrix} \cos\theta & \sin\theta \\ -\sin\theta & \cos\theta \end{pmatrix} \quad \text{with} \quad \theta = \frac{1}{2} \arctan\left(\frac{2m_D}{m_R - m_L} \right).$$

and we have

$$\mathbf{V}^T \mathbf{M} \mathbf{V} = \text{diag}(m_1, m_2),$$

where $m_{1,2}$ are eigenvalues of $\mathbf{M}$ given by

$$m_{1,2} = \frac{1}{2} \left(m_L + m_R \pm \sqrt{(m_L - m_R)^2 + 4m_D^2} \right).$$

---

[a] A particular case of a more general relation $\overline{\psi}_1 \Gamma \psi_2 = \overline{\psi}_2^c C \Gamma^T C^{-1} \psi_1^c$, where $\psi_{1,2}$ are Dirac spinors and Γ represents a product of the Dirac γ matrices.

The eigenvalues are real if (as we assume) $m_{D,L,R}$ are real, but not necessarily positive. Let us define $\zeta_k = \mathrm{sign}\, m_k$ and rewrite the mass term in the new basis:

$$\mathcal{L}_m = -\frac{1}{2}\left[\zeta_1 |m_1| \overline{\nu}_{1L} (\nu_{1L})^c + \zeta_2 |m_2| (\overline{\nu}_{2R})^c \nu_{2R}\right] + \text{H.c.}, \tag{4}$$

The new fields ν_{1L} and ν_{2R} represent chiral components of two different neutrino states with "masses" m_1 and m_2, respectively:

$$\begin{pmatrix} \nu_L \\ \nu_R^c \end{pmatrix} = \mathbf{V} \begin{pmatrix} \nu_{1L} \\ \nu_{2R}^c \end{pmatrix} \quad \Longrightarrow \quad \begin{cases} \nu_{1L} = \cos\theta\, \nu_L - \sin\theta\, \nu_R^c, \\ \nu_{2R} = \sin\theta\, \nu_L^c + \cos\theta\, \nu_R. \end{cases}$$

Now we define two 4-component fields

$$\nu_1 = \nu_{1L} + \zeta_1 (\nu_{1L})^c \quad \text{and} \quad \nu_2 = \nu_{2R} + \zeta_2 (\nu_{2R})^c.$$

Certainly, these fields are self-conjugate with respect to the C transformation:

$$\nu_k^c = \zeta_k \nu_k \quad (k = 1, 2)$$

and therefore they describe Majorana neutrinos. In terms of these fields Eq. (5) reads

$$\mathcal{L}_m = -\frac{1}{2}\left(|m_1| \overline{\nu}_1 \nu_1 + |m_2| \overline{\nu}_2 \nu_2\right). \tag{5}$$

We can conclude therefore that $\nu_k(x)$ is the Majorana neutrino field with the definite (physical) mass $|m_k|$.

There are several special cases of the Dirac-Majorana mass matrix $\mathbf{M}$ which are of considerable phenomenological importance, in particular,

(A): $\mathbf{M} = \begin{pmatrix} 0 & m \\ m & 0 \end{pmatrix} \quad \Longrightarrow \quad |m_{1,2}| = m, \quad \theta = \frac{\pi}{4}$ (maximal mixing)

two Majorana fields are equivalent to one Dirac field;

(B): $\mathbf{M} = \begin{pmatrix} m_L & m \\ m & m_L \end{pmatrix} \quad \Longrightarrow \quad m_{1,2} = m_L \pm m_D, \quad \theta = \frac{\pi}{4}$ (maximal mixing);

(C): $\mathbf{M} = \begin{pmatrix} 0 & m \\ m & M \end{pmatrix}$ or, more generally, $|m_L| \ll |m_R|, \quad m_D > 0.$

A generalization of case (A), $|m_{L,R}| \ll |m_D|$, leads to the so-called "Pseudo-Dirac neutrinos" and to the ν_L (active) $\leftrightarrow$ ν_R (sterile) oscillations with almost maximal mixing ($\tan 2\theta \gg 1$).

4.2 The see-saw

The case (C) with $m \ll M$ is the simplest example of the see-saw mechanism. It leads to two masses, one very large, $m_1 \approx M$, other very small, $m_2 \approx m^2/M \ll m$, suppressed compared to the entries in $\mathbf{M}$. In particular, one can assume

$$m \sim m_\ell \text{ or } m_q \quad (0.5 \text{ MeV to } 200 \text{ GeV}) \quad \text{and} \quad M \sim M_{\mathsf{GUT}} \sim 10^{15-16} \text{ GeV}.$$

Then m_2 can ranges from $\sim 10^{-14}$ eV to ~ 0.04 eV. The mixing between the heavy and light neutrinos is extremely small: $\theta \approx m/M \sim 10^{-20} - 10^{-13} \lll 1$.

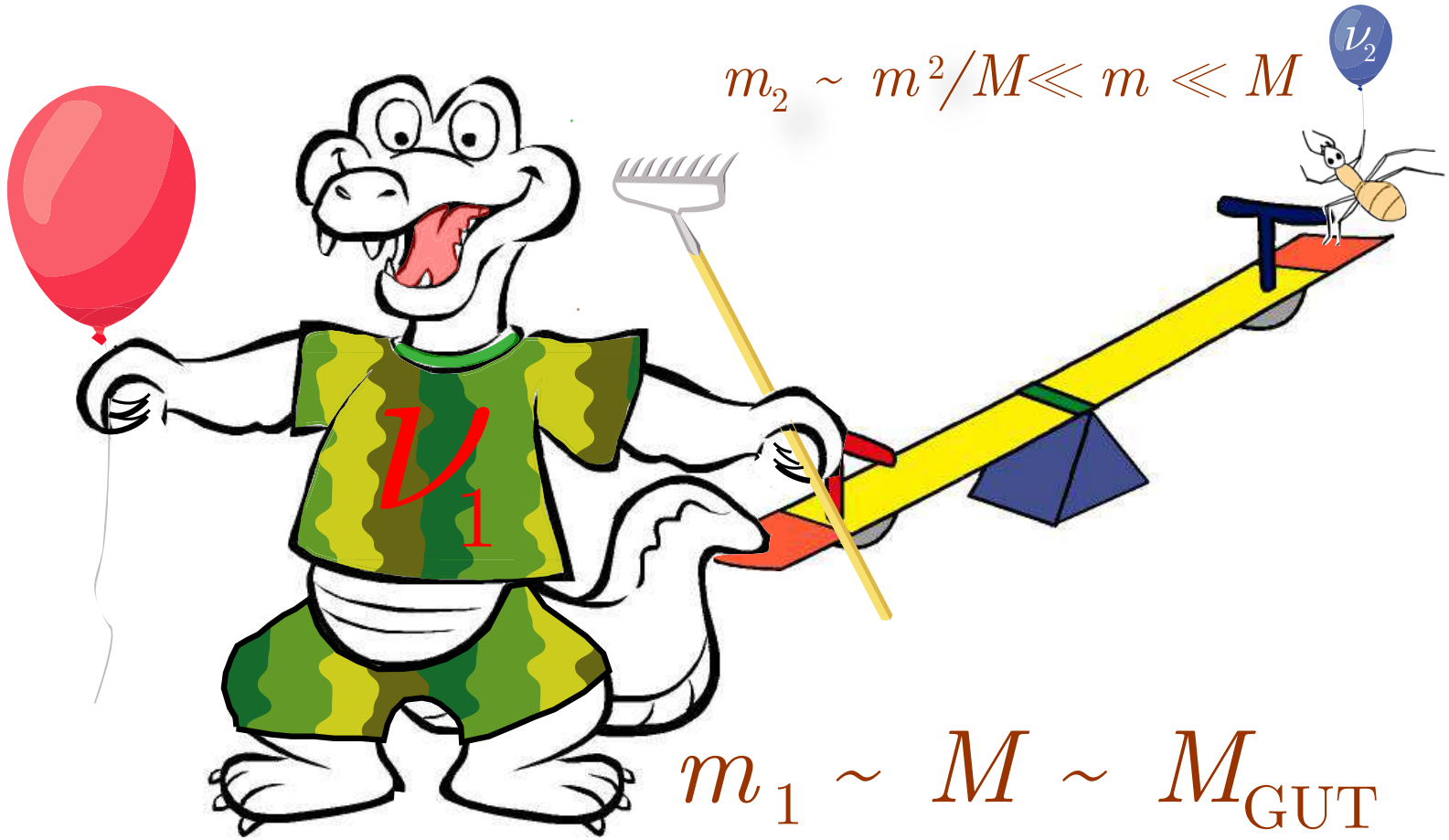

If one of the eigenvalues m_i *goes up*, the other *goes down*, and vice versa. This is the reason why the name see-saw was given to the mechanism. [Too witty for so simple idea...]

4.3 More neutral fermions

A generalization of the above scheme to N generations is almost straightforward but technically rather cumbersome. Let's consider it schematically for the $N = 3$ case.

- If neutral fermions are added to the set of the SM fields, then the flavour neutrinos can acquire mass by mixing with them.
- The additional fermions can be[a]
  - Gauge chiral singlets per family (e.g., right-handed neutrinos) [Type I seesaw], or
  - $SU(2) \times U(1)$ doublets (e.g., Higgsino in SUSY), or
  - $Y = 0$, $SU(2)_L$ triplets (e.g., Wino in SUSY) [Type III seesaw].
- Addition of three right-handed neutrinos $\mathcal{N}_{iR}$ leads to the see-saw mechanism with the following mass terms:

$$\mathcal{L}_m = -\sum_{ij} \left[\overline{\nu}_{iL} M^D_{ij} \mathcal{N}_{jR} - \frac{1}{2} \left(\mathcal{N}_{iR}\right)^c M^R_{ij} \mathcal{N}_{jR} + \text{H.c.} \right] .$$

- The above equation gives the see-saw 6×6 mass matrix

$$\mathbf{M} = \begin{pmatrix} \mathbf{0} & \mathbf{m}_D \\ \mathbf{m}_D^T & \mathbf{M}_R \end{pmatrix}.$$

  Both $\mathbf{m}_D$ and $\mathbf{m}_R$ are 3×3 matrices in the generation space.

[a] Type II seesaw operates with an additional scalar triplet.

When $\mathbf{M}_R$ is nonsingular and its scale M is much larger than that in $\mathbf{m}_R$,[a] one gets

$$\mathbf{m}_\nu \sim -\mathbf{m}_D \mathbf{M}_R^{-1} \mathbf{m}_D^T.$$

All the neutrino masses are automatically suppressed due to the large scale $M \sim M_{\mathsf{GUT}}$ in $\mathbf{M}_R$. One gets the following mass hierarchy for a diagonal $\mathbf{M}_R$:

$$m_1 : m_2 : m_3 \propto m_{D1}^2 : m_{D2}^2 : m_{D3}^2.$$

Here m_{Dk} are eigenvalues of $\mathbf{m}_D$. As long as these eigenvalues are hierarchical, the Majorana neutrino masses also display the hierarchy. The mass eigenfields are surely Majorana neutrinos.

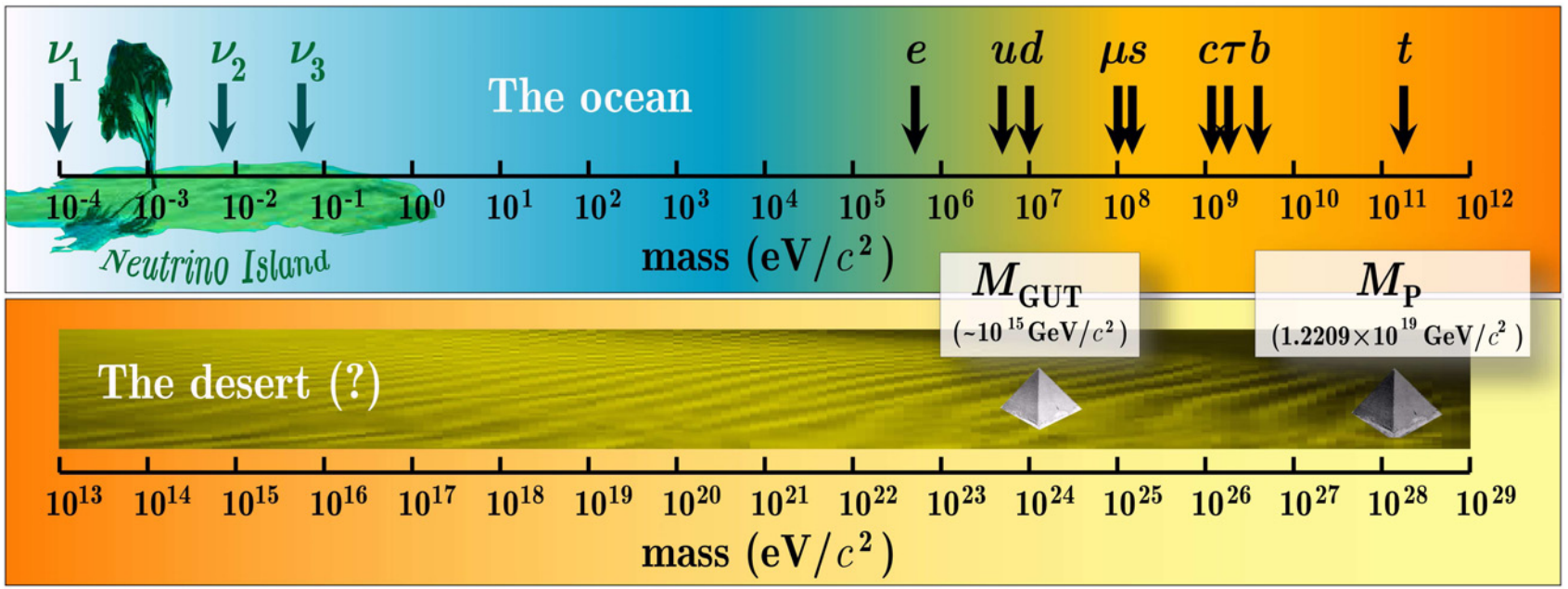

[a] A large M is natural in, e.g., grand unified $SO(10)$ theories.

Часть III

Neutrino Oscillations in Vacuum

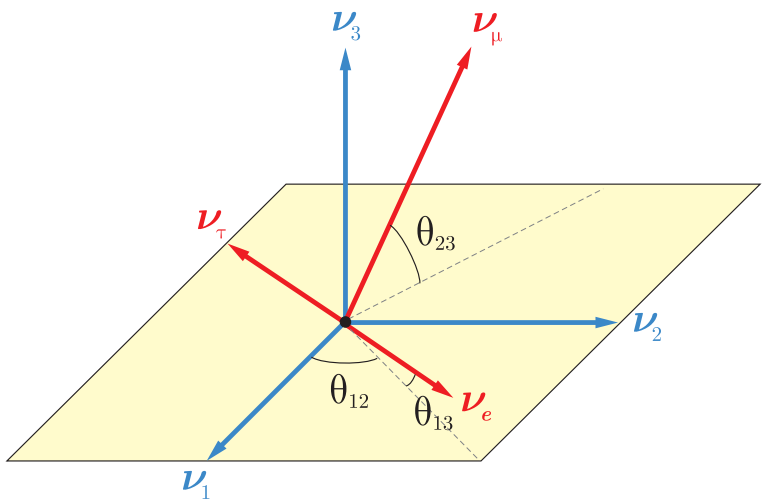

5 Quantum mechanical treatment

Let us introduce two types of neutrino eigenstates:

- The flavor neutrino eigenstates which can be written as a vector

$$|\boldsymbol{\nu}\rangle_f = (|\nu_e\rangle, |\nu_\mu\rangle, |\nu_\tau\rangle, \ldots)^T \equiv (|\nu_\alpha\rangle)^T$$

are defined as the states which correspond to the charge leptons $\alpha = e, \mu, \tau$. The correspondence is established through the charged current interactions of active neutrinos and charged leptons.[a] In general, the flavor states have no definite masses. Therefore, they can have either definite momentum, or definite energy but not both.

- The neutrino mass eigenstates

$$|\boldsymbol{\nu}\rangle_m = (|\nu_1\rangle, |\nu_2\rangle, |\nu_3\rangle, \ldots)^T \equiv (|\nu_k\rangle)^T$$

are, by definition, the states with the definite masses m_k, $k = 1, 2, 3, \ldots$.

Since $|\nu_\alpha\rangle$ and $|\nu_k\rangle$ are not identical, they are related to each other through a unitary transformation

$$|\nu_\alpha\rangle = \sum_k \hat{V}_{\alpha k} |\nu_k\rangle \quad \text{or} \quad |\boldsymbol{\nu}\rangle_f = \hat{\mathbf{V}} |\boldsymbol{\nu}\rangle_m,$$

where $\hat{\mathbf{V}} = \| \hat{V}_{\alpha k} \|$ is a unitary (in general, $N \times N$) matrix.

[a] Together with the standard νs, $|\boldsymbol{\nu}\rangle_f$ may include also neutrino states allied with additional heavy charged leptons, as well as the states not associated with charge leptons, like sterile neutrinos, ν_s.

To find out the correspondence between $\hat{\mathbf{V}}$ and the PMNS mixing matrix $\mathbf{V}$ we can normalize the "f" and "m" states by the following conditions

$$\langle 0|\nu_{\alpha L}(x)|\nu_{\alpha'}\rangle = \delta_{\alpha\alpha'} \quad \text{and} \quad \langle 0|\nu_{kL}(x)|\nu_{k'}\rangle = \delta_{kk'}.$$

From these conditions we obtain

$$\sum_k V_{\alpha k}\hat{V}_{\alpha' k} = \delta_{\alpha\alpha'} \quad \text{and} \quad \sum_\alpha V_{\alpha k}\hat{V}_{\alpha k'} = \delta_{kk'}.$$

Therefore

$$\hat{\mathbf{V}} \equiv \mathbf{V}^\dagger$$

and

$$\boxed{|\boldsymbol{\nu}\rangle_f = \mathbf{V}^\dagger|\boldsymbol{\nu}\rangle_m \iff |\boldsymbol{\nu}\rangle_m = \mathbf{V}|\boldsymbol{\nu}\rangle_f.} \tag{6}$$

The time evolution of a single mass eigenstate $|\nu_k\rangle$ with momentum p_ν is trivial,

$$i\frac{d}{dt}|\nu_k(t)\rangle = E_k|\nu_k(t)\rangle \implies |\nu_k(t)\rangle = e^{-iE_k(t-t_0)}|\nu_k(t_0)\rangle,$$

where $E_k = \sqrt{p_\nu^2 + m_k^2}$ is the total energy in the state $|\nu_k\rangle$. Now, assuming that all N states $|\nu_k\rangle$ have the same momentum, one can write

$$i\frac{d}{dt}|\boldsymbol{\nu}(t)\rangle_m = \mathbf{H}_0|\boldsymbol{\nu}(t)\rangle_m, \quad \text{where} \quad \mathbf{H}_0 = \text{diag}\,(E_1, E_2, E_3, \ldots). \tag{7}$$

From Eqs. (6) and (7) we have

$$i\frac{d}{dt}|\boldsymbol{\nu}(t)\rangle_f = \mathbf{V}^\dagger \mathbf{H}_0 \mathbf{V} |\boldsymbol{\nu}(t)\rangle_f. \tag{8}$$

Solution to this equation is obvious:

$$\begin{aligned} |\boldsymbol{\nu}(t)\rangle_f &= \mathbf{V}^\dagger e^{-i\mathbf{H}_0(t-t_0)}\mathbf{V}\,|\boldsymbol{\nu}(t_0)\rangle_f \\ &= \mathbf{V}^\dagger \,\mathrm{diag}\left(e^{-iE_1(t-t_0)}, e^{-iE_2(t-t_0)}, \ldots\right)\,\mathbf{V}\,|\boldsymbol{\nu}(t_0)\rangle_f. \end{aligned} \tag{9}$$

Now we can derive the survival and transition probabilities

$$\begin{aligned} P_{\alpha\beta}(t-t_0) &= P\left[\nu_\alpha(t_0) \to \nu_\beta(t)\right] = \left|\langle \nu_\beta(t)|\nu_\alpha(t_0)\rangle\right|^2 \\ &= \left|\sum_k V_{\alpha k} V^*_{\beta k}\, \exp\left[iE_k(t-t_0)\right]\right|^2 \\ &= \sum_{jk} V_{\alpha j} V_{\beta k}\left(V_{\alpha k} V_{\beta j}\right)^*\, \exp\left[i(E_j - E_k)(t-t_0)\right]. \end{aligned}$$

In the ultrarelativistic limit $p_\nu^2 \gg m_k^2$, which is undoubtedly valid for all interesting circumstances (except relic neutrinos),

$$E_k = \sqrt{p_\nu^2 + m_k^2} \approx p_\nu + \frac{m_k^2}{2p_\nu} \approx E_\nu + \frac{m_k^2}{2E_\nu}.$$

Therefore in VERY good approximation

$$P_{\alpha\beta}(t-t_0) \approx \sum_{jk} V_{\alpha j} V_{\beta k} \left(V_{\alpha k} V_{\beta j}\right)^* \exp\left[\frac{i\Delta m^2_{jk}(t-t_0)}{2E_\nu}\right].$$

Before MINOS and OPERA there was now way to measure t_0 and t in the same experiment. But it is usually possible to measure the distance L between the source and detector. So we have to connect $t - t_0$ with L. The standard and almost "evident" approximation is

$$v_k = p_\nu / E_k \approx c = 1,$$

from which it follows that $t - t_0 \approx L$ and finally we arrive at the following formula

$$\boxed{P_{\alpha\beta}(L) = \sum_{jk} V_{\alpha j} V_{\beta k} \left(V_{\alpha k} V_{\beta j}\right)^* \exp\left(\frac{2i\pi L}{L_{jk}}\right),} \tag{10}$$

where

$$\boxed{L_{jk} = \frac{4\pi E_\nu}{\Delta m^2_{jk}}} \tag{11}$$

are the neutrino oscillation lengths. Just this result is the basis for the "oscillation interpretation" of the current neutrino experiments.

5.1 Simplest example: two-flavor oscillations

Let us now consider the simplest 2-flavor case with $i = 2, 3$ and $\alpha = \mu, \tau$ (the most favorable due to the SK and other underground experiments). The 2×2 vacuum mixing matrix can be parametrized (due to the unitarity) with a single parameter, $\theta = \theta_{23}$, the vacuum mixing angle,

$$\mathbf{V} = \begin{pmatrix} \cos\theta & \sin\theta \\ -\sin\theta & \cos\theta \end{pmatrix}, \qquad 0 \leq \theta \leq \pi/2.$$

Equation (10) then becomes very simple:

$$P_{\alpha\alpha'}(L) = \frac{1}{2}\sin^2 2\theta \left[1 - \cos\left(\frac{2\pi L}{L_\nu}\right)\right],$$

$$L_\nu \equiv L_{23} = \frac{4\pi E_\nu}{\Delta m^2_{23}} \approx 2R_\oplus \left(\frac{E_\nu}{10\ \text{GeV}}\right)\left(\frac{0.002\ \text{eV}^2}{\Delta m^2_{23}}\right).$$

Here $R_\oplus$ is the mean radius of Earth and 10 GeV is a typical energy in the (very wide) atmospheric neutrino spectrum.

Since Earth provides variable "baseline" [from about 15 km to about 12700 km], it is surprisingly suitable for studying the atmospheric (as well as accelerator and reactor) neutrino oscillations in rather wide range of the parameter Δm^2_{23} at not too small mixing angle θ.

5.2 The oscillation parameter plot (current status)

The regions of neutrino squared-mass splitting ($\Delta m^2 = |\Delta m^2_{ij}| = |m^2_j - m^2_i|$) and mixing angle favored or excluded by various experiments. Contributed to RPP-2010 [J. Phys. G **37** (2010) 075021, Fig. 13.10] by Hitoshi Murayama (University of California, Berkeley).

[From URL http://hitoshi.berkeley.edu/neutrino/]

Figure shows the most rigorous current results; it does not include the new data of BOREXINO and neutrino telescopes Baikal and AMANDA. Also the data from many earlier underground experiments (BUST, NUSEX, Fréjus, IMB, Kamiokande, MACRO, SOUDAN 2), are ignored. However, all these very weakly affect the global analysis.

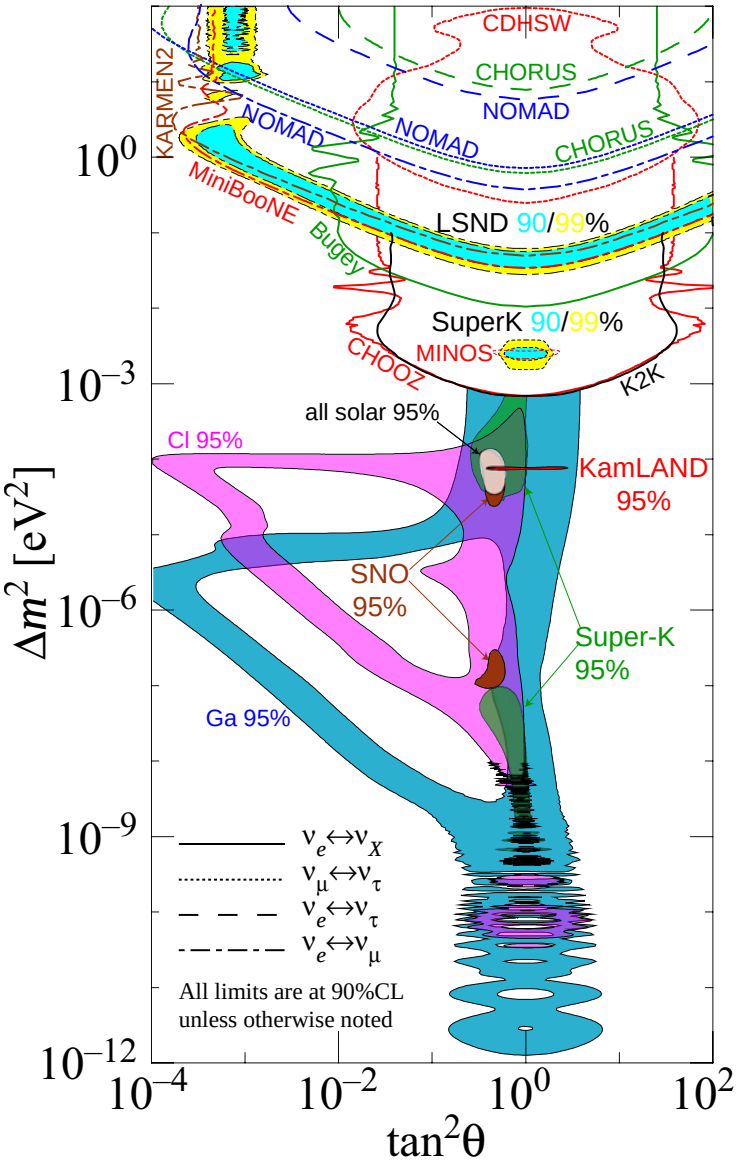

The current analyses actually neglect possible CP violation. In this approximation

$$\mathbf{V} = \begin{pmatrix} c_{12}c_{31} & s_{12}c_{31} & s_{13} \\ -s_{12}c_{23} - c_{12}s_{23}s_{31} & c_{12}c_{23} - s_{12}s_{23}s_{31} & s_{23}c_{31} \\ s_{12}s_{23} - c_{12}c_{23}s_{31} & -c_{12}s_{23} - s_{12}c_{23}s_{31} & c_{23}c_{31} \end{pmatrix}.$$

Таблица 2: **Tentative** summary of squared-mass splitting ($\Delta m^2_{ij} = m^2_j - m^2_i$) & mixing angles. [The central values are from the current update for the PDG 2012 edition, <http://pdg.lbl.gov> and from the recent Double CHOOZ (DC) eprint arXiv:1112.6353v2 [hep-ex]. The 99% C.L. ranges are a bit obsolete.]

Oscillation parameter		Central value	99% C.L. range
solar mass splitting	Δm^2_{12}	$(7.59 \pm 0.21) \times 10^{-5}\,\text{eV}^2$	$(7.1 \div 8.3) \times 10^{-5}\,\text{eV}^2$
atmospheric mass splitting	$\lvert\Delta m^2_{23}\rvert$	$(2.43 \pm 0.13) \times 10^{-3}\,\text{eV}^2$	$(2.1 \div 2.8) \times 10^{-3}\,\text{eV}^2$
solar mixing angle	$\sin^2 2\theta_{12}$	$0.861^{+0.026}_{-0.022}$	$30^\circ < \theta_{12} < 38^\circ$
atmospheric mixing angle	$\sin^2 2\theta_{23}$	> 0.92	$36^\circ < \theta_{23} < 54^\circ$
DC mixing angle	$\sin^2 2\theta_{31}$	0.086 ± 0.051	$3.75^\circ < \theta_{31} < 11.8^\circ$

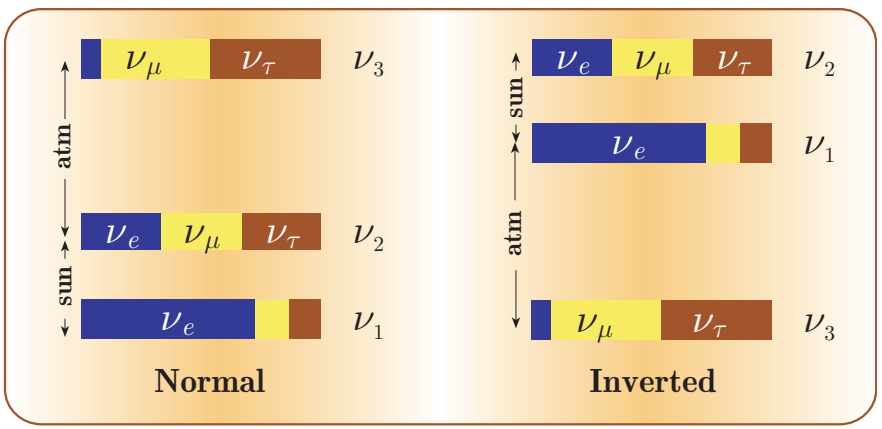

5.3 Summary of the standard QM theory.

The standard assumptions are intuitively transparent and (almost) commonly accepted.

[1] The neutrino flavor states $|\nu_\alpha\rangle$ associated with the charged leptons $\alpha = e, \mu, \tau$ (that is having definite lepton numbers) are not identical to the neutrino mass eigenstates $|\nu_i\rangle$ with the definite masses m_i $(i = 1, 2, 3)$.
Both sets of states are orthonormal: $\langle\nu_\beta|\nu_\alpha\rangle = \delta_{\alpha\beta}$, $\langle\nu_j|\nu_i\rangle = \delta_{ij}$.

$\Downarrow$

They are related to each other through a unitary transformation $\mathbf{V} = ||V_{\alpha i}||$, $\mathbf{V}\mathbf{V}^\dagger = 1$,

$$|\nu_\alpha\rangle = \sum_i V^*_{\alpha i}|\nu_i\rangle, \quad |\nu_i\rangle = \sum_\alpha V_{\alpha i}|\nu_\alpha\rangle.$$

[2] Massive neutrino states originated from any reaction or decay have the same definite momenta $\mathbf{p}_\nu$ ["equal momentum (EM) assumption"]. [a]

> To simplify matter, we do not consider exotic processes with multiple neutrino production.

$\Downarrow$

The flavor states $|\nu_\alpha\rangle$ have the same momentum $\mathbf{p}_\nu$ but have no definite mass and energy.

[a] Sometimes – the same definite energies ["equal energy (EE) assumption"].

[3] Neutrino masses are so small that in essentially all experimental circumstances the neutrinos are ultrarelativistic.

$$\Downarrow$$

$$E_i = \sqrt{\mathbf{p}_\nu^2 + m_i^2} \simeq |\mathbf{p}_\nu| + m_i^2/(2|\mathbf{p}_\nu|).$$

Moreover, in the evolution equation, one can safely replace the time parameter t by the distance L between the neutrino source and detector. [Everywhere $\hbar = c = 1$.]

The enumerated assumptions are enough to derive the nice and commonly accepted expression for the neutrino flavor transition probability [L_{jk} are the neutrino oscillation lengths]:

$$\mathscr{P}(\nu_\alpha \to \nu_\beta; L) \equiv \mathscr{P}_{\alpha\beta}(L) = \sum_{jk} V_{\alpha j} V_{\beta k} \left(V_{\alpha k} V_{\beta j}\right)^* \exp\left(\frac{2i\pi L}{L_{jk}}\right),$$

$$L_{jk} = \frac{4\pi E_\nu}{\Delta m_{jk}^2}, \qquad E_\nu = |\mathbf{p}_\nu|, \qquad \Delta m_{jk}^2 = m_j^2 - m_k^2.$$

Just this result is the basis for the "oscillation interpretation" of the current experiments with the natural and artificial (anti)neutrino beams.

The QM formula satisfies the probability conservation law:

$$\sum_\alpha \mathscr{P}_{\alpha\beta}(L) = \sum_\beta \mathscr{P}_{\alpha\beta}(L) = 1.$$

5.4 Some challenges against the QM approach.

Equal-momentum assumption

Massive neutrinos ν_i have, by assumption, equal momenta $\mathbf{p}_i = \mathbf{p}_\nu$. But this key assumption is reference-frame (RF) dependent and thus unphysical. Indeed, if $\mathbf{p}_i = \mathbf{p}_\nu$ in a certain RF, then in another RF moving with the velocity $\mathbf{v}$,

$$E_i' = \Gamma_\mathbf{v}\left[E_i - (\mathbf{v}\mathbf{p}_\nu)\right], \quad \mathbf{p}_i' = \mathbf{p}_\nu + \Gamma_\mathbf{v}\left[\frac{\Gamma_\mathbf{v}(\mathbf{v}\mathbf{p}_\nu)}{\Gamma_\mathbf{v}+1} - E_i\right]\mathbf{v},$$

$$\Downarrow$$

$$\mathbf{p}_i' - \mathbf{p}_j' = \left(E_j' - E_i'\right)\mathbf{v} = \Gamma_\mathbf{v}\left(E_j - E_i\right)\mathbf{v} \neq 0.$$

Treating the Lorentz transformation as active, we conclude that the EM assumption cannot be applied to the neutrinos arising from a non-monoenergetic beam of parent particles (the case in the real-life experiments).

* Similar objection is against the alternative equal-energy assumption. Indeed, in this case

$$E_i' - E_j' = \Gamma_\mathbf{v}\left(\mathbf{p}_j - \mathbf{p}_i\right)\mathbf{v} \neq 0, \quad \left|\mathbf{p}_i' - \mathbf{p}_j'\right| = \sqrt{\left|\mathbf{p}_i - \mathbf{p}_j\right|^2 + \Gamma_\mathbf{v}^2\left[\left(\mathbf{p}_i - \mathbf{p}_j\right)\mathbf{v}\right]^2} \neq 0.$$

* Can the EM (or EE) assumption be at least a good approximation? Alas, no, it cannot.

Let ν_μ arise from $\pi_{\mu 2}$ decays. If the pion beam has a wide momentum spectrum – from subrelativistic to ultrarelativistic (like that of CR), the EM condition cannot be valid even approximately within the whole spectral range of the pion neutrinos.

Light-ray approximation

The propagation time T is, by assumption, equal to the distance L traveled by the neutrino between production and detection points. But, if the massive neutrino components have the same momentum $\mathbf{p}_\nu$, their velocities are in fact different:

$$\mathbf{v}_k = \frac{\mathbf{p}_\nu}{\sqrt{\mathbf{p}_\nu^2 + m_k^2}} \quad \Longrightarrow \quad |\mathbf{v}_k - \mathbf{v}_j| \approx \frac{\Delta m^2_{jk}}{2E_\nu^2}.$$

One may naively expect that during the time T the neutrino ν_k travels the distance $L_k = |\mathbf{v}_k|T$; therefore, there must be a spread in distances of each neutrino pair

$$\delta L_{kj} = L_k - L_j \approx \frac{\Delta m^2_{jk}}{2E_\nu^2}\, L, \quad \text{where} \quad L = cT = T.$$

Δm^2_{jk}	E_ν	L	L_{kj}	$\lvert\delta L_{kj}\rvert$
Δm^2_{23}	1 GeV	$2R_\oplus$	$0.1R_\oplus$	$\sim 10^{-12}$ cm
Δm^2_{23}	1 TeV	$R_G \sim 100$ kps	$100R_\oplus$	$\sim 10^{-4}$ cm
Δm^2_{21}	1 MeV	1 AU	$0.25R_\oplus$	$\sim 10^{-3}$ cm

The values of δL_{kj} listed in the Table seem to be **fantastically** small.
But are they sufficiently small to preserve the coherence in any circumstance?

Can light neutrinos oscillate into heavy ones or vise versa? [Can active neutrinos oscillate into sterile ones or vise versa?]

The naive QM answer is Yes. Why not? If, at least, both ν_α (light) and ν_s (heavy) are ultrarelativistic [$|\mathbf{p}_\nu| \gg \max(m_1, m_2, m_3, \ldots, M)$,] one obtains the same formula for the oscillation probability $\mathscr{P}_{\alpha s}(L)$, since the QM formalism has no any limitation to the neutrino mass hierarchy.

Possibility of such transitions is a basis for many speculations in astrophysics and cosmology.

But! Assume again that the neutrino source is $\pi_{\mu 2}$ decay and $M > m_\pi$. Then the transition $\nu_\alpha \to \nu_s$ in the pion rest frame is forbidden by the energy conservation.

$\Downarrow$

There must be some limitations & flaws in the QM formula. What are they?

Do relic neutrinos oscillate?

The lightest (standard) relic neutrinos are most probably relativistic or even ultrarelativistic while the heaviest ones can be subrelativistic. The QM approach cannot operate with such a set of neutrinos.

Does the motion of the neutrino source affect the transition probabilities?

To answer these and similar questions

one has to unload the UR approximation & develop a covariant formalism.

In the QFT approach: the effective (most probable) energies and momenta of virtual ν_is are *found to be* functions of the masses, most probable momenta and momentum spreads of all particles (wave packets) involved into the neutrino production and detection processes.
In particular, in the two limiting cases – ultrarelativistic (UR) and nonrelativistic (NR):

Ultrarelativistic case

$(|q^0_{s,d}| \sim |\mathbf{q}_{s,d}| \gg m_i)$

$$\begin{cases} E_i = E_\nu \left[1 - \mathfrak{n} r_i - \mathfrak{m} r_i^2 + \ldots\right], \\ |\mathbf{p}_i| = E_\nu \left[1 - (\mathfrak{n}+1)\, r_i - \left(\mathfrak{m} + \mathfrak{n} + \frac{1}{2}\right) r_i^2 + \ldots\right], \\ v_i = 1 - r_i - \left(2\mathfrak{n} + \frac{1}{2}\right) r_i^2 + \ldots < 1, \end{cases}$$

Nonrelativistic case

$(|q^0_{s,d}| \sim m_i \gg |\mathbf{q}_{s,d}|)$

$$\begin{cases} E_i = m_i + \dfrac{m_i v_i^2}{2}\left(1 + \dfrac{3}{4}\delta_i + \ldots\right), \\ |\mathbf{p}_i| = m_i v_i \left(1 + \dfrac{1}{2}\delta_i + \ldots\right), \\ v_i \approx \dfrac{\boldsymbol{\varrho}_i \mathbf{l}}{1 + \varrho_i^0} \ll 1, \end{cases}$$

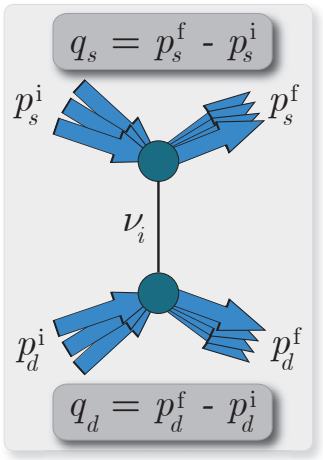

$$E_\nu \approx q_s^0 \approx -q_d^0, \quad r_i = \frac{m_i^2}{2E_\nu^2} \ll 1 \text{ (UR)},$$

$$\varrho_i^\mu = \frac{1}{m_i \mathscr{R}} \left[\widetilde{\mathfrak{K}}_s^{\mu 0}\left(m_i - q_s^0\right) + \widetilde{\mathfrak{K}}_d^{\mu 0}\left(m_i + q_d^0\right) - \widetilde{\mathfrak{K}}_s^{\mu k} q_s^k + \widetilde{\mathfrak{K}}_d^{\mu k} q_d^k\right], \quad |\varrho_i^\mu| \ll 1 \text{ (NR)}.$$

Definite momentum assumption

In the naive QM approach, the assumed definite momenta of neutrinos (both ν_α and ν_i) imply that the spatial coordinates of neutrino production ($\mathbf{X}_s$) and detection ($\mathbf{X}_d$) are fully uncertain (Heisenberg's principle).

$\Downarrow$

The distance $L = |\mathbf{X}_d - \mathbf{X}_s|$ is uncertain too, that makes the standard QM formula for the flavor transition probabilities to be strictly speaking senseless.

In the correct theory, the neutrino momentum uncertainty $\delta|\mathbf{p}_\nu|$ must be at least of the order of $\min(1/D_s, 1/D_d)$, where D_s and D_d are the characteristic dimensions of the source and detector "machines" along the neutrino beam.

$\Downarrow$

The neutrino states must be some wave packets (WP) [though having very small spreads] dependent, in general, on the quantum states of the particles [or, more exactly, also WPs] which participate in the production and detection processes.

In the QFT approach: the effective WPs of virtual UR ν_is are *found to be*

$$\psi_i^{(*)} = \exp\left\{\pm i(p_i X_{s,d}) - \frac{\widetilde{\mathfrak{D}}_i^2}{E_\nu^2}\left[(p_i X)^2 - m_i^2 X^2\right]\right\}, \qquad X = X_d - X_s,$$

where $p_i = (E_i, \mathbf{p}_i)$ and $X_{s,d}$ are the 4-vectors which characterize the space-time location of the ν production and detection processes, while $\widetilde{\mathfrak{D}}_i$ are certain (in general, complex-valued) functions of the masses, mean momenta and momentum spreads of all particles involved into these processes. [$\widetilde{\mathfrak{D}}_i/E_\nu$ and thereby ψ_i are Lorentz invariants.]

5.5 The aims and concepts of the field-theoretical approach.

The main purposes:

To define the domain of applicability of the standard quantum-mechanical (QM) theory of vacuum neutrino oscillations and obtain the QFT corrections to it.

The basic concepts:

- The "ν-oscillation" phenomenon in QFT is nothing else than a result of interference of the macroscopic Feynman diagrams perturbatively describing the lepton number violating processes with the massive neutrino fields as internal lines (propagators).
- The external lines of the macrodiagrams are wave packets rather than plane waves (therefore the standard S matrix approach should be revised).
- The external wave packet states are the covariant superpositions of the standard one-particle Fock states, satisfying a correspondence principle.

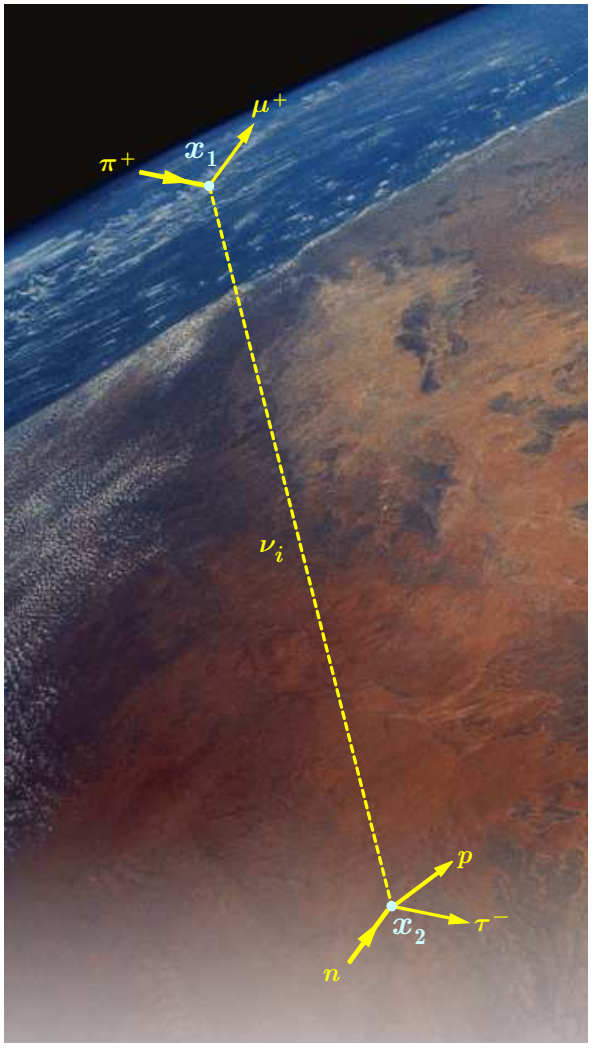

References: D. V. Naumov & VN, J. Phys. G **37** (2010) 105014 [arXiv:1008.0306 [hep-ph]]; Russ. Phys. J. **53** (2010) 549–574; arXiv:1110.0989 [hep-ph].

Most relevant papers

- C. Giunti, C.W. Kim, J.A. Lee, & U.W. Lee, Phys. Rev. D **48** (1993) 4310.
- ✓ W. Grimus & P. Stockinger, Phys. Rev. D **54** (1996) 3414.
- J.E. Campagne, Phys. Lett. B **400** (1997) 135.
- K. Kiers & N. Weiss, Phys. Rev. D **57** (1998) 3091.
- W. Grimus, P. Stockinger, & S. Mohanty, Phys. Rev. D **59** (1999) 013011.
- W. Grimus, S. Mohanty, & P. Stockinger, arXiv:hep-ph/9909341; hep-ph/9904340.
- A. Ioannisian & A. Pilaftsis, Phys. Rev. D **59** (1999) 053003.
- ✓ C.Y. Cardall, Phys. Rev. D **61** (2000) 073006.
- P. Stockinger, Pramana **54** (2000) 203.
- M. Beuthe, Ph.D. Thesis (Universit´e catholique de Louvain, Sep. 4, 2000), UCL-IPT-00-12 [arXiv:hep-ph/0010054].
- ✓ M. Beuthe, Phys. Rev. D **66** (2002) 013003.
- M. Beuthe, Phys. Rept. **375** (2003) 105.
- A.D. Dolgov, L.B. Okun, M.V. Rotaev, & M.G. Schepkin, arXiv:hep-ph/0407189. A.D. Dolgov, O.V. Lychkovskiy, A.A. Mamonov, L.B. Okun, & M.G. Schepkin, Eur. Phys. J. C **44** (2005) 431.
- C.C. Nishi, Phys. Rev. D **73** (2006) 053013.
- C.Y. Cardall & D.J.H. Chung, Phys. Rev. D **60** (1999) 073012.
- K. Fujii, C. Habe, & M. Blasone, arXiv:hep-ph/0212076.
- D. Pallin & H. Snellman, arXiv:hep-ph/0303173.
- M. Garbutt & B.H.J. McKellar, arXiv:hep-ph/0308111.
- A.D. Dolgov, O. V. Lychkovskiy, A. A. Mamonov, L.B. Okun, M.V. Rotaev, & M.G. Schepkin, Nucl. Phys. B **729** (2005) 79.
- L. Visinelli & P. Gondolo, arXiv:0810.4132 [hep-ph].
- E.Kh. Akhmedov & A.Yu. Smirnov, arXiv:0905.1903 [hep-ph].

6 Wave packets in quantum mechanics

Let $|\mathbf{k}\rangle$ be the eigenstate of the on-shell (with mass m) 4-momentum operator $\hat{P} = (\hat{P}_0, \hat{\mathbf{P}})$:

$$\hat{P}_\mu |\mathbf{k}\rangle = k_\mu |\mathbf{k}\rangle \quad (\mu = 0, 1, 2, 3).$$

$$k^2 = k_0^2 - \mathbf{k}^2 = m^2 \quad \Longrightarrow \quad \hat{P}^2 |\mathbf{k}\rangle = m^2 |\mathbf{k}\rangle.$$

So the proper Lorentz transformation $k \longmapsto k' = \Lambda k$ transforms the state $|\mathbf{k}\rangle$ into $|\mathbf{k}'\rangle$:

$$|\mathbf{k}\rangle \overset{\Lambda}{\longmapsto} |\mathbf{k}'\rangle.$$

Notation : $k_0 = E_\mathbf{k} = \sqrt{\mathbf{k}^2 + m^2}$,

Normalization : $\langle \mathbf{q} | \mathbf{k} \rangle = (2\pi)^3 2E_\mathbf{k} \delta(\mathbf{q} - \mathbf{k})$,

$$\Longrightarrow \quad \int \frac{d\mathbf{k}}{(2\pi)^3 2E_\mathbf{k}} |\mathbf{k}\rangle\langle\mathbf{k}| = 1.$$

Let now $|a\rangle$ be an arbitrary «one-particle» spinless state. It can be decomposed into the full set $\{|\mathbf{k}\rangle\}$ that is represented as a wave packet:

$$|a\rangle = \int \frac{d\mathbf{k}}{(2\pi)^3 \sqrt{2E_\mathbf{k}}} \psi_\mathbf{k} |\mathbf{k}\rangle, \quad \psi_\mathbf{k} = \frac{\langle \mathbf{k} | a \rangle}{\sqrt{2E_\mathbf{k}}}.$$

But $|a\rangle$ can be decomposed in the eigenvectors of any other self-adjoint operator, e.g. – the position operator $\hat{\mathbf{X}} = (\hat{X}_1, \hat{X}_2, \hat{X}_3)$:

$$\hat{X}_i|\mathbf{x}\rangle = x_i|\mathbf{x}\rangle, \quad (i = 1, 2, 3); \qquad \langle \mathbf{y}|\mathbf{x}\rangle = \delta(\mathbf{y} - \mathbf{x}) \implies \int d\mathbf{x}|\mathbf{x}\rangle\langle\mathbf{x}| = 1.$$

Therefore

$$|a\rangle = \int d\mathbf{x}\psi_{\mathbf{x}}|\mathbf{x}\rangle, \quad \psi_{\mathbf{x}} = \langle\mathbf{x}|a\rangle.$$

Since the operator $\hat{\mathbf{P}}$ in x representation is $-i\boldsymbol{\nabla}_{\mathbf{x}}$ then

$$\mathbf{k}\langle\mathbf{k}|\mathbf{x}\rangle = \langle\mathbf{k}|\hat{\mathbf{P}}|\mathbf{x}\rangle = \langle\mathbf{k}|(-i\boldsymbol{\nabla}_{\mathbf{x}})|\mathbf{x}\rangle = -i\boldsymbol{\nabla}_{\mathbf{x}}\langle\mathbf{k}|\mathbf{x}\rangle, \quad \implies \quad \langle\mathbf{k}|\mathbf{x}\rangle = \sqrt{2E_{\mathbf{k}}}e^{i\mathbf{k}\mathbf{x}},$$

$$|\mathbf{x}\rangle = \int \frac{d\mathbf{k}e^{i\mathbf{k}\mathbf{x}}}{(2\pi)^3\sqrt{2E_{\mathbf{k}}}}|\mathbf{k}\rangle, \quad |\mathbf{k}\rangle = \sqrt{2E_{\mathbf{k}}}\int d\mathbf{x}e^{-i\mathbf{k}\mathbf{x}}|\mathbf{x}\rangle.$$

Therefore the wavefunctions $\psi_{\mathbf{k}}$ and $\psi_{\mathbf{x}}$ are Fourier transforms of each other:

$$\psi_{\mathbf{x}} = \int \frac{d\mathbf{k}}{(2\pi)^3}e^{-i\mathbf{k}\mathbf{x}}\psi_{\mathbf{k}}, \qquad \psi_{\mathbf{k}} = \int d\mathbf{x}e^{i\mathbf{k}\mathbf{x}}\psi_{\mathbf{x}}.$$

The norm of the state $|a\rangle$ is

$$\langle a|a\rangle = \int \frac{d\mathbf{k}}{(2\pi)^3}|\psi_{\mathbf{k}}|^2 = \int d\mathbf{x}|\psi_{\mathbf{x}}|^2.$$

6.1 Space-time localization (local limit).

- If the state $|a\rangle$ is localized in the point $\mathbf{x}_a$ that is $|a\rangle = \text{const}\,|\mathbf{x}_a\rangle$, then

$$\psi_{\mathbf{x}} = \text{const}\,\delta(\mathbf{x}-\mathbf{x}_a) \quad \Longleftrightarrow \quad \psi_{\mathbf{k}} = \text{const}\,e^{i\mathbf{k}\mathbf{x}_a}.$$

  Of course, such a state cannot be the state of a real physical particle, since its momentum is absolutely uncertain. Moreover, particle cannot be localized in a region smaller than its Compton length $\sim 1/m$. It is however important that in this mathematical limit, wavefunctions $\psi_{\mathbf{x}}$ and $\psi_{\mathbf{k}}$ depend explicitly on the spatial coordinate $\mathbf{x}_a$.

- In Real World, any physical ("particle-like") state $|a\rangle$ is localized within a finite space region S. **More formally**: the probability density $|\psi_{\mathbf{x}}|^2$ vanishes well beyond S.

In general S can be described by some equations, inequalities, or by a set of coordinates. Let's limit ourselves to the simplest case when it can be characterized by a single 3-vector $\mathbf{x}_a$ (the simples example is a sphere with the center in $\mathbf{x}_a$). Then

$\psi_{\mathbf{x}}$ must be a function of $\mathbf{x}_a$ $\Longleftrightarrow$ $\psi_{\mathbf{k}}$ must be a function of $\mathbf{x}_a$

- Similarly, if the state $|a\rangle$ has a finite lifetime, $\psi_{\mathbf{x}}$ and $\psi_{\mathbf{k}}$ must be functions of x_a^0.
- In a more general case of a space-time localization the wavefunctions depend on $\mathbf{x}_a$ & x_a^0.
- Since any Lorentz boost entangles the space-time variables, the wavefunctions $\psi_{\mathbf{x}}$ and $\psi_{\mathbf{k}}$ must depend on a 4-vector $x_a = (x_a^0, \mathbf{x}_a)$, which describes the evolution of the state in the configuration space.

6.2 Momentum localization (plane wave limit)

- Let's assume that the state $|a\rangle$ has a definite 3-momentum $\mathbf{p}_a$: $|a\rangle = \text{const}\,|\mathbf{p}_a\rangle$. Then

$$\psi_{\mathbf{k}} = \text{const}\,(2\pi)^3\sqrt{2E_{\mathbf{k}}}\,\delta(\mathbf{k}-\mathbf{p}_a) \quad \Longleftrightarrow \quad \psi_{\mathbf{x}} = \text{const}\,\sqrt{2p_a^0}\,e^{-i\mathbf{p}_a\mathbf{x}}.$$

  This state is also unphysical since it is fully delocalized in space.

  However, just such kind of states are used for description of the asymptotically free particles in the quantum scattering theory. Sometimes the plane waves are astonishingly associated with point particles... Fortunately such "interpretation" does not (usually) affect the calculations of the microscopic scattering amplitudes.

- In Real World, any physical ("particle-like") state $|a\rangle$ is localized in some finite region of the momentum space. Considerations similar to the above ones allow us to conclude that

$$\boxed{\psi_{\mathbf{k}} \text{ must be a function of } \mathbf{p}_a} \Longleftrightarrow \boxed{\psi_{\mathbf{x}} \text{ must be a function of } \mathbf{p}_a}$$

  Note: the energy variable p_a^0 (in contrast with the time variable x_a^0) is not independent since in the PW limit it becomes $\sqrt{\mathbf{p}_a^2 + m^2}$.

Finally we may conclude that the simplest wave packet $|a\rangle$ suitable for description of the particle states localized in both the configuration space and momentum space must depend on the space-time variable x_a and momentum variable $\mathbf{p}_a$:

$$\boxed{\psi_{\mathbf{k}} = \psi_{\mathbf{k}}(\mathbf{p}_a, x_a) \quad \text{and} \quad \psi_{\mathbf{x}} = \psi_{\mathbf{x}}(\mathbf{p}_a, x_a).}$$

6.3 Quasistable wave packets

The foregoing qualitative considerations do not provide us with the exact physical meaning of variables x_a and $\mathbf{p}_a$. Let us precisely specify the latter for the special class of the states.

Definition: The quasistable packet (QSP) is the state whose norm does not depend on x_a in any inertial reference frame.

- For QSP, the 4-vector x_a can enter the function $\psi_{\mathbf{k}}$ only through a phase factor $\exp[if(x_a)]$, where $f(x_a)$ is a real function.
- Since $f(x_a)$ is dimensionless and (by assumption) does not depend on any dimension parameters, it can only depend on the dimensionless combinations of the components of the 4-vectors k, p_a ($k^2 = p_a^2 = m^2$) and x_a.
- Due to Lorentz invariance of the norm $\langle a|a\rangle$, the function $f(x_a)$ is also a Lorentz invariant. Therefore it is a function of the scalar products (kx_a), $(p_a x_a)$, and $m^2 x_a^2$ only.
- The function $f(x_a)$ must satisfy the aforementioned limiting cases, namely, it must contain the term $\mathbf{k}\mathbf{x}_a$ in the local limit ($|a\rangle \to \text{const}\,|\mathbf{x}_a\rangle$) and does not depend on x_a in the plane wave limit ($|a\rangle \to \text{const}\,|\mathbf{p}_a\rangle$).

It is easy to see that the simplest choice of the function $f(x_a)$, which satisfies the above requirements is

$$f(x_a) = (p_a - k)x_a.$$

If we wish to describe the states which are sufficiently well localized in both the momentum space and configuration space, than this form is intrinsically unique.

Therefore our quasistable state is of the form

$$\boxed{|a\rangle \equiv |\mathbf{p}_a, x_a\rangle = \int \frac{d\mathbf{k}}{(2\pi)^3 2E_{\mathbf{k}}} e^{i(p_a - k)x_a} \phi(\mathbf{k}, \mathbf{p}_a)|\mathbf{k}\rangle,}$$

where the "form factor" $\phi(\mathbf{k}, \mathbf{p}_a)$ does not depend on x_a and the extra factor in the denominator is added to simplify at most the form factor's properties.[a] From above we find:

$$\langle \mathbf{p}_a, x_a | \mathbf{p}_a, x_a\rangle = \int \frac{d\mathbf{k}}{(2\pi)^3 2E_{\mathbf{k}}} |\phi(\mathbf{k}, \mathbf{p}_a)|^2.$$

Therefore $|\phi(\mathbf{k}, \mathbf{p}_a)|^2$ is a Lorentz scalar. Without loss of generality, we require that

$$\phi(\mathbf{k}', \mathbf{p}'_a) = \phi(\mathbf{k}, \mathbf{p}_a) \quad (k' = \Lambda k, \;\; p'_a = \Lambda p_a).$$

$$\Updownarrow$$

$$|\mathbf{p}_a, x_a\rangle \overset{\Lambda}{\longmapsto} |\mathbf{p}'_a, x'_a\rangle \quad (p'_a = \Lambda p_a, \;\; x'_a = \Lambda x_a),$$

Clearly, the wavefunctions $\psi_{\mathbf{x}}(\mathbf{p}_a, x_a)$ and $\psi_{\mathbf{k}}(\mathbf{p}_a, x_a)$ are not Lorentz scalars:

$$\psi_{\mathbf{k}}(\mathbf{p}_a, x_a) = \frac{1}{\sqrt{2E_{\mathbf{k}}}} e^{i(p_a - k)x_a} \phi(\mathbf{k}, \mathbf{p}_a),$$

$$\psi_{\mathbf{x}}(\mathbf{p}_a, x_a) = e^{ip_a x_a} \int \frac{d\mathbf{k}}{(2\pi)^3 \sqrt{2E_{\mathbf{k}}}} e^{-i\left[\mathbf{k}(\mathbf{x} - \mathbf{x}_a) + k^0 x_a^0\right]} \phi(\mathbf{k}, \mathbf{p}_a).$$

[a] And also for better accommodation to the QFT case.

6.3.1 Further properties of QSP

Particular case of the Lorentz invariance is the invariance of $\phi(\mathbf{k}, \mathbf{p}_a)$ relative to rotations

$$\mathbf{k} \longmapsto \mathbf{k}' = \mathbf{O}\mathbf{k}, \quad \mathbf{p}_a \longmapsto \mathbf{p}'_a = \mathbf{O}\mathbf{p}_a.$$

$$\Downarrow$$

- $\psi_{\mathbf{k}}(\mathbf{p}_a, x_a)$ and $\psi_{\mathbf{x}}(\mathbf{p}_a, x_a)$ are rotation invariants:

  $$\psi_{\mathbf{k}'}(\mathbf{p}'_a, x'_a) = \psi_{\mathbf{k}}(\mathbf{p}_a, x_a), \;\; \psi_{\mathbf{x}'}(\mathbf{p}'_a, x'_a) = \psi_{\mathbf{x}}(\mathbf{p}_a, x_a) \quad (\mathbf{x}' = \mathbf{O}\mathbf{x}, \;\; x'_a = (\mathbf{O}\mathbf{x}_a, x^0_a)).$$

  Since $|\psi_{\mathbf{x}_a}(\mathbf{p}_a, x_a)|$ does not depend on $\mathbf{x}_a$, the latter can be identified with the center of symmetry of the packet; we'll call it the center of the packet.
- $|\psi_{\mathbf{x}}(\mathbf{p}_a, x_a)|$ is invariant relative to spatial translations is space but not in time.
- $|\psi_{\mathbf{x}}(\mathbf{p}_a, x_a)| \to 0$ as $|x^0_a| \to \infty$ (the packet spreads with time in the configuration space).
- The form factor $\phi(\mathbf{k}, \mathbf{p})$ can be function of the only Lorentz invariant quantity

  $$(k-p)^2 = 2[m^2 - (kp)] = (E_{\mathbf{k}} - E_{\mathbf{p}})^2 - (\mathbf{k}-\mathbf{p})^2.$$

  $\Longrightarrow$
  - $\phi(\mathbf{k}, \mathbf{p}) = \phi(\mathbf{p}, \mathbf{k})$, $\phi(\mathbf{p}, \mathbf{p}) \equiv \phi_0$ does not depend on $\mathbf{p}$;
  - $\phi(\mathbf{k}, \mathbf{0}) = \phi(\mathbf{0}, \mathbf{k}) = \widetilde{\phi}(k_0)$ is a rotation-invariant function of $k_0 = E_{\mathbf{k}}$;
  - the norm $\langle \mathbf{p}_a, x_a | \mathbf{p}_a, x_a \rangle$ does not depend on $\mathbf{x}_a$ and $\mathbf{p}_a$.
- The states $|\mathbf{p}_a, x_a\rangle$ form a complete vector set:

  $$|\mathbf{p}_a\rangle = \frac{2p^0_a}{\phi_0} \int d\mathbf{x}_a |p_a, x_a\rangle \quad \Longrightarrow \quad \int d\mathbf{p} d\mathbf{x} d\mathbf{y} \frac{E_{\mathbf{p}}}{4\pi^3 |\phi_0|^2} |\mathbf{p}, x\rangle\langle \mathbf{p}, y| = 1.$$

6.3.2 Physical meaning of the vector $\mathbf{p}_a$.

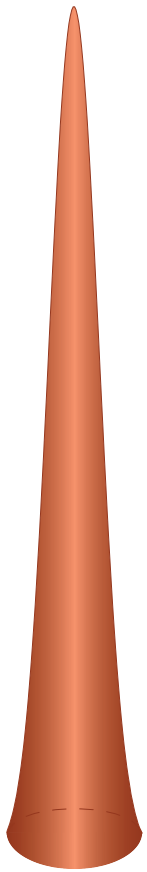

From the definition of the QSP $|\mathbf{p}_a, x_a\rangle$ it follows that

$$|\langle \mathbf{k}|\mathbf{p}_a, x_a\rangle|^2 = |\phi(\mathbf{k}, \mathbf{p}_a)|^2.$$

So $|\phi(\mathbf{k}, \mathbf{p}_a)|^2$ defines the weight with which the state $|\mathbf{k}\rangle$ enters into the wave packet state $|\mathbf{p}_a, x_a\rangle$.

It is natural to adopt that the function $|\phi(\mathbf{k}, \mathbf{p})|$ has the only maximum in the point $\mathbf{k} = \mathbf{p}$ (at that $|\phi|_{\max} = |\phi_0| > 0$) and drops rapidly as $|\mathbf{k} - \mathbf{p}| \to \infty$.

$$\Downarrow$$

$$[\nabla_{\mathbf{k}}|\phi(\mathbf{k}, \mathbf{p})|]_{\mathbf{k}=\mathbf{p}} = [\nabla_{\mathbf{p}}|\phi(\mathbf{k}, \mathbf{p})|]_{\mathbf{p}=\mathbf{k}} = 0.$$

For the form factors $\phi(\mathbf{k}, \mathbf{p}_a)$ of such class, the physical meaning of the vector $\mathbf{p}_a$ is clear:

The vector $\mathbf{p}_a$ is the most probable 3-momentum of the state $|\mathbf{p}_a, x_a\rangle$.

Note: After this, the transition to the local limit becomes impossible and we can forget about this "strut" (which is in any case absent in QFT).

6.3.3 Mean 4-momentum and mass of QSP.

- The mean 4-momentum $\overline{P} = (\overline{P}_0, \overline{\mathbf{P}})$ of the packet is defined by the standard QM rule:

$$\overline{P}_\mu = \overline{P}_\mu(\mathbf{p}) = \frac{\langle \mathbf{p}, x|\hat{P}_\mu|\mathbf{p}, x\rangle}{\langle \mathbf{p}, x|\mathbf{p}, x\rangle} = \frac{1}{2m\mathrm{V}_\star}\int \frac{d\mathbf{k}k_\mu|\phi(\mathbf{k},\mathbf{p})|^2}{(2\pi)^3 2E_\mathbf{k}}.$$

Here and below the index a is dropped for short; the positive constant

$$\mathrm{V}_\star = \frac{\langle \mathbf{p}, x|\mathbf{p}, x\rangle}{2m} = \frac{1}{2m}\int \frac{d\mathbf{k}\,|\phi(\mathbf{k},\mathbf{p})|^2}{(2\pi)^3 2E_\mathbf{k}} = \frac{1}{8\pi^2 m}\int_m^\infty dk_0\sqrt{k_0^2-m^2}\,|\widetilde{\phi}(k_0)|^2$$

has dimension of volume. The mean 4-momentum is the integral of motion.

- $\overline{\mathbf{P}}(\mathbf{0}) = \mathbf{0}$ due to the evenness of the function $\phi(\mathbf{k}, \mathbf{0})$. Therefore the mean (effective) mass of the packet, $\overline{m}$, is the mean energy $\overline{P}_0$ in RF:

$$\overline{m} = \overline{P}_0(\mathbf{0}) = \int \frac{d\mathbf{k}|\phi(\mathbf{k},\mathbf{0})|^2}{4(2\pi)^3 m\mathrm{V}_\star} = \frac{1}{8\pi^2 m\mathrm{V}_\star}\int_m^\infty dk_0 k_0\sqrt{k_0^2-m^2}\,|\widetilde{\phi}(k_0)|^2,$$

$$\Longrightarrow \quad \frac{\overline{m}}{m} = \int_m^\infty dk_0 k_0\sqrt{k_0^2-m^2}\,|\widetilde{\phi}(k_0)|^2\left[\int_m^\infty dk_0 m\sqrt{k_0^2-m^2}\,|\widetilde{\phi}(k_0)|^2\right]^{-1} \geq 1;$$

the equality $\overline{m} = m$ only holds in the PW limit.

The QSP is heavier than its plane-wave constituents.

This very general effect is a manifestation of the nonadditivity of the relativistic mass.

In our case: the transversal to $\mathbf{p}$ components of the momenta of the states $|\mathbf{k}\rangle$ do not contribute to the mean momentum ($\mathbf{p} \times \overline{\mathbf{P}} = 0$), but do contribute to the mean energy.

Some analogy:

The mass of a gas in a bulb increases under (uniform) heating: the bulb does not get an extra momentum, but internal energy of the gas grows.

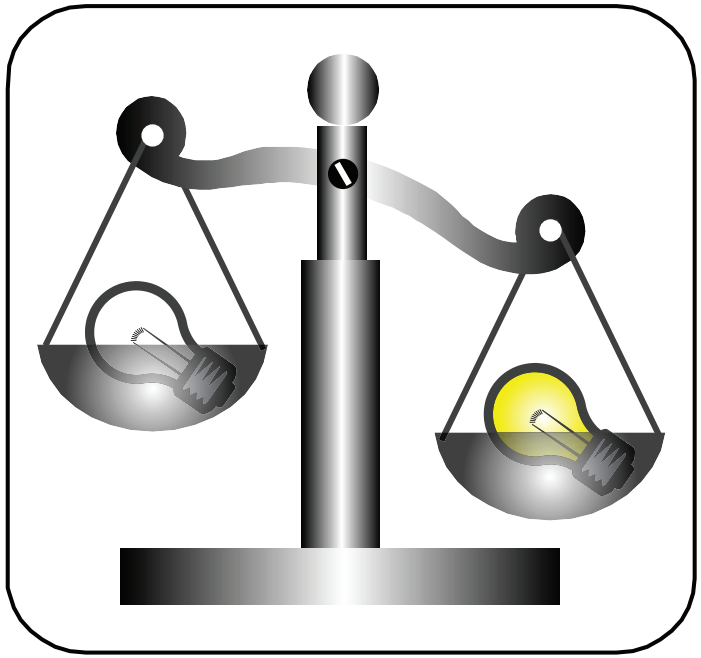

Proposal of an experiment.

Note that the mean value of the squared mass $\overline{P^2}$ is equal to m^2 and thus

$$\overline{P}^2 \geq \overline{P^2} = m^2.$$

One can prove that $\overline{P}_0 = (\overline{m}/m)E_{\mathbf{p}}$, $\overline{\mathbf{P}} = (\overline{m}/m)\mathbf{p}$. So, in the mean, QSP is on-shell:

$$\overline{P}^2 = \overline{P}_\mu \overline{P}^\mu = \overline{m}^2.$$

The mean velocity $\overline{\mathbf{P}}/\overline{P}_0$ coincides with most probable velocity $\mathbf{v}_\mathbf{p} = \mathbf{p}/E_\mathbf{p}$.

6.4 Mean position of QSP. Meaning of the space-time parameter.

Let us inquire the exact physical meaning of the space-time dependence of the state $|\mathbf{p}, x\rangle$. Consider the mean value of the position operator $\hat{\mathbf{X}}$:

$$\begin{aligned}\overline{\mathbf{x}} = \overline{\mathbf{x}}(\mathbf{p}, x) &= \frac{\langle \mathbf{p}, x|\hat{\mathbf{X}}|\mathbf{p}, x\rangle}{\langle \mathbf{p}, x|\mathbf{p}, x\rangle} = \frac{1}{2m\mathrm{V}_\star}\int d\mathbf{y}\mathbf{y}|\psi_{\mathbf{y}}(\mathbf{p}, x)|^2 \\ &= \frac{1}{4m\mathrm{V}_\star}\int d\mathbf{y}\mathbf{y}\int \frac{d\mathbf{k}d\mathbf{q}}{(2\pi)^6\sqrt{E_{\mathbf{k}}E_{\mathbf{q}}}} e^{i[(\mathbf{q}-\mathbf{k})(\mathbf{y}-\mathbf{x})+(q_0-k_0)x_0]}\phi(\mathbf{k}, \mathbf{p})\phi^*(\mathbf{q}, \mathbf{p}) \\ &= \frac{1}{4m\mathrm{V}_\star}\int d\mathbf{y}(\mathbf{y}+\mathbf{x})\int \frac{d\mathbf{k}d\mathbf{q}}{(2\pi)^6\sqrt{E_{\mathbf{k}}E_{\mathbf{q}}}} e^{i[(\mathbf{q}-\mathbf{k})\mathbf{y}+(q_0-k_0)x_0]}\phi(\mathbf{k}, \mathbf{p})\phi^*(\mathbf{q}, \mathbf{p}).\end{aligned}$$

$$\Downarrow$$

$\overline{\mathbf{x}} = \boldsymbol{\xi}(\mathbf{p}, x_0) + \mathbf{x}$, where $\boldsymbol{\xi}(\mathbf{p}, x_0) = \dfrac{1}{2m\mathrm{V}_\star}\displaystyle\int d\mathbf{y}\mathbf{y}\,|\chi_{\mathbf{y}}(\mathbf{p}, x_0)|^2$ and $\chi_{\mathbf{y}}(\mathbf{p}, x_0) \equiv \psi_{\mathbf{y}}(\mathbf{p}, x)|_{\mathbf{x}=\mathbf{0}}$.

Due to the rotation invariance of $\psi_{\mathbf{y}}(\mathbf{p}, x)$, the function $\chi_{\mathbf{y}}(\mathbf{0}, x_0)$ is even function of $\mathbf{y}$. Thus

$$\boldsymbol{\xi}(\mathbf{0}, x_0) = \mathbf{0}.$$

Since $\boldsymbol{\xi}$ is a 3-vector, and the last equality is valid for any x_0, it is equivalent to the following:

$$\boldsymbol{\xi}_\star = \mathbf{0}.$$

Here and below, the star symbol ($\star$) is used to denote the rest-frame quantities.

Let ξ_0 be the 0-component of the 4-vector $\xi = (\xi_0, \boldsymbol{\xi})$. The Lorentz boost connecting RF with lab. frame (LF) can be written as

$$\boldsymbol{\xi}_\star = \boldsymbol{\xi} + \Gamma_{\mathbf{p}} \left[\frac{\Gamma_{\mathbf{p}}(\mathbf{v}_{\mathbf{p}}\boldsymbol{\xi})}{\Gamma_{\mathbf{p}} + 1} - \xi_0 \right] \mathbf{v}_{\mathbf{p}},$$

where

$$\mathbf{v}_{\mathbf{p}} = \mathbf{p}/E_{\mathbf{p}}, \quad \Gamma_{\mathbf{p}} = E_{\mathbf{p}}/m, \quad \text{and} \quad \boldsymbol{\xi} = \boldsymbol{\xi}(\mathbf{p}, x_0).$$

So we obtain the equation

$$\boldsymbol{\xi} = \frac{E_{\mathbf{p}}}{m} \left[\xi_0 - \frac{E_{\mathbf{p}}(\mathbf{v}_{\mathbf{p}}\boldsymbol{\xi})}{E_{\mathbf{p}} + m} \right] \mathbf{v}_{\mathbf{p}},$$

which has the only solution

$$\boldsymbol{\xi}(\mathbf{p}, x_0) = \mathbf{v}_{\mathbf{p}} \xi_0.$$

Next, it is easy to prove that $|\chi_{\mathbf{y}}(\mathbf{p}, 0)|$ is even function of $\mathbf{y}$. Hence $\boldsymbol{\xi}(\mathbf{p}, 0) = \mathbf{0}$ that is

$$\xi_0 = 0 \quad \text{as} \quad x_0 = 0.$$

Therefore ξ_0 must be identified with x_0 and we have

$$\boxed{\overline{\mathbf{x}}(\mathbf{p}, x) = \mathbf{x} + \mathbf{v}_{\mathbf{p}} x_0.}$$

Conclusions:

- In the mean, QSP follows the classical trajectory, with the most probable velocity $\mathbf{v}_{\mathbf{p}}$.
- In RF, the mean position of the packet is just its center, $\mathbf{x}$.
- The parameter x_0 is the time counted from the moment when the mean position of the packet has been coincided with its center $\mathbf{x}$ in LF.

6.5 Effective volume of QSP.

Which is the area of localization of a wave packet in the configuration space?

> Making the perfect definition of the size or volume of a wave packet (an infinite quantum object) is an almost as thankless job as defining the size of a cloud. Nevertheless, we have to have a quantitative characteristic of the degree of localization of the packet, allowing to compare the effective sizes of different packets.

Clouds over Sochi city (April 1, 2011)

Simple example: Let $\rho(\mathbf{x})$ be the spherically symmetric density distribution of some quantity, say mass, with the center in the point $\mathbf{x} = \mathbf{0}$. Let both the full mass

$$\int d\mathbf{x}\rho(\mathbf{x}) = M$$

and the central density $\rho_0 = \rho(\mathbf{0})$ are finite. We may define the effective spatial volume V as the volume of a uniform ball of mass M with density ρ_0:

$$\mathrm{V} = M/\rho_0.$$

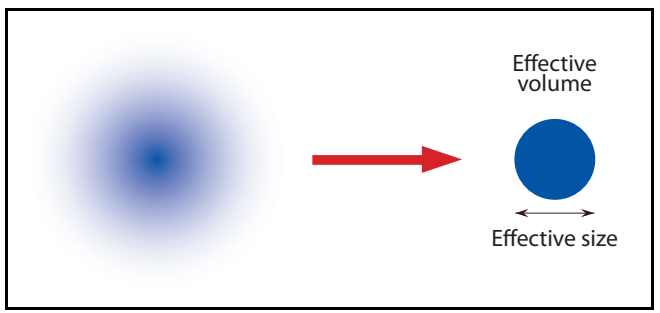

This definition, being no better and no worse than any other, is the most appropriate since it can easily be translated to the covariant quantum language.

By following the above example, we define the effective spatial volume of QSP in RF as

$$\mathrm{V}(\mathbf{0}) = \frac{1}{\rho_\star}\int d\mathbf{y}\,|\psi_{\mathbf{y}}(\mathbf{0},x)|^2\,.$$

Here, the analog of the central density is the central value of the function $|\psi_{\mathbf{y}}(\mathbf{0},x)|^2$ (proportional to the probability density in RF), $\rho_\star$, taken at the moment $x_0 = 0$:

$$\rho_\star \equiv |\psi_{\mathbf{x}}(\mathbf{0},x)|^2\big|_{x_0=0} = \left|\int \frac{d\mathbf{k}\,\widetilde{\phi}(k_0)}{(2\pi)^3\sqrt{2k_0}}\right|^2 = \frac{1}{8\pi^2}\left|\int_m^\infty dk_0\sqrt{k_0(k_0^2-m^2)}\,\widetilde{\phi}(k_0)\right|^2\,.$$

This is just a constant. It's easy to see that

$$\boldsymbol{\nabla}_{\mathbf{y}}|\psi_{\mathbf{y}}(\mathbf{0},x)|^2\big|_{\mathbf{y}=\mathbf{x},\,x_0=0} = \mathbf{0}.$$

Hence $\rho_\star$ is the extremum of the density function

$$|\psi_{\mathbf{y}}(\mathbf{0},x)|^2 = \int \frac{d\mathbf{k}d\mathbf{q}}{2(2\pi)^6\sqrt{k_0q_0}}e^{i[(\mathbf{q}-\mathbf{k})(\mathbf{y}-\mathbf{x})+(q_0-k_0)x_0]}\widetilde{\phi}(k_0)\widetilde{\phi}^*(q_0).$$

One more (the last) restriction: $\widetilde{\phi}(k_0) > 0$ or, equivalently, $\arg[\phi(\mathbf{k},\mathbf{p})] = 0$.

This condition, unclaimed till now, is connected with the same PW limit, in which the phase of the function $\phi(\mathbf{k},\mathbf{p})$ is zero. So it is sufficient to put $\arg[\phi(\mathbf{k},\mathbf{p})] = 0$.

In this case, it is obvious that $\rho_\star$ is the absolute maximum of $|\psi_{\mathbf{y}}(\mathbf{0},x)|^2$.

By using the definition of the norm $\langle \mathbf{p}, x | \mathbf{p}, x \rangle = 2m\mathrm{V}_\star$ we obtain

$$\mathrm{V}(\mathbf{0}) = 2m\mathrm{V}_\star/\rho_\star.$$

Taking into account the Lorentz transformation law for the volume, we find the effective volume of the packet in LF:

$$\boxed{\mathrm{V}(\mathbf{p}) = \frac{\mathrm{V}(\mathbf{0})}{\Gamma_{\mathbf{p}}} = \frac{1}{\Gamma_{\mathbf{p}}\rho_\star}\int d\mathbf{y}\,|\psi_{\mathbf{y}}(\mathbf{p}, x)|^2.}$$

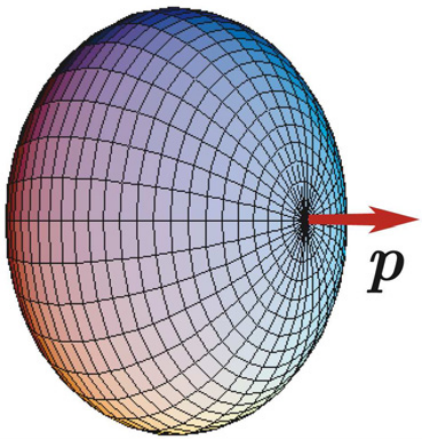

In the PW limit:

$$\phi(\mathbf{k}, \mathbf{0}) \to 16\pi^3 m\delta(\mathbf{k}) \implies \rho_\star \to 2m \implies \mathrm{V}(\mathbf{0}) \to \mathrm{V}_\star \to \infty.$$

Thus, for the packets well localized in the momentum space, one can put approximately

$$\mathrm{V}(\mathbf{0}) = \mathrm{V}_\star, \quad \mathrm{V}(\mathbf{p}) = \mathrm{V}_\star/\Gamma_{\mathbf{p}}.$$

The above definition of $\mathrm{V}(\mathbf{p})$ is formally applicable to any form factor. It is therefore instructive to check its self-consistency also in the local limit. While in this (unphysical) case, the integrals defining the constants $\mathrm{V}_\star$, $\rho_\star$ diverge at the upper limit of integration in k_0, their ratio vanishes $\implies \mathrm{V}(\mathbf{p}) \to 0$ *as it should be*. Formally this fact can be proved by the standard regularization of the integrals in k_0:

$$\frac{\mathrm{V}_\star}{\rho_\star} \propto \lim_{M\to\infty} \frac{\int_m^M dk_0\sqrt{k_0^2 - m^2}\,|\widetilde{\phi}(k_0)|^2}{\left|\int_m^M dk_0\sqrt{k_0(k_0^2 - m^2)}\,\widetilde{\phi}(k_0)\right|^2} = \lim_{M\to\infty}\left(\int_m^M dk_0 k_0\sqrt{k_0^2 - m^2}\right)^{-1} = \lim_{M\to\infty}\frac{3}{M^3}.$$

The effective size of QSP in RF is naturally defined as the diameter of a ball of volume $\mathrm{V}(\mathbf{0})$.

7 Wave packets in quantum field theory.

7.1 Fock states.

The S-matrix formalism of QFT usually deals with the one-particle Fock states (FS) as the asymptotically-free states of the spin-s fields. The FS are constructed from the vacuum state:

$$|\mathbf{k},s\rangle = \sqrt{2E_{\mathbf{k}}}\, a^{\dagger}_{\mathbf{k}s}|0\rangle, \qquad a_{\mathbf{k}s}|0\rangle = 0, \qquad (E_{\mathbf{k}} = k_0 = \sqrt{\mathbf{k}^2 + m^2}),$$

and provide the QFT realization of the abstract QM states $|\mathbf{k}\rangle$ with the fixed 3-momentum.

- The conventional (anti)commutation relations for the creation/annihilation operators hold:

$$\{a_{\mathbf{q}r}, a_{\mathbf{k}s}\} = \{a^{\dagger}_{\mathbf{q}r}, a^{\dagger}_{\mathbf{k}s}\} = 0, \qquad \{a_{\mathbf{q}r}, a^{\dagger}_{\mathbf{k}s}\} = (2\pi)^3 \delta_{sr} \delta\left(\mathbf{k} - \mathbf{q}\right).$$

- The Lorentz-invariant normalization of FS is therefore singular since

$$\langle \mathbf{q},r|\mathbf{k},s\rangle = (2\pi)^3 2E_{\mathbf{k}} \delta_{sr} \delta\left(\mathbf{k} - \mathbf{q}\right).$$

- The proper Lorentz transformation induces the unitary transformation of FS:

$$k \longmapsto k' = \Lambda k \quad \Longrightarrow \quad |\mathbf{k},s\rangle \longmapsto U_{\Lambda}|\mathbf{k},s\rangle = |\mathbf{k}',s\rangle,$$

  assuming that the axis of spin quantization is oriented along the boost or rotation axis.

- This is equivalent to the following unitary transformation of the operators $a^{\dagger}_{\mathbf{k}s}$ and $a_{\mathbf{k}s}$:

$$a^{\dagger}_{\mathbf{k}s} \longmapsto U_{\Lambda} a^{\dagger}_{\mathbf{k}s} U^{-1}_{\Lambda} = \sqrt{E_{\mathbf{k}'}/E_{\mathbf{k}}}\, a^{\dagger}_{\mathbf{k}'s}, \quad a_{\mathbf{k}s} \longmapsto U_{\Lambda} a_{\mathbf{k}s} U^{-1}_{\Lambda} = \sqrt{E_{\mathbf{k}'}/E_{\mathbf{k}}}\, a_{\mathbf{k}'s}.$$

7.2 Wave-packet states.

By the same, as above (QM), arguments referring to the localization of the state in the configuration space and momentum space, we can build the QFT wave-packet (WP) as a linear combination of the Fock states. The most general construction is

$$|\mathbf{p}, s, x\rangle = \int \frac{d\mathbf{k}}{(2\pi)^3 2E_{\mathbf{k}}} \sum_{s'} \Phi_{ss'}\left(\mathbf{k}, \mathbf{p}, x; \boldsymbol{\sigma}\right) |\mathbf{k}, s'\rangle,$$

In general, the function $\Phi_{ss'}(\mathbf{k}, \mathbf{p}, x; \boldsymbol{\sigma})$ depends not only on the momentum, space-time, and spin variables, but also on a (finite or infinite) set of parameters (constants)

$$\boldsymbol{\sigma} = \{\sigma_1, \sigma_2, \ldots\},$$

governing the shape of WP. All momenta are, by definition, on-shell [can be avoided in future].

Correspondence principle:

The wave packet state passes into the Fock state in the plane-wave limit:

$$|\mathbf{p}, s, x\rangle \overset{\text{PW}}{\longmapsto} |\mathbf{p}, s\rangle.$$

Since the parameters σ_i can always be defined in such a way to approach the PW limit as $\sigma_i \to 0$ $(\forall i)$, we can formulate the correspondence principle in the following way:

$$\lim_{\boldsymbol{\sigma}\to 0} \Phi_{ss'}\left(\mathbf{k}, \mathbf{p}, x; \boldsymbol{\sigma}\right) = (2\pi)^3 2E_{\mathbf{p}} \delta_{ss'} \delta(\mathbf{k} - \mathbf{p}).$$

Below, we'll only interested in the quasistable WP very close to FS that is very narrow in the momentum space ($\Longleftrightarrow$ all σ_i are small). Then the correspondence principle suggests that

- functions $\Phi_{ss'}$ must be Lorentz invariants (scalars),
- the x dependence of $|\Phi_{ss'}|$ can be neglected,
- $|\Phi_{ss'}| \ll |\Phi_{ss}|$ for $s' \neq s$.

These requirements can be accumulated in the following simple ansatz:

$$\Phi_{ss'}\left(\mathbf{k},\mathbf{p},x;\boldsymbol{\sigma}\right) = \delta_{ss'} e^{i\varsigma(k-p)x}\phi(\mathbf{k},\mathbf{p};\boldsymbol{\sigma}),$$

in which $\phi(\mathbf{k},\mathbf{p};\boldsymbol{\sigma})$ is a spin- and coordinate-independent Lorentz-invariant function, such that

$$\lim_{\boldsymbol{\sigma}\to 0}\phi(\mathbf{k},\mathbf{p};\boldsymbol{\sigma}) = (2\pi)^3 2E_{\mathbf{p}}\delta(\mathbf{k}-\mathbf{p})$$

(so $\phi(\mathbf{k},\mathbf{p};\boldsymbol{\sigma})$ is a "smeared" δ-function), and ς is the sign which will be fixed in a short while. Finally, the quasistable QFT wave packet [abbreviated as above by QSP] can be written as

$$\boxed{|\mathbf{p},s,x\rangle = \int \frac{d\mathbf{k}\, e^{i\varsigma(k-p)x}}{(2\pi)^3 2E_{\mathbf{k}}}\phi(\mathbf{k},\mathbf{p})|\mathbf{k},s\rangle,} \tag{12}$$

[Here and below the argument $\boldsymbol{\sigma}$ is dropped for short, but is implied.]

From (12) it is in particular follows the (expected) transformation rule:

$$|\mathbf{p},s,x\rangle \overset{\Lambda}{\longmapsto} |\mathbf{p}',s,x'\rangle \quad (p'=\Lambda p,\ \ x'=\Lambda x),$$

where again the axis of spin quantization is oriented along the boost or rotation axis.

7.2.1 The most general properties of QSP.

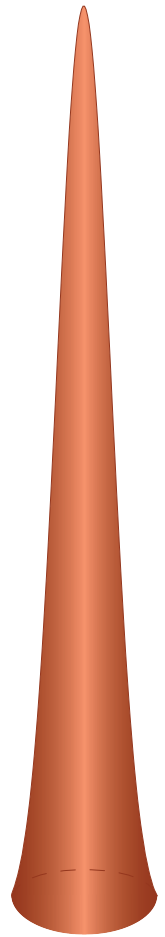

The function $\phi(\mathbf{k},\mathbf{p})$ has exactly the same properties as its QM analog.
Thus, the major properties of QSP can be summarized without derivation:

- the form factor $\phi(\mathbf{k},\mathbf{p})$ can be function of the only quantity $(k-p)^2$;
- $\phi(\mathbf{k},\mathbf{p}) = \phi(\mathbf{p},\mathbf{k})$;
- $\phi(\mathbf{p},\mathbf{p}) \equiv \phi_0$ does not depend on $\mathbf{p}$;
- $\phi(\mathbf{k},\mathbf{0}) = \phi(\mathbf{0},\mathbf{k}) = \widetilde{\phi}(k_0)$ is a rotation-invariant function of $k_0 = E_{\mathbf{k}}$;
- the norm $\langle \mathbf{p},s,x|\mathbf{p},s,x\rangle = 2m\mathrm{V}_\star$ is a constant and, moreover, the inner product $\langle \mathbf{q},r,y|\mathbf{p},s,x\rangle = \delta_{sr}e^{i(qy-px)}\mathcal{D}(\mathbf{p},\mathbf{q};x-y)$ is defined by the nonsingular and relativistic-invariant function

$$\mathcal{D}(\mathbf{p},\mathbf{q};x) = \int \frac{d\mathbf{k}}{(2\pi)^3 2E_{\mathbf{k}}}\, e^{ikx}\phi(\mathbf{k},\mathbf{p})\phi^*(\mathbf{k},\mathbf{q}) \quad [\text{for } \varsigma = +1].$$

- As in the QM case, we require that the function $\phi(\mathbf{k},\mathbf{p})$ is positive definite, has the only maximum at $\mathbf{k}=\mathbf{p}$, and drops rapidly as $|\mathbf{k}-\mathbf{p}| \to \infty$. Hence

The vector $\mathbf{p}$ is the most probable 3-momentum of the state $|\mathbf{p},s,x\rangle$.

Technical condition [ensues from the correspondence principle; not necessary but practical.]

$$\int \frac{d\mathbf{k}}{(2\pi)^3 2E_{\mathbf{k}}}\,\phi(\mathbf{k},\mathbf{0}) = 1.$$

- The mean 4-momentum, $\overline{P}$, of QSP is the integral of motion.
- In the mean, the QSP is on-shell: $\overline{P}^2 = \overline{m}^2$, but $\overline{P^2} = m^2$.
- The QSP is heavier than its Fock constituents: $\overline{m} > m$.

The relevant formulas remain formally the same as in the QM case.

7.2.2 A nuisance (metaphysical notes).

Treating the QSP as a physical quantum state, created in collisions or decays of other particles $\varkappa$, one may expect that the function $\phi(\mathbf{k}, \mathbf{p})$ depends parametrically (through the set $\boldsymbol{\sigma}$) on the 4-momenta $Q_\varkappa$ of both primary and secondary particles participated in the creation process.

Moreover, in the most general case the set of the progenitor and accompanying particles may include ones from the whole net of the reactions which led to the production of the packet.

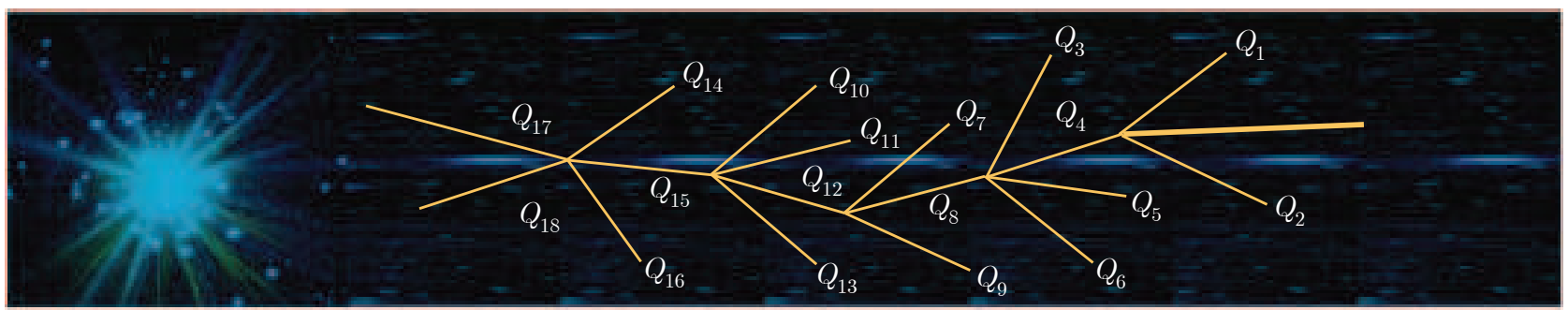

The 4-momenta $Q_\varkappa$ can enter the scalar function $\phi(\mathbf{k},\mathbf{p})$ only through the scalar products $(Q_\varkappa k)$, $(Q_\varkappa p)$ and $(Q_\varkappa Q_{\varkappa'})$. Owing to the required properties of $\phi(\mathbf{k},\mathbf{p})$, it satisfies the conditions

$$\left[\frac{\partial\phi(\mathbf{k},\mathbf{p})}{\partial k_l}\right]_{\mathbf{k}=\mathbf{p}} = \left[\frac{\partial(k-p)^2}{\partial k_l}\,\frac{\partial\phi(\mathbf{k},\mathbf{p})}{\partial(k-p)^2}\right]_{\mathbf{k}=\mathbf{p}} + \sum_\varkappa \left[\frac{\partial(Q_\varkappa k)}{\partial k_l}\,\frac{\partial\phi(\mathbf{k},\mathbf{p})}{\partial(Q_\varkappa k)}\right]_{\mathbf{k}=\mathbf{p}}$$

$$= \sum_\varkappa Q^0_\varkappa \left(\frac{p^l}{p^0} - \frac{Q^l_\varkappa}{Q^0_\varkappa}\right)\left[\frac{\partial\phi(\mathbf{k},\mathbf{p})}{\partial(Q_\varkappa k)}\right]_{\mathbf{k}=\mathbf{p}} = 0 \qquad (l=1,2,3).$$

The last equations are satisfied identically only in the unphysical case, when the velocities of all particles $\varkappa$, are equal to each other, $\mathbf{Q}_\varkappa/Q^0_\varkappa = \mathbf{p}/E_\mathbf{p}$. Thus, from the arbitrariness of the 4-momentum configurations $\{Q_\varkappa\}$, we conclude that $[\partial\phi(\mathbf{k},\mathbf{p})/\partial(Q_\varkappa k)]_{\mathbf{k}=\mathbf{p}} = 0$. Similarly we obtain $[\partial\phi(\mathbf{k},\mathbf{p})/\partial(Q_\varkappa p)]_{\mathbf{p}=\mathbf{k}} = 0$. Hence the dependence of $\phi(\mathbf{k},\mathbf{p})$ upon $(Q_\varkappa k)$ and $(Q_\varkappa p)$ must vanish, at least in the vicinity of the maximum of $\phi(\mathbf{k},\mathbf{p})$. Since only this vicinity is really important for the smeared δ-function, it is safe to neglect this dependence everywhere.

The remaining scalar products $(Q_\varkappa Q_{\varkappa'})$ can be then "absorbed" into the definition of the parameters σ_i. In other words, σ_i can be, in general, the scalar functions of the 4-momenta of the "network particles" $\varkappa$ rather than constants. As a result, the WP composed by identical one-particle Fock states but produced in different reactions (or reaction chains) are not, generally speaking, identical. To avoid this serious complication we will be forced to sacrifice the generality in some stages of our study, assuming voluntary that σ_i are still constants.

A note in excuse: this problem is not specific to the covariant approach...

7.3 Wave packet in the configuration space.

Consider, as a representative example, a spin-$\frac{1}{2}$ free-field operator

$$\Psi(x) = \int \frac{d\mathbf{k}}{(2\pi)^3\sqrt{2E_{\mathbf{k}}}} \sum_s \left[a_{\mathbf{k}s}u_s(\mathbf{k})e^{-ikx} + b^\dagger_{\mathbf{k}s}v_s(\mathbf{k})e^{ikx}\right].$$

The coordinate representation of FS is a plane wave uniformly distributed over the space-time:

$$\langle 0|\Psi(x)|\mathbf{p},s\rangle = u_s(\mathbf{p})e^{-ipx},$$

So, the QFT analog of the QM wavefunction $\psi_y(\mathbf{p},x)$ in x representation is the spinor function

$$\psi_y(\mathbf{p},s,x) = \langle 0|\Psi(y)|\mathbf{p},s,x\rangle = \int \frac{d\mathbf{k}}{(2\pi)^3 2E_{\mathbf{k}}} u_s(\mathbf{k})e^{-i[ky+\varsigma(p-k)x]}\phi(\mathbf{k},\mathbf{p}). \qquad (13)$$

Moreover, in the S-matrix perturbation theory, just this factor will provide the modified Feynman-rule factor for any Feynman diagram with the corresponding incoming fermion leg.

It is natural to demand that $|\psi_x(\mathbf{p},s,x)|$ does not depend on $\mathbf{x}$ in RF because, in this case, the point $\mathbf{x}$ can be identified with the symmetry center of the packet.

$$\psi_x(\mathbf{p},s,x) = \langle 0|\Psi(x)|\mathbf{p},s,x\rangle = e^{-i\varsigma(px)} \int \frac{d\mathbf{k}}{(2\pi)^3 2E_{\mathbf{k}}} u_s(\mathbf{k})e^{-i(1-\varsigma)(kx)}\phi(\mathbf{k},\mathbf{p}).$$

$$\Downarrow$$

The requirement is fulfilled for any form factor $\phi(\mathbf{k},\mathbf{p})$ only if $\varsigma = 1$.

So instead of Eqs. (12) and (13) we finally obtain

$$\boxed{|\mathbf{p},s,x\rangle = \int \frac{d\mathbf{k}\,\phi(\mathbf{k},\mathbf{p})e^{i(k-p)x}}{(2\pi)^3 2E_{\mathbf{k}}}|\mathbf{k},s\rangle,} \tag{14}$$

$$\boxed{\psi_y(\mathbf{p},s,x) = e^{-ipx}\int \frac{d\mathbf{k}}{(2\pi)^3 2E_{\mathbf{k}}}u_s(\mathbf{k})\phi(\mathbf{k},\mathbf{p})e^{ik(x-y)}.} \tag{15}$$

The opposed (in comparison with the QM WP) sign in the exponent in Eq. (14) is caused by the identification of the function $\psi_y(\mathbf{p},s,x)$ with the matrix element $\langle 0|\Psi(y)|\mathbf{p},s,x\rangle$ (what is with the in wave packet) rather than with its complex conjugate. Indeed, quite similarly it can be constructed the wave function for the wave packet related to the *outgoing* fermion line:

$$\overline{\psi}_y(\mathbf{p},s,x) = \langle \mathbf{p},s,x|\overline{\Psi}(y)|0\rangle = e^{ipx}\int \frac{d\mathbf{k}}{(2\pi)^3 2E_{\mathbf{k}}}\overline{u}_s(\mathbf{k})\phi^*(\mathbf{k},\mathbf{p})e^{ik(y-x)}. \tag{16}$$

Obviously,

$$\overline{\psi}_y(\mathbf{p},s,x) = \psi_y^\dagger(\mathbf{p},s,x)\gamma_0,$$

and hence, for definiteness, below we will only discuss the incoming wave packets.

Clearly, the same constructions can be released for the free fields of arbitrary tensor structure.

This finalizes the construction of QSP. However we'll need to do some simplifications.

7.4 Narrow QSP approximation.

From this point we'll consider only very narrow (in the momentum space) packets, for which the function $\phi(\mathbf{k},\mathbf{p})$ is strongly peaked at the point $\mathbf{k}=\mathbf{p}$. In this case, considering that the Dirac spinor $u_s(\mathbf{k})$ is a smooth function of $\mathbf{k}$, we can write

$$\psi_y(\mathbf{p},s,x)=\langle 0|\Psi(y)|\mathbf{p},s,x\rangle \approx e^{-ipx}u_s(\mathbf{p})\psi(\mathbf{p},x-y), \tag{17}$$

where we have introduced the Lorentz-invariant function

$$\boxed{\psi(\mathbf{p},x)=\int\frac{d\mathbf{k}}{(2\pi)^3 2E_{\mathbf{k}}}\,e^{ikx}\phi(\mathbf{k},\mathbf{p})=\psi(\mathbf{0},x_\star).}$$

satisfying the Klein-Gordon equation: $(\Box_x-m^2)\psi(\mathbf{p},x)=0$. [Therefore it is a relativistic wave packet in terms of conventional scattering theory.]

The approximation (17) is valid under the condition

$$|i\nabla_{\mathbf{y}}\ln\psi(\mathbf{p},x-y)+\mathbf{p}|\ll 2E_{\mathbf{p}}, \tag{18}$$

which is fully consistent with other approximations in the subsequent analysis.

The relations analogous to (17) can be obtained for the free fields of any spin, providing us with the modified Feynman-rule factors for the external legs of any diagram. In particular, it is pertinent to note that the equality

$$\langle 0|\Phi(y)|\mathbf{p},s=0,x\rangle = e^{-ipx}\psi(\mathbf{p},x-y)$$

is exact for the scalar and pseudoscalar fields $\Phi(x)$.

From definition of $\psi(p,x)$ and the correspondence principle it follows that

$$\lim_{\sigma\to 0}\psi(\mathbf{p},x)=e^{ipx} \quad \text{and} \quad \lim_{\sigma\to 0}\psi_y(\mathbf{p},s,x)=e^{-ipy}u_s(\mathbf{p})=\langle 0|\Psi(y)|\mathbf{p},s\rangle.$$

$$\Downarrow$$

An infinitely narrow wave packet in the momentum space corresponds to a plane wave in the configuration space and vice versa.

- The effective spatial volume can be defined in the full analogy with the QM case:

$$\mathrm{V}(\mathbf{p})\stackrel{\text{def}}{=}\int d\mathbf{y}\,\frac{\psi_y^\dagger(\mathbf{p},s,x)\psi_y(\mathbf{p},s,x)}{\psi_x^\dagger(\mathbf{p},s,x)\psi_x(\mathbf{p},s,x)}=\int d\mathbf{x}|\psi(\mathbf{p},x)|^2=\int\frac{d\mathbf{k}}{(2\pi)^3}\frac{|\phi(\mathbf{k},\mathbf{p})|^2}{(2E_{\mathbf{k}})^2}=\frac{\mathrm{V}(\mathbf{0})}{\Gamma_{\mathbf{p}}}.$$

- In a similar way, we can define the mean position of the packet:

$$\overline{\mathbf{x}}\stackrel{\text{def}}{=}\frac{\int d\mathbf{y}\,\psi_y^\dagger(\mathbf{p},s,x)\,\mathbf{y}\,\psi_y(\mathbf{p},s,x)}{\int d\mathbf{y}\,\psi_y^\dagger(\mathbf{p},s,x)\psi_y(\mathbf{p},s,x)}=\frac{1}{\mathrm{V}(\mathbf{p})}\int d\mathbf{y}\,\mathbf{y}|\psi(\mathbf{p},x-y)|^2.$$

By using the properties of the function $\psi(\mathbf{p},x)$, it can be proved that

$$\overline{\mathbf{x}}=\mathbf{x}+\mathbf{v}_{\mathbf{p}}(y_0-x_0).$$

So, in the mean, the packet follows the classical trajectory, with the most probable velocity $\mathbf{v}_{\mathbf{p}}$.

7.5 Commutation function.

It is useful to introduce the auxiliary operator (wave-packet creation operator)

$$A^{\dagger}_{\mathbf{p}s}(x) = \int \frac{d\mathbf{k}\,\phi(\mathbf{k},\mathbf{p})e^{i(k-p)x}}{2(2\pi)^3\sqrt{E_{\mathbf{k}}E_{\mathbf{p}}}} a^{\dagger}_{\mathbf{k}r}. \tag{19}$$

Then the state $|\mathbf{p},s,x\rangle$ can be written in the form similar to the Fock state:

$$|\mathbf{p},s,x\rangle = \sqrt{2E_{\mathbf{p}}}A^{\dagger}_{\mathbf{p}s}(x)\,|0\rangle.$$

Clearly $A^{\dagger}_{\mathbf{p}s}(x)$ passes into $a^{\dagger}_{\mathbf{p}s}$ in the limit $\boldsymbol{\sigma} \to 0$. It can be easily proved that under the Lorentz transformation $p \longmapsto p' = \Lambda p$ and $x \longmapsto x' = \Lambda x$ the operator (19) is transformed as

$$A^{\dagger}_{\mathbf{p}s}(x) \longmapsto U_{\Lambda}A^{\dagger}_{\mathbf{p}s}(x)U^{-1}_{\Lambda} = \sqrt{E_{\mathbf{p}'}/E_{\mathbf{p}}}\,A^{\dagger}_{\mathbf{p}'s}(x').$$

The following (anti)commutation relations can be derived:

$$\left\{a_{\mathbf{q}r}, A^{\dagger}_{\mathbf{p}s}(x)\right\} = \delta_{sr}\,(4E_{\mathbf{q}}E_{\mathbf{p}})^{-1/2}\,e^{i(q-p)x}\,\phi(\mathbf{q},\mathbf{p}),$$

$$\{A_{\mathbf{q}r}(y), A_{\mathbf{p}s}(x)\} = \left\{A^{\dagger}_{\mathbf{q}r}(y), A^{\dagger}_{\mathbf{p}s}(x)\right\} = 0,$$

$$\left\{A_{\mathbf{q}r}(y), A^{\dagger}_{\mathbf{p}s}(x)\right\} = \delta_{sr}\,(4E_{\mathbf{q}}E_{\mathbf{p}})^{-1/2}\,e^{i(qy-px)}\mathcal{D}(\mathbf{p},\mathbf{q};x-y).$$

Here we have defined the Lorentz- and translation-invariant commutation function

$$\mathcal{D}(\mathbf{p},\mathbf{q};x-y)=\int\frac{d\mathbf{k}}{(2\pi)^3 2E_{\mathbf{k}}}\,\phi(\mathbf{k},\mathbf{p})\phi^*(\mathbf{k},\mathbf{q})e^{ik(x-y)}.$$

From the last (anti)commutation relation it follows that

$$\langle\mathbf{q},r,y|\mathbf{p},s,x\rangle=\delta_{sr}e^{i(qy-px)}\mathcal{D}(\mathbf{p},\mathbf{q};x-y).$$

It provides, in particular, the invariant and non-singular (assuming $\boldsymbol{\sigma}\neq 0$) normalization of the wave-packet states:

$$\langle\mathbf{p},s,x|\mathbf{p},s,x\rangle=\mathcal{D}(\mathbf{p},\mathbf{p};0)=2m\mathrm{V}_\star\approx 2E_{\mathbf{p}}\mathrm{V}(\mathbf{p}). \tag{20}$$

7.5.1 Plane-wave limit.

In virtue of the correspondence principle, we have for arbitrary (smooth) function $F(\mathbf{p})$:

$$\lim_{\boldsymbol{\sigma}\to 0}\int\frac{d\mathbf{p}\,\mathcal{D}(\mathbf{p},\mathbf{q};x-y)}{(2\pi)^3 2E_{\mathbf{p}}}F(\mathbf{p})=\lim_{\boldsymbol{\sigma}\to 0}\int\frac{d\mathbf{k}\,\phi^*(\mathbf{k},\mathbf{q})}{(2\pi)^3 2E_{\mathbf{k}}}e^{ik(x-y)}F(\mathbf{k})=e^{iq(x-y)}F(\mathbf{q}),$$

$$\Downarrow$$

$$\lim_{\boldsymbol{\sigma}\to 0}\mathcal{D}(\mathbf{p},\mathbf{q};x-y)=(2\pi)^3 2E_{\mathbf{p}}\delta(\mathbf{p}-\mathbf{q})e^{ip(x-y)},$$

$$\Downarrow$$

$$\lim_{\boldsymbol{\sigma}\to 0}\left\{A_{\mathbf{q}r}(y),A^\dagger_{\mathbf{p}s}(x)\right\}=(2\pi)^3\delta_{sr}\delta\left(\mathbf{p}-\mathbf{q}\right),\quad\lim_{\boldsymbol{\sigma}\to 0}\langle\mathbf{q},r,y|\mathbf{p},s,x\rangle=(2\pi)^3\delta_{sr}2E_{\mathbf{p}}\delta\left(\mathbf{p}-\mathbf{q}\right).$$

7.5.2 Behavior of the commutation function in the center-of-inertia frame.

Certain properties of the commutation function become especially transparent in the center-of-inertia frame (CIF) of the two packets ($\mathbf{p}_* + \mathbf{q}_* = 0$) in which

$$\mathcal{D}(\mathbf{p}_*, -\mathbf{p}_*; x_* - y_*) = \int \frac{d\mathbf{k}}{(2\pi)^3 2E_{\mathbf{k}}} \phi(\mathbf{k}, \mathbf{p}_*)\phi^*(\mathbf{k}, -\mathbf{p}_*)e^{ik(x_* - y_*)}.$$

- Due to the assumed behaviour of $\phi(\mathbf{k}, \mathbf{p})$ in the vicinity of the point $\mathbf{k} = \mathbf{p}$, one may expect that $|\mathcal{D}(\mathbf{p}_*, -\mathbf{p}_*; x_* - y_*)|$ has a sharp maximum at $\mathbf{p}_* = 0$.
- On the contrary, the function $|\mathcal{D}(\mathbf{p}_*, -\mathbf{p}_*; x_* - y_*)|$ vanishes at large $|\mathbf{p}_*|$, since the maxima of the factors $|\phi(\mathbf{k}, \mathbf{p}_*)|$ and $|\phi(\mathbf{k}, -\mathbf{p}_*)|$ in the integrand are widely separated in this case and thus $|\phi(\mathbf{k}, \mathbf{p}_*)\phi^*(\mathbf{k}, -\mathbf{p}_*)| \ll 1$ for any $\mathbf{k}$.

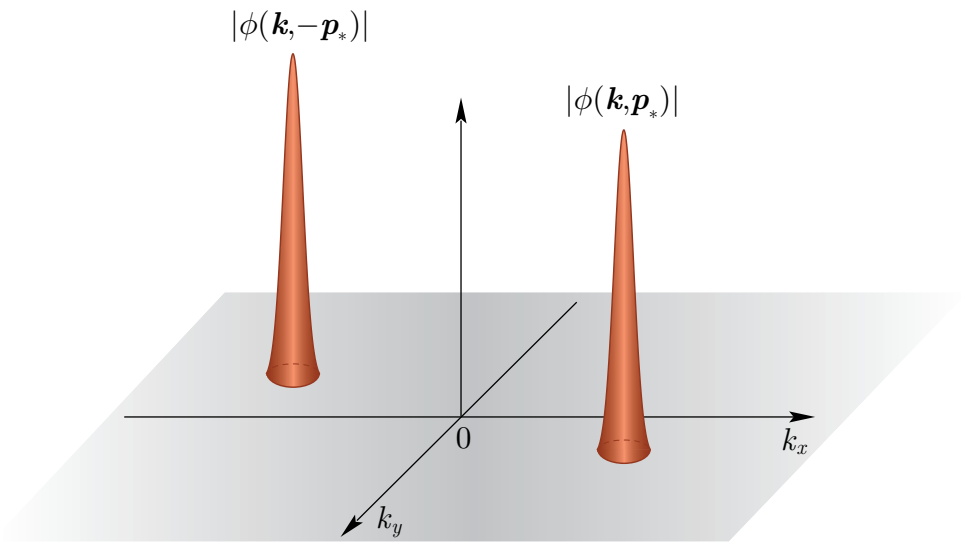

- Function $\mathcal{D}(\mathbf{p}_*, -\mathbf{p}_*; x_* - y_*)$ must vanish when the points x_* and y_* are widely separated in space (that is $|\mathbf{x}_* - \mathbf{y}_*|$ is large) because the phase factor $e^{-i\mathbf{k}(\mathbf{x}_* - \mathbf{y}_*)}$ in the integrand rapidly oscillates in this case.

7.5.3 Summary of kinematic relations.

To come back into the laboratory (or any other) frame we have to express the asterisked variables in terms of the non-asterisked ones.

- The Lorentz-transformation rules:

$$x_*^0 = \Gamma\left(x^0 - \mathbf{vx}\right), \quad \mathbf{x}_* = \mathbf{x} + \Gamma\left[\frac{\Gamma}{\Gamma+1}(\mathbf{vx}) - x^0\right]\mathbf{v},$$

- The velocity and Lorentz factor of CIF in the lab. frame:

$$\mathbf{v} = \frac{\mathbf{p}+\mathbf{q}}{E_\mathbf{p}+E_\mathbf{q}}, \quad \Gamma = \frac{1}{\sqrt{1-\mathbf{v}^2}} = \frac{E_\mathbf{p}+E_\mathbf{q}}{E_{\mathbf{p}_*}+E_{\mathbf{q}_*}}$$

- The energies and momenta in CIF:

$$E_{\mathbf{p}_*} = E_{\mathbf{q}_*} = \frac{1}{2}\sqrt{(p+q)^2} \equiv E_*, \quad |\mathbf{p}_*| = |\mathbf{q}_*| = \frac{1}{2}\sqrt{-(p-q)^2} \equiv P_*.$$

It is seen from the last relation that P_* vanishes as $\mathbf{p} \to \mathbf{q}$ and grows with increasing $|\mathbf{p}-\mathbf{q}|$. [Hence from the above consideration it follows that the function $|\mathcal{D}(\mathbf{p},\mathbf{q};x-y)|$ reaches its maximum at $\mathbf{p}=\mathbf{q}$ and vanishes at large values of $|\mathbf{p}-\mathbf{q}|$.]

- Useful identities:

$$2E_*x_*^0 = (p+q)x, \quad 2\mathbf{p}_*\mathbf{x}_* = (q-p)x, \quad \mathbf{vx}_* = \Gamma\left(\mathbf{vx} - \mathbf{v}^2x^0\right),$$

$$\mathbf{x}_*^2 = \frac{[(p+q)x]^2}{(p+q)^2} - x^2 = \Gamma^2\left(\left|\mathbf{x} - \mathbf{v}x^0\right|^2 - |\mathbf{v}\times\mathbf{x}|^2\right), \quad \mathbf{x}_* = 0 \Longleftrightarrow \mathbf{x} = \mathbf{v}x^0.$$

7.6 Multi-packet states ☕.

[This item is important as a "prearrangement" for an extension of the formalism to include the effects of coherent forward neutrino scattering from the matter background particles.]

Let's define the ket-state (and consequently bra-states) of n identical wave packets by

$$\begin{aligned}
|\,\{\mathbf{p},s,x\}_n\rangle &\equiv |\,\mathbf{p}_1,s_1,x_1;\mathbf{p}_2,s_2,x_2;\ldots;\mathbf{p}_n,s_n,x_n\rangle \\
&= \widetilde{A}^\dagger_{\mathbf{p}_1 s_1}(x_1)\widetilde{A}^\dagger_{\mathbf{p}_2 s_2}(x_2)\cdots\widetilde{A}^\dagger_{\mathbf{p}_n s_n}(x_n)|0\rangle \\
&= (\pm 1)^{n(n-1)/2}\widetilde{A}^\dagger_{\mathbf{p}_n s_n}(x_n)\cdots\widetilde{A}^\dagger_{\mathbf{p}_2 s_2}(x_2)\widetilde{A}^\dagger_{\mathbf{p}_1 s_1}(x_n)|0\rangle, \\
\langle\{\mathbf{p},s,x\}_n\,| &\equiv \langle\mathbf{p}_1,s_1,x_1;\mathbf{p}_2,s_2,x_2;\ldots;\mathbf{p}_n,s_n,x_n\,| \\
&= \langle 0|\widetilde{A}_{\mathbf{p}_n s_n}(x_n)\cdots\widetilde{A}_{\mathbf{p}_2 s_2}(x_2)\widetilde{A}_{\mathbf{p}_1 s_1}(x_1) \\
&= (\pm 1)^{n(n-1)/2}\langle 0|\widetilde{A}_{\mathbf{p}_1 s_1}(x_1)\widetilde{A}_{\mathbf{p}_2 s_2}(x_2)\cdots\widetilde{A}_{\mathbf{p}_n s_n}(x_1),
\end{aligned}$$

where the sign "$+$" ("$-$") is for bosons (fermions) and

$$\widetilde{A}^\dagger_{\mathbf{p}s}(x) = \sqrt{2E_{\mathbf{p}}}\,A^\dagger_{\mathbf{p}s}(x), \quad \widetilde{A}_{\mathbf{p}s}(x) = \sqrt{2E_{\mathbf{p}}}\,A_{\mathbf{p}s}(x).$$

It is easy to see that this state is fully (anti)symmetric relative to permutation

$$(\mathbf{p}_i,s_i,x_i) \longleftrightarrow (\mathbf{p}_j,s_j,x_j) \text{ for any } 1\le i,j\le n \ (i\ne j).$$

To determine the normalization of the multi-packet states we define the $n\times n$ matrix

$$\mathbb{D}_n = \mathbb{D}\left(\{\mathbf{q},r,y\}_n, \{\mathbf{p},s,x\}_n\right) = \left|\left|\delta_{s_i r_j}(\mp 1)^{i+j}\mathcal{D}(\mathbf{p}_i,\mathbf{q}_j;x_i-y_j)\right|\right|.$$

It can be proved by induction (not so easy, see Appendix 16 ☕) that

$$\boxed{\langle\{\mathbf{q},r,y\}_n \,|\, \{\mathbf{p},s,x\}_n\rangle = \exp\left[i\sum_{i=1}^{n}(q_i y_i - p_i x_i)\right]\det\left(\mathbb{D}_n\right).}$$

$$\mathcal{D}(\mathbf{p},\mathbf{q};x-y) = \mathcal{D}^*(\mathbf{q},\mathbf{p};y-x) \Longrightarrow \begin{cases} \mathbb{D}\left(\{\mathbf{p},s,x\}_n, \{\mathbf{p},s,x\}_n\right) \text{ is Hermitian,} \\ \langle\{\mathbf{p},s,x\}_n \,|\, \{\mathbf{p},s,x\}_n\rangle \text{ is real.} \end{cases}$$

Examples

$$\langle\{\mathbf{p},s,x\}_1 \,|\, \{\mathbf{p},s,x\}_1\rangle = 2m\mathrm{V}_\star,$$

$$\langle\{\mathbf{p},s,x\}_2 \,|\, \{\mathbf{p},s,x\}_2\rangle = (2m\mathrm{V}_\star)^2 \pm \delta_{s_1 s_2}|\mathcal{D}(\mathbf{p}_1,\mathbf{p}_2;x_1-x_2)|^2,$$

$$\langle\{\mathbf{p},s,x\}_3 \,|\, \{\mathbf{p},s,x\}_3\rangle = (2m\mathrm{V}_\star)^3 \pm 2m\mathrm{V}_\star \sum_{1\le i<j\le 3}\delta_{s_i s_j}|\mathcal{D}(\mathbf{p}_i,\mathbf{p}_j;x_i-x_j)|^2$$
$$+2\mathrm{Re}\prod_{1\le i<j\le 3}\left[\delta_{s_i s_j}\mathcal{D}(\mathbf{p}_i,\mathbf{p}_j;x_i-x_j)\right].$$

Simplest repercussions

Non-overlapping regime: If the space-time points $x_1, x_2, \ldots, x_n$ $(n \geq 2)$ are well separated and/or the 3-momenta $\mathbf{p}_1, \mathbf{p}_2, \ldots, \mathbf{p}_n$ essentially differ from each other, the n-packet matrix element is approximately equal to $(2m\mathrm{V}_\star)^n$.

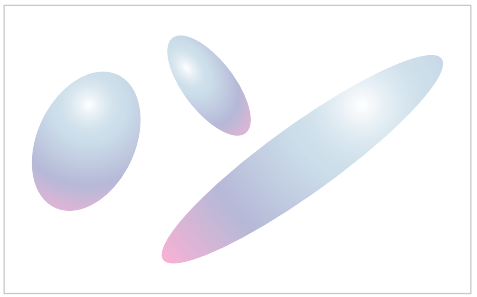

Overlapping regime: If the wave packets having the same spin projections strongly overlap in both the momentum and the configuration spaces, the n-boson matrix element tends to $n!(2m\mathrm{V}_\star)^n$, while the n-fermion matrix element vanishes.

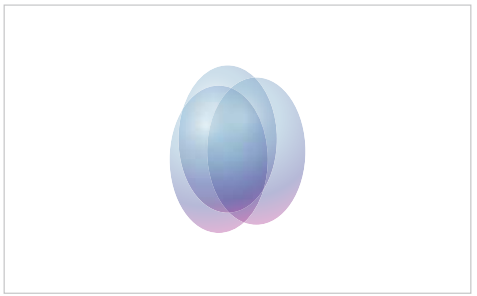

The behaviour of the n-particle matrix element in the overlapping regime is merely a manifestation of the effects of Bose attraction and Pauli blocking for identical bosons and fermions, respectively.

It is less trivial that the wave-packet formalism reproduces another intuitively evident result that the identical non-interacting bosons (fermions) with the same momenta and the same spin projections do not condense (may well coexist) if they are separated by a sufficiently large space-time interval. This result cannot be understood within the framework of the plane-wave approach.

We will return to this conceptually important issue in order to clarify the exact meaning of the words "sufficiently large space-time interval".

7.7 Relativistic Gaussian packets (RGP).

In further consideration we will use a simple model of the QFT WP state – relativistic Gaussian packet (RGP), in which the form-factor function $\phi(\mathbf{k},\mathbf{p})$ is of the form

$$\boxed{\phi(\mathbf{k},\mathbf{p}) = \frac{2\pi^2}{\sigma^2 K_1(m^2/2\sigma^2)} \exp\left(-\frac{E_\mathbf{k}E_\mathbf{p} - \mathbf{kp}}{2\sigma^2}\right) \stackrel{\text{def}}{=} \phi_G(\mathbf{k},\mathbf{p}),} \tag{21}$$

where K_1 is the modified Bessel function of the 3rd kind of order 1.

$$K_1(z) = z\int_1^\infty dt e^{-zt}\sqrt{t^2-1} \qquad \left(|\arg z| < \frac{\pi}{2}\right).$$

One can check that the function (21) has the correct plane-wave limit and satisfies the normalization conditions.

In what follows we assume $\boxed{\sigma^2 \ll m^2.}$ Then the function (21) can be rewritten as an asymptotic expansion:

$$\phi_G(\mathbf{k},\mathbf{p}) = \frac{2\pi^{3/2}}{\sigma^2}\frac{m}{\sigma}\exp\left[\frac{(k-p)^2}{4\sigma^2}\right]\left[1+\frac{3\sigma^2}{4m^2}+\mathcal{O}\left(\frac{\sigma^4}{m^4}\right)\right].$$

In the nonrelativistic case, $(|\mathbf{k}|+|\mathbf{p}|)^2 \ll 4m^2$, and only in this case this form factor coincides, up to a normalization factor, with the usual (noncovariant) Gaussian distribution:

$$\varphi_G(\mathbf{k}-\mathbf{p}) \propto \exp\left[-\frac{(\mathbf{k}-\mathbf{p})^2}{4\sigma^2}\right].$$

But it is not the case at relativistic and especially ultrarelativistic momenta, when the functions ϕ_G and φ_G significantly differ from each other.

7.7.1 Example: ultrarelativistic case.

In the UR limit ($\mathbf{p}^2 \gg m^2$, $\mathbf{k}^2 \gg m^2$) the function $\phi_G(\mathbf{k},\mathbf{p})$ behaves as

$$\phi_G(\mathbf{k},\mathbf{p}) \approx \frac{2\pi^{3/2}}{\sigma^2}\frac{m}{\sigma}\exp\left[-\frac{m^2\left(|\mathbf{k}|-|\mathbf{p}|\right)^2}{4\sigma^2|\mathbf{k}||\mathbf{p}|}-\frac{(1-\cos\theta)\,|\mathbf{k}||\mathbf{p}|}{2\sigma^2}\right] \equiv \phi_G^{\mathsf{UR}}(\mathbf{k},\mathbf{p}),$$

where θ is the angle between the vectors $\mathbf{k}$ and $\mathbf{p}$.

In particular, for $\theta = 0$ and $\pi/2$ we have

$$\phi_G^{\mathsf{UR}}\Big|_{\theta=0} \propto \exp\left[-\frac{(\mathbf{k}-\mathbf{p})^2}{4\sigma^2\Gamma_{\mathbf{k}}\Gamma_{\mathbf{p}}}\right] \quad \text{and} \quad \phi_G^{\mathsf{UR}}\Big|_{\theta=\pi/2} \propto \exp\left[-\frac{|\mathbf{k}||\mathbf{p}|}{2\sigma^2}\right].$$

In the first case, the relativistic effect consists in a widening of the packet (in comparison with the NR case) in the momentum space ("renormalization" of the WP width):

$$\sigma \longmapsto \sigma\sqrt{\Gamma_{\mathbf{k}}\Gamma_{\mathbf{p}}}.$$

This effect is essential for the neutrino production and absorption processes involving relativistic particles.

7.7.2 Plane-wave limit.

To illustrate the importance of the correct normalization it is useful to verify that the limit of $\phi_G(\mathbf{k},\mathbf{p})$ as $\sigma \to 0$ is indeed $\propto \delta(\mathbf{k}-\mathbf{p})$. To do this it is sufficient to prove that for any smooth function $F(\mathbf{k})$

$$\lim_{\sigma\to 0}\int \frac{d\mathbf{k}\,\phi_G(\mathbf{k},\mathbf{0})}{(2\pi)^3 2E_{\mathbf{k}}}\,F(\mathbf{k}) = F(\mathbf{0}). \tag{22}$$

The left part of the latter equality can be transformed to the following form

$$\lim_{\sigma\to 0}\frac{m}{(4\pi)^{3/2}\sigma^3}\int d\Omega_{\mathbf{k}}\int_0^\infty d|\mathbf{k}|\,\frac{\mathbf{k}^2}{E_{\mathbf{k}}}\exp\left[-\frac{m^2}{2\sigma^2}\left(\frac{E_{\mathbf{k}}}{m}-1\right)\right]F(\mathbf{k})$$

$$= \lim_{\sigma\to 0}\left(\frac{m^2}{4\pi\sigma^2}\right)^{3/2}\int d\mathbf{n}\int_0^\infty dt\exp\left(-\frac{m^2 t}{2\sigma^2}\right)\sqrt{t(t+2)}\,F\left(m\sqrt{t(t+2)}\,\mathbf{n}\right),$$

where $\mathbf{n}=\mathbf{k}/|\mathbf{k}|$. In order to estimate the integral in t one can use the famous formula[a]

$$\int_0^\infty dt t^{a-1}e^{-\nu t}f(t) \sim \nu^{-a}\Gamma(a)f(0)\,[1+o(1)] \qquad (a>0,\ \nu\to\infty), \tag{23}$$

which is valid for arbitrary continuous function $f(t)$, $t\in[0,\infty)$. Since in our case

$$a=\frac{3}{2},\quad \nu=\frac{m^2}{2\sigma^2} \quad \text{and} \quad f(t)=\sqrt{t+2}\,F\left(m\sqrt{t(t+2)}\,\mathbf{n}\right),$$

the identity (22) becomes evident.

As a result we see that the function $\phi_G(\mathbf{k},\mathbf{p})$ actually represents the simplest model of the form factor satisfying all the conditions imposed to the generic function $\phi(\mathbf{k},\mathbf{p})$.

[a] See, e.g., М. В. Федорюк. Метод перевала. М.: Наука. 1977.

7.7.3 Function $\psi_G(\mathbf{p}, x)$.

The function $\psi(\mathbf{p}, x)$ in the RGP model is

$$\psi(\mathbf{p}, x) = \frac{K_1(\zeta m^2/2\sigma^2)}{\zeta K_1(m^2/2\sigma^2)} \stackrel{\text{def}}{=} \psi_G(\mathbf{p}, x).$$

Here we have defined the dimensionless Lorentz-invariant complex variable

$$\zeta = \sqrt{1 - \frac{4\sigma^2}{m^2}\,[\sigma^2 x^2 + i(px)]};$$

$$|\zeta|^4 = \left[1 - \frac{4\sigma^4 x^2}{m^2}\right]^2 + \frac{16\sigma^4 (px)^2}{m^4},$$

$$\varphi = \arg\zeta = -\frac{1}{2}\arcsin\left[\frac{4\sigma^2(px)}{m^2|\zeta|^2}\right].$$

It can be proved that for any $\mathbf{p}$ and x

$$|\zeta| \geq 1 \quad \text{and} \quad |\varphi| < \pi/2.$$

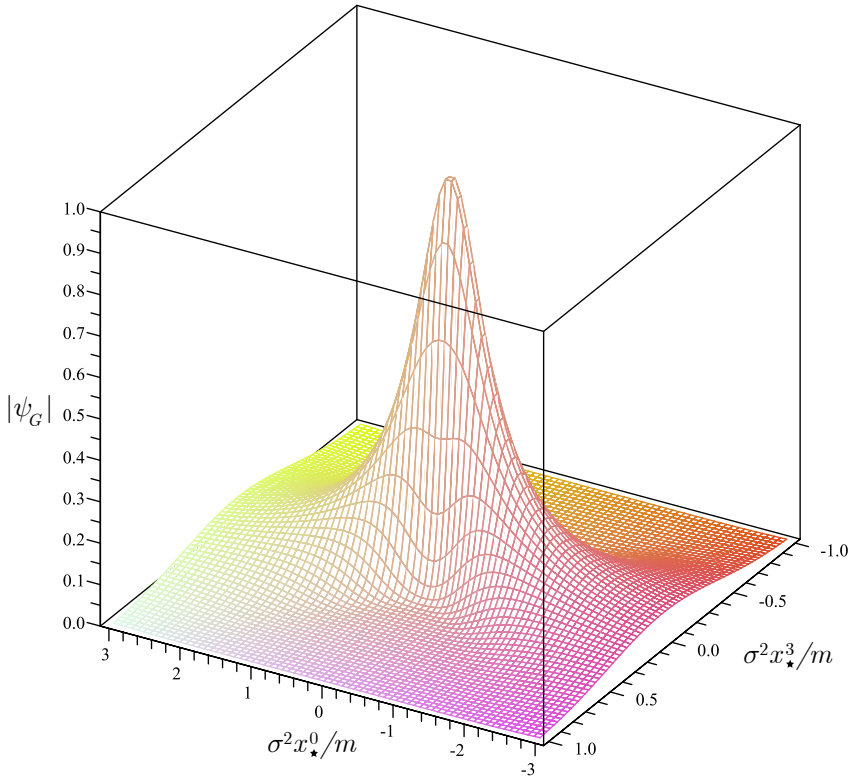

A 3D plot of $|\psi_G(\mathbf{0}, x_\star)|$ as a function of $\sigma^2 x^0_\star/m$ and $\sigma^2 x^3_\star/m$ [assuming that $\mathbf{x}_\star = (0, 0, x^3_\star)$]. The calculations are done for $\sigma/m = 0.1$.

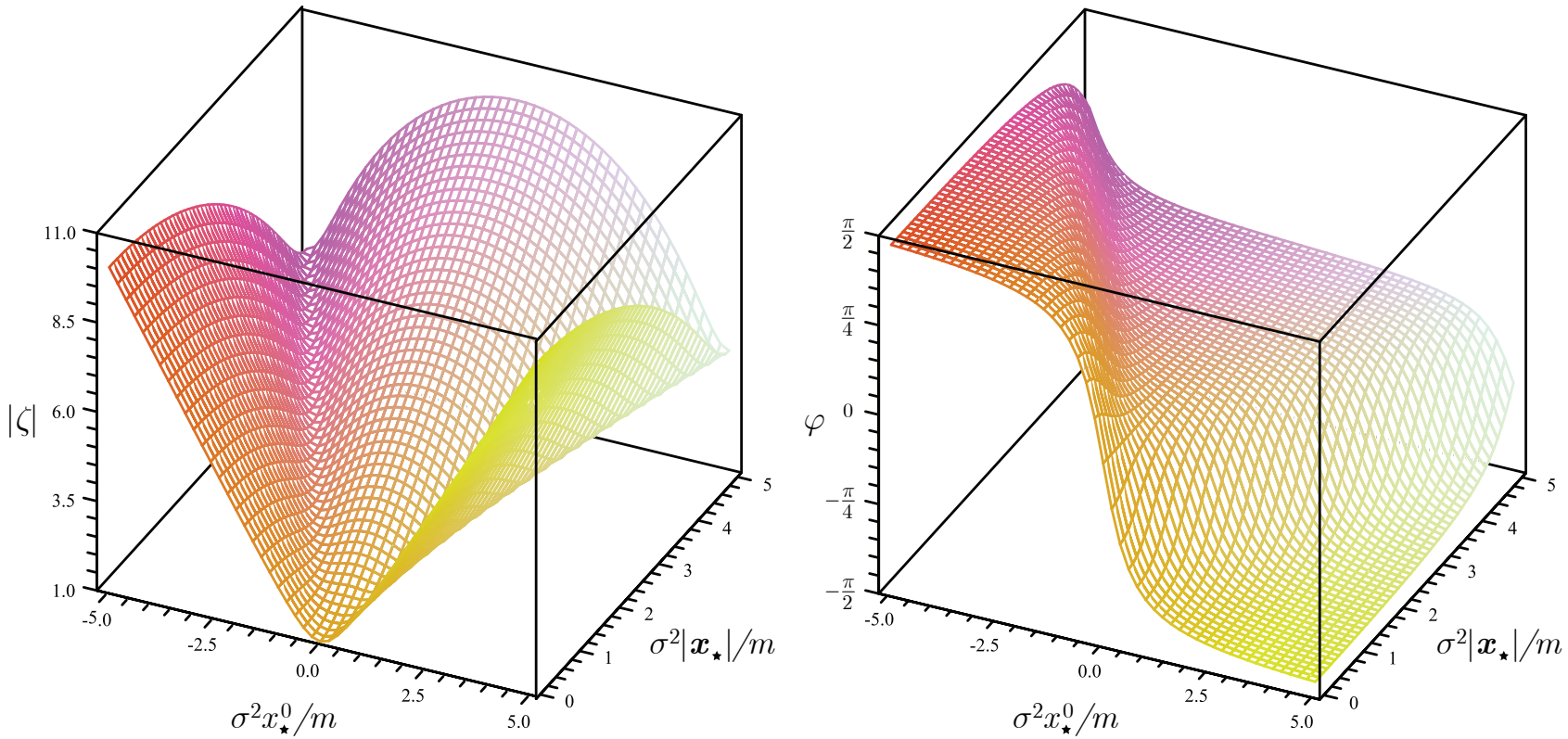

3D plots of $|\zeta|$ and $\varphi = \arg\zeta$ as functions of $\sigma^2 x^0_\star/m$ and $\sigma^2 x^3_\star/m$ [assuming that $\mathbf{x}_\star = (0, 0, x^3_\star)$]. The calculations are done for $\sigma/m = 0.1$.

Training

It is useful to ascertain that the function ψ_G satisfies the Klein-Gordon equation. Taking into account that

$$K_0'(z) = -K_1(z) \quad \text{and} \quad K_1'(z) = -K_0(z) - K_1(z)/z,$$

we find

$$\partial_\mu \left[\frac{K_1(z)}{z}\right] = -\left[K_0(z) + \frac{2}{z}K_1(z)\right]\frac{\partial_\mu z}{z}, \quad \text{where} \quad z = m^2\zeta/(2\sigma^2),$$

$$\Downarrow$$

$$\Box\left[\frac{K_1(z)}{z}\right] = \left[K_0(z) + \frac{2}{z}K_1(z)\right]\frac{\Box z}{z} - \left[\frac{3}{z}K_0(z) + \left(1 + \frac{6}{z^2}\right)K_1(z)\right]\frac{(\partial_\mu z)(\partial^\mu z)}{z}. \quad (24)$$

Next step:

$$\partial_\mu z = -\frac{m^2}{\sigma^2 z}\left(\sigma^2 x_\mu + \frac{i}{2}p_\mu\right)$$

$$\Downarrow$$

$$\Box z = -\partial_\mu\partial^\mu z = \frac{3m^2}{z} \quad \text{and} \quad (\partial_\mu z)(\partial^\mu z) = -m^2.$$

Substituting these identities into Eq. (24) and taking into account the explicit form of ψ_G we see that

$$(\Box - m^2)\psi_G = 0.$$

7.7.4 Nondiffluent regime. Contracted RGP (CRGP).

An analysis of the asymptotic expansion of $\ln\left[\psi_G(\mathbf{0},x_\star)\right]$ in powers of $\sigma^2/(m^2\zeta)$ provides the necessary and sufficient conditions of the nondiffluent behavior.

Due to the inequalities

$$|\zeta|\geq 1,\quad |\varphi|<\pi/2,\quad \text{and}\quad \sigma^2\ll m^2,$$

one can use the asymptotic expansion

$$K_1(z)\sim\sqrt{\frac{\pi}{2z}}\,e^{-z}\left[1+\frac{3}{8z}+\frac{15}{2(8z)^2}+\mathcal{O}\left(\frac{1}{z^3}\right)\right]\qquad\left(|\arg z|<\frac{3\pi}{2}\right),\tag{25}$$

which gives

$$\psi_G(\mathbf{p},x)=\frac{1}{\zeta^{3/2}}\exp\left[\frac{m^2(1-\zeta)}{2\sigma^2}\right]\left[1-\frac{3\sigma^2}{4m^2}\left(1-\frac{1}{\zeta}\right)+\frac{3\sigma^4}{32m^4}\left(1-\frac{1}{\zeta}\right)\left(11+\frac{5}{\zeta}\right)+\mathcal{O}\left(\frac{\sigma^6}{m^6}\right)\right].$$

This formula is valid for any $\mathbf{p}$ and x, but it is still too involved for our aims. Under additional restrictions the above expression can be essentially simplified by using an expansion of the variable ζ in powers of the small parameter σ^2/m^2. In the rest frame of the packet we obtain

$$\begin{aligned}\ln\left[\psi_G(\mathbf{0},x_\star)\right]=imx_\star^0&\left[1+\frac{3\sigma^2}{m^2}-\frac{\sigma^4}{m^4}\left(2m^2\mathbf{x}_\star^2-\frac{3}{2}\right)\right]\\&-\sigma^2\mathbf{x}_\star^2-\frac{3\sigma^4}{m^2}\left[(x_\star^0)^2+\mathbf{x}_\star^2\right]+\mathcal{O}\left(\frac{\sigma^6}{m^6}\right).\end{aligned}\tag{26}$$

We see that $|\psi_G(\mathbf{0},x_\star)|$ depends on time only in the $\mathcal{O}\left(\sigma^4/m^4\right)$ order.

An elementary analysis suggests that the asymptotic series (26) can be truncated by neglecting the $\mathcal{O}\left(\sigma^4/m^4\right)$ terms under the following (necessary and sufficient) conditions:

$$\boxed{\sigma^2(x^0_\star)^2 \ll m^2/\sigma^2, \quad \sigma^2|\mathbf{x}_\star|^2 \ll m^2/\sigma^2.} \tag{27a}$$

They can be rewritten in the equivalent but explicitly Lorentz-invariant form:

$$\boxed{(px)^2 \ll m^4/\sigma^4, \quad (px)^2 - m^2x^2 \ll m^4/\sigma^4.} \tag{27b}$$

Under these conditions $\psi_G(\mathbf{p},x)$ reduces to the very simple and transparent result:

$$\begin{aligned}\psi_G(\mathbf{p},x) &= \exp\left(imx^0_\star - \sigma^2\mathbf{x}^2_\star\right)\\ &= \exp\left\{iE\left(x_0 - \mathbf{v_p}\mathbf{x}\right) - \sigma^2\Gamma^2_\mathbf{p}\left[\left(\mathbf{x} - \mathbf{v_p}x_0\right)^2 - \left(\mathbf{v_p}\times\mathbf{x}\right)^2\right]\right\}\\ &= \exp\left[iE\left(x_0 - \mathbf{v_p}\mathbf{x}\right) - \sigma^2\Gamma^2_\mathbf{p}\left(\mathbf{x}_\parallel - \mathbf{v_p}x_0\right)^2 - \sigma^2\mathbf{x}^2_\perp\right]\\ &= \exp\left\{i(px) - (\sigma/m)^2\left[(px)^2 - m^2x^2\right]\right\}.\end{aligned} \tag{28}$$

Some properties of CRGP:

1. The mean coordinate of the packet follows the classical trajectory (CT) $\mathbf{x} = \mathbf{v_p}x_0$.
2. $|\psi_G(\mathbf{p},x)| = 1$ along the CT and $|\psi_G(\mathbf{p},x)| < 1$ with any deviation from it.
3. $|\psi_G(\mathbf{p},x)|$ is invariant under the transformations $\{x_0 \longmapsto x_0 + \tau,\ \mathbf{x} \longmapsto \mathbf{x} + \mathbf{v_p}\tau\}$.
4. The nonrelativistic limit of (28) is $\psi^{(\mathsf{NR})}_G(\mathbf{p},x) \approx \exp\left[im\left(x_0 - \mathbf{v_p}\mathbf{x}\right) - \sigma^2\left|\mathbf{x} - \mathbf{v_p}x_0\right|^2\right]$.

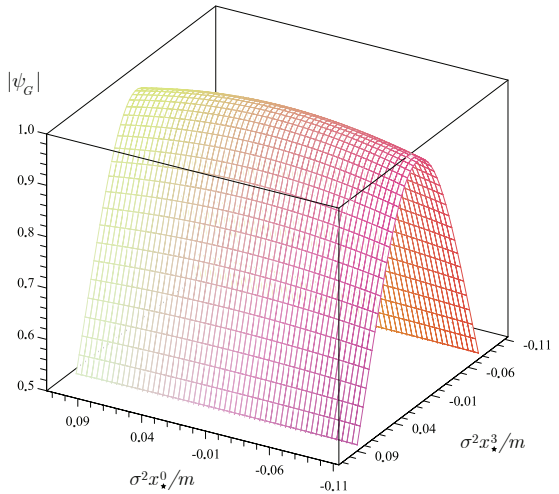

A 3D plot of $|\psi_G(\mathbf{0}, x_\star)|$ in the small vicinity of the maximum as a function of $\sigma^2 x^0_\star/m$ and $\sigma^2 x^3_\star/m$ [assuming that $\mathbf{x}_\star = (0, 0, x^3_\star)$]. The calculations are done for $\sigma/m = 0.1$.

The CRGP model permits to check the validity of the condition (18) necessary for the applicability of the factorization formula (17) – an essential element of the formalism. As is follows from the explicit form of $\psi_G(\mathbf{p}, x)$ in the CRGP approximation,

$$i\nabla_{\mathbf{x}} \ln \psi_G(\mathbf{p}, x) = \mathbf{p} + 2i\frac{\sigma^2}{m^2}\left[(px)\mathbf{p} - m^2\mathbf{x}\right].$$

Therefore the condition (18) can be written in the form

$$\left|(pX)\mathbf{p} - m^2\mathbf{X}\right| \ll \left(m^2/\sigma^2\right) E_{\mathbf{p}}, \qquad (29)$$

where $X = (X_0, \mathbf{X}) = (y_0 - x_0, \mathbf{y} - \mathbf{x})$. Then the elementary algebra yields

$$\begin{aligned}\left|(pX)\mathbf{p} - m^2\mathbf{X}\right|^2 &= (pX)^2\mathbf{p}^2 - 2m^2(pX)(\mathbf{pX}) + m^4\mathbf{X}^2 \\ &= (pX)^2 E_{\mathbf{p}}^2 + m^2\left[(\mathbf{pX})^2 + m^2\mathbf{X}^2 - E_{\mathbf{p}}^2 X_0^2\right] \\ &\le (pX)^2 E_{\mathbf{p}}^2 + m^2\left(\mathbf{p}^2\mathbf{X}^2 + m^2\mathbf{X}^2 - E_{\mathbf{p}}^2 X_0^2\right).\end{aligned}$$

As a result we have proved that

$$\left|(pX)\mathbf{p} - m^2\mathbf{X}\right| \le E_{\mathbf{p}}\sqrt{(pX)^2 - m^2X^2}.$$

Therefore the inequality (29) is not an independent condition but is satisfied automatically in the CRGP approximation.

It can be also proved that the quantum correction to the classical momentum vanishes on the classical trajectory $\mathbf{X} = \mathbf{v}_{\mathbf{p}} X_0$.

7.7.5 Function $\mathcal{D}_G(\mathbf{p},\mathbf{q};x)$

One can derive the explicit formula for the commutation function:

$$\mathcal{D}(\mathbf{p},\mathbf{q};x) = 2m\mathrm{V}_\star \frac{K_1(zm^2/\sigma^2)}{zK_1(m^2/\sigma^2)} \stackrel{\text{def}}{=} \mathcal{D}_G(\mathbf{p},\mathbf{q};x),$$

$$z = \frac{E_*}{m}\sqrt{1-\frac{\sigma^2}{E_*^2}\left[\sigma^2 x_*^2 + 2iE_* x_*^0\right]} = \frac{1}{2m}\sqrt{(p+q)^2 - 4\sigma^2\left[\sigma^2 x^2 + i(p+q)x\right]}.$$

The module and phase of z are determined by

$$|z|^4 = \frac{1}{4}\left(1+\frac{pq-2\sigma^4x^2}{m^2}\right)^2 + \left[\frac{\sigma^2(p+q)x}{m^2}\right]^2, \quad \arg z = -\frac{1}{2}\arcsin\left[\frac{\sigma^2(p+q)x}{m^2|z|^2}\right].$$

From these relations it can be proved that

$$|z| \geq E_*/m \geq 1 \quad \text{and} \quad |\arg z| < \pi/2.$$

Owing to these inequalities and condition $\sigma^2 \ll m^2$, we can write the asymptotic expansion:

$$\mathcal{D}_G(\mathbf{p},\mathbf{q};x) = \frac{2m\mathrm{V}_\star}{z^{3/2}}\exp\left[\frac{m^2(1-z)}{\sigma^2}\right]\left[1-\frac{3\sigma^2}{8m^2}\left(1-\frac{1}{z}\right)\right.$$
$$\left.+\frac{3\sigma^4}{128m^4}\left(1-\frac{1}{z}\right)\left(11+\frac{5}{z}\right)+\mathcal{O}\left(\frac{\sigma^6}{m^6}\right)\right].$$

The self-consistency demands to write down the approximation of this formula which would be accordant with the CRGP approximation for the function $\psi_G(\mathbf{p}, x)$.

$$z = \frac{E_*}{m}\left(1 + \frac{\sigma^4 \mathbf{x}_*^2}{2E_*^2}\right) - i\frac{\sigma^2 x_*^0}{m}\left(1 - \frac{\sigma^4 \mathbf{x}_*^2}{2E_*^2}\right) + \mathcal{O}\left(\frac{\sigma^8}{m^8}\right).$$

$$\Downarrow$$

$$\begin{aligned}\ln\left[\frac{\mathcal{D}_G(\mathbf{p}_*, -\mathbf{p}_*; x_*)}{2m\mathrm{V}_\star}\right] = {} & \frac{3}{2}\ln\left(\frac{m}{E_*}\right) - \frac{m(E_* - m)}{\sigma^2} - \frac{m\sigma^2 \mathbf{x}_*^2}{2E_*} + \frac{3\sigma^2(E_* - m)}{8mE_*} \\ & + imx_*^0\left\{1 + \frac{3\sigma^2}{2mE_*}\left[1 + \frac{\sigma^2}{4mE_*}\left(1 - \frac{4}{3}m^2\mathbf{x}_*^2\right)\right]\right\} \\ & - \frac{3\sigma^4}{4m^2E_*^2}\left\{m^2\left[(x_*^0)^2 + \mathbf{x}_*^2\right] - \frac{P_*^2}{4m^2}\right\} + \mathcal{O}\left(\frac{\sigma^6}{m^6}\right).\end{aligned}$$

It is now seen that, under the conditions [equivalent to those for the function $\psi_G(\mathbf{p}, x)$]

$$\boxed{\sigma^2(x_*^0)^2 \ll E_*^2/\sigma^2 \quad \text{and} \quad \sigma^2\mathbf{x}_*^2 \ll E_*^2/\sigma^2,} \tag{30}$$

one can retain only the four leading terms in powers of σ^2/m^2, finally obtaining:

$$\boxed{\mathcal{D}_G(\mathbf{p}_*, -\mathbf{p}_*; x_*) = \frac{2m\mathrm{V}_\star}{\Gamma_*^{3/2}}\exp\left[imx_*^0 - \frac{m^2(\Gamma_* - 1)}{\sigma^2} - \frac{\sigma^2\mathbf{x}_*^2}{2\Gamma_*}\right],} \tag{31}$$

where $\Gamma_* = E_*/m$ (Lorentz factor of CIF) and $\mathrm{V}_\star = [\pi/(2\sigma^2)]^{3/2}$ (effective volume).

Hence, as expected, $\mathcal{D}_G(\mathbf{p}_*, -\mathbf{p}_*; x_*)$ quickly vanishes when either $|\mathbf{p}_*|$ or $|\mathbf{x}_*|$ (or both) are large enough.

Some scarcely foreseeable features:

- The dependence of $|\mathcal{D}_G|$ on variables x_0 and $\mathbf{x}$ disappears for the classical trajectories $\mathbf{x} = \mathbf{v_p} x_0$;
- $|\mathcal{D}_G|/(2m\mathrm{V}_\star)$ exponentially vanishes at sub-relativistic energies ($\Gamma_* - 1 \sim 1$) and is nearly independent of $\mathbf{x}_*$ at ultrarelativistic energies ($\Gamma_* - 1 \gg 1$).
- For the nonrelativistic energies one gets (after transforming into the lab. frame)

$$\mathcal{D}_G(\mathbf{p}, \mathbf{q}; x) \approx 2m\mathrm{V}_\star \exp\left[im\,(x_0 - \mathbf{v}\mathbf{x}) - \frac{m^2}{8\sigma^2}\,|\mathbf{v_p} - \mathbf{v_q}|^2 - \frac{\sigma^2}{2}\,|\mathbf{x} - \mathbf{v}x_0|^2\right],$$

$$\left[\mathbf{v_p} = \mathbf{p}/m, \quad \mathbf{v_q} = \mathbf{q}/m, \quad \mathbf{v} = \tfrac{1}{2}\,(\mathbf{v_p} + \mathbf{v_q}), \qquad |\mathbf{v_p}| \ll 1, \;\; |\mathbf{v_q}| \ll 1\right]$$

  The term $\propto (m^2/\sigma^2)$ yet can be large (if $\mathbf{v_p} \neq \mathbf{v_q}$ and σ is small enough).

The correspondence principle:

All these nice features fade away in the plane-wave limit since (as it can be proved),

$$\lim_{\sigma \to 0} \mathcal{D}_G(\mathbf{p}, \mathbf{q}; x) = (2\pi)^3 2E_\mathbf{p} \delta(\mathbf{p} - \mathbf{q}) e^{ipx}.$$

7.7.6 Multi-packet matrix elements (examples).

Consider the ME $\langle \{\mathbf{p}, s, x\}_n \,|\, \{\mathbf{p}, s, x\}_n \rangle$ with equal momenta ($\mathbf{p}_i = \mathbf{p}$, $\forall i$) for $n = 2$ and 3.
In the CIF, which coincides now with the rest frame (the same for all 1-packet "sub-states")

$$\langle \{\mathbf{p}, s, x\}_2 \,|\, \{\mathbf{p}, s, x\}_2 \rangle = (2m\mathrm{V}_\star)^2 \left[1 \pm \delta_{s_1 s_2} \exp\left(-\sigma^2 |\mathbf{x}_1^\star - \mathbf{x}_2^\star|^2\right)\right],$$

$$\langle \{\mathbf{p}, s, x\}_3 \,|\, \{\mathbf{p}, s, x\}_3 \rangle = (2m\mathrm{V}_\star)^3 \left[1 \pm \sum_{i<j} \delta_{s_i s_j} \exp\left(-\sigma^2 |\mathbf{x}_i^\star - \mathbf{x}_j^\star|^2\right) + 2\delta_{s_1 s_2}\delta_{s_2 s_3}\delta_{s_3 s_1} \exp\left(-\frac{\sigma^2}{2} \sum_{i<j} |\mathbf{x}_i^\star - \mathbf{x}_j^\star|^2\right)\right].$$

So the effects of Bose-Einstein attraction and Pauli repulsion, appearing when $s_i = s_j$ for any pair (i, j), are only essential at short distances satisfying

$$\sigma^2 |\mathbf{x}_i^\star - \mathbf{x}_j^\star|^2 \lesssim 1.$$

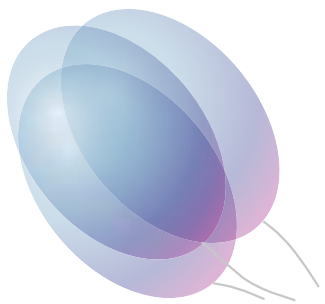

In other words, both effects are essential when the spatial distance between the identical one-packet states (measured in their common rest frame) is comparable with or shorter than the packet's dimension.

In the lab. frame the "attraction/repulsion regions" is restricted by the following condition:

$$\left|\mathbf{x}_i - \mathbf{x}_j - \mathbf{v}\left(x_i^0 - x_j^0\right)\right|^2 - |\mathbf{v} \times (\mathbf{x}_i - \mathbf{x}_j)|^2 \lesssim \mathrm{V}^{2/3}(\mathbf{p}) \qquad (\mathbf{v} = \mathbf{p}/E_\mathbf{p}).$$

7.7.7 Effective dimensions & momentum uncertainty of CRGP.

In the CRGP approximation, the effective volume is explicitly calculated to be

$$\mathrm{V}(\mathbf{0}) \approx \mathrm{V}_\star = \frac{2\pi^2 m K_1(m^2/\sigma^2)}{\sigma^2 \left[K_1(m^2/2\sigma^2)\right]^2} \approx \left(\frac{\pi}{2\sigma^2}\right)^{3/2}.$$

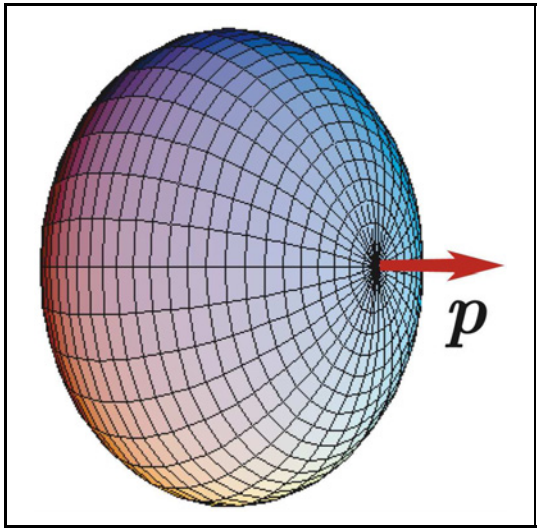

In the RF of the packet, one can define its effective size as the diameter $d_\star$ of a ball of volume $\mathrm{V}_\star$,

$$d_\star = \left(\frac{6\mathrm{V}_\star}{\pi}\right)^{1/3} \approx \left(\frac{9\pi}{2}\right)^{1/6} \frac{1}{\sigma} \approx \frac{1.555}{\sigma}.$$

Then, in the lab. frame, the effective size of the packet along its momentum $\mathbf{p}$ is $d_\star/\Gamma_{\mathbf{p}}$. The pictorial model of the packet is therefore an oblate spheroid with the transversal diameter of about $1.555/\sigma$ and eccentricity of $1/\Gamma_{\mathbf{p}}$.

The volume density difference between the center and effective edge of any wave packet does not depend on mass and spread and is $\exp[(\sigma d_\star)^2/2] = \exp[(9\pi/16)^{1/3}] \approx 3.350$.

The momentum uncertainty can be evaluated as follows:

$$\begin{cases} |\delta\mathbf{p}_T|^2 = \dfrac{2}{3}\,|\delta\mathbf{p}_\star|^2 \approx 4\ln 2\,\sigma^2, \\ |\delta\mathbf{p}_L|^2 = \dfrac{1}{3}\,|\delta\mathbf{p}_\star|^2 \Gamma_{\mathbf{p}}^2 \approx 2\ln 2\,\sigma^2 \Gamma_{\mathbf{p}}^2, \end{cases} \Longrightarrow \boxed{|\delta\mathbf{p}| \approx \sqrt{2\ln 2\,(\Gamma_{\mathbf{p}}^2+2)}\,\sigma.}$$

7.7.8 The range of applicability of CRGP.

The inherent (probably inaccessible in reality) "upper limit" for the packet dimension, $d_\star^{\max}$, for an unstable particle is of the order of its decay length $c\tau$ (which is macroscopic for long-lived particles), while the "lower limit", $d_\star^{\min}$, is just the size of the particles composing the packet: ~ 1 fm for hadrons and $\sim 1/m$ (the Compton wavelength) for the structureless particles (leptons, gauge bosons). Any rate, due to the general restriction $\sigma^2 \ll m^2$, the permissible in the formalism dimension of the packet must be much larger than $d_\star^{\min}$.

But, for unstable particles, the conditions of applicability of the CRGP approximation (27) impose an additional and rather strong restriction to the maximum permissible value of the parameter σ. These condition should be valid during at least the life of the particle that is for

$$0 \leq |x_\star^0| \lesssim \tau = 1/\Gamma.$$

Therefore the following condition is necessary: $\sigma^4\tau^2 \ll m^2$. So $\sigma_{\max} = \sqrt{m/\tau} = \sqrt{m\Gamma}$ is the absolute upper limit for the permissible in CRGP values of σ. Correspondingly, the value

$$d_\star^{\min} = \left(\frac{9\pi}{2}\right)^{1/6} \frac{1}{\sigma_{\max}} = \left(\frac{9\pi}{2}\right)^{1/6} \left(\frac{\tau}{m}\right)^{1/2}$$

is the lower limit for the spatial dimension of the packet. Next, since we consider just the quasistable packets, σ must be much larger than Γ (or, more precisely, $\sigma^2 \gg \Gamma^2$).
Finally the combined range of applicability is given by

$$\boxed{\Gamma^2 \ll \sigma^2 \ll m\Gamma \ll m^2.}$$

Table: Maximum permissible values of σ ($\sigma_{\max} = \sqrt{m\Gamma}$), the ratio $\Gamma/\sigma_{\max} = \sqrt{\Gamma/m}$ and minimum permissible effective dimensions $d_\star^{\min} \approx 1.55/\sqrt{m\Gamma}$ in the CRGP approximation for some particles.

Particle	$\sigma_{\max}$ (eV)	$\Gamma/\sigma_{\max}$	$d_\star^{\min}$ (cm)
$\mu^\pm$	1.78×10^{-1}	1.68×10^{-9}	1.72×10^{-4}
$\tau^\pm$	2.01×10^{3}	1.13×10^{-6}	1.53×10^{-8}
$\pi^\pm$	1.88	1.35×10^{-8}	1.63×10^{-5}
π^0	3.25×10^{4}	2.41×10^{-4}	0.94×10^{-9}
$K^\pm$	5.12	1.04×10^{-8}	5.99×10^{-6}
K_S^0	6.05×10^{1}	1.22×10^{-7}	5.07×10^{-7}
K_L^0	2.53	5.08×10^{-9}	1.21×10^{-5}
$D^\pm$	1.09×10^{3}	5.82×10^{-7}	2.82×10^{-8}
D^0	1.73×10^{3}	9.28×10^{-7}	1.77×10^{-8}
$D_s^\pm$	1.61×10^{3}	8.18×10^{-7}	1.91×10^{-8}
$B^\pm$	1.46×10^{3}	2.76×10^{-7}	2.11×10^{-8}
B^0	1.51×10^{3}	2.86×10^{-7}	2.03×10^{-8}
B_s^0	1.55×10^{3}	2.89×10^{-7}	1.98×10^{-8}
n	2.64×10^{-5}	2.81×10^{-14}	1.16
Λ	5.28×10^{1}	4.74×10^{-7}	5.81×10^{-7}
$\Lambda_c^\pm$	2.74×10^{3}	1.87×10^{-6}	1.12×10^{-8}

The maximum permissible deviation of the mean mass of CRGP from the field mass, $\delta m = \overline{m} - m$, is equal to

$$\delta m_{\max} \approx \frac{3\sigma_{\max}^2}{2m} = 1.5\Gamma,$$

So, the correction to the field mass of the short-lived resonances can be essential, but for the long-lived particles we can (and we must) to neglect the weighting effect.

7.8 Examples of macroscopic diagrams.

- The *pep* fusion

$$^1\mathrm{H} + {}^1\mathrm{H} + e^- \to {}^2\mathrm{D} + \nu_e \quad (E_\nu = 1.44\ \mathrm{MeV})$$

accounts for about 0.25% of the deuterium created in the Sun in the *pp* chain. It has a characteristic time scale $\sim 10^{12}$ yr that is larger than the age of the Universe. So it is *insignificant* in the Sun as far as energy generation is concerned. Enough *pep* fusions happen to produce a detectable number of neutrinos in Ga-Ge detectors. Hence the reaction must be accounted for by those interested in the *solar neutrino problem*.

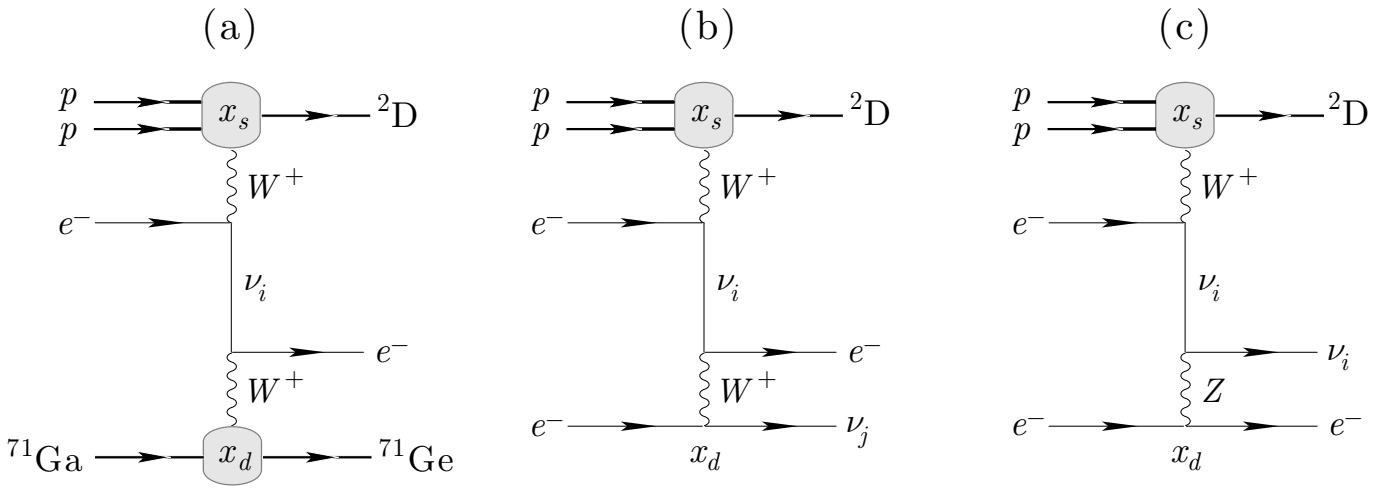

The Figure illustrates the detection of *pep* neutrinos with gallium (a) and electron (b,c) targets. Unfortunately, the current detection thresholds for electrons in SK and SNO is higher then the expected maximum of 1.44 MeV.

- The μ_{e3} decay

$$\mu^- \to e^- + \overline{\nu}_e + \nu_\mu$$

in the source can be detected through quasielastic scattering with production of $e^\pm$, $\mu^\pm$, or $\tau^\pm$; of course, only $\mu^\pm$ production is permitted in SM. The diagrams (a) and (b) are for both Dirac and Majorana (anti)neutrinos, while diagrams (c) and (d) are only for Majorana neutrinos.

In the Majorana case, the diagrams (a), (d) and (b), (c) interfere. Potentially this provides a way for distinguishing between the Dirac and Majorana cases. Unfortunately, the diagrams (c) and (d) are suppressed by a factor $\propto m_i/E_\nu$.

Dirac or Majorana

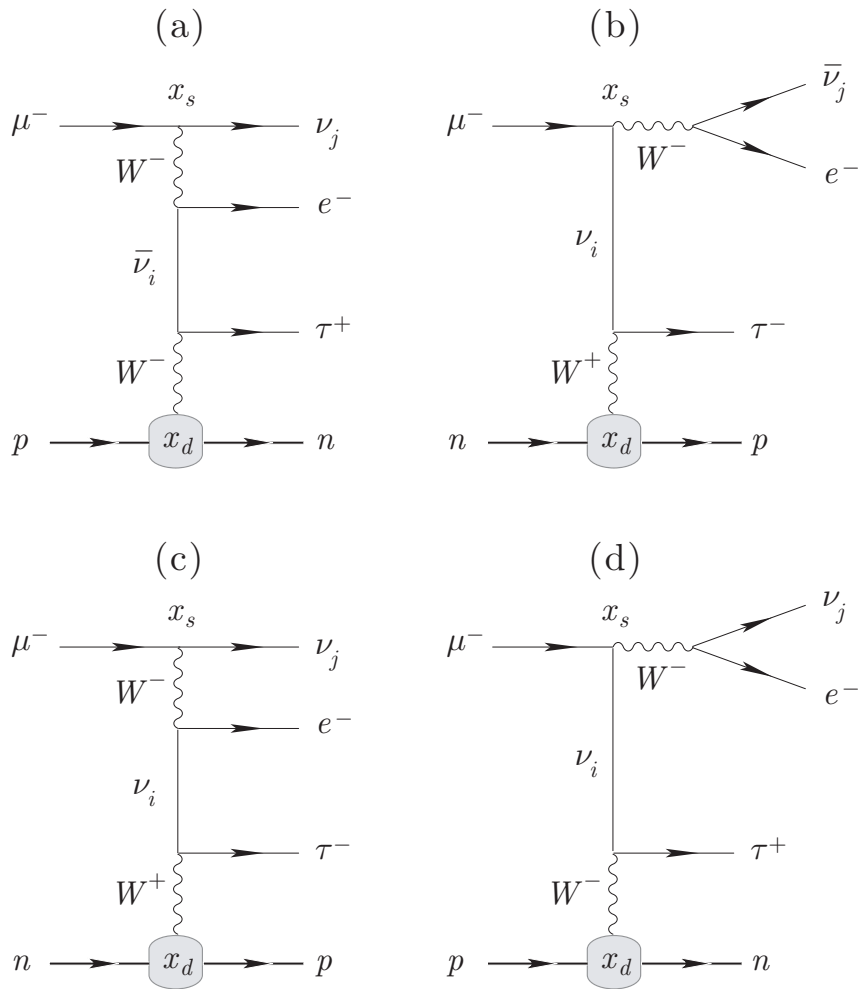

Similar diagrams can be drawn for τ_{e3} and $\tau_{\mu 3}$ decays.

7.9 Feynman rules and overlap integrals.

We will deal with the generic Feynman diagrams. ▷

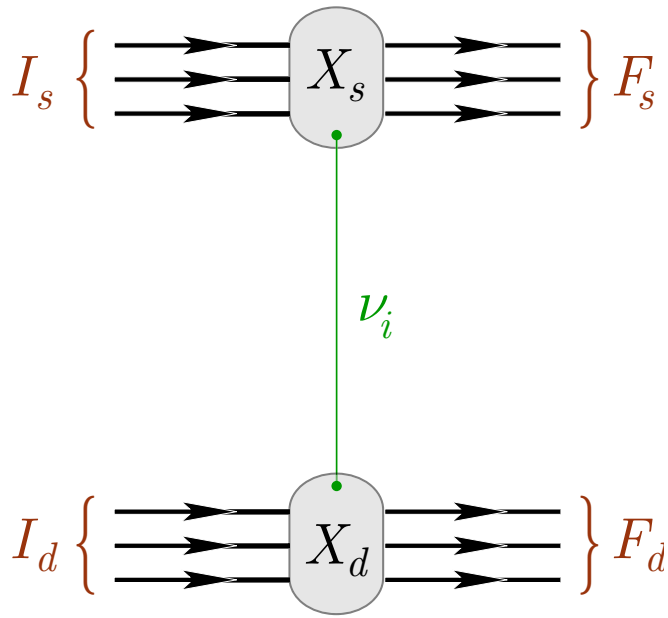

- The external legs correspond to asymptotically free incoming ("in") and outgoing ("out") WPs in the coordinate representation. Here and below: I_s (F_s) is the set of in (out) packets in the block X_s ("source"), I_d (F_d) is the set of in (out) packets in the block X_d ("detector").
- The internal line denotes the causal Green's function of the neutrino mass eigenfield ν_i ($i = 1, 2, 3, \ldots$). The blocks X_s and X_d are assumed to be macroscopically separated in space-time.
- For narrow WPs, the Feynman rules in the formalism are to be modified in a trivial way: for each external line, the *standard* (plain-wave) factor must be multiplied by

$$\begin{cases} e^{-ip_a(x_a - x)}\psi_a\left(\mathbf{p}_a, x_a - x\right) & \text{for } a \in I_s \oplus I_d, \\ e^{+ip_b(x_b - x)}\psi_b^*\left(\mathbf{p}_b, x_b - x\right) & \text{for } b \in F_s \oplus F_d, \end{cases} \tag{32}$$

  where each function $\psi_\varkappa\left(\mathbf{p}_\varkappa, x\right)$ ($\varkappa = a, b$) is specified by the mass $m_\varkappa$ and momentum spread $\sigma_\varkappa$.
- The internal lines and loops remain unchanged.

The additional factors (32) provide the following two common multipliers in the integrand of the scattering amplitude [we will call these the overlap integrals]:

$$\begin{aligned}\mathbb{V}_s(q) &= \int dx e^{+iqx}\Big[\prod_{a\in I_s} e^{-ip_a x_a}\psi_a\left(\mathbf{p}_a, x_a - x\right)\Big]\Big[\prod_{b\in F_s} e^{ip_b x_b}\psi_b^*\left(\mathbf{p}_b, x_b - x\right)\Big],\\ \mathbb{V}_d(q) &= \int dx e^{-iqx}\Big[\prod_{a\in I_d} e^{-ip_a x_a}\psi_a\left(\mathbf{p}_a, x_a - x\right)\Big]\Big[\prod_{b\in F_d} e^{ip_b x_b}\psi_b^*\left(\mathbf{p}_b, x_b - x\right)\Big].\end{aligned} \tag{33}$$

The function $\mathbb{V}_s$ ($\mathbb{V}_d$) characterizes the 4D overlap of the "in" and "out" wave-packet states in the source (detector) vertex, integrated over the infinite space-time volume.

In the plane-wave limit ($\sigma_\varkappa \to 0$, $\forall \varkappa$)

$$\mathbb{V}_s(q) \to (2\pi)^4\delta\left(q - q_s\right) \quad \text{and} \quad \mathbb{V}_d(q) \to (2\pi)^4\delta\left(q + q_d\right),$$

where q_s and q_d are the 4-momentum transfers defined by

$$q_s = \sum_{a\in I_s} p_a - \sum_{b\in F_s} p_b \quad \text{and} \quad q_d = \sum_{a\in I_d} p_a - \sum_{b\in F_d} p_b.$$

The δ functions provide the energy-momentum conservation in the vertices s and d (that is in the "subprocesses" $I_s \to F_s + \nu_i^*$ and $\nu_i^* + I_d \to F_d$) and, as a result, – in the whole process:

$$I_s \oplus I_d \to F_s \oplus F_d: \qquad \sum_{a\in I_s\oplus I_d} p_a = \sum_{b\in F_s\oplus F_d} p_b.$$

Information about the space-time coordinates of the interacting packets is completely lost.

In the general case of *nonzero* spreads σ_x, we may expect no more than an approximate conservation of energy and momentum and lack of any singularities.

To quantify this expectation, we apply the CRGP model. It is a good approximation since the main contribution to the overlap integral comes from the very narrow space-time region of intersection of the maxima of all wave packets (see schematic illustration).

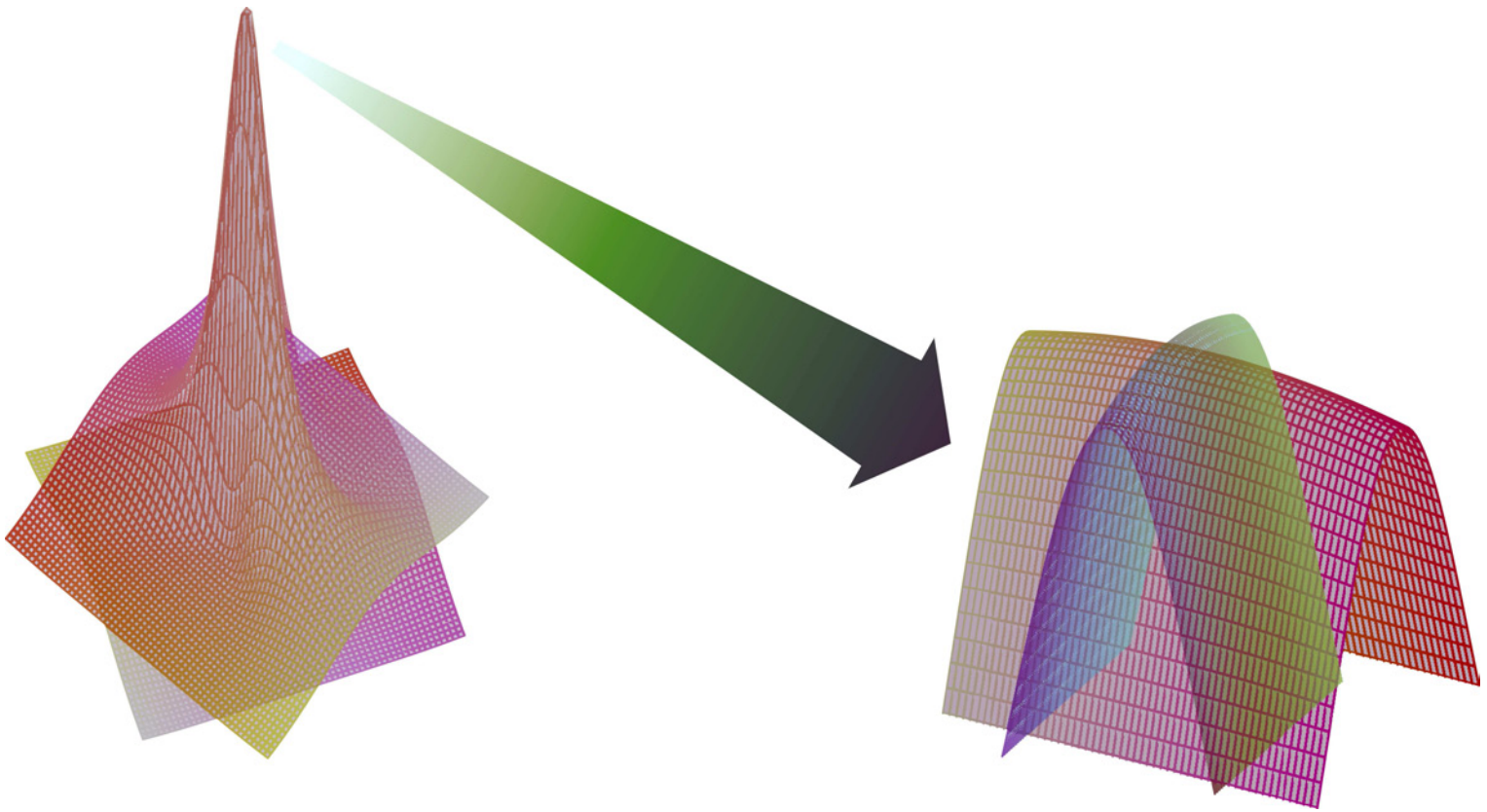

We define the tensors

$$T_{\varkappa}^{\mu\nu} \stackrel{\text{def}}{=} \sigma_{\varkappa}^{2}\,(u_{\varkappa}^{\mu}u_{\varkappa}^{\nu} - g^{\mu\nu}), \qquad [u_{\varkappa} = p_{\varkappa}/m_{\varkappa} = \Gamma_{\varkappa}(1, \mathbf{v}_{\varkappa})]$$

$$\Downarrow$$

$$\mathbb{V}_{s,d}(q) = \int dx \exp\left[i\,(\pm qx - q_{s,d}x) - \sum_{\varkappa\in S,D} T_{\varkappa}^{\mu\nu}\,(x_{\varkappa} - x)_{\mu}\,(x_{\varkappa} - x)_{\nu}\right],$$

where $S = I_s \oplus F_s$ and $D = I_d \oplus F_d$. It is useful to define the overlap tensors

$$\boxed{\mathfrak{R}_{s}^{\mu\nu} = \sum_{\varkappa\in S} T_{\varkappa}^{\mu\nu} \quad \text{and} \quad \mathfrak{R}_{d}^{\mu\nu} = \sum_{\varkappa\in D} T_{\varkappa}^{\mu\nu}.}$$

A crucial property:

$$T_{\varkappa}^{\mu\nu}x_{\mu}x_{\nu} = \sigma_{\varkappa}^{2}\left[(u_{\varkappa}x)^{2} - x^{2}\right] = \sigma_{\varkappa}^{2}\mathbf{x}_{(\varkappa)}^{2} \geq 0$$

$$\Downarrow$$

$$\mathfrak{R}_{s,d}^{\mu\nu}\,x_{\mu}x_{\nu} > 0.$$

Consequently, there exist the positive-definite tensors $\widetilde{\mathfrak{R}}_{s}^{\mu\nu}$ and $\widetilde{\mathfrak{R}}_{d}^{\mu\nu}$ such that

$$\widetilde{\mathfrak{R}}_{s,d} = ||\widetilde{\mathfrak{R}}_{s,d}^{\mu\nu}|| = g\,\mathfrak{R}_{s,d}^{-1}\,g, \quad \mathfrak{R}_{s,d} = ||\mathfrak{R}_{s,d}^{\mu\nu}||.$$

The explicit form and properties of these tensors and relevant convolutions are established (studied in detail for the most important reactions $1 \to 2,\ 1 \to 3,\ 2 \to 2$).

The overlap integrals in CRGP are the 4D Gaussian integrals in Minkowski space.

$$\mathbb{V}_{s,d}(q) = (2\pi)^4 \widetilde{\delta}_{s,d}\left(q \mp q_{s,d}\right) \exp\left[-\mathfrak{S}_{s,d} \pm i\left(q \mp q_{s,d}\right)\cdot X_{s,d}\right],$$

$$\widetilde{\delta}_{s,d}(K) = (4\pi)^{-2} |\Re_{s,d}|^{-1/2} \exp\left(-\frac{1}{4}\widetilde{\Re}^{\mu\nu}_{s,d} K_\mu K_\nu\right),$$

$$\mathfrak{S}_{s,d} = \sum_{\varkappa,\varkappa'} \left(\delta_{\varkappa\varkappa'} T^{\mu\nu}_{\varkappa} - T^{\mu}_{\varkappa\mu'}\, \widetilde{\Re}^{\mu'\nu'}_{s,d}\, T^{\nu}_{\varkappa'\nu'}\right) x_{\varkappa\mu} x_{\varkappa'\nu},$$

$$X^{\mu}_{s,d} = \widetilde{\Re}^{\mu\nu}_{s,d} \sum_{\varkappa} T^{\lambda}_{\varkappa\nu} x_{\varkappa\lambda}.$$

Physical meaning of $\widetilde{\delta}_{s,d}$, $\mathfrak{S}_{s,d}$, and $X_{s,d}$.

- From the integral representation $\widetilde{\delta}_{s,d}(K) = \int \frac{dx}{(2\pi)^4} \exp\left(-\Re^{\mu\nu}_{s,d} x_\mu x_\nu + iKx\right)$ it follows that $\widetilde{\delta}_{s,d}(K) \to \delta(K)$ in the plane-wave limit $[\sigma_\varkappa \to 0,\ \forall \varkappa \Rightarrow \widetilde{\Re}^{\mu\nu}_{s,d} \to 0]$.
  $\Longrightarrow$ just the factors $\widetilde{\delta}_s\left(q - q_s\right)$ and $\widetilde{\delta}_d\left(q + q_d\right)$ are responsible for the approximate energy–momentum conservation (with the accuracy governed by the momentum spreads of the interacting packets) in the neutrino production and detection points.

- The functions $\exp\left(-\mathfrak{S}_s\right)$ and $\exp\left(-\mathfrak{S}_d\right)$ are the geometric suppression factors conditioned by a partial overlap of the in and out WPs in the space-time regions of their interaction in the source and detector.

This can be seen after converting $\mathfrak{S}_{s,d}$ to the form[a]

$$\mathfrak{S}_{s,d} = \sum_{\varkappa} T_{\varkappa}^{\mu\nu} \left(x_\varkappa - X_{s,d}\right)_\mu \left(x_\varkappa - X_{s,d}\right)_\nu \tag{34}$$

and taking into account that both $\mathfrak{S}_{s,d}$ and $X_{s,d}$ are invariants under the group of uniform rectilinear motions (here, $\tau_\varkappa$ are arbitrary real time parameters)

$$\left\{x_\varkappa^0 \longmapsto \tilde{x}_\varkappa^0 = x_\varkappa^0 + \tau_\varkappa,\ \boldsymbol{x}_\varkappa \longmapsto \tilde{\mathbf{x}}_\varkappa = \boldsymbol{x}_\varkappa + \boldsymbol{v}_\varkappa \tau_\varkappa\right\}$$

Due to this symmetry, (34) can be rewritten as

$$\mathfrak{S}_{s,d} = \sum_{\varkappa} \sigma_\varkappa^2 \left[\left(\Gamma_\varkappa^2 - 1\right)\left(b_\varkappa^0\right)^2 + \boldsymbol{b}_\varkappa^2\right] = \sum_{\varkappa} \sigma_\varkappa^2 |\boldsymbol{b}_\varkappa^{(\varkappa)}|^2,$$

$$b_\varkappa^0 = \left(x_\varkappa^0 - X_{s,d}^0\right) - |\boldsymbol{v}_\varkappa|^{-1} \boldsymbol{n}_\varkappa \cdot \left(\boldsymbol{x}_\varkappa - \boldsymbol{X}_{s,d}\right),$$

$$\boldsymbol{b}_\varkappa = \left(\boldsymbol{x}_\varkappa - \boldsymbol{X}_{s,d}\right) - \left[\boldsymbol{n}_\varkappa \cdot \left(\boldsymbol{x}_\varkappa - \boldsymbol{X}_{s,d}\right)\right] \boldsymbol{n}_\varkappa,$$

$$\left[\boldsymbol{n}_\varkappa = \begin{cases} \boldsymbol{v}_\varkappa/|\boldsymbol{v}_\varkappa|, & \text{for } \mathbf{v}_\varkappa \neq 0, \\ 0, & \text{for } \mathbf{v}_\varkappa = 0. \end{cases}\right]$$

The 4-vector $b_\varkappa = (b_\varkappa^0, \boldsymbol{b}_\varkappa)$ is a relativistic analog of the usual impact parameter, so it is natural to call it the impact vector. [Note that $|\mathbf{b}_\varkappa| = |\mathbf{n}_\varkappa \times (\mathbf{x}_\varkappa - \mathbf{X}_{s,d})|$ for $\mathbf{v}_\varkappa \neq 0$.] The 4-vectors $X_{s,d}$ can be called, accordingly, the impact points.

[a] In this derivation we have used the translation invariance of the functions $\mathfrak{S}_{s,d}$.

The suppression of the overlap integral caused by the factors $\exp(-\mathfrak{S}_s)$ and $\exp(-\mathfrak{S}_d)$ can be small only if all the world tubes in the source/detector inter-cross each other.

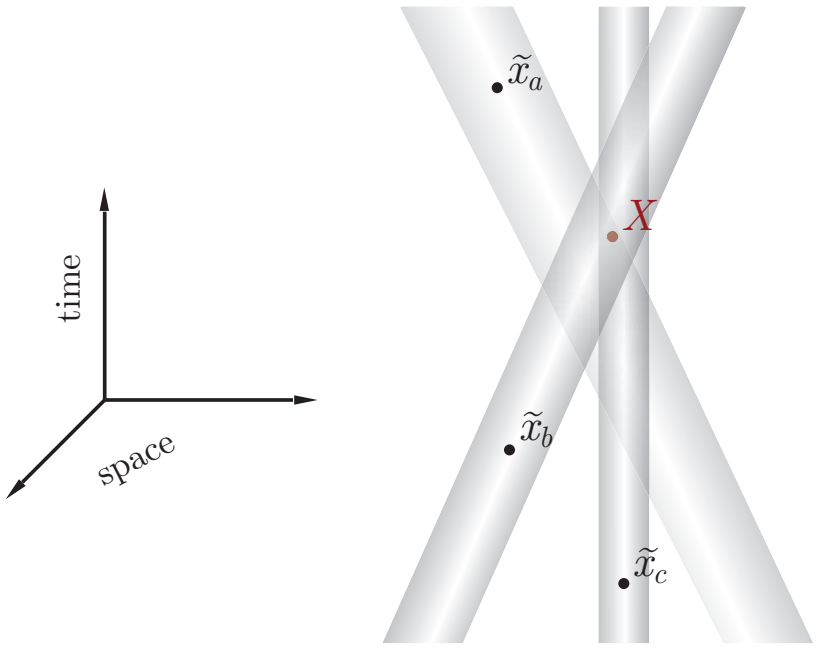

Artistic view of the "classical world tubes" of interacting wave packets. The tubes reproduce the space-time cylindrical volumes swept by the classically moving spheroids which represent the wave-packet patterns. The impact point X is defined by the velocities $\mathbf{v}_\varkappa$ of the packets and the space-time points $\tilde{x}_\varkappa = \tilde{x}_\varkappa(\tau_\varkappa)$ arbitrarily chosen on the axes of the tubes. The axes do not necessarily cross the point X.

The interacting packets behave, bluntly speaking, like colliding interpenetrative cloudlets.

7.9.1 Asymptotic conditions.

Now we can elaborate the physical conditions at which the in and out packets can be considered as free. If the geometric suppression factors are not too small (only such configurations of the momenta and coordinates contribute to the observables) then the condition of macroscopic separation of the interaction regions in S и D is equivalent to the macroscopic separation of the impact points $X_{s,d}$. We'll hold that the intervals $X^0_d - X^0_s$ and $|\mathbf{X}_d - \mathbf{X}_s|$ are large in comparison with $|x^0_\varkappa - x^0_{\varkappa'}|$ and $|\mathbf{x}_\varkappa - \mathbf{x}_{\varkappa'}|$ for $\varkappa, \varkappa' \in S$ and $\varkappa, \varkappa' \in D$. Under such assumptions the packets certainly do not overlap $\Longrightarrow$ the sought conditions for the packets in S and D must be independent.

> We assume that the dimensions of the packets are large in comparison with the interaction radius in the corresponding vertex of the diagram. Therefore our analysis will be based *exclusively* on the properties of the geometric suppression factors $\exp\left(-\mathfrak{S}_{s,d}\right)$ which do not depend on the dynamics and do not appellate to the energy-momentum conservation.

1. First of all it is necessary to demand that the time intervals $X^0_{s,d} - x^0_a$ $(a \in I_{s,d})$ and $x^0_b - X^0_{s,d}$ $(b \in F_{s,d})$ are sufficiently large. They however cannot be arbitrarily large since the packets $\varkappa$ remain stable (do not spread) during the time $\left|X^0_{s,d} - x^0_\varkappa\right|$ only under the condition

$$\left|X^{0(\varkappa)}_{s,d} - x^{0(\varkappa)}_\varkappa\right|^2 \ll m^2_\varkappa/\sigma^4_\varkappa, \quad \forall \varkappa \in S, D. \tag{35}$$

Since $\mathfrak{S}_s$ and $\mathfrak{S}_d$ do not depend from $X^{0(\varkappa)}_{s,d}$ and $x^{0(\varkappa)}_\varkappa$ it is permissible to demand that the left part of Eq. (35) is larg in comparison with the squared effective size of the packet that is

$$\left|X^{0(\varkappa)}_{s,d} - x^{0(\varkappa)}_\varkappa\right|^2 \gg 1/\sigma^2_\varkappa. \tag{36}$$

Inequalities (36) do not contradict the stationarity condition since $\sigma_\varkappa^2 \ll m_\varkappa^2$. If, in addition, $\varkappa$ is an unstable particle then one can expect that

$$\left|X_{s,d}^{0(\varkappa)} - x_\varkappa^{0(\varkappa)}\right| \sim \tau_\varkappa = 1/\Gamma_\varkappa. \tag{37}$$

The conditions (36) and (37) do not contradict to each other if $\sigma_\varkappa^2 \tau_\varkappa^2 \gg 1$; the latter is one of the conditions of applicability of the CRGP approximation, the *full set of which* is

$$1/\tau_\varkappa^2 \ll \sigma_\varkappa^2 \ll m_\varkappa/\tau_\varkappa \ll m_\varkappa^2. \tag{38}$$

Since for all known long-lived elementary particles $m_\varkappa \tau_\varkappa \lggg 1$, the allowed values of the parameters $\sigma_\varkappa$ can vary in rather wide limits.

Thus the relativistic-invariant conditions for the time parameters $x_\varkappa^0$ is fully consistent with the range of applicability of the CRGP approximation (38), has the form (36) and the correct time sequence in LF is given by

$$x_a^0 < X_{s,d}^0 < x_b^0 \quad (a \in I_{s,d},\ \ b \in F_{s,d}). \tag{39}$$

These inequalities are Lorentz invariant if the points $x_{a,b}$ and $X_{s,d}$ are separated by the time-like intervals. If otherwise for some $\varkappa$ the intervals $(x_\varkappa - X_{s,d})^2$ are space-like the inequalities (39) have sense only in LF.

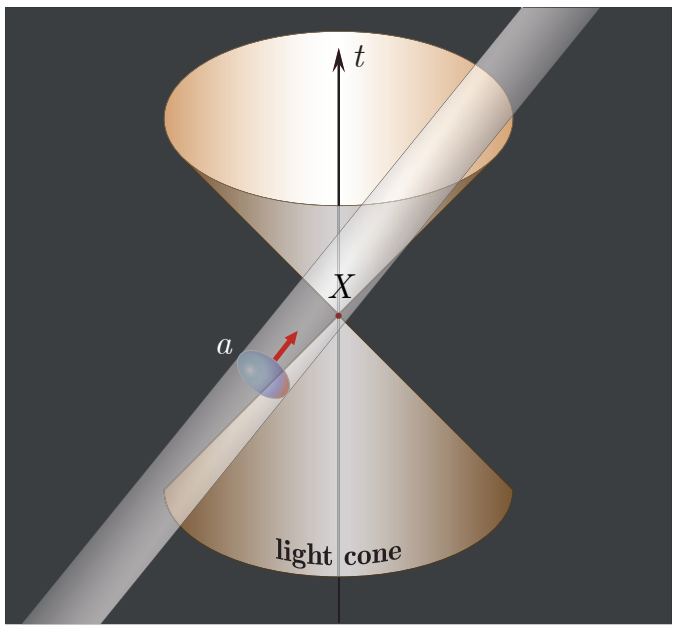

This instance must be taken into account since the packet (e.g., $a \in I_s$) can participate in the interaction even if $(x_a - X_s)^2 < 0$, but under the condition that the points inside a part of its effective volume are separated with the impact point by a time-like interval because the latter can come to be inside the classical world tube of the packet a.

From the geometric considerations it can be proved that for such events $0 < |\mathbf{b}_a^\star| < d_a^\star/2$ Therefore

$$\sigma_a^2 |\mathbf{b}_a^\star|^2 < 0.605 \quad \text{and} \quad \exp\left(-\sigma_a^2 |\mathbf{b}_a^\star|^2\right) \gtrsim 0.546.$$

Clearly there the micro-causality is not violated here since all "signals" propagate strictly inside the light cones. However, in principle, the interactions of such kind would lead to observable effect which imitate the causality violation.

2. The conditions of spatial remoteness of the packets from the impact points are not in general necessary. Indeed, some packets (e.g., decaying meson or secondary charged lepton in the source, a target nucleus in the detector, etc.) can be at rest in LF before or after interaction. In this case they must be spatially close to the corresponding impact points; otherwise the amplitude will be small due to the smallness of the factors $\exp\left(-\mathfrak{S}_{s,d}\right)$.

However, all the packets must be spatially separated from each other, that is the differences of the spatial coordinates for each pair of the packets $\varkappa, \varkappa'$ must be large in comparison with the dimensions of these packets. The simplest reference frame to formulate this condition is the CIF of the pair.

Since the packet momenta in CIF are collinear ($\mathbf{p}_\varkappa^* = -\mathbf{p}_{\varkappa'}^* = \mathbf{n}_* |\mathbf{p}_\varkappa^*|$) and the only case is interesting when the classical impact parameter $\left|\mathbf{n}_* \times \left(\mathbf{x}_\varkappa^* - \mathbf{x}_{\varkappa'}^*\right)\right|$ is not larger than the transversal sizes of the packets, the distance between the packets must be large in comparison with these dimensions.

$$\left|\mathbf{x}_\varkappa^* - \mathbf{x}_{\varkappa'}^*\right|^2 \gg \frac{1}{\left(\sigma_\varkappa \Gamma_\varkappa^*\right)^2} + \frac{1}{\left(\sigma_{\varkappa'} \Gamma_{\varkappa'}^*\right)^2}. \tag{40}$$

It is not a simple matter to prove that these conditions do not contradict the conditions

$$\left|\mathbf{X}_{s,d}^{(\varkappa)} - \mathbf{x}_\varkappa^{(\varkappa)}\right|^2 \ll m_\varkappa^2/\sigma_\varkappa^4. \tag{41}$$

7.10 Calculation of a macroscopic amplitude.

As a practically important example, we consider the charged-current induced production of charged leptons ℓ_α^+ and ℓ_β^- ($\ell_{\alpha,\beta} = e, \mu, \tau$) in the process

$$I_s \oplus I_d \to F'_s + \ell_\alpha^+ \oplus F'_d + \ell_\beta^-, \qquad (42)$$

We assume for definiteness that all the external substates I_s, I_d, F'_s, and F'_d consist exclusively of (asymptotically free) hadronic WPs. Consequently, if $\alpha \neq \beta$, the process (42) violates the lepton numbers L_α and L_β that is only possible via exchange of massive neutrinos (no matter whether they are Dirac or Majorana particles).
In the lowest nonvanishing order in electroweak interactions, the process (42) is described by the sum of the diagrams shown in the figure.

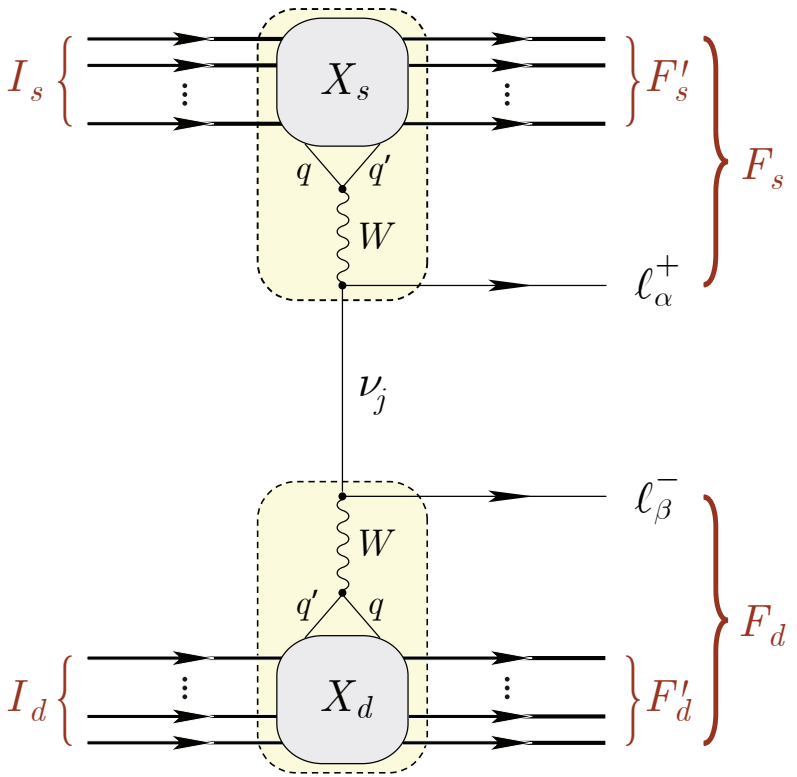

A macroscopic Feynman diagram describing the flavor-violating process (42).

The impact points X_s and X_d in the figureare macroscopically separated and the asymptotic conditions are assumed to be fulfilled.

7.11 Sketch of the calculation.

1. Quark-lepton blocks. We use the Standard Model (SM) phenomenologically extended by inclusion of a neutrino mass term. The quark-lepton blocks are described by the Lagrangian

$$\mathcal{L}_W(x) = -\frac{g}{2\sqrt{2}}\left[j_\ell(x)W(x) + j_q(x)W(x) + \text{H.c.}\right],$$

where g is the $SU(2)$ coupling constant, j_ℓ and j_q are the weak charged currents:

$$j^\mu_\ell(x) = \sum_{\alpha i} V^*_{\alpha i}\,\overline{\nu}_i(x)O^\mu\ell_\alpha(x), \qquad j^\mu_q(x) = \sum_{qq'} V^{'*}_{qq'}\,\overline{q}(x)O^\mu q'(x), \qquad \left[O^\mu = \gamma^\mu(1-\gamma_5)\right].$$

Here $V_{\alpha i}$ ($\alpha = e,\mu,\tau$; $i = 1,2,3$) and $V'_{qq'}$ ($q = u,c,t$; $q' = d,s,b$) are the elements of the neutrino and quark mixing matrices ($\boldsymbol{V}$ and $\boldsymbol{V}'$, respectively).

The normalized amplitude is given by the 4th order of the perturbation theory in g:

$$\begin{aligned}\mathcal{A}_{\beta\alpha} &= \langle \mathbf{out}|\mathbb{S}|\mathbf{in}\rangle\left(\langle \mathbf{in}|\mathbf{in}\rangle\langle \mathbf{out}|\mathbf{out}\rangle\right)^{-1/2} \\ &= \frac{1}{\mathcal{N}}\left(\frac{-ig}{2\sqrt{2}}\right)^4 \langle F_s\oplus F_d|\,T\int dxdx'dydy' : j_\ell(x)W(x) :: j_q(x')W^\dagger(x') : \\ &\quad \times : j^\dagger_\ell(y)W^\dagger(y) :: j^\dagger_q(y')W(y') : \mathbb{S}_h|I_s\oplus I_d\rangle. \end{aligned} \tag{43}$$

The normalization factor $\mathcal{N}$ in the CRGP approximation is given by

$$\mathcal{N}^2 = \langle \mathbf{in}|\mathbf{in}\rangle\langle \mathbf{out}|\mathbf{out}\rangle = \prod_{\varkappa\in I_s\oplus I_d\oplus F_s\oplus F_d} 2E_\varkappa \mathrm{V}_\varkappa(\boldsymbol{p}_\varkappa).$$

2. Hadronic blocks. The strong and (possibly) electromagnetic interactions responsible for nonperturbative processes of fragmentation and hadronization are described by the hadronic (QCD) interaction Lagrangian $\mathcal{L}_{\rm h}(x)$ and the corresponding part of the full S-matrix is

$$\mathbb{S}_h = \exp\left[i\int dz \mathcal{L}_{\rm h}(z)\right].$$

The following factorization theorem can be proved

$$\langle F'_s \oplus F'_d | T\left[: j_q^{\mu}(x) : \mathbb{S}_h : j_q^{\dagger\nu}(y) :\right] | I_s \oplus I_d\rangle = \mathcal{J}_s^{\mu}(p_S)\mathcal{J}_d^{\nu\dagger}(p_D)$$
$$\times\Big[\prod_{a\in I_s} e^{-ip_a x_a}\psi_a(\boldsymbol{p}_a, x_a - x)\Big]\Big[\prod_{b\in F'_s} e^{ip_b x_b}\psi_b^*(\boldsymbol{p}_b, x_b - x)\Big]$$
$$\times\Big[\prod_{a\in I_d} e^{-ip_a x_a}\psi_a(\boldsymbol{p}_a, x_a - y)\Big]\Big[\prod_{b\in F'_d} e^{ip_b x_b}\psi_b^*(\boldsymbol{p}_b, x_b - y)\Big].$$

Here $\mathcal{J}_s(p_S)$ and $\mathcal{J}_d(p_D)$ are the c-number hadronic currents in which the strong interactions are taken into account nonperturbatively, and p_S and p_D denote the sets of the momentum and spin variables of the hadronic states.

The proof is based on the assumed narrowness of the WPs in the momentum space, macroscopic remoteness of the interaction regions in the source and detector vertices, and the consideration of translation invariance.

The explicit form of the hadronic currents $\mathcal{J}_s$ and $\mathcal{J}_d$ is not needed for our purposes.

Now, by applying Wick's theorem, factorization theorem, and the known properties of the leptonic WPs, the amplitude (43) can be rewritten in the following way:

$$\mathcal{A}_{\beta\alpha} = \frac{g^4}{64\mathcal{N}} \sum_j V_{\beta j} \mathcal{J}_d^{\nu\dagger} \overline{u}(\boldsymbol{p}_\beta) O_{\nu'} \mathbb{G}_{\nu\mu}^{j\nu'\mu'} \left(\{\boldsymbol{p}_\varkappa, x_\varkappa\}\right) O_{\mu'} v(\boldsymbol{p}_\alpha) \mathcal{J}_s^\mu V_{\alpha j}^*, \tag{44}$$

$$\mathbb{G}_{\nu\mu}^{j\nu'\mu'} \left(\{\boldsymbol{p}_\varkappa, x_\varkappa\}\right) = \int \frac{dq}{(2\pi)^4} \mathbb{V}_d(q) \Delta_\nu^{\nu'}(q - p_\beta) \Delta^j(q) \Delta_\mu^{\mu'}(q + p_\alpha) \mathbb{V}_s(q). \tag{45}$$

Here $\mathbb{V}_s(q)$ and $\mathbb{V}_d(q)$ are the overlap integrals; Δ^j and Δ_μ^ν are the propagators of, respectively, the massive neutrino ν_j and W boson.[a]

$$\Delta^j(q) = \frac{i}{\hat{q} - m_j + i0} = i \frac{\hat{q} + m_j}{q^2 - m_j^2 + i0}. \tag{47}$$

[a] The bare W boson propagator has the form

$$\Delta_{\mu\nu}(k) = -i \frac{g_{\mu\nu} - k_\mu k_\nu / m_W^2}{k^2 - m_W^2 + i0} \tag{46}$$

However, the explicit form of $\Delta_{\mu\nu}$ is not used below. So $\Delta_{\mu\nu}$ can be thought of as the *renormalized* propagator.

7.12 Large-distance asymptotics.

At large spatial distances between the impact points $\mathbf{X}_s$ and $\mathbf{X}_d$, the integral (45) can be evaluated by means of the Grimus-Stockinger (GS) theorem.[a]

> Let $F(\boldsymbol{q})$ be a thrice continuously differentiable function such that F itself and its 1st and 2nd derivatives decrease not slowly than $|\boldsymbol{q}|^{-2}$ as $|\boldsymbol{q}| \to \infty$. Then in the asymptotic limit of $L = |\boldsymbol{L}| \to \infty$,
>
> $$\int \frac{d\mathbf{q}}{(2\pi)^3} \frac{\Phi(\mathbf{q}) e^{i\mathbf{q}\mathbf{L}}}{s - \mathbf{q}^2 + i0} \sim \begin{cases} -\dfrac{\Phi\left(\sqrt{s}\,\mathbf{L}/L\right)}{4\pi L} \exp\left(i\sqrt{s}L\right) + \mathcal{O}\left(L^{-3/2}\right) & \text{for } s > 0, \\ \mathcal{O}\left(L^{-2}\right) & \text{for } s < 0. \end{cases}$$

Taking into account the definition (45), implicit form of the overlap integrals and neutrino propagator (47) we conclude that in our case

$$\mathbf{L} = \mathbf{X}_d - \mathbf{X}_s, \quad T = X_d^0 - X_s^0, \quad s = q_0^2 - m_j^2.$$

The integrand in (45) satisfies the formulated requirements.

---

[a] W. Grimus and P. Stockinger, *Real oscillations of virtual neutrinos*, Phys. Rev. D **54** (1996) 3414 [arXiv:hep-ph/9603430].

The function corresponding the function $\Phi(\mathbf{q})$ in the GS theorem is, up to an inessential (q independent) multiplier[a],

$$\widetilde{\delta}_s\,(q-q_s)\,\widetilde{\delta}_d\,(q+q_d)\,\Delta_{\nu\nu'}(q-p_\beta)(\hat{q}+m_j)\Delta_{\mu'\mu}(q+p_\alpha), \tag{48}$$

The first requirement of the theorem can be formally violated by the poles in the bare W propagators (46). In order to exclude this small trouble, we will use instead of (46) the renormalized propagator which has no singularity in the resonance region.

> The simplest recipe consists in the standard substitution $m_W^2 \longmapsto m_W^2 - i m_W \Gamma_W$, in the denominator of the bare propagator (46); Γ_W is the full width of the W boson.

Since the functions $\widetilde{\delta}_s\,(q-q_s)$ and $\widetilde{\delta}_d\,(q+q_d)$ decay faster that any power of $|\mathbf{q}|^{-1}$ as $|\mathbf{q}| \to \infty$, we conclude that the function (48) satisfies the conditions of the GS theorem. As a result, in the leading order in $1/L$ the function (45) behaves as

$$\begin{aligned}\mathbb{G}^j_{\nu\nu'\mu'\mu}\left(\{\mathbf{p}_\varkappa, x_\varkappa\}\right) = \frac{e^{-\mathfrak{S}-i\Theta}}{8\pi^2 L}\int_{-\infty}^{\infty} dq_0 e^{-i\left(q_0 T - |\mathbf{q}_j|\,L\right)}\widetilde{\delta}_s\,(q_j-q_s)\,\widetilde{\delta}_d\,(q_j+q_d)\\ \times\Delta_{\nu\nu'}(q_j-p_\beta)\,(\hat{q}_j+m_j)\,\Delta_{\mu'\mu}(q_j+p_\alpha),\end{aligned} \tag{49}$$

where

$$q_j = (q_0, \mathbf{q}_j), \quad \mathbf{q}_j = \sqrt{q_0^2 - m_j^2}\;\mathbf{l}, \quad \mathbf{l} = \mathbf{L}/L, \quad \mathfrak{S} = \mathfrak{S}_s + \mathfrak{S}_d, \quad \text{and} \quad \Theta = X_s q_s + X_d q_d.$$

[a] We have to note that the term in Eq. (48) proportional to the neutrino mass m_j does not contribute to the amplitude due to the matrix multipliers $O^{\mu'}$ и $O^{\nu'}$.

7.12.1 Integration in q_0.

Since the factors $\widetilde{\delta}_s\left(q_j - q_s\right)$ and $\widetilde{\delta}_d\left(q_j + q_d\right)$ under the integral sign in the right-hand part of Eq. (49) have, as the functions of q_0, very sharp maxima close to each other, the integral is saturated by the narrow vicinity of these maxima. So it cam be estimated by the standard saddle-point technique. All calculations will be performed within the CRGP model. According the the definition of the "smeared" δ functions,

$$\widetilde{\delta}_s\left(q_j - q_s\right)\widetilde{\delta}_d\left(q_j + q_d\right) = \frac{1}{(4\pi)^4\sqrt{|\Re_s||\Re_d|}}\exp\left[-\frac{1}{4}F_j(q_0)\right],$$

$$F_j(q_0) = \widetilde{\Re}_s^{\mu\nu}\left(q_j - q_s\right)_\mu\left(q_j - q_s\right)_\nu + \widetilde{\Re}_d^{\mu\nu}\left(q_j + q_d\right)_\mu\left(q_j + q_d\right)_\nu.$$

We denote

$$F_0 = \widetilde{\Re}_s^{\mu\nu}q_{s\mu}q_{s\nu} + \widetilde{\Re}_d^{\mu\nu}q_{d\mu}q_{d\nu}, \quad Y^\mu = \widetilde{\Re}_s^{\mu\nu}q_{s\nu} - \widetilde{\Re}_d^{\mu\nu}q_{d\nu}, \quad R^{\mu\nu} = \widetilde{\Re}_s^{\mu\nu} + \widetilde{\Re}_d^{\mu\nu}, \tag{50}$$

and rewrite $F_j(q_0)$ in the following form:

$$F_j(q_0) = F_0 - 2Y_\mu q_j^\mu + R_{\mu\nu}q_j^\mu q_j^\nu. \tag{51}$$

The extremum of this function is given by

$$\frac{dF_j(q_0)}{dq_0} = \frac{2}{|\mathbf{q}_j|}\left[Rq_0|\mathbf{q}_j| - (\mathbf{Rl})\left(q_0 - |\mathbf{q}_j|\right)^2 - Y_0|\mathbf{q}_j| + (\mathbf{Yl})q_0\right] = 0, \tag{52}$$

where

$$R = R^{\mu\nu} l_\mu l_\nu = R_{00} - 2(\mathbf{Rl}) + \mathscr{R},$$
$$\mathscr{R} = R_{kn} l_k l_n,$$
$$\mathbf{R} = (R_{01}, R_{02}, R_{03}), \tag{53}$$
$$\mathbf{Y} = (Y_1, Y_2, Y_3),$$
$$l = (1, \mathbf{l}), \quad \mathbf{l} = \mathbf{L}/L.$$

Here and be below we suppose conventional summation on repeating Latin indices ($k, n = 1, 2, 3$). The root of Eq. (52), $q_0 = E_j$, will be the saddle point, if the 2nd derivative

$$\frac{d^2 F_j(q_0)}{dq_0^2} = 2R + \frac{2\,(q_0 - |\mathbf{q}_j|)}{|\mathbf{q}_j|^3}\left[(\mathbf{Rl})\,(q_0 + 2|\mathbf{q}_j|)\,(q_0 - |\mathbf{q}_j|) - (\mathbf{Yl})\,(q_0 + |\mathbf{q}_j|)\right] \tag{54a}$$

is positive in this point. Let's define

$$v_j = |\mathbf{q}_j|/q_0 \quad \text{and} \quad \Gamma_j = q_0/m_j$$

Then Eq. (54a) can be rewritten in the following form:

$$\frac{d^2 F_j(q_0)}{dq_0^2} = R + \frac{2}{v_j^3}\left[(\mathbf{Rl})\,(1 + 2v_j)\,(1 - v_j)^2 - \frac{(\mathbf{Yl})}{m_j \Gamma_j^3}\right]. \tag{54б}$$

The straightforward method of the exact solution of Eq. (52) in the general case is described in Appendix 18. Here we only consider the most interesting ultrarelativistic case, for which one can obtain comparatively simple approximate solutions. The nonrelativistic case is described in Appendix 19.

7.12.2 Ultrarelativistic case.

Let's consider the following configurations of the external momenta:

$$q_s^0 \sim -q_d^0 \sim |\mathbf{q}_s| \sim |\mathbf{q}_d|. \tag{55}$$

This particular case is realized in all (without exceptions) modern neutrino experiments and thus is the most interesting.

PW_0 limit: In the plane-wave limit ($\sigma_\varkappa = 0$, $\forall \varkappa$) and for a massless neutrino ($m_j = 0$) the exact energy-momentum conservation in each vertex of the diagram requires the strict equalities

$$q_s^0 = -q_d^0, \quad \mathbf{q}_s = -\mathbf{q}_d = q_s^0 \mathbf{l}, \quad \mathbf{l} = \mathbf{L}/L.$$

So, according to Eqs. (50) and (53), the root of Eq. (52) is

$$q_0 = \lim_{\sigma_\varkappa = 0,\, \forall \varkappa} \frac{Y_0 - (\mathbf{Y}\mathbf{l})}{R} = q_s^0. \tag{56}$$

It is nothing else than the energy of the real massless neutrino. Therefore

$$q_j = q_s^0 l = (q_s^0, q_s^0 \mathbf{l}) = (q_s^0, \mathbf{q}_s), \quad q_j^2 = 0.$$

Below, we'll call this special case the "PW_0 limit".

The PW_0 limit suggests us the way of finding the saddle point in the general (ultrarelativistic) case.

General UR case: In the general case, $\sigma_{\varkappa} \neq 0$, under the conditions (55) and natural assumption that $m_j \ll \min(q_s^0, -q_d^0)$ [where the minimization is performed on the set of the most probable external momenta in S and D, defined by the given experimental conditions] the solution (52) can be found as a series in powers of the small dimensionless parameter

$$r_j = m_j^2/(2E_\nu^2). \tag{57}$$

In Eq. (57) E_ν is the "representative" energy of virtual neutrino:

$$E_\nu = (Yl)/R \quad (\nu \text{ is not the Lorentz index!}) \tag{58}$$

which coincides with the energy transfer q_s^0 in the PW_0 limit and close to it in magnitude at sufficiently small $\sigma_{\varkappa}$. Due to Eq. (58), E_ν is a rotation-invariant function of momenta, masses, and momentum spreads of all external wave packets. Due to the approximate energy-momentum conservation this value is nonnegative and transformed (approximately) as a zero component of a 4-momentum.

Now we can seek q_0 and $|\mathbf{q}_j| = \sqrt{q_0 - m_j^2}$ as the power series

$$q_0 \equiv E_j = E_\nu \left(1 - \sum_{n=1}^{\infty} C_n^E r_j^n\right), \quad |\mathbf{q}_j| \equiv P_j = E_\nu \left(1 - \sum_{n=1}^{\infty} C_n^P r_j^n\right). \tag{59}$$

It is convenient to rewrite Eq. (52) in the form

$$q_0|\mathbf{q}_j| - \mathfrak{m}\,(q_0 - |\mathbf{q}_j|)^2 - E_\nu\,[(\mathfrak{n}+1)|\mathbf{q}_j| - \mathfrak{n}q_0] = 0, \tag{60}$$

where we introduced two rotation-invariant dimensionless functions

$$\mathfrak{n} = \frac{(\mathbf{Yl})}{(Yl)} \quad \text{and} \quad \mathfrak{m} = \frac{(\mathbf{Rl})}{R}.$$

From Eq. (60) it follows that the coefficients C_n^E and C_n^P, $\forall n \geq 1$ are expressed only through these two functions. The coefficients can be found by the standard recurrent procedure. The firs three pairs are

$$\begin{aligned} C_1^E &= \mathfrak{n}, \\ C_2^E &= \mathfrak{n}\left(2\mathfrak{n} + \frac{3}{2}\right) - \mathfrak{m}, \\ C_3^E &= \mathfrak{n}\left(7\mathfrak{n}^2 + 9\mathfrak{n} + \frac{5}{2}\right) - (5\mathfrak{n} + 2)\mathfrak{m}; \end{aligned} \tag{61}$$

$$\begin{aligned} C_1^P &= \mathfrak{n} + 1, \\ C_2^P &= (\mathfrak{n} + 1)\left(2\mathfrak{n} + \frac{1}{2}\right) - \mathfrak{m}, \\ C_3^P &= (\mathfrak{n} + 1)\left(7\mathfrak{n}^2 + 5\mathfrak{n} + \frac{1}{2}\right) - (5\mathfrak{n} + 3)\mathfrak{m}. \end{aligned} \tag{62}$$

The quantities E_j and $\mathbf{p}_j = P_j\mathbf{l}$ can be naturally treated as effective (or most probable) energy and 3-momentum of the virtual massive neutrino ν_j.

Then the effective neutrino velocity is $\mathbf{v}_j = v_j \mathbf{l} = \mathbf{p}_j / E_j$;

$$v_j = 1 - r_j - \left(2\mathfrak{n} + \frac{1}{2}\right) r_j^2 - \left(7\mathfrak{n}^2 + 5\mathfrak{n} + \frac{1}{2} - 2\mathfrak{m}\right) r_j^3 + \mathcal{O}\left(r_j^4\right). \tag{63}$$

As it could be expected,

$$0 < 1 - v_j \ll 1,$$

that is the neutrino is ultrarelativistic.

Considering that

$$R = R^{\mu\nu} l_\mu l_\nu = \mathfrak{F} E_\nu^{-2}, \tag{64}$$

where

$$\mathfrak{F} = \left[R^{\mu\nu} q_\mu q_\nu\right]_{q = E_\nu l} > 0, \tag{65}$$

we conclude that the 2nd derivative (54) is positive in the point $q_0 = E_j$ and thus the function $F_j(q_0)$ has the absolute minimum in this point.

The quantities E_j, $\mathbf{p}_j$, and $\mathbf{v}_j$ are unambiguously defined by the most probable momenta $\mathbf{p}_\varkappa$, masses $m_\varkappa$, and momentum spreads $\sigma_\varkappa$ of the external packets in S and D.

It will be demonstrated that the functions $\mathfrak{n}$ and $\mathfrak{m}$ can vary within orders of magnitude in different kinematic regions of the reaction (42). Hence the smallness of the parameter r_j does not yet ensure that that the corrections $\sim r_j^n$ with $n \geq 2$ in Eqs. (59) and (63) are small in the whole phase space of the reaction. Now we'l just assume that

$$|\mathfrak{n}| r_j \ll 1 \quad \text{and} \quad |\mathfrak{m}| r_j \ll |\mathfrak{n}|, \quad \forall j. \tag{66}$$

A summary: The integral over q_0 has been evaluated by the regular saddle-point method. In the ultrarelativistic approximation ($q_s^0 \approx -q_d^0 \gg m_j$, $j = 1, 2, 3$) the stationary saddle point $q_0 = E_j$ was found as a series in powers of the small parameter $r_j = m_j^2/(2E_\nu^2) \approx \Gamma_j^2/2$. The NLO result reads

$$\begin{aligned} q_0 &\equiv E_j = E_\nu \left[1 - \mathfrak{n} r_j - \mathfrak{m} r_j^2 + \mathcal{O}\left(r_j^3\right)\right], \\ |\mathbf{q}_j|_{q_0=E_j} &\equiv P_j = E_\nu \left[1 - (\mathfrak{n}+1) r_j - \left(\mathfrak{n} + \mathfrak{m} + \frac{1}{2}\right) r_j^2 + \mathcal{O}\left(r_j^3\right)\right], \\ \frac{P_i}{E_j} &\equiv v_j = 1 - r_j - \left(2\mathfrak{n} + \frac{1}{2}\right) r_j^2 + \mathcal{O}\left(r_j^3\right), \quad E_j^2 - P_j^2 = m_j^2; \end{aligned}$$

$$\mathfrak{n} = \frac{\mathbf{Y}\boldsymbol{l}}{Yl}, \quad \mathfrak{m} = \mathfrak{n}\left(\frac{3}{2} + 2\mathfrak{n}\right) + \frac{1}{R} \sum_{n=1,2,3} \left(\widetilde{\Re}_s^{0n} + \widetilde{\Re}_d^{0n}\right) l_n,$$

$$Y^\mu = \widetilde{\Re}_s^{\mu\nu} q_{s\nu} - \widetilde{\Re}_d^{\mu\nu} q_{d\nu}, \quad R = \left(\widetilde{\Re}_s^{\mu\nu} + \widetilde{\Re}_d^{\mu\nu}\right) l_\mu l_\nu,$$

$$E_\nu = \frac{Yl}{R}, \quad l = (1, \boldsymbol{l}), \quad \boldsymbol{l} = \frac{\boldsymbol{L}}{L}, \quad \boldsymbol{L} = \boldsymbol{X}_d - \boldsymbol{X}_s.$$

The quantities E_j, $\mathbf{P}_j = P_j \mathbf{l}$ and $\mathbf{v}_j = v_j \mathbf{l}$ can naturally be treated as, respectively, the effective energy, momentum and velocity of the virtual neutrino ν_j.

The ultrarelativistic approximation is, of course, reference-frame dependent. That is why the obtained result is not explicitly Lorentz-invariant.

In the limit of $m_j = 0$ and assuming the exact energy-momentum conservation,

$$E_j = P_j = E_\nu = q_s^0 = -q_d^0.$$

But, in the general case, the effective neutrino 4-momentum $p_j = (E_j, \boldsymbol{p}_j)$ is determined by the mean momenta and momentum spreads of the external WPs involved in the process (42).

Below, we'll limit ourselves to the 1st order of the expansion in r_j. However, the next-order corrections are needed to define properly the range of applicability of the obtained result.

Finally, by introducing the notation

$$\Omega_j(T,L) = i\,(E_jT - P_jL) + 2\left(\widetilde{\mathfrak{D}}_j/P_j\right)^2 (P_jT - E_jL)^2\,,$$

$$\Theta = X_s q_s + X_d q_d, \quad L = |\boldsymbol{X}_d - \boldsymbol{X}_s|, \quad T = X_d^0 - X_s^0,$$

$$\widetilde{\mathfrak{D}}_j = \mathfrak{D}_j \left(1 + \frac{8ir_jE_\nu^2\mathfrak{D}_j^2 L}{P_j^3}\right)^{-1/2}, \quad \mathfrak{D}_j = \frac{1+\mathfrak{n}r_j}{\sqrt{2R}},$$

we arrive at the saddle-point estimate of the function (45):

$$\mathbb{G}_{\nu\mu}^{j\nu'\mu'} = \Delta_\nu^{\nu'}(p_j - p_\beta)(\hat{p}_j + m_j)\Delta_\mu^{\mu'}(p_j + p_\alpha)|\mathbb{V}_d(p_j)\mathbb{V}_s(p_j)|\,\frac{\widetilde{\mathfrak{D}}_j e^{-\Omega_j(T,L)-i\Theta}}{i(2\pi)^{3/2}L}. \qquad (67)$$

This formula can be (and must be) somewhat simplified by putting $r_j = 0$ everywhere wherever it is not a factor multiplying L or T (whose values can be arbitrary large).
Somewhere the 4-vector p_j is replaced by the light-cone 4-vector $p_\nu = (E_\nu, \boldsymbol{p}_\nu) = E_\nu l$.

7.13 Source-detector factorization.

Now, by applying the identity

$$P_- \hat{p}_\nu P_+ = P_- u_-(\boldsymbol{p}_\nu)\overline{u}_-(\boldsymbol{p}_\nu)P_+, \quad P_\pm = \frac{1}{2}(1 \pm \gamma_5),$$

where $u_-(\boldsymbol{p}_\nu)$ is the Dirac bispinor for the LH massless ν, we define the matrix elements

$$M_s = (g^2/8)\,\overline{u}_-(\boldsymbol{p}_\nu)\mathcal{J}_s^\mu \Delta_\mu^{\mu'}(p_\nu + p_\alpha)O_{\mu'}u(\boldsymbol{p}_\alpha) \quad (I_s \to F_s' + \ell_\alpha^+ + \nu)$$

$$M_d^* = (g^2/8)\,\overline{v}(\boldsymbol{p}_\beta)O_{\mu'}\Delta_\mu^{\mu'}(p_\nu - p_\beta)\mathcal{J}_d^{\mu\dagger}u_-(\boldsymbol{p}_\nu) \quad (\nu + I_d \to F_d' + \ell_\beta^-).$$

These describe the reactions with production and absorption of a real massless neutrino ν.

The final expression for the amplitude (44) is

$$\boxed{\mathcal{A}_{\beta\alpha} = \frac{M_s M_d^*}{i(2\pi)^{3/2}\mathcal{N}L}\sum_j \widetilde{\mathfrak{D}}_j |\mathbb{V}_s(p_j)\mathbb{V}_d(p_j)| V_{\alpha j}^* V_{\beta j}\, e^{-\Omega_j(T,L) - i\Theta}.} \qquad (68)$$

- The form of eq. (68) suggests that it is common for essentially any class of macrodiagrams, with exchange of virtual neutrinos between the source and detector, until we do not specify the explicit form of the matrix elements M_s and M_d.
- To obtain similar answer for the macrodiagrams with an exchange of virtual antineutrinos, one has to replace (besides the matrix elements) $\mathbf{V} \longmapsto \mathbf{V}^\dagger$.

7.14 Effective wave packet for ultrarelativistic neutrino.

Фазовая функция (144) может быть тождественно переписана в приближенно[a] лоренц-инвариантной форме:

$$\Omega_j(T,L) = i(p_j X) + \frac{2\widetilde{\mathfrak{D}}_j^2}{E_\nu^2}\left[(p_j X)^2 - m_j^2 X^2\right], \tag{69}$$

где $X = X_d - X_s$. Рассмотрим следующий фактор в амплитуде (146):

$$\overline{u}_-(\mathbf{p}_\nu)\frac{1}{L}e^{-\Omega_j(T,L)}u_-(\mathbf{p}_\nu) \approx \overline{u}_-(\mathbf{p}_j)\frac{1}{L}e^{-\Omega_j(T,L)}u_-(\mathbf{p}_j)$$

Пренебрегая $\mathrm{Im}\widetilde{\mathfrak{D}}_j^2$ этот фактор можно записать в виде произведения

$$|\mathbf{X}_d - \mathbf{X}_s|^{-1}\overline{\psi}^j_{X_s}(\mathbf{p}_j, X_d - X_s)\psi^j_{X_d}(\mathbf{p}_j, X_s - X_d), \tag{70}$$

в котором

$$\psi^j_y(\mathbf{p}_j, x) = \exp\left\{-i(p_j y) - \frac{\mathfrak{D}_j^2}{E_\nu^2}\left[(p_j x)^2 - m_j^2 x^2\right]\right\}u_-(\mathbf{p}_j),$$

$$\overline{\psi}^j_y(\mathbf{p}_j, x) = \left[\psi^j_y(\mathbf{p}_j, x)\right]^\dagger\gamma_0 = \overline{u}_-(\mathbf{p}_j)\exp\left\{i(p_j y) - \frac{\mathfrak{D}_j^2}{E_\nu^2}\left[(p_j x)^2 - m_j^2 x^2\right]\right\}.$$

[a] Функция $\widetilde{\mathfrak{D}}_j/E_\nu$ инвариантна с точностью до поправок $\mathcal{O}(\mathfrak{r}_j^2)$.

Сравнивая спинорную функцию $\psi_y(\mathbf{p}_j, x)$ с волновой функцией фермионного пакета общего вида в приближении СРГП

$$\psi_y(\mathbf{p}, s, x) = e^{-ipx} u_s(\mathbf{p}) \psi(\mathbf{p}, x-y) = u_s(\mathbf{p}) \exp\left\{-i(py) - \frac{\sigma^2}{m^2}\left[(px)^2 - m^2 x^2\right]\right\},$$

видим, что спинорную функцию $\psi^j_{X_d}(\mathbf{p}_j, X_s - X_d)$ можно интерпретировать как волновую функцию в x-представлении, описывающую *входящий* волновой пакет *реального* массивного нейтрино ν_j, роль параметра σ в которой играет величина

$$\sigma_j = \frac{\mathfrak{D}_j}{\Gamma_j} \qquad \left(\Gamma_j = \frac{E_j}{m_j} \simeq \frac{E_\nu}{m_j}\right).$$

Второй спинорный сомножитель в (70), $\overline{\psi}^j_{X_s}(\mathbf{p}_j, X_d - X_s)/|\mathbf{X}_d - \mathbf{X}_s|$, естественно интерпретировать как *выходящую* из источника сферическую волну нейтрино на расстоянии $|\mathbf{X}_d - \mathbf{X}_s|$ от точки рождения $\mathbf{X}_s$.

Поскольку $\widetilde{\mathfrak{D}}_j$ – комплекснозначная функция, факторизация вида (70) в общем случае становится невозможной. Соответствующую поправку, представляющую очевидный интерес для нейтринной астрофизики, можно интерпретировать как результат своеобразной интерференции расплывающихся in- и out-пакетов нейтрино. Поправка становится существенной при очень больших расстояниях L и приводит к общему подавлению амплитуды (44) и к модификации осцилляционных факторов $\propto \exp\left[i\mathrm{Im}\Omega_j(T, L)\right]$. Детальное изучение этих эффектов возможно только посредством анализа наблюдаемых величин (таких, как скорость счета событий данного типа в установке), которые получаются после надлежащего усреднения квадрата модуля амплитуды по всем неизмеряемым переменным, от которых зависит амплитуда (44).

Такое усреднение зависит от статистических распределений (в более общем случае – от кинетики) ансамблей in-пакетов и от процедуры детектирования. Здесь мы ограничимся случаем, когда этими эффектами можно пренебречь. Используя (143) и (145) запишем:

$$\mathfrak{r}_j \simeq \frac{10^5}{\mathfrak{F}} \left(\frac{m_j}{1\ \text{эВ}}\right)^2 \left(\frac{1\ \text{ГэВ}}{E_\nu}\right) \left(\frac{L}{10^4\ \text{км}}\right). \tag{71}$$

Отсюда видно, что $\mathfrak{r}_j \ll 1$ для всех современных экспериментов с

- реакторными ($E_\nu \gtrsim 1$ МэВ, $L \lesssim 10^3$ км),
- ускорительными ($E_\nu \gtrsim 100$ МэВ, $L \lesssim 10^3$ км) и
- атмосферными ($E_\nu \gtrsim 100$ МэВ, $L \lesssim 1.3 \times 10^4$ км) (анти)нейтрино

при условии, что $m_j \lesssim 1$ эВ и $\mathfrak{F} \gg 10^7$. Мы убедимся на типичных примерах, что при выполнении условий применимости модели СРГП условие $\mathfrak{F} \gg 10^7$ выполняется "с большим запасом". При этом $\widetilde{\mathfrak{D}}_j^2 \simeq \mathfrak{D}_j^2 \simeq \mathfrak{D}^2$ и, следовательно,

$$\frac{\sigma_j^2}{m_j^2} \simeq \frac{\mathfrak{D}^2}{E_\nu^2} = \frac{1}{2E_\nu^2 R} \simeq \frac{1}{2\mathfrak{F}}. \tag{72}$$

Отсюда, с учетом принятых нами условий узости внешних пакетов в импульсном пространстве, $\sigma_\varkappa^2 \ll m_\varkappa^2$, автоматически следует, что $\sigma_j^2/m_i^2 \ll 10^{-7}$ и $\sigma_j^2 L^2 \ll m_i^2/\sigma_j^2$ (условие стабильности пакета).

Неопределенности энергии и компонент импульса ультрарелятивистского волнового пакета в приближении СРГП есть

$$\delta E_{\mathbf{p}} \approx |\delta\mathbf{p}| \approx |\delta\mathbf{p}_\parallel| \approx \sqrt{2\ln 2}\Gamma_{\mathbf{p}}\sigma, \quad |\delta\mathbf{p}_\perp| \approx 2\sqrt{\ln 2}\,\sigma \quad (\delta\mathbf{p}_\parallel \times \mathbf{p} = 0,\ \ \delta\mathbf{p}_\perp \cdot \mathbf{p} = 0).$$

Т.о. соответствующие неопределенности для ультрарелятивистского нейтринного пакета равны

$$\delta E_j \approx |\delta \mathbf{p}_j| \approx |\delta \mathbf{p}_{j\parallel}| \approx 2\sqrt{\ln 2}\mathfrak{D}, \quad |\delta \mathbf{p}_{j\perp}| \approx 2\sqrt{2\ln 2}\,\mathfrak{D}/\Gamma_j \ll |\delta \mathbf{p}_{j\parallel}|,$$

т.е., функция $\mathfrak{D}$, зависящая от масс, импульсов и размазок импульсов внешних in- и out-пакетов, характеризует неопределенность энергии нейтрино, а $1/\mathfrak{D}$ определяет (с точностью до числового множителя порядка единицы) эффективный размер нейтринного волнового пакета поперечный к импульсу $\mathbf{p}_j$.

Наглядным образом волнового пакета ультрарелятивистского нейтринно может служить огромный, но чрезвычайно тонкий диск, отношение поперечного и продольного размеров которого равно $\Gamma_j \gg 1$. Относительная неопределенность энергии и импульса нейтрино

$$\delta E_j/E_j \simeq \delta P_j/P_j \sim \mathfrak{D}/E_\nu \sim 1/\sqrt{\mathfrak{F}}$$

всегда очень мала и не зависит от энергии и массы нейтрино. Именно в этом смысле следует понимать стандартное квантовомеханическое предположение о том, что состояния нейтрино с определенными массами $|\nu_j\rangle$ (а следовательно и состояния с определенными флейворами $|\nu_\alpha\rangle$) обладают определенными 4-импульсами.

Как и всякий СРГП, нейтринный волновой пакет в среднем движется по "классической траектории" $\overline{\mathbf{L}}_j = \mathbf{v}_j T$, квантовые отклонения от которой, $\delta\mathbf{L}_j$, подавлены фактором

$$\exp\left\{-2\mathfrak{D}^2\left[(\delta\mathbf{L}_j)^2/\Gamma_j^2 + (\mathbf{L}\delta\mathbf{L}_j)^2/L^2\right]\right\}.$$

Из-за малости величины $\mathfrak{D}^2/\Gamma_j^2 \sim m_j^2/\mathfrak{F}$ поперечные отклонения могут быть макроскопически велики (бесконечно велики в случае безмассового нейтрино).

Итак, мы убедились, что эффективный волновой пакет ультрарелятивистского нейтрино воспроизводит все свойства СРГП общего вида, с той лишь существенной оговоркой, что параметр σ_j зависит, вообще говоря, от импульсов (а также масс и дисперсий импульсов) всех внешних пакетов.

Здесь необходимо отметить, что эта зависимость отнюдь не является специфическим свойством нейтрино или ковариантного формализма, поскольку волновой пакет, описываюший состояние *любой* массивной частицы должен зависеть от импульсов частиц, участвовавших как в ее образовании так и, вообще говоря, поглощении, а использованное нами соглашение $\sigma_\varkappa = \text{const}$ является не более чем приближением, принятым для упрощения теории.

Ниже мы вернемся к этому вопросу при рассмотрении процесса двухчастичного распада $a \to \ell\nu_j^*$ в источнике.

7.15 Squared amplitude.

It can be shown that

$$|\mathbb{V}_{s,d}(p_\nu)|^2 = (2\pi)^4 \delta_{s,d}(p_\nu \mp q_{s,d}) \mathrm{V}_{s,d}, \tag{73}$$

where $\delta_{s,d}$ are the "smeared" δ functions (analogous to the functions $\widetilde{\delta}_{s,d}$) and $\mathrm{V}_{s,d}$ are the effective 4D overlap volumes of the external packets in the source and detector;

$$\delta_{s,d}(K) = (2\pi)^{-2} |\Re_{s,d}|^{-1/2} \exp\left(-\frac{1}{2}\,\widetilde{\Re}^{\mu\nu}_{s,d} K_\mu K_\nu\right), \tag{74}$$

$$\mathrm{V}_{s,d} = \int dx \prod_{\varkappa \in S,D} |\psi_\varkappa(\boldsymbol{p}_\varkappa, x_\varkappa - x)|^2 = \frac{\pi^2}{4} |\Re_{s,d}|^{-1/2} \exp\left(-2\mathfrak{S}_{s,d}\right). \tag{75}$$

$$\Downarrow$$

$$\begin{aligned} |\mathcal{A}_{\beta\alpha}|^2 = & \frac{(2\pi)^4 \delta_s(p_\nu - q_s) \mathrm{V}_s |M_s|^2}{\prod_{\varkappa\in S} 2E_\varkappa \mathrm{V}_\varkappa} \; \frac{(2\pi)^4 \delta_d(p_\nu + q_d) \mathrm{V}_d |M_d|^2}{\prod_{\varkappa\in D} 2E_\varkappa \mathrm{V}_\varkappa} \\ & \times \frac{\mathfrak{D}^2}{(2\pi)^3 L^2} \left| \sum_j V^*_{\alpha j} V_{\beta j}\, e^{-\Omega_j(T,L) - \Theta_j} \right|^2. \end{aligned} \tag{76}$$

Here

$$\Theta_j \approx \frac{m_j^4 \left[R_{00}\mathscr{R} - (\mathbf{Rl})^2\right]}{4RE_\nu^2}; \tag{77}$$

see Appendix 21 for details.

Equation (76) defines the microscopic probability dependent on the mean momenta $\boldsymbol{p}_\varkappa$, initial coordinates $x_\varkappa$, masses $m_\varkappa$, and parameters $\sigma_\varkappa$ of all external wave packets participated in the reaction. By using the explicit form of the functions $\delta_{s,d}$ and $\mathfrak{D}$, one can prove the following approximate relation:

$$2\sqrt{\pi}\mathfrak{D}\delta_s\left(p_\nu - q_s\right)\delta_d\left(p_\nu + q_d\right)F(p_\nu) = \int dE'_\nu \delta_s\left(p'_\nu - q_s\right)\delta_d\left(p'_\nu + q_d\right)F(p'_\nu), \qquad (78)$$

where $F(p_\nu)$ is an arbitrary slowly varying function and $p'_\nu = (E'_\nu, \boldsymbol{p}'_\nu) = E'_\nu l$. The relation is valid with the same accuracy with which the amplitude (68) itself has been deduced that is, with the accuracy of the saddle-point method. With help of (78) the squared amplitude (76) transforms to

$$|\mathcal{A}_{\beta\alpha}|^2 = \int dE_\nu \frac{(2\pi)^4\delta_s(p_\nu - q_s)\mathrm{V}_s|M_s|^2}{\prod_{\varkappa\in S}2E_\varkappa \mathrm{V}_\varkappa} \frac{(2\pi)^4\delta_d(p_\nu + q_d)\mathrm{V}_d|M_d|^2}{\prod_{\varkappa\in D}2E_\varkappa \mathrm{V}_\varkappa} \times \frac{\mathfrak{D}}{2\sqrt{\pi}(2\pi)^3L^2}\left|\sum_j V^*_{\alpha j}V_{\beta j}\, e^{-\Omega_j(T,L)-\Theta_j}\right|^2. \qquad (79)$$

The expressions (76) and (79) are equivalent within the adopted accuracy, but from (79) it is apparent that the energy-momentum conservation is governed by the factors $\delta_s(p_\nu - q_s)$ and $\delta_d(p_\nu + q_d)$ which, at sufficiently small $\sigma_\varkappa$, could be substituted by the usual δ functions.

The probability (79) is the most general result of this work. However, it is too general to be directly applied to the contemporary neutrino oscillation experiments.

7.16 Properties of the overlap tensors $\widetilde{\Re}^{\mu\nu}_{s,d}$.

7.16.1 General formulas for $\Re^{\mu\nu}_{s,d}$ and $\widetilde{\Re}^{\mu\nu}_{s,d}$.

Consider the general properties of the tensors

$$\Re^{\mu\nu}_{s,d} = \sum_{\varkappa} T^{\mu\nu}_{\varkappa} = \sum_{\varkappa} \sigma^2_{\varkappa} \left(u^{\mu}_{\varkappa} u^{\nu}_{\varkappa} - g^{\mu\nu}\right) \quad \text{and} \quad \widetilde{\Re}^{\mu\nu}_{s,d} = \left(\Re^{-1}_{s,d}\right)_{\mu\nu}.$$

The explicit form of the matrices $\Re_{s,d}$ reads

$$\Re_{s,d} = \sum_{\varkappa} \sigma^2_{\varkappa} \begin{pmatrix} \Gamma^2_{\varkappa} - 1 & -\Gamma_{\varkappa} u_{\varkappa 1} & -\Gamma_{\varkappa} u_{\varkappa 2} & -\Gamma_{\varkappa} u_{\varkappa 3} \\ -\Gamma_{\varkappa} u_{\varkappa 1} & 1 + u^2_{\varkappa 1} & u_{\varkappa 1} u_{\varkappa 2} & u_{\varkappa 1} u_{\varkappa 3} \\ -\Gamma_{\varkappa} u_{\varkappa 2} & u_{\varkappa 2} u_{\varkappa 1} & 1 + u^2_{\varkappa 2} & u_{\varkappa 2} u_{\varkappa 3} \\ -\Gamma_{\varkappa} u_{\varkappa 3} & u_{\varkappa 3} u_{\varkappa 1} & u_{\varkappa 3} u_{\varkappa 2} & 1 + u^2_{\varkappa 3} \end{pmatrix}$$

$$= \sum_{\varkappa} (\sigma_{\varkappa} \Gamma_{\varkappa})^2 \begin{pmatrix} \mathbf{v}^2_{\varkappa} & -v_{\varkappa 1} & -v_{\varkappa 2} & -v_{\varkappa 3} \\ -v_{\varkappa 1} & 1 - v^2_{\varkappa 2} - v^2_{\varkappa 3} & v_{\varkappa 1} v_{\varkappa 2} & v_{\varkappa 1} v_{\varkappa 3} \\ -v_{\varkappa 2} & v_{\varkappa 2} v_{\varkappa 1} & 1 - v^2_{\varkappa 3} - v^2_{\varkappa 1} & v_{\varkappa 2} v_{\varkappa 3} \\ -v_{\varkappa 3} & v_{\varkappa 3} v_{\varkappa 1} & v_{\varkappa 3} v_{\varkappa 2} & 1 - v^2_{\varkappa 1} - v^2_{\varkappa 2} \end{pmatrix}.$$

As above, the index $\varkappa$ ranges over the sets of initial ($I_{s,d}$) and final ($F_{s,d}$) one-packet states; $u_{\varkappa i}$ and $v_{\varkappa i}$ ($i = 1, 2, 3$) are the components of the vectors $\mathbf{u}_{\varkappa} = \mathbf{p}_{\varkappa}/m_{\varkappa}$ and $\mathbf{v}_{\varkappa}$, respectively ($u_{\varkappa i} = \Gamma_{\varkappa} v_{\varkappa i}$). Clearly, $|T_{\varkappa}| = |T_{\varkappa}|_{\mathbf{v}_{\varkappa}=0} = 0$ while $|\Re_{s,d}| \geq 0$, as judged by strength of positivity of the quadratic form $\Re^{\mu\nu}_{s,d} x_{\mu} x_{\nu}$ and assuming that $\sigma_{\varkappa} > 0$ for all $\varkappa$. Moreover, all principal minors of $|\Re_{s,d}|$ are positive.

We will use the following notation:

$$\omega_i = \sum_\varkappa \sigma_\varkappa^2 \left(1 + u_{\varkappa i}^2\right), \quad \omega = \sum_\varkappa \sigma_\varkappa^2 \mathbf{u}_\varkappa^2, \quad \upsilon_i = \sum_\varkappa \sigma_\varkappa^2 \Gamma_\varkappa u_{\varkappa i}, \quad w_i = \sum_\varkappa \sigma_\varkappa^2 u_{\varkappa j} u_{\varkappa k}. \tag{80}$$

Here and below in this Section, the indices s and d are omitted for short. The spatial indices denoted by i, j, k range over 1,2,3, and (if not stipulated otherwise) $i \neq j \neq k$. With this notation, the determinants of $\Re_s$ and $\Re_d$ are given by

$$\begin{aligned} |\Re_{s,d}| = \omega \prod_i \omega_i + 2\omega \prod_i w_i + \sum_i \upsilon_i w_i \left(\upsilon_i w_i - \upsilon_j w_j - \upsilon_k w_k\right) \\ + \sum_i \left[w_i \omega_i \left(2\upsilon_j \upsilon_k - \omega w_i\right) - \upsilon_i^2 \omega_j \omega_k\right]. \end{aligned} \tag{81}$$

The matrices inverse to $\Re_{s,d}$ are straightforwardly (but not trivially) determined through the adjuncts $\mathfrak{A}_{s,d}^{\mu\nu}$ of $|\Re_{s,d}|$:

$$\Re_{s,d}^{-1} = |\Re_{s,d}|^{-1} ||\mathfrak{A}_{s,d}^{\mu\nu}||, \tag{82}$$

$$\begin{aligned} \mathfrak{A}_{s,d}^{00} &= \prod_i \omega_i - \sum_i w_i^2 \omega_i + 2 \prod_i w_i, \\ \mathfrak{A}_{s,d}^{0i} &= \upsilon_i \omega_j \omega_k - \upsilon_j w_k \omega_k - \upsilon_k w_j \omega_j + w_i \left(\upsilon_j w_j + \upsilon_k w_k - \upsilon_i w_i\right), \\ \mathfrak{A}_{s,d}^{ii} &= \omega \left(\omega_j \omega_k - w_i^2\right) + 2 w_i \upsilon_j \upsilon_k - \upsilon_j^2 \omega_k - \upsilon_k^2 \omega_j, \\ \mathfrak{A}_{s,d}^{jk} &= \left(\upsilon_j \upsilon_k - \omega w_i\right) \omega_i + \upsilon_i \left(\upsilon_i w_i - \upsilon_j w_j - \upsilon_k w_k\right) + \omega w_j w_k. \end{aligned} \tag{83}$$

The elements of the matrices $\widetilde{\Re}_s$ and $\widetilde{\Re}_d$ are given by

$$\widetilde{\Re}^{\mu\nu}_{s,d} = |\Re_{s,d}|^{-1}\widetilde{\mathfrak{A}}^{\mu\nu}_{s,d},$$

where

$$\widetilde{\mathfrak{A}}^{00}_{s,d} = \mathfrak{A}^{00}_{s,d}, \quad \widetilde{\mathfrak{A}}^{0i}_{s,d} = \widetilde{\mathfrak{A}}^{i0}_{s,d} = -\mathfrak{A}^{0i}_{s,d}, \quad \widetilde{\mathfrak{A}}^{ij}_{s,d} = \widetilde{\mathfrak{A}}^{ji}_{s,d} = \mathfrak{A}^{ij}_{s,d}.$$

The positive-definiteness of the quadratic forms $\Re^{\mu\nu}_{s,d}q_\mu q_\nu$ provides a set of strict inequalities, in particular,

$$\widetilde{\Re}^{\mu\mu}_{s,d} > 0, \quad \widetilde{\Re}^{00}_{s,d}\widetilde{\Re}^{ii}_{s,d} - \left(\widetilde{\Re}^{0i}_{s,d}\right)^2 > 0, \quad \widetilde{\Re}^{jj}_{s,d}\widetilde{\Re}^{kk}_{s,d} - \left(\widetilde{\Re}^{jk}_{s,d}\right)^2 > 0. \tag{84a}$$

The left parts of these inequalities correspond to the principal minors of the matrix $\widetilde{\Re}_{s,d}$ of the 1-st and 2-nd orders. It is assumed here that there is no summation in repeating indices but, of course, the sums of the corresponding minors are also positive. One more useful set of inequalities is

$$\omega\omega_i > \upsilon_i^2.$$

Similar inequalities are valid also for adjuncts $\mathfrak{A}^{\mu\nu}_{s,d}$ and $\widetilde{\mathfrak{A}}^{\mu\nu}_{s,d}$ (since $|\widetilde{\Re}_{s,d}| > 0$), and for the elements of the matrix $||R^{\mu\nu}|| = ||\widetilde{\Re}^{\mu\nu}_s + \widetilde{\Re}^{\mu\nu}_d||$:

$$R_{\mu\mu} > 0, \quad R_{00}R_{ii} - R^2_{0i} > 0, \quad R_{jj}R_{kk} - R^2_{jk} > 0. \tag{84b}$$

These inequalities lead to important corollaries, in particular, to the positivity of the functions $\mathscr{R}$ and $\mathfrak{m} - \mathfrak{n}_0 - \mathfrak{n}_0^2$ which enter the amplitude.

Indeed, in the coordinate frame where the z axis is directed along the unit vector $\mathbf{l}$ we have

$$\mathscr{R} = R_{33}, \quad \mathfrak{m} - \mathfrak{n}_0 - \mathfrak{n}_0^2 = \frac{R_{00}\mathscr{R} - (\mathbf{Rl})^2}{R^2} = \frac{R_{00}R_{33} - R_{03}^2}{(R_{00} - 2R_{03} + R_{33})^2}.$$

Since these quantities are rotation invariant, from Eqs. (84b) it follows that

$$\mathscr{R} > 0 \quad \text{and} \quad \mathfrak{m} - \mathfrak{n}_0 - \mathfrak{n}_0^2 > 0.$$

From the last inequality it is seen that

$$\Theta_j \approx \frac{m_j^4 R\left(\mathfrak{m} - \mathfrak{n}_0 - \mathfrak{n}_0^2\right)}{4E_\nu^2} = \frac{m_j^4\left[R_{00}\mathscr{R} - (\mathbf{Rl})^2\right]}{4RE_\nu^2} > 0.$$

(see (150)). This leads to a suppression of the probability (79).

The functions $\mathfrak{n}$ and $\bar{\mathfrak{m}}$ can be now constructed from the tensor components $R^{0i} = \widetilde{\mathfrak{R}}_s^{0i} + \widetilde{\mathfrak{R}}_d^{0i}$ and 4-vector $Y = Y_s + Y_d$, where $Y_s^\mu = \widetilde{\mathfrak{R}}_s^{\mu\nu} q_{s\nu}$ and $Y_d^\mu = -\widetilde{\mathfrak{R}}_d^{\mu\nu} q_{d\nu}$.

> Note that for computing the functions $\mathfrak{n}$ and $\bar{\mathfrak{n}}$ we actually only need to know the inner product $Yl = (Y_s + Y_d)l = E_\nu R$ and zero-component $Y^0 = Y_s^0 + Y_d^0$. Moreover, it is sufficient to calculate these quantities in the PW_0 limit, in which the calculations are essentially simplified.

From here on we will use the symbol $[\![f]\!]$ to indicate that the function f is calculated in the PW_0 limit. In these terms

$$Y_{s,d}l \to \widetilde{\mathfrak{R}}_{s,d}^{\mu\nu} q_\mu l_\nu\Big|_{q=E_\nu l} = E_\nu^{-1}\left[\!\!\left[\widetilde{\mathfrak{R}}_{s,d}^{\mu\nu} q_\mu q_\nu\right]\!\!\right] \quad \text{and} \quad Y_{s,d}^0 \to \left[\!\!\left[\widetilde{\mathfrak{R}}_{s,d}^{0\mu} q_\mu\right]\!\!\right].$$

To illustrate the general formulas, we consider several examples important for applications.

7.16.2 Two-particle decay in the source.

Let us investigate the simplest process – the leptonic decay $a \to \ell \nu_*$ in the source, where a is a charged meson ($\pi^\pm$, $K^\pm$, $D_s^\pm$, ...), ℓ is a charged lepton and ν_* denotes a virtual neutrino or antineutrino. Forasmuch as such decays provide the main source of accelerator, atmospheric and astrophysical neutrinos of high energies, we will study this example circumstantially.

Assuredly, the formulas of this section can be straightforwardly translated to *any* 2-body decay $a \to b \nu_*$, for example, to an electron capture decay of relativistic ions (e.g., $^{140}\mathrm{Pr}^{57+} \to {}^{140}\mathrm{Ce}^{57+} \nu_*$) in a gedanken experiment capable of detecting the electron-capture neutrino interactions. With certain stipulations, they can also be applied to the sequential processes of emission and resonant absorption (by induced orbital e-capture) of M¨ossbauer antineutrinos, e.g., $^3\mathrm{H} \to {}^3\mathrm{He} + \overline{\nu}_*$, $\overline{\nu}_* + {}^3\mathrm{He} \to {}^3\mathrm{H}$).

Arbitrary momenta.

In the considered case, the determinant of the matrix $\Re_s$ can readily be obtained from Eq. (81) written in the rest frame of the meson wave packet:[a]

$$\boxed{|\Re_s| = \sigma_a^2 \sigma_\ell^2 \sigma_2^4 |\mathbf{u}_\ell^\star|^2.} \tag{85}$$

Here $\sigma_2^2 = \sigma_a^2 + \sigma_\ell^2$ and $\mathbf{u}_\ell = \mathbf{p}_\ell / m_\ell = \Gamma_\ell \mathbf{v}_\ell$.

[a] We use the star superscript to denote the meson rest frame. The subscripts a and ℓ indicate the corresponding particles and should not be confused with Lorentz indices. A similar index convention is used in the subsequent text.

Since $|\Re_s|$ is a Lorentz invariant, Eq. (85) can be transformed to the laboratory frame just by substitution

$$|\mathbf{u}_\ell^\star| = \frac{\sqrt{(E_\ell \mathbf{p}_a - E_a \mathbf{p}_\ell)^2 - |\mathbf{p}_a \times \mathbf{p}_\ell|^2}}{m_a m_\ell} = (u_a u_\ell)\mathrm{V}_{a\ell}, \quad \mathrm{V}_{a\ell} = \frac{\sqrt{(\mathbf{v}_a - \mathbf{v}_\ell)^2 - |\mathbf{v}_a \times \mathbf{v}_\ell|^2}}{1 - \mathbf{v}_a \mathbf{v}_\ell}.$$

Here $\mathrm{V}_{a\ell}$ is the relative velocity of the meson and lepton in the lab. frame.

Notice that the kinematic variables in this formula are not in general constrained by the energy-momentum conservation. By adopting that the virtual neutrino is on-mass-shell and neglecting both the neutrino masses and the smearing of the meson and lepton momenta, one may use the standard 2-particle kinematics, according to which

$$|\mathbf{v}_\ell^\star| = \mathrm{V}_{a\ell} = \frac{m_a^2 - m_\ell^2}{m_a^2 + m_\ell^2} \quad \text{and} \quad |\mathbf{u}_\ell^\star| = \frac{m_a^2 - m_\ell^2}{2 m_a m_\ell}.$$

In a little bit more complicated way one can calculate the adjuncts $\mathfrak{A}_s^{\mu\nu}$ defined by Eqs. (83):

$$\begin{aligned}
\mathfrak{A}_s^{00} &= \sigma_2^2 \left[\sigma_2^2 \left(\sigma_a^2 \Gamma_a^2 + \sigma_\ell^2 \Gamma_\ell^2\right) + \sigma_a^2 \sigma_\ell^2 \left|\mathbf{u}_a \times \mathbf{u}_\ell\right|^2\right], \\
\mathfrak{A}_s^{0i} &= \sigma_2^2 \left\{\sigma_a^2 \left[\sigma_a^2 \Gamma_a + \sigma_\ell^2 \Gamma_\ell (u_a u_\ell)\right] u_{ai} + \sigma_\ell^2 \left[\sigma_\ell^2 \Gamma_\ell + \sigma_a^2 \Gamma_a (u_a u_\ell)\right] u_{\ell i}\right\}, \\
\mathfrak{A}_s^{ii} &= \sigma_2^2 \left\{\sigma_a^2 \left[\sigma_a^2 u_{ai} + \sigma_\ell^2 (u_a u_\ell) u_{\ell i}\right] u_{ai} + \sigma_\ell^2 \left[\sigma_\ell^2 u_{\ell i} + \sigma_a^2 (u_a u_\ell) u_{ai}\right] u_{\ell i}\right. \\
&\qquad \left. + \sigma_a^2 \sigma_\ell^2 \left[\left(\Gamma_\ell \mathbf{u}_a - \Gamma_a \mathbf{u}_\ell\right)^2 - \left|\mathbf{u}_a \times \mathbf{u}_\ell\right|^2\right]\right\}, \\
\mathfrak{A}_s^{jk} &= \sigma_2^2 \left[\sigma_a^4 u_{aj} u_{ak} + \sigma_\ell^4 u_{\ell j} u_{\ell k} + \sigma_a^2 \sigma_\ell^2 (u_a u_\ell) \left(u_{aj} u_{\ell k} + u_{\ell j} u_{ak}\right)\right], \quad j \neq k.
\end{aligned} \tag{86}$$

No kinematic constraints were imposed for derivation of these formulas.

Using Eqs. (86) and taking into account Eq. (82), we obtain (for arbitrary q)

$$\widetilde{\Re}_s^{\mu\nu} q_\mu q_\nu = \frac{1}{|\Re_s|} \left[\mathfrak{A}_s^{00} q_0^2 + \sum_i \left(-2\mathfrak{A}_s^{0i} q_0 + \mathfrak{A}_s^{ii} q_i \right) q_i + 2 \sum_{j<k} \mathfrak{A}_s^{jk} q_j q_k \right]$$
$$= \frac{A_2}{\sigma_a^2 \sigma_\ell^2 \sigma_2^2 |\mathbf{u}_\ell^\star|^2} - \frac{q^2}{\sigma_2^2}, \tag{87}$$

where we have defined the Lorentz-invariant function

$$\begin{aligned} A_2 = & \left[\sigma_2^2 \left(\sigma_a^2 \Gamma_a^2 + \sigma_\ell^2 \Gamma_\ell^2 \right) + \sigma_a^2 \sigma_\ell^2 \left(\Gamma_\ell \mathbf{u}_a - \Gamma_a \mathbf{u}_\ell \right)^2 \right] q_0^2 \\ & - 2 \left\{ \sigma_a^2 \left[\sigma_a^2 \Gamma_a + \sigma_\ell^2 \Gamma_\ell (u_a u_\ell) \right] \mathbf{u}_a \mathbf{q} + \sigma_\ell^2 \left[\sigma_\ell^2 \Gamma_\ell + \sigma_a^2 \Gamma_a (u_a u_\ell) \right] \mathbf{u}_\ell \mathbf{q} \right\} q_0 \\ & + \sum_i \left[\sigma_a^4 u_{ai}^2 + \sigma_\ell^4 u_{\ell i}^2 + 2 \sigma_a^2 \sigma_\ell^2 (u_a u_\ell) u_{ai} u_{\ell i} \right] q_i^2 \\ & + 2 \sum_{j<k} \left[\sigma_a^4 u_{aj} u_{ak} + \sigma_\ell^4 u_{\ell j} u_{\ell k} + \sigma_a^2 \sigma_\ell^2 (u_a u_\ell) \left(u_{aj} u_{\ell k} + u_{ak} u_{\ell j} \right) \right] q_j q_k . \end{aligned}$$

By applying the identities

$$\left(u_a q \right) \left(u_\ell q \right) = \Gamma_a \Gamma_\ell q_0^2 - \left[\Gamma_a \left(\mathbf{u}_\ell \mathbf{q} \right) + \Gamma_\ell \left(\mathbf{u}_a \mathbf{q} \right) \right] q_0 + \left(\mathbf{u}_a \mathbf{q} \right) \left(\mathbf{u}_\ell \mathbf{q} \right),$$
$$\left(\mathbf{u}_a \mathbf{q} \right) \left(\mathbf{u}_\ell \mathbf{q} \right) = \sum_i \left[\left(u_{ai} q_i \right) \left(u_{\ell i} q_i \right) + \left(u_{aj} q_j \right) \left(u_{\ell k} q_k \right) + \left(u_{ak} q_k \right) \left(u_{\ell j} q_j \right) \right],$$

we arrive at the compact formula for the function A_2:

$$A_2 = \sigma_a^4 \left(u_a q \right)^2 + \sigma_\ell^4 \left(u_\ell q \right)^2 + 2 \sigma_a^2 \sigma_\ell^2 \left(u_a u_\ell \right) \left(u_a q \right) \left(u_\ell q \right). \tag{88}$$

Now we can write out the 4-vector Y_s whose components are defined by

$$Y_s^0 = \widetilde{\Re}_s^{0\nu} q_{s\nu} = \frac{1}{|\Re_s|}\left[\mathfrak{A}^{00}\left(E_a - E_\ell\right) - \mathfrak{A}^{0i}\left(p_a - p_\ell\right)_i\right],$$
$$Y_s^i = \widetilde{\Re}_s^{i\nu} q_{s\nu} = \frac{1}{|\Re_s|}\left[\mathfrak{A}^{ij}\left(p_a - p_\ell\right)_j - \mathfrak{A}^{i0}\left(E_a - E_\ell\right)\right].$$

After elementary manipulations with Eqs. (86), we arrive at the expression:

$$Y_s^\mu = \frac{1}{|\mathbf{u}_\ell^\star|^2}\left\{\left[\frac{(p_a p_\ell)}{m_a^2} - 1\right]\frac{p_a^\mu}{\sigma_\ell^2} - \left[\frac{(p_a p_\ell)}{m_\ell^2} - 1\right]\frac{p_\ell^\mu}{\sigma_a^2}\right\}. \tag{89}$$

Even simpler:

$$(\mathbf{Rq}) = \frac{1}{\sigma_2^2|\mathbf{u}_\ell^\star|^2}\left\{\left[\frac{\sigma_a^2\Gamma_a}{\sigma_\ell^2} + \Gamma_\ell(u_a u_\ell)\right](\mathbf{u}_a\mathbf{q}) + \left[\frac{\sigma_\ell^2\Gamma_\ell}{\sigma_a^2} + \Gamma_a(u_a u_\ell)\right](\mathbf{u}_\ell\mathbf{q})\right\}.$$

PW$_0$ limit.

In the PW$_0$ limit ($q \to p_a - p_\ell = p_\nu = E_\nu l$, $p_\nu^2 = 0$ in this instance) we have

$$u_a u_\ell = \frac{E_\ell^\star}{m_\ell}, \quad u_a q = E_\nu^\star, \quad u_\ell q = \frac{m_a E_\nu^\star}{m_\ell},$$

where

$$E_\ell^\star = \frac{m_a^2 + m_\ell^2}{2m_a} \quad \text{and} \quad E_\nu^\star = \frac{m_a^2 - m_\ell^2}{2m_a}$$

are, respectively, the lepton and neutrino energies in the meson rest frame.

By applying the above relations to Eqs. (88) and (87), we obtain

$$\boxed{\left[\!\left[\widetilde{\Re}_s^{\mu\nu} q_\mu q_\nu\right]\!\right] = \frac{m_\ell^2}{\sigma_\ell^2} + \frac{m_a^2}{\sigma_a^2}.} \tag{90}$$

The shape of the effective neutrino wavepacket.

To illustrate Eq. (90) let us consider the special but quite realistic case when one can neglect the contributions into the full function $\mathfrak{D}$ caused by the reaction in the detector. For this we have to assume that the parameters $\sigma_\varkappa$ for all $\varkappa \in D$ are large enough in comparison with σ_a and σ_ℓ.). Then from Eq. (90) we obtain:

$$\mathfrak{D}^2 \approx E_\nu^2 \left[2\left(\frac{m_\ell^2}{\sigma_\ell^2} + \frac{m_a^2}{\sigma_a^2}\right)\right]^{-1} \ll E_\nu^2, \quad \sigma_j^2 \approx \frac{m_j^2}{2}\left(\frac{m_\ell^2}{\sigma_\ell^2} + \frac{m_a^2}{\sigma_a^2}\right)^{-1} \ll m_j^2. \tag{91}$$

So, in this simplest case, the effective wavepacket of virtual neutrino with a given mass definitely defined by the mass and momentum spreads of the packets of a and ℓ and the values of σ_j for all three known neutrino are *mightily small* for any values of σ_a and σ_ℓ allowed by the CRGP approximation.

Moreover, taking into account that the masses of the known neutrinos are many orders of magnitude smaller than the masses of all other known (massive) elementary particles, we can conclude that $\sigma_j^2 \lll \sigma_{a,\ell}^2$.

While the estimations were done neglecting the detector contributions, they partially explain the success of the standard quantum-mechanical assumptions that the light neutrinos have definite momenta in spite of the fact that they are produced in the processes with the particles having comparatively large momentum spreads.

From (91) it in particular follows that $\sigma_j = 0$ as $m_j = 0$ that is the massless neutrinos can be treated as plane waves. With obvious limitations this remarkable fact can be used in the analyses of the processes in which the light massive (or massless) neutrinos participate as external wavepackets.

From the conditions of applicability of the CRGP approximation for unstable particles

$$(\sigma_\varkappa/\sigma_\varkappa^{\max})^4 \ll 1, \quad \sigma_\varkappa^{\max} = \sqrt{m_\varkappa \Gamma_\varkappa}$$

(where $\Gamma_\varkappa = 1/\tau_\varkappa$ is the full decay width of the particle $\varkappa$) it follows the important limitation:

$$\sigma_j^2 \ll \frac{m_j^2}{2}\left(\frac{m_\ell}{\Gamma_\ell} + \frac{m_a}{\Gamma_a}\right)^{-1}.$$

Therefore, for the two-particle decays of *any* mesons with a muon in the final state ($\pi_{\mu 2}$, $K_{\mu 2}$, etc.) we obtain the upper limit

$$\frac{\sigma_j^2}{m_j^2} \ll \frac{\Gamma_\mu}{m_\mu} \approx 1.4 \times 10^{-18} \quad \Longrightarrow \quad \frac{\sigma_j^{\max}}{\sigma_\mu^{\max}} \approx \frac{m_j}{m_\mu} \lll 1.$$

This leads to the lower limit for the effective transversal and longitudinal dimensions of the neutrino wavepacket:

$$d_j^{\perp} \gg 2.5 \left(\frac{0.1 \text{ eV}}{m_j}\right) \text{ km} \quad \text{and} \quad d_j^{\parallel} = \frac{d_j^{\perp}}{\Gamma_j} \gg 2.5 \times 10^{-5} \left(\frac{1 \text{ GeV}}{E_\nu}\right) \left(\frac{0.1 \text{ eV}}{m_j}\right) \text{ cm}.$$

- The size $d_j^{\perp}$ is on no account the size of the neutrino wavepacket in rest, since all our estimations were performed in the ultrarelativistic approximation and are therefore valid only for such frames in which the neutrinos remain ultrarelativistic. The Lorentz invariance of the effective neutrino wavefunction $\psi_y^j(\mathbf{p}_j, x)$ also takes place up to the same reserve requirement.
- The limitations for the characteristics of the neutrino wavepackets created in $a_{\tau 2}$ decays depend on the type of the decaying particle. For example, in the case of a D_s meson decay we obtain $\sigma_j^2/m_j^2 \ll 2.2 \times 10^{-13}$.
- The effective dimensions $d_j^{\perp}$ and $d_j^{\parallel}$ define (on the order of magnitude) the allowed transversal and longitudinal quantum deviations of the center of the neutrino packet from the "classical trajectory" $\overline{\mathbf{L}}_j = \mathbf{v}_j T$.
- The transversal deviations $\delta \mathbf{L}_j^{\perp} \sim d_j^{\perp}$ can be huge, wittingly larger than the dimensions of the present-day neutrino detectors and the natural widening of the accelerator neutrino beams even in the distances of about $\sim 10^3$ km from the source. This fact should not cause bewilderment and confusion if we remind ourselves that the standard quantum-mechanical description of the massive neutrino as a state with definite momentum implicates, as a direct consequence of the Heisenberg uncertainty relation,

that its "dimensions" (both transversal and longitudinal) are *infinitely large*. Such description does not lead to unphysical results since the neither transversal dimensions nor transversal quantum fluctuations enter the transition amplitude and thus do not affect the observables.

Вклады в функции $\mathfrak{n}$ и $\mathfrak{m}$. Из общей формулы (89) находим 4-вектор Y_s в ПВ$_0$-приближении:

$$Y_s = \frac{1}{m_a E_\nu^\star}\left[\left(\frac{m_\ell^2}{\sigma_\ell^2}+\frac{m_a^2}{\sigma_a^2}\right)p_a - \frac{m_a^2}{\sigma_a^2}\,p_\nu\right] = \frac{1}{m_a E_\nu^\star}\left[\left(\frac{m_\ell^2}{\sigma_\ell^2}+\frac{m_a^2}{\sigma_a^2}\right)p_\ell - \frac{m_\ell^2}{\sigma_\ell^2}\,p_\nu\right].$$

Скалярные произведения, которые требуются для расчета $a_{\ell 2}$ вкладов в функции $\mathfrak{n}$ и $\mathfrak{m}$, имеют вид

$$Y_s l = \left[\!\left[\widetilde{\Re}_s^{\mu\nu} q_\mu q_\nu\right]\!\right]\frac{1}{E_\nu} = \left(\frac{m_\ell^2}{\sigma_\ell^2}+\frac{m_a^2}{\sigma_a^2}\right)\frac{1}{E_\nu},$$

$$\mathbf{Y}_s\mathbf{l} = Y_s^0 - Y_s l = \frac{\mathit{\Gamma}_a}{E_\nu^\star}\left[\left(\frac{m_\ell^2}{\sigma_\ell^2}+\frac{m_a^2}{\sigma_a^2}\right)\left(1-\frac{m_a E_\nu^\star}{E_a E_\nu}\right) - \frac{m_a^2}{\sigma_a^2}\frac{E_\nu}{E_a}\right].$$

Отсюда находим:

$$\frac{\mathbf{Y}_s\mathbf{l}}{Y_s l} = \mathit{\Gamma}_a\left[1-\left(\frac{m_a^2\sigma_\ell^2}{m_a^2\sigma_\ell^2+m_\ell^2\sigma_a^2}\right)\frac{E_\nu}{E_a}\right]\frac{E_\nu}{E_\nu^\star} - 1 \equiv \mathfrak{n}_s\left(E_a, E_\nu\right).$$

Поскольку, при фиксированном значении E_ν функция $\mathfrak{n}_s$ линейно зависит от E_a, то имеет место следующее неравенство:

$$\mathfrak{n}_s \geq \mathfrak{n}_s \left(E_a^{\min}, E_\nu \right),$$

в котором

$$E_a^{\min} = \frac{m_a}{2} \left(\frac{E_\nu}{E_\nu^\star} + \frac{E_\nu^\star}{E_\nu} \right)$$

есть минимальная энергия частицы a, необходимая для рождения безмассового нейтрино с энергией E_ν в $a_{\ell 2}$-распаде. Таким образом, абсолютный минимум функции $\mathfrak{n}_s$ отрицателен:

$$\mathfrak{n}_s^{\min} = \mathfrak{n}_s \left(m_a, E_\nu^\star \right) = -\frac{\left(m_a^2 - m_\ell^2 \right) \sigma_\ell^2}{2 \left(m_a^2 \sigma_\ell^2 + m_\ell^2 \sigma_a^2 \right)}, \quad |\mathfrak{n}_s^{\min}| < \frac{1}{2} \left(1 - \frac{m_\ell^2}{m_a^2} \right).$$

Функция $\mathfrak{n}_s$ возрастает с увеличением энергии нейтрино и может быть сколь угодно велика при $E_\nu \gg E_\nu^\star$;

$$\mathfrak{n}_s \geq \mathfrak{n}_s \left(E_a^{\min}, E_\nu \right) = \frac{1}{2} \left(1 - 2|\mathfrak{n}_s^{\min}| \right) \left(\frac{E_\nu}{E_\nu^\star} \right)^2 \left[1 + \mathcal{O} \left(\frac{E_\nu^\star}{E_\nu} \right) \right].$$

Если предположить, что $|Y_s^0| \gg |Y_d^0|$ и $Y_s l \gg Y_d l$, то функция $\mathfrak{n}_s$ может служить оценкой для полной функции $\mathfrak{n}$. Как хорошо известно, распределение энергии нейтрино в $a_{\ell 2}$-распаде равномерно (т.е. не зависит от E_ν) внутри кинематических границ

$$E_\nu^\star \Gamma_a (1 - |\mathbf{v}_a|) \leq E_\nu \leq E_\nu^\star \Gamma_a (1 + |\mathbf{v}_a|),$$

откуда следует, что средняя энергия распадного нейтрино равна $\overline{E}_\nu = \Gamma_a E^\star_\nu$. Поэтому при высоких энергиях распадающихся мезонов, $\Gamma_a \gg 1$, с точностью до $\mathcal{O}(\Gamma_a^{-2})$ имеем:

$$\mathfrak{n}_s\left(E_a, \overline{E}_\nu\right) \approx \Gamma_a^2 \left(1 - |\mathfrak{n}_s^{\min}|\right) = \left(1 - |\mathfrak{n}_s^{\min}|\right) \left(\frac{\overline{E}_\nu}{E^\star_\nu}\right)^2$$

и, следовательно,

$$\mathfrak{n}_s r_i\big|_{E_\nu = \overline{E}_\nu} \approx \frac{1}{2}\left(1 - |\mathfrak{n}_s^{\min}|\right) \left(\frac{m_i}{E^\star_\nu}\right)^2 \ll 1.$$

При тех же предположениях и удерживая только лидирующие по Γ_a и $E_\nu/E^\star_\nu$ члены, можно оценить вклад $a_{\ell 2}$-распада в функцию $\mathfrak{m}$:

$$\mathfrak{m}_s \approx \Gamma_a^2 \left\{1 + \frac{\sigma_\ell^4 m_a^4}{\left(m_\ell^2\sigma_a^2 + m_a^2\sigma_\ell^2\right)^2}\left[1 + \frac{2\sigma_a^2 E^\star_\nu}{m_a\left(\sigma_a^2 + \sigma_\ell^2\right)}\right]\left(\frac{E_\nu}{E_a}\right)^2\right\}\left(\frac{E_\nu}{E^\star_\nu}\right)^2.$$

Отсюда видно, что $\mathfrak{m}_s \gg \mathfrak{n}_s$; тем не менее предполагаемые в разделе 7.12.2 неравенства (66) остаются справедливыми при $E_\nu \sim \overline{E}_\nu$.

7.16.3 Quasielastic scattering in detector

В качестве простейшего (и наиболее важного) примера реакции в детекторной вершине диаграммы рассмотрим «квазиупругое» рассеяние виртуального нейтрино $\nu_* a \to b\ell$, в котором частица-мишень a может быть электроном, нуклоном или ядром, а ℓ – заряженный лептон. Поскольку в типичном нейтринном эксперименте частицы-мишени обладают очень малыми (тепловыми) скоростями относительно лаб. системы, будем считать, что лаб. система совпадает с с.с.о. волнового пакета, описывающего состояние частицы a. Разумеется, при необходимости все формулы могут быть преобразованы в любую другую систему отсчета, поскольку мы имеем дело лишь с векторами и тензорами, законы преобразования которых хорошо известны.

Arbitrary momenta.

В с.с.о. пакета a определитель матрицы $\Re_d$ имеет вид

$$|\Re_d| = \sigma_3^2 \left\{ \left(\sigma_3^2 + \sigma_a^2\right) \sigma_b^2 \sigma_\ell^2 \left(u_b u_\ell\right)^2 \mathrm{V}_{b\ell}^2 + 2\sigma_a^2 \sigma_b^2 \sigma_\ell^2 \left(u_b u_\ell\right) \left(\mathbf{u}_b \mathbf{u}_\ell\right) + \right. \\ \left. + \sigma_a^2 \left[\sigma_b^2 \left(\sigma_a^2 + \sigma_b^2\right) \mathbf{u}_b^2 + \sigma_\ell^2 \left(\sigma_a^2 + \sigma_\ell^2\right) \mathbf{u}_\ell^2 \right] \right\}. \tag{92}$$

Здесь $\mathrm{V}_{b\ell}$ есть относительная скорость частиц b и ℓ, а $\sigma_3^2 \equiv \sigma_a^2 + \sigma_b^2 + \sigma_\ell^2$. Важный вывод, следующий из этой формулы заключается в том, что определитель $|\Re_d|$ остается *неотрицательным* даже если одна (но только одна) из частиц a, b или ℓ описывается

плоской волной. Если, например, пренебречь членами, пропорциональными σ_ℓ^2, формула для определителя (92) приобретает вид, совпадающий с (85):

$$|\Re_d| \approx \sigma_a^2 \sigma_b^2 \left(\sigma_a^2 + \sigma_b^2\right)^2 |\mathbf{u}_b|^2. \tag{93}$$

Это важное свойство дает возможность значительно упростить анализ многопакетных in- и out-состояний, пренебрегая вкладами пакетов очень больших пространственных размеров (характеризующихся очень малыми значениями параметров $\sigma_\varkappa$). При этом следует иметь в виду, что приближенная формула (93) применима только при условии $|\mathbf{u}_b| \neq 0$[a]. Аналогичная оговорка должна быть учтена и в общем случае, т.е. при отбрасывании вкладов пакетов с очень малыми значениями $\sigma_\varkappa$ следует вырезать окрестности фазового пространства, внутри которых определители $|\Re_s|$ и $|\Re_d|$, вычисленные в таком приближении, обращаются в нуль. Как правило, такие области расположены вблизи кинематических границ фазового пространства и не дают вклада в экспериментально измеряемые характеристики.

[a] Напомним, что величина $|\mathbf{u}_\ell^\star|$ в (85) всегда отлична от нуля.

Согласно (83), алгебраические дополнения $\mathfrak{A}_d^{\mu\nu}$ имеют вид

$$
\begin{aligned}
\mathfrak{A}_d^{00} &= \sigma_3^2\left[\sigma_3^2\left(\sigma_a^2+\sigma_b^2\Gamma_b^2+\sigma_\ell^2\Gamma_\ell^2\right)+\sigma_b^2\sigma_\ell^2\left|\mathbf{u}_b\times\mathbf{u}_\ell\right|^2\right],\\
\mathfrak{A}_d^{0i} &= \sigma_3^2\sigma_b^2\left[\left(\sigma_a^2+\sigma_b^2\right)\Gamma_b+\sigma_\ell^2(u_bu_\ell)\right]u_{pi}+\sigma_3^2\sigma_\ell^2\left[\left(\sigma_a^2+\sigma_\ell^2\right)\Gamma_\ell+\sigma_b^2(u_bu_\ell)\right]u_{\ell i},\\
\mathfrak{A}_d^{ii} &= \sigma_b^2\left(\sigma_3^2\sigma_b^2-\sigma_a^2\sigma_\ell^2\mathbf{u}_\ell^2\right)u_{pi}^2+\sigma_\ell^2\left(\sigma_3^2\sigma_\ell^2-\sigma_a^2\sigma_b^2\mathbf{u}_b^2\right)u_{\ell i}^2+\\
&\quad+2\sigma_b^2\sigma_\ell^2\left[\sigma_a^2\Gamma_b\Gamma_\ell+\left(\sigma_b^2+\sigma_\ell^2\right)(u_bu_\ell)\right]u_{pi}u_{\ell i}+\sigma_3^{-2}|\Re_d|,\\
\mathfrak{A}_d^{jk} &= \sigma_b^2\left(\sigma_3^2\sigma_b^2-\sigma_a^2\sigma_\ell^2\mathbf{u}_\ell^2\right)u_{pj}u_{pk}+\sigma_\ell^2\left(\sigma_3^2\sigma_\ell^2-\sigma_a^2\sigma_b^2\mathbf{u}_b^2\right)u_{\ell j}u_{\ell k}+\\
&\quad+\sigma_b^2\sigma_\ell^2\left[\sigma_a^2\Gamma_b\Gamma_\ell+\left(\sigma_b^2+\sigma_\ell^2\right)(u_bu_\ell)\right]\left(u_{pj}u_{\ell k}+u_{pk}u_{\ell j}\right),\quad j\neq k.
\end{aligned}
\tag{94}
$$

Отсюда для произвольного 4-вектора q получаем:

$$
\begin{aligned}
|\Re_d|\widetilde{\Re}_d^{\mu\nu}q_\mu q_\nu &= \mathfrak{A}_d^{00}q_0^2+\sum_i\left(-2\mathfrak{A}_d^{0i}q_0+\mathfrak{A}_d^{ii}q_i\right)q_i+2\sum_{j<k}\mathfrak{A}_d^{jk}q_jq_k\\
&= \sigma_3^2\left[\sigma_3^2\left(\sigma_a^2+\sigma_b^2\Gamma_b^2+\sigma_\ell^2\Gamma_\ell^2\right)+\sigma_b^2\sigma_\ell^2\left|\mathbf{u}_b\times\mathbf{u}_\ell\right|^2\right]q_0^2-\\
&\quad-2\sigma_3^2\sigma_b^2\left[\left(\sigma_a^2+\sigma_b^2\right)\Gamma_b+\sigma_\ell^2\Gamma_\ell(u_bu_\ell)\right](\mathbf{u}_b\mathbf{q})\,q_0-\\
&\quad-2\sigma_3^2\sigma_\ell^2\left[\left(\sigma_a^2+\sigma_\ell^2\right)\Gamma_\ell+\sigma_b^2\Gamma_b(u_bu_\ell)\right](\mathbf{u}_\ell\mathbf{q})\,q_0+\\
&\quad+\sigma_3^2\left[\sigma_b^4\left(\mathbf{u}_b\mathbf{q}\right)^2+\sigma_\ell^4\left(\mathbf{u}_\ell\mathbf{q}\right)^2+2\sigma_b^2\sigma_\ell^2\left(u_bu_\ell\right)\left(\mathbf{u}_b\mathbf{q}\right)\left(\mathbf{u}_\ell\mathbf{q}\right)\right]+\\
&\quad+\sigma_a^2\sigma_b^2\sigma_\ell^2\left\{\left[(\mathbf{u}_b\times\mathbf{u}_\ell)\mathbf{q}\right]^2-\left(\mathbf{u}_b\times\mathbf{u}_\ell\right)^2\mathbf{q}^2\right\}+\sigma_3^{-2}|\Re_d|\mathbf{q}^2.
\end{aligned}
$$

Компоненты 4-импульса Y_d найдем, используя (94):

$$Y_d^0 = \frac{\sigma_3^2}{|\Re_d|}\left(c_a^0 m_a - c_b^0 E_b - c_\ell^0 E_\ell\right), \quad \mathbf{Y}_d = \frac{\sigma_3^2}{|\Re_d|}\left(c_b \mathbf{u}_b + c_\ell \mathbf{u}_\ell\right).$$

Фигурирующие здесь коэффицентные функции даются следующими формулами:

$$\begin{aligned}
c_a^0 &= \sigma_a^2\left(\sigma_3^2 + \sigma_b^2 \Gamma_b^2 + \sigma_\ell^2 \Gamma_\ell^2\right) + \sigma_b^2\sigma_\ell^2\left[\left(\Gamma_b\Gamma_\ell - 1\right)^2 - \left(\mathbf{u}_b\mathbf{u}_\ell\right)^2\right] + \left(\sigma_b^2\Gamma_b + \sigma_\ell^2\Gamma_\ell\right)^2, \\
c_b^0 &= \sigma_3^2\left[\sigma_a^2 + \sigma_b^2 + \sigma_\ell^2\Gamma_\ell^2\left(1 - \mathbf{v}_b\mathbf{v}_\ell\right)\right], \\
c_\ell^0 &= \sigma_3^2\left[\sigma_a^2 + \sigma_\ell^2 + \sigma_b^2\Gamma_b^2\left(1 - \mathbf{v}_b\mathbf{v}_\ell\right)\right], \\
c_b &= \sigma_b^2\left\{\left[m_a\sigma_\ell^2\Gamma_\ell - m_\ell\left(\sigma_b^2 + \sigma_\ell^2\right)\right]\left(u_b u_\ell\right) + m_a\sigma_b^2\Gamma_b - m_b\left(\sigma_b^2 + \sigma_\ell^2\right)\right\} + \\
&\quad + \sigma_a^2\left\{m_b\sigma_\ell^2\mathbf{u}_\ell^2 + \sigma_b^2\left[\Gamma_b\left(m_a - m_\ell\Gamma_\ell\right) - m_b\right]\right\}, \\
c_\ell &= \sigma_\ell^2\left\{\left[m_a\sigma_b^2\Gamma_b - m_b\left(\sigma_b^2 + \sigma_\ell^2\right)\right]\left(u_b u_\ell\right) + m_a\sigma_\ell^2\Gamma_\ell - m_\ell\left(\sigma_b^2 + \sigma_\ell^2\right)\right\} + \\
&\quad + \sigma_a^2\left\{m_\ell\sigma_b^2\mathbf{u}_b^2 + \sigma_\ell^2\left[\Gamma_\ell\left(m_a - m_b\Gamma_b\right) - m_\ell\right]\right\}.
\end{aligned}$$

Как и должно быть, вышеприведенные выражения симметричны по отношению к замене индексов $b \leftrightarrow \ell$, а их явно нековариантная форма связана с использованием специальной системы отсчета.

PW_0 limit.

В $\mathrm{ПВ}_0$-пределе кинематика реакции $2 \to 2$ позволяет записать величины $|\Re_d|$, $\widetilde{\Re}_d^{\mu\nu} q_\mu q_\nu$ и $\mathbf{Y}_d \mathbf{l}$ в терминах двух произвольных независимых инвариантных переменных; мы будем использовать стандартную пару переменных:

$$s = (p_a + p_\nu)^2 = m_a \left(2E_\nu + m_a\right) \quad \text{и} \quad Q^2 = -(p_\nu - p_\ell)^2.$$

Для того, чтобы записать выражения предыдущего раздела через эти переменные примем во внимание точные кинематические соотношения:

$$E_b = \frac{1}{m_a}\left(E_b^* E_a^* - E_\nu^* P_\ell^* \cos\theta_*\right), \quad \mathbf{p}_b \mathbf{p}_\nu = \frac{E_\nu}{m_a}\left(E_b^* E_\nu^* - E_a^* P_\ell^* \cos\theta_*\right),$$
$$E_\ell = \frac{1}{m_a}\left(E_\ell^* E_a^* + E_\nu^* P_\ell^* \cos\theta_*\right), \quad \mathbf{p}_\ell \mathbf{p}_\nu = \frac{E_\nu}{m_a}\left(E_\ell^* E_\nu^* + E_a^* P_\ell^* \cos\theta_*\right),$$
$$|\mathbf{u}_b \times \mathbf{u}_\ell| = \frac{E_\nu P_\ell^* \sin\theta_*}{m_b m_\ell}, \quad (\mathbf{u}_b \times \mathbf{u}_\ell)\, \mathbf{p}_\nu = 0,$$
$$u_b u_\ell = \frac{s - m_b^2 - m_\ell^2}{2 m_b m_\ell}, \quad \mathrm{V}_{b\ell} = \frac{2\sqrt{s} P_\ell^*}{s - m_b^2 - m_\ell^2},$$

в которых $E_\nu = |\mathbf{p}_\nu| = \left(s - m_a^2\right)/2m_a$ и $\mathbf{p}_\nu = E_\nu \mathbf{l}$ есть, соответственно, энергия и

импульс безмассового нейтрино в лабораторной системе отсчета, а

$$E^*_\nu = \frac{s - m_a^2}{2\sqrt{s}}, \quad E^*_\ell = \frac{s + m_\ell^2 - m_b^2}{2\sqrt{s}},$$
$$E^*_a = \frac{s + m_a^2}{2\sqrt{s}} \quad \text{и} \quad E^*_b = \frac{s - m_\ell^2 + m_b^2}{2\sqrt{s}}$$

есть энергии частиц ν^*, ℓ, a и b в с.ц.м. сталкивающихся частиц ν^* и a, которая задается условиями

$$E^*_\nu + E^*_a = E^*_a + E^*_\ell, \quad \mathbf{p}^*_\nu + \mathbf{p}^*_a = \mathbf{p}^*_\ell + \mathbf{p}^*_b = 0;$$

наконец, $P^*_\ell = |\mathbf{p}^*_\ell|$. Угол рассеяния лептона θ_* в с.ц.м. связан с Q^2:

$$Q^2 = 2E^*_\nu \left(E^*_\ell - P^*_\ell \cos\theta_*\right) - m_\ell^2.$$

Кинематически допустимая область фазового пространства дается неравенствами

$$s \geq s_{\mathsf{th}} = \max\left[m_a^2, (m_b + m_\ell)\right], \tag{95}$$

$$Q^2_- \leq Q^2 \leq Q^2_+, \quad Q^2_\pm = 2E^*_\nu \left(E^*_\ell \pm P^*_\ell\right) - m_\ell^2. \tag{96}$$

Теперь, после элементарных, хотя и довольно громоздких алгебраических

преобразований, находим:

$$[\![|\Re_d|]\!] = \frac{\sigma_3^2}{4m_a^2 m_b^2 m_\ell^2} \sum_{k,l=0}^{2} A_{kl} s^k Q^{2l},$$

$$\left[\!\!\left[|\Re_d| \widetilde{\Re}_d^{\mu\nu} q_\mu q_\nu\right]\!\!\right] = \frac{\sigma_3^2}{4m_a^2 m_b^2 m_\ell^2} \sum_{k,l=0}^{2} B_{kl} s^k Q^{2l},$$

$$[\![|\Re_d| \mathbf{Y}_d \mathbf{q}]\!] = \frac{\sigma_3^2}{8m_a^2 m_b^2 m_\ell^2} \sum_{k,l=0}^{3} C_{kl} s^k Q^{2l}.$$

Явные формулы для коэффициентов A_{kl}, B_{kl} и C_{kl} выписаны в Приложении 22. Там же приведены дополнительные результаты, относящиеся к рассматриваемому примеру.

Таким образом, квадратичная форма $\widetilde{\Re}_d^{\mu\nu} q_\mu q_\nu$ и скалярное произведение $\mathbf{Y}_d \mathbf{q}$ являются рациональными функциями двух переменных s и Q^2:

$$\left[\!\!\left[\widetilde{\Re}_d^{\mu\nu} q_\mu q_\nu\right]\!\!\right] = \frac{\sum_{k,l} B_{kl} s^k Q^{2l}}{\sum_{k,l} A_{kl} s^k Q^{2l}} \equiv \mathfrak{F}_d(s, Q^2),$$

$$[\![\mathbf{Y}_d \mathbf{q}]\!] = \frac{1}{2} \frac{\sum_{k,l} C_{kl} s^k Q^{2l}}{\sum_{k,l} A_{kl} s^k Q^{2l}} \equiv \mathfrak{n}_d(s, Q^2) \mathfrak{F}_d(s, Q^2).$$

Здесь мы ввели функцию[a]

$$\mathfrak{n}_d = \frac{[\![\mathbf{Y}_d\mathbf{l}]\!]}{[\![Y_d l]\!]} = \frac{1}{2}\,\frac{\sum_{k,l} C_{kl} s^k Q^{2l}}{\sum_{k,l} B_{kl} s^k Q^{2l}}.$$

Полезно также ввести функцию $\mathfrak{D}_d$ с помощью следующего определения:

$$\frac{\mathfrak{D}_d^2}{E_\nu^2} = \frac{1}{2\mathfrak{F}_d} = \frac{1}{2}\,\frac{\sum_{k,l} A_{kl} s^k Q^{2l}}{\sum_{k,l} B_{kl} s^k Q^{2l}}.$$

Хотя ни $\mathfrak{D}_d$, ни $\mathfrak{n}_d$ не имеют сами по себе очевидного физического смысла, они полезны для иллюстрации поведения интересующих нас функций $\mathfrak{D}$ и $\mathfrak{n}$ в том специальном случае, когда можно пренебречь соответствующими вкладами в $\mathfrak{D}$ и $\mathfrak{n}$, обусловленными реакцией в источнике[b], а именно, при выполнении условий

$$\left[\!\!\left[\widetilde{\Re}_d^{\mu\nu} q_\mu q_\nu\right]\!\!\right] \gg \left[\!\!\left[\widetilde{\Re}_s^{\mu\nu} q_\mu q_\nu\right]\!\!\right] \quad \text{и} \quad [\![|\mathbf{Y}_d\mathbf{l}|]\!] \gg [\![|\mathbf{Y}_s\mathbf{l}|]\!]\,.$$

В простейшем частном случае, когда $\sigma_a/m_a = \sigma_b/m_b = \sigma_\ell/m_\ell = \lambda = \text{const}$, (эти соотношения описывают своеобразный скейлинг эффективных размеров пакетов) можно показать, что функции $\lambda^2\mathfrak{F}_d$ (а следовательно и $\mathfrak{D}_d/\lambda$) и $\mathfrak{n}_d$ не зависят от параметра λ и определяются исключительно кинематикой. Этот «изысканный» (хотя, возможно, и не очень реалистичный) случай иллюстрируется на рисунках 33 и 34 для шести реакций

---

[a] Следует обратитить внимание, что, в отличие от $\mathfrak{F}_d$, функция $\mathfrak{n}_d$ не является релятивистским инвариантом, несмотря на то, что выражается (в л.с.) в терминах двух инвариантов.

[b] Этот случай прямо противоположен рассмотренному для $a_{\ell 2}$-распада.

квазиупругого рассеяния нейтрино и антинейтрино на свободных нуклонах. Области определения функций $\mathfrak{F}_d$ и $\mathfrak{n}_d$ ограничены кинематическими условиями (95), (96), и различия формы поверхностей, изображенных на разных панелях, обусловлены, главным образом, разными порогами реакций (95), т.е., по существу, массами конечных лептонов. Поэтому различия нивелируются при достаточно высоких энергиях, т.е. при $s \gg \max(s_{\mathsf{th}})$. Обращение функции $\mathfrak{F}_d$ в нуль при $E_\nu \to 0$ для беспороговой реакции $\nu n \to pe^-$ не имеет отношения к нашей задачей, ограниченной рассмотрением ультрарелятивистских нейтрино (напомним, что в случае $E_\nu \sim m_j$ формулы для дисперсии сильнейшим образом видоизменяются.

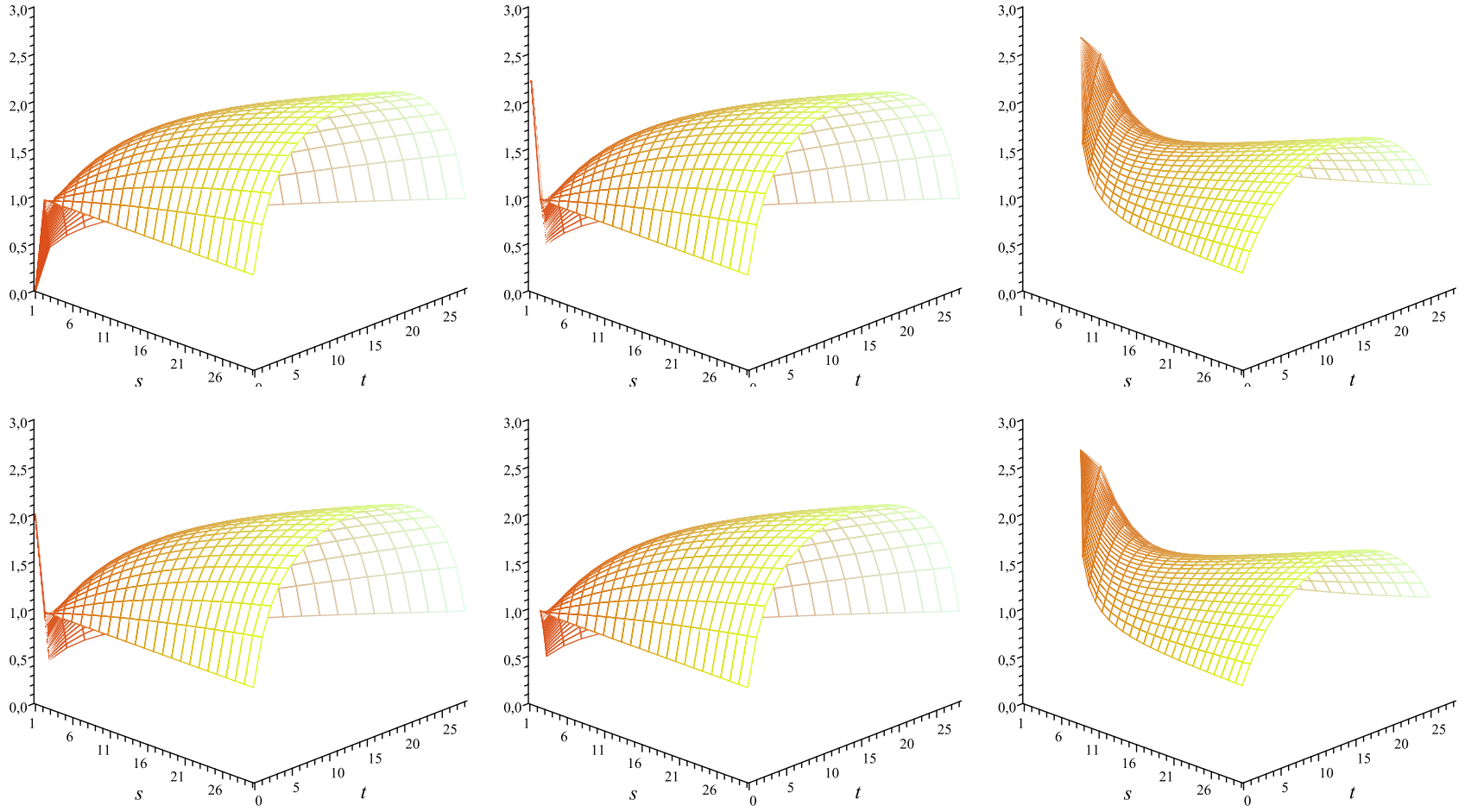

Рис. 33: Function $\lambda^2\mathfrak{F}_d$ vs. s and $t = Q^2$ (both variables are in GeV^2) for quasielastic reactions $\nu n \to p e^-$ (top left), $\nu n \to p \mu^-$ (top mid), $\nu n \to p \tau^-$ (top right), $\overline{\nu} p \to n e^+$ (bottom left), $\overline{\nu} p \to n \mu^+$ (bottom mid), and $\overline{\nu} p \to n \tau^+$ (bottom right). Calculations are done with $\sigma_p/m_p = \sigma_n/m_n = \sigma_\ell/m_\ell = \lambda$.

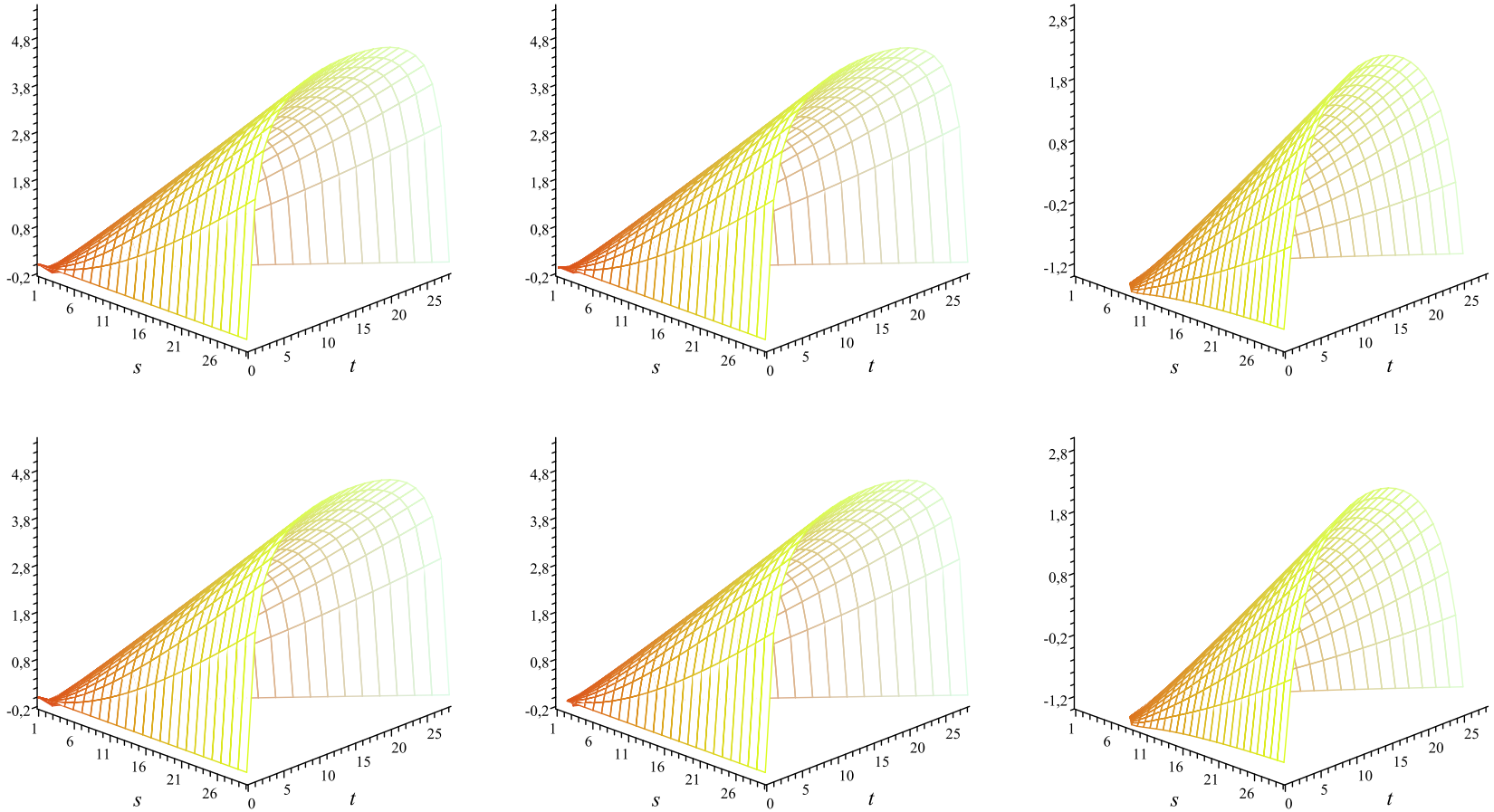

Рис. 34: Function $\mathfrak{n}_d$ vs. s and $t = Q^2$ (both variables are in GeV^2) for quasielastic reactions $\nu n \to p e^-$ (top left), $\nu n \to p \mu^-$ (top mid), $\nu n \to p \tau^-$ (top right), $\overline{\nu} p \to n e^+$ (bottom left), $\overline{\nu} p \to n \mu^+$ (bottom mid), and $\overline{\nu} p \to n \tau^+$ (bottom right). Calculations are done with $\sigma_p/m_p = \sigma_n/m_n = \sigma_\ell/m_\ell = \lambda$.

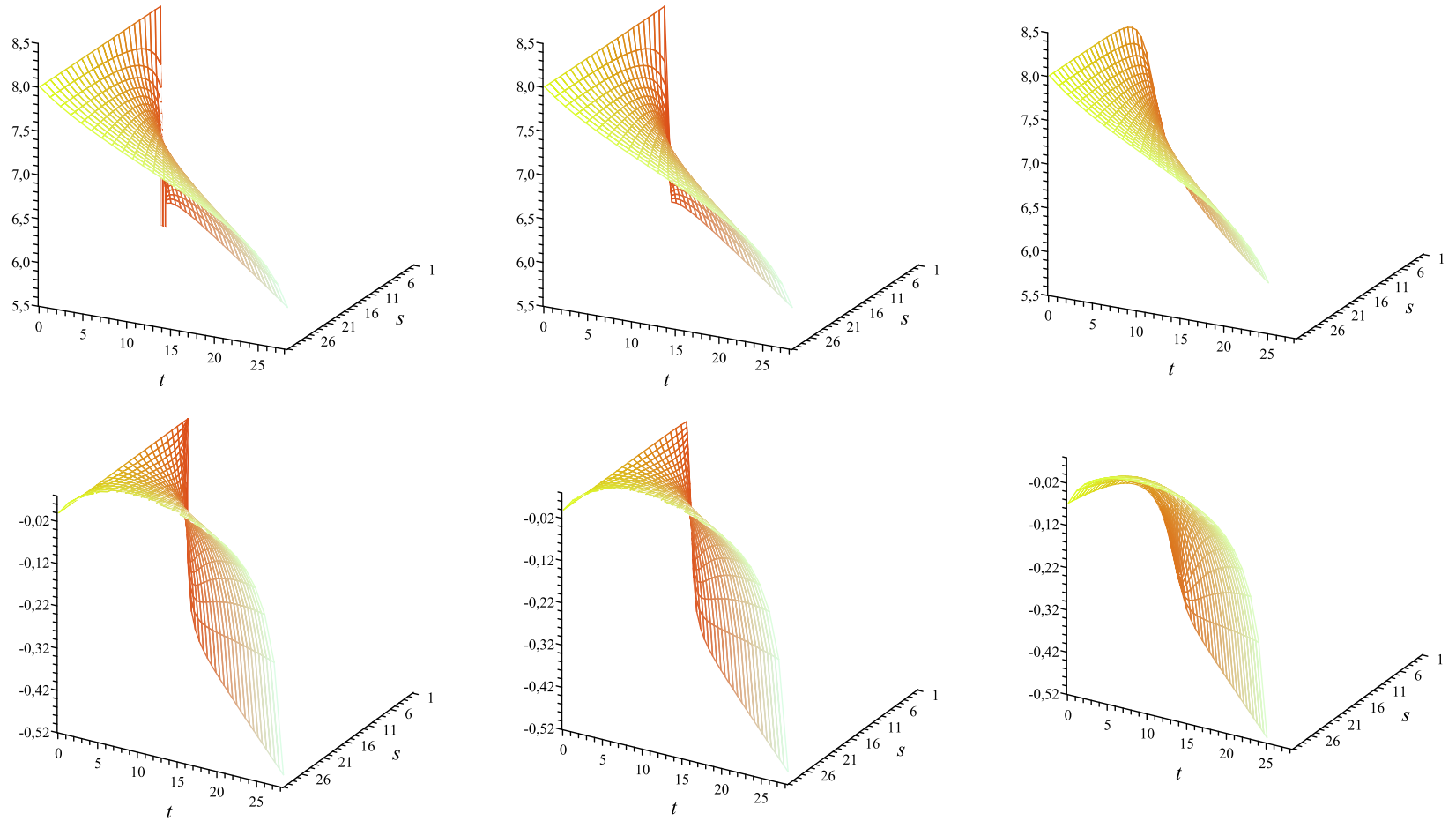

Рис. 35: Functions $\lg(\mathfrak{F}_d)$ (top panels) and $\mathfrak{n}_d$ (bottom panels) vs. s and $t = Q^2$ (both variables are in GeV^2) for quasielastic reactions $\nu n \to p e^-$, $\nu n \to p \mu^-$, and $\nu n \to p \tau^-$ (from left to right). Calculations are done with $\sigma_p/m_p = \sigma_n/m_n = 10^{-3}$, $\sigma_\ell/m_\ell = 10^{-4}$.

В общем случае поведение функций $\mathfrak{F}_d$ и $\mathfrak{n}_d$ становится гораздо более сложным. На рис. 35 показаны примеры функций $\lg(\mathfrak{F}_d)$ и $\mathfrak{n}_d$ для реакций $\nu n \to p e^-$, $\nu n \to p \mu^-$ и $\nu n \to p \tau^-$, в предположении, что $\sigma_p/m_p = \sigma_n/m_n = 10\sigma_\ell/m_\ell = 10^{-3}$. Разумеется, это предположение, принятое здесь исключительно в иллюстративных целях, совершенно произвольно и, более того, совершенно нереалистично. В более реалистичной ситуации, $\sigma_\varkappa/m_\varkappa \lll 1$, даже функция $\lg(\mathfrak{F}_d)$ очень сильно изменяется внутри своей области определения и детали ее поведения трудновоспроизводимы на двумерном графике. Для лучшего понимания свойств функций $\mathfrak{F}_d$ и $\mathfrak{n}_d$, мы приводим в Приложении 22 наиболее важные предельные случаи, асимптотики и неравенства.

7.16.4 Three-particle decay in the source.

Общие формулы, описывающие трехчастичный распад $a \to b + \ell + \nu_*$ формально совпадают с таковыми для рассеяния $2 \to 2$, если рассматривать их в с.с.о. частицы a. Главное различие обусловлено кинематикой. Поэтому мы рассмотрим этот случай кратко. Подобно случаю рассеяния $2 \to 2$, в функции $|\Re_s|$ и $\widetilde{\Re}_s^{\mu\nu} q_\mu q_\nu$ могут быть записаны в терминах двух независимых инвариантных переменных, в качестве которых можно использовать, например, любую пару инвариантов

$$s_1 = (p_b + p_\ell)^2 = (p_a - p_\nu)^2\,, \quad s_2 = (p_\nu + p_\ell)^2 = (p_a - p_b)^2\,, \quad s_3 = (p_\nu + p_b)^2 = (p_a - p_\ell)^2\,,$$

связанных тождеством $s_1 + s_2 + s_3 = m_a^2 + m_b^2 + m_\ell^2$. Физическая область для этих переменных задается условиями

$$(m_b + m_\ell)^2 \le s_1 \le m_a^2, \quad m_\ell^2 \le s_2 \le (m_a - m_\ell)^2\,, \quad m_b^2 \le s_3 \le (m_a - m_b)^2\,.$$

Для определенности будем использовать пару (s_1, s_2). Область определения для этой пары является диаграмма Далитца

$$s_1^- \le s_1 \le s_1^+, \quad m_\ell^2 \le s_2 \le (m_a - m_\ell)^2,$$

где

$$s_1^\pm = m_b^2 + m_\ell^2 - \frac{\left(s_2 + m_b^2\right)\left(s_2 - m_a^2 + m_\ell^2\right) \mp \left(s_2 - m_b^2\right)\sqrt{\left(s_2 - m_a^2 - m_\ell^2\right)^2 - 4m_a^2 m_\ell^2}}{2s_2}.$$

Воспользовавшись результатами предыдущего раздела, найдем, например,

$$[\![|\Re_s|]\!] = \frac{\sigma_3^2}{4m_a^2 m_b^2 m_\ell^2} \sum_{k,l=0}^{2} A'_{kl} s_1^k s_2^l,$$

$$\left[\!\!\left[|\Re_s| \widetilde{\Re}_d^{\mu\nu} q_\mu q_\nu\right]\!\!\right] = \frac{\sigma_3^2}{4m_a^2 m_b^2 m_\ell^2} \sum_{k,l=0}^{2} B'_{kl} s_1^k s_2^l.$$

Следовательно, квадратичная форма $\widetilde{\Re}_s^{\mu\nu} q_\mu q_\nu$ является рациональной функцией переменных s_1 и s_2,

$$\left[\!\!\left[\widetilde{\Re}_s^{\mu\nu} q_\mu q_\nu\right]\!\!\right] = \frac{\sum_{k,l} B'_{kl} s_1^k s_2^l}{\sum_{k,l} A'_{kl} s_1^k s_2^l} \equiv \mathfrak{F}_s(s_1, s_2).$$

Отличные от нуля коэффициенты A'_{kl} и B'_{kl} выписаны в Приложении 22. Там же приведены формулы для функции $\mathfrak{F}_s(s_1, s_2)$ в случае сильной иерархии параметров $\sigma_{\varkappa}$.

7.17 Macroscopic averaging.

To obtain the observable quantities, the probability must be averaged/integrated over all the unmeasurable or unused variables of incoming/outgoing WP states.

> Such a procedure can only be realized by taking into account the conditions of a real experimental environment. For these reasons and in this sense, further analysis is model-dependent.

A thought experiment:

Assume that the statistical distributions of the incoming WPs $a \in I_{s,d}$ over the mean momenta, spin projections, and space-time coordinates in the source and detector "devices" can be described by the one-particle distribution functions $f_a(\boldsymbol{p}_a, s_a, x_a)$. It is convenient to normalize each function f_a to the total number, $N_a(x_a^0)$, of the packets a at a time x_a^0:

$$\sum_{s_a} \int \frac{d\boldsymbol{x}_a d\boldsymbol{p}_a}{(2\pi)^3} f_a(\boldsymbol{p}_a, s_a, x_a) = N_a(x_a^0) \qquad (a \in I_{s,d}).$$

For clarity purposes, we (re)define the terms "source" and "detector":

$$\mathcal{S} = \mathrm{supp}_{\{x_a;\ a \in I_s\}} \prod_a f_a(\boldsymbol{p}_a, s_a, x_a), \quad \mathcal{D} = \mathrm{supp}_{\{x_a;\ a \in I_d\}} \prod_a f_a(\boldsymbol{p}_a, s_a, x_a).$$

We'll use the same terms and notation $\mathcal{S}$ and $\mathcal{D}$ also for the corresponding devices.

Suppositions:

[1] $\mathcal{S}$ and $\mathcal{D}$ are finite and mutually disjoint within the space domain.

[2] Effective spatial dimensions of $\mathcal{S}$ and $\mathcal{D}$ are small compared to the mean distance between them but very large compared to the effective dimensions ($\sim \sigma_{\varkappa}^{-1}$) of all WPs in $\mathcal{S}$ and $\mathcal{D}$.

[3] The experiment measures only the momenta of the secondaries in $\mathcal{D}$ and (due to [2]) the background events caused by the secondaries falling into $\mathcal{D}$ from $\mathcal{S}$ can be neglected.

[4] The detection efficiency in $\mathcal{D}$ is 100%.

With these assumptions, the macroscopically averaged probability (79) represents the total number, $dN_{\alpha\beta}$, of the events recorded in $\mathcal{D}$ and consisted of the secondaries $b{\in}F_d$ having the mean momenta between $\boldsymbol{p}_b$ and $\boldsymbol{p}_b + d\boldsymbol{p}_b$:

$$\begin{aligned}\langle\!\langle |\mathcal{A}_{\beta\alpha}|^2 \rangle\!\rangle \equiv dN_{\alpha\beta} = &\sum_{\text{spins}} \int \prod_{a\in I_s} \frac{d\boldsymbol{x}_a d\boldsymbol{p}_a f_a(\boldsymbol{p}_a, s_a, x_a)}{(2\pi)^3 2E_a \mathrm{V}_a} \int \prod_{b\in F_s} \frac{d\boldsymbol{x}_b d\boldsymbol{p}_b}{(2\pi)^3 2E_b \mathrm{V}_b} \mathrm{V}_s \\ &\times \int \prod_{a\in I_d} \frac{d\boldsymbol{x}_a d\boldsymbol{p}_a f_a(\boldsymbol{p}_a, s_a, x_a)}{(2\pi)^3 2E_a \mathrm{V}_a} \int \prod_{b\in F_d} \frac{d\boldsymbol{x}_b [d\boldsymbol{p}_b]}{(2\pi)^3 2E_b \mathrm{V}_b} \mathrm{V}_d \\ &\times \int dE_\nu (2\pi)^4 \delta_s(p_\nu - q_s) |M_s|^2 (2\pi)^4 \delta_d(p_\nu + q_d) |M_d|^2 \\ &\times \frac{\mathfrak{D}}{2\sqrt{\pi}(2\pi)^3 L^2} \Big| \sum_j V_{\alpha j}^* V_{\beta j}\, e^{-\Omega_j(T,L) - \Theta_j} \Big|^2 .\end{aligned} \tag{97}$$

- $\sum_{\text{spins}}$ denotes the averaging/summation over the spin projections of the in/out states.
- Symbol $[d\boldsymbol{p}_b]$ indicates that integration in variable $\boldsymbol{p}_b$ is not performed, i.e., $\int [d\boldsymbol{p}_b] = d\boldsymbol{p}_b$.

Under additional assumptions, the unwieldy expression (97) can be simplified in a few steps.

Step 1: Multidimensional integration in WP positions.

Supposition 5: The distribution functions $f_a(\boldsymbol{p}_a, s_a, x_a)$, as well as the factors $e^{-\Omega_j - \Omega_i^*}/L^2$ vary at large (macroscopic) scales.

> The integrand $\prod_{\varkappa} |\psi_{\varkappa}(\boldsymbol{p}_{\varkappa}, x_{\varkappa} - x)|^2$ in the integral representation of the overlap volumes (75) is essentially different from zero only if the classical word lines of all packets $\varkappa$ pass through a small (though not necessarily microscopic) vicinity of the integration variable.

Supposition 6: The edge effects can be neglected (a harmless extension of supposition [2]).

As a result, expression (97) is reduced to the following:

$$dN_{\alpha\beta} = \sum_{\text{spins}} \int dx \int dy \int d\mathfrak{P}_s \int d\mathfrak{P}_d \int dE_\nu \frac{\mathfrak{D} \left| \sum_j V_{\alpha j}^* V_{\beta j}\, e^{-\Omega_j(T,L) - \Theta_j} \right|^2}{16\pi^{7/2} |\boldsymbol{y} - \boldsymbol{x}|^2}, \tag{98}$$

where $T = y_0 - x_0$, $L = |\boldsymbol{y} - \boldsymbol{x}|$ and we have defined the differential forms

$$d\mathfrak{P}_s = \prod_{a \in I_s} \frac{d\boldsymbol{p}_a f_a(\boldsymbol{p}_a, s_a, x)}{(2\pi)^3 2E_a} \prod_{b \in F_s} \frac{d\boldsymbol{p}_b}{(2\pi)^3 2E_b} (2\pi)^4 \delta_s(p_\nu - q_s) |M_s|^2, \tag{99a}$$

$$d\mathfrak{P}_d = \prod_{a \in I_d} \frac{d\boldsymbol{p}_a f_a(\boldsymbol{p}_a, s_a, y)}{(2\pi)^3 2E_a} \prod_{b \in F_d} \frac{[d\boldsymbol{p}_b]}{(2\pi)^3 2E_b} (2\pi)^4 \delta_d(p_\nu + q_d) |M_d|^2. \tag{99b}$$

Step 2: Integration in time variables.

Supposition 7: During the experiment, the distribution functions f_a in $\mathcal{S}$ and $\mathcal{D}$ vary slowly enough with time so that they can be modelled by the "rectangular ledges"

$$\begin{aligned} f_a(\boldsymbol{p}_a, s_a; x) &= \theta\left(x^0 - x_1^0\right)\theta\left(x_2^0 - x^0\right)\overline{f}_a(\boldsymbol{p}_a, s_a; \boldsymbol{x}) \ \text{ for } \ a\in I_s, \\ f_a(\boldsymbol{p}_a, s_a; y) &= \theta\left(y^0 - y_1^0\right)\theta\left(y_2^0 - y^0\right)\overline{f}_a(\boldsymbol{p}_a, s_a; \boldsymbol{y}) \ \text{ for } \ a\in I_d. \end{aligned} \tag{100}$$

Supposition 8: The time intervals needed to switch on and switch off the source and detector are negligibly small in comparison with periods of stationarity $\tau_s = x_2^0 - x_1^0$ and $\tau_d = y_2^0 - y_1^0$.

> In case of detector, the step functions in (100) can be thought as the "hardware" or "software" trigger conditions. The periods of stationarity τ_s and τ_d can be astronomically long, as it is for the solar and atmospheric neutrino experiments ($\tau_s \ggg \tau_d$ in these cases), or very short, like in the experiments with short-pulsed accelerator beams (when usually $\tau_s \lesssim \tau_d$).

Within the model (100), the only time-dependent factor in the integrand of (98) is $e^{-\Omega_j - \Omega_i^*}$. So the problem is reduced to the (comparatively) simple integral

$$\int_{y_1^0}^{y_2^0} dy^0 \int_{x_1^0}^{x_2^0} dx^0 \; e^{-\Omega_j(y^0-x^0,L)-\Omega_i^*(y^0-x^0,L)} = \frac{\sqrt{\pi}}{2\mathfrak{D}}\tau_d \exp\left(i\varphi_{ij} - \mathscr{A}_{ij}^2\right) S_{ij}. \tag{101}$$

In relation (101) we have adopted the following notation:

$$S_{ij} = \frac{\exp\left(-\mathscr{B}_{ij}^2\right)}{4\tau_d \mathfrak{D}} \sum_{l,l'=1}^{2} (-1)^{l+l'+1} \mathsf{lerf}\left[2\mathfrak{D}\left(x_l^0 - y_{l'}^0 + \frac{L}{v_{ij}}\right) - i\mathscr{B}_{ij}\right], \tag{102}$$

$$\mathscr{A}_{ij} = (v_j - v_i)\mathfrak{D}L = \frac{2\pi\mathfrak{D}L}{E_\nu L_{ij}}, \qquad \mathscr{B}_{ij} = \frac{\Delta E_{ji}}{4\mathfrak{D}} = \frac{\pi\mathfrak{n}}{2\mathfrak{D}L_{ij}}, \tag{103}$$

$$\varphi_{ij} = \frac{2\pi L}{L_{ij}}, \qquad L_{ij} = \frac{4\pi E_\nu}{\Delta m_{ij}^2}, \qquad \frac{1}{v_{ij}} = \frac{1}{2}\left(\frac{1}{v_i} + \frac{1}{v_j}\right),$$

$$\Delta m_{ij}^2 = m_i^2 - m_j^2, \qquad \Delta E_{ij} = E_i - E_j,$$

$$\mathsf{lerf}(z) = \int_0^z dz' \mathsf{erf}(z') + \frac{1}{\sqrt{\pi}} = z\,\mathsf{erf}(z) + \frac{1}{\sqrt{\pi}} e^{-z^2},$$

For a more realistic description of the beam pulse experiments, the model (100) could be readily extended by inclusion of a series of rectangular ledges followed by pauses during which $f_a = 0$.

Then substituting (101) into (98) we obtain:

$$dN_{\alpha\beta} = \tau_d \sum_{\text{spins}} \int d\boldsymbol{x} \int d\boldsymbol{y} \int d\mathfrak{P}_s \int d\mathfrak{P}_d \int dE_\nu \frac{\mathcal{P}_{\alpha\beta}(E_\nu, |\boldsymbol{y} - \boldsymbol{x}|)}{4(2\pi)^3 |\boldsymbol{y} - \boldsymbol{x}|^2}, \tag{104a}$$

$$\equiv \frac{\tau_d}{V_{\mathcal{D}} V_{\mathcal{S}}} \int d\boldsymbol{x} \int d\boldsymbol{y} \int d\Phi_\nu \int d\sigma_{\nu\mathcal{D}} \mathcal{P}_{\alpha\beta}(E_\nu, |\boldsymbol{y} - \boldsymbol{x}|). \tag{104b}$$

The differential forms $d\mathfrak{P}_{s,d}$ in (104a) are are given by eq. (99) after substitution $f_a \longmapsto \overline{f}_a$.

Explanation of the factors in eq. (104b).

- $V_{\mathcal{S}}$ and $V_{\mathcal{D}}$ are the spatial volumes of the source and detector, respectively.
- The differential form $d\Phi_\nu$ is defined in such a way that the integral

$$\frac{d\boldsymbol{x}}{V_{\mathcal{S}}}\int\frac{d\Phi_\nu}{dE_\nu}=d\boldsymbol{x}\sum_{\text{spins}\,\in\,S}\int\frac{d\mathfrak{P}_s E_\nu}{2(2\pi)^3|\boldsymbol{y}-\boldsymbol{x}|^2} \tag{105}$$

is the flux density of neutrinos in $\mathcal{D}$, produced through the processes $I_s\to F'_s\ell^+_\alpha\nu$ in $\mathcal{S}$.

> More precisely, it is the number of neutrinos appearing per unit time and unit neutrino energy in an elementary volume $d\boldsymbol{x}$ around the point $\boldsymbol{x}\in\mathcal{S}$, travelling within the solid angle $d\boldsymbol{\Omega}_\nu$ about the flow direction $\boldsymbol{l}=(\boldsymbol{y}-\boldsymbol{x})/|\boldsymbol{y}-\boldsymbol{x}|$ and crossing a unit area, placed around the point $\boldsymbol{y}\in\mathcal{D}$ and normal to $\boldsymbol{l}$.

- The differential form $d\sigma_{\nu\mathcal{D}}$ is defined in such a way that

$$\frac{1}{V_{\mathcal{D}}}\int d\boldsymbol{y}d\sigma_{\nu\mathcal{D}}=\sum_{\text{spins}\,\in\,D}\int\frac{d\boldsymbol{y}d\mathfrak{P}_d}{2E_\nu} \tag{106}$$

represents the differential cross section of the neutrino scattering off the detector as a whole.

> In the particular (and the most basically important) case of neutrino scattering in the reaction $\nu a\to F'_d\ell^-_\beta$, provided that the momentum distribution of the target scatterers a is sufficiently narrow, the differential form $d\sigma_{\nu\mathcal{D}}$ becomes exactly the elementary differential cross section of this reaction multiplied by the total number of the particles a in $\mathcal{D}$.

▷ Now let us address the last sub-integral multiplier of (104b), given by

$$\mathcal{P}_{\alpha\beta}(E_\nu, L) = \sum_{ij} V^*_{\alpha i} V_{\alpha j} V_{\beta i} V^*_{\beta j} S_{ij} \exp\left(i\varphi_{ij} - \mathscr{A}^2_{ij} - \Theta_{ij}\right), \tag{107}$$

$$\Theta_{ij} = \Theta_i + \Theta_j, \tag{108}$$

$$\Theta_j = \frac{m_j^2}{2\mathfrak{D}^2}\left[(\mathfrak{n}_0 - \mathfrak{n}) + \frac{1}{2}\left(\mathfrak{m} - \mathfrak{n} - \mathfrak{n}^2\right) r_j + \left(\mathfrak{n} + \frac{1}{2}\right)\left(\mathfrak{m} - \mathfrak{n} - \mathfrak{n}^2\right) r_j^2 + \mathcal{O}(r_j^3)\right]. \tag{109}$$

Let's remind that the function $\mathfrak{n}_0$ coincides with $\mathfrak{n}$ in the case of exact energy-momentum conservation in the vertices of our diagram. Therefore in the vicinity of the maximum of the product $\widetilde{\delta}_s(p_\nu - q_s)\widetilde{\delta}_d(p_\nu + q_d)$ (that is at $q_s \approx -q_d \approx p_\nu$), which gives the main contribution into the event rate, one can neglect the alternating quantity $\mathfrak{n}_0 - \mathfrak{n}$ in (109). Taking into account the properties of the function $\mathfrak{n}$ one can also neglect the $\mathcal{O}(r_j^2)$ contributions in (109). In this approximation

$$\Theta_j \approx \frac{m_j^4 R\left(\mathfrak{m} - \mathfrak{n} - \mathfrak{n}^2\right)}{4E_\nu^2} \approx \frac{m_j^4 R\left(\mathfrak{m} - \mathfrak{n}_0 - \mathfrak{n}_0^2\right)}{4E_\nu^2} = \frac{m_j^4\left[R_{00}\mathscr{R} - (\mathbf{Rl})^2\right]}{4RE_\nu^2} \geq 0.$$

• The factor (107) coincides with the QM expression for the neutrino flavor transition probability,

$$\mathcal{P}^{(\mathsf{QM})}_{\alpha\beta}(E_\nu, L) = \sum_{ij} V_{\alpha i} V_{\beta j} V^*_{\alpha j} V^*_{\beta i} \exp\left(i\varphi_{ij}\right). \tag{110}$$

provided that $S_{ij} = 1$, $\Theta_{ij} = 0$, and $\mathscr{A}_{ij} = 0$. So it can be considered as a QFT refinement of the QM result.

BUT!

• A probabilistic interpretation of the function $\mathcal{P}_{\alpha\beta}$ can be only provisionally true, because the factors S_{ij} and $\mathscr{A}_{ij}$ involve the functions $\mathfrak{D}$, $\mathfrak{n}$, and $\mathfrak{m}$ strongly dependent on the neutrino energy E_ν and external momenta $\boldsymbol{p}_{\varkappa}$; all these (except for the momenta of secondaries in $\mathcal{D}$) are variables of integration in (104b).

As a result, the factor $\mathcal{P}_{\alpha\beta}$, as function of α and β, does not satisfy the unitarity relations

$$\sum_{\alpha} \mathcal{P}^{(\mathrm{QM})}_{\alpha\beta} = \sum_{\beta} \mathcal{P}^{(\mathrm{QM})}_{\alpha\beta} = 1,$$

which are a commonplace in the QM theory of neutrino oscillations.

The point is that the domains and shapes of the functions $\mathfrak{D}$, $\mathfrak{n}$, and $\mathfrak{m}$ are essentially different for each of the nine leptonic pairs $(\ell_\alpha, \ell_\beta)$. These differences are governed by kinematics of the subprocesses in $\mathcal{S}$ and $\mathcal{D}$ (in particular, their thresholds), that is, eventually, by the leptonic masses (m_e, m_μ, m_τ) and by the momentum spreads (σ_e, σ_μ, σ_τ) of the leptonic WPs, which are not necessarily equal to each other, perhaps even within an order of magnitude.

So $\mathcal{P}_{\alpha\beta}(E_\nu, L)$ is not the flavor transition probability!

Having this in mind, we will call it probability factor for short.

Two more drawbacks.

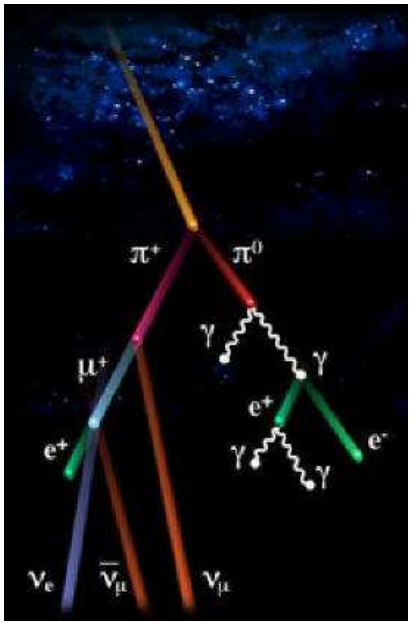

• The probabilistic treatment of $\mathcal{P}_{\alpha\beta}$ is even more problematic in real-life experiments, because the detector event rate (with ℓ_β appearance in our case) is defined by many subprocesses of different types in the source and detector.

E.g., in the astrophysical, atmospheric and accelerator neutrino experiments, the major processes of neutrino production are in-flight decays of light mesons ($\pi_{\mu 2}$, $K_{\mu 2}$, $K_{\mu 3}$, K_{e3}, etc.) and muons, and neutrino interactions with a detector medium consist of an incoherent superposition of exclusive reactions of many types, – from (quasi)elastic to deep-inelastic.

• A "technical" drawback is the dependence of the function S_{ij} (which will be referred to as decoherence factor) on the four "instrumental" time parameters x_1^0, x_2^0, y_1^0, y_2^0.

So far we have made no assumption concerning a "synchronization" of the time windows (x_1^0, x_2^0) and (y_1^0, y_2^0). Thus, it is no wonder that the decoherence factor turns to be vanishingly small in magnitude if these windows are not adjusted to account that the representative time of ultrarelativistic neutrino propagation from $\mathcal{S}$ to $\mathcal{D}$ is equal to the mean distance, $\overline{L}$, between $\mathcal{S}$ and $\mathcal{D}$.

Before discussing the role of the decoherence factor, we perform one more, and the last, simplification of the formula for $dN_{\alpha\beta}$.

Step 3: Spatial averaging.

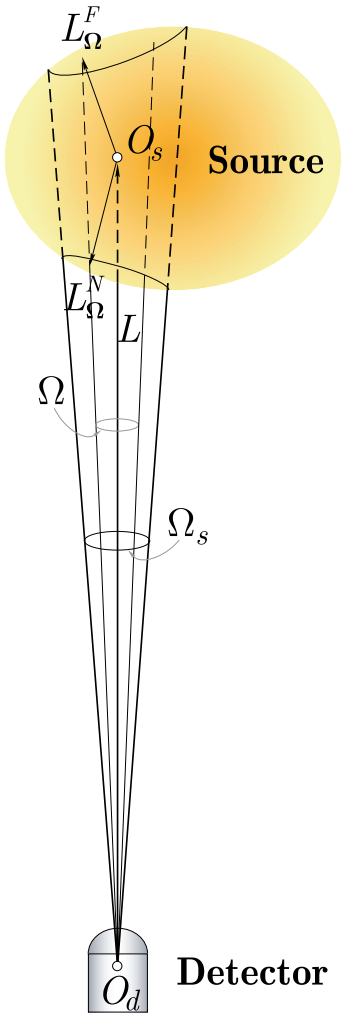

We'll use again the requirement that the characteristic dimensions of $\mathcal{S}$ and $\mathcal{D}$ are small compared to $\overline{L}$. Under certain conditions, this allows us to replace approximately

$$|\boldsymbol{y}-\boldsymbol{x}| \longmapsto \overline{L} = \frac{1}{2\Omega_s}\int_{\Omega_s} d\boldsymbol{\Omega}\left(L^F_{\boldsymbol{\Omega}} + L^N_{\boldsymbol{\Omega}}\right),$$

$$d\Phi_\nu \longmapsto d\overline{\Phi}_\nu, \quad d\sigma_{\nu\mathcal{D}} \longmapsto d\overline{\sigma}_{\nu\mathcal{D}}.$$

The range of applicability of this approximation is in general much more limited than that of (104b), as a consequence of additional restrictions implicitly imposed on the distribution functions $\overline{f}_a$, absolute dimensions and geometry of $\mathcal{S}$ and $\mathcal{D}$.
These issues are bit more complicated then the considered above and must be the subject of special attention in the neutrino oscillation experiments.

Finally, we arrive at the very simple but rather rough expression:

$$dN_{\alpha\beta} = \tau_d \int d\overline{\Phi}_\nu \int d\overline{\sigma}_{\nu\mathcal{D}} \mathcal{P}_{\alpha\beta}(E_\nu, \overline{L}). \tag{111}$$

In particular, it is not applicable to the short base-line experiments.

7.18 Synchronized measurements.

Let us now return to the decoherence factor, limiting ourselves to a consideration of "synchronized" measurements, in which

$$x^0_{1,2} = \mp\frac{\tau_s}{2}, \quad y^0_{1,2} = \overline{L} \mp \frac{\tau_d}{2}.$$

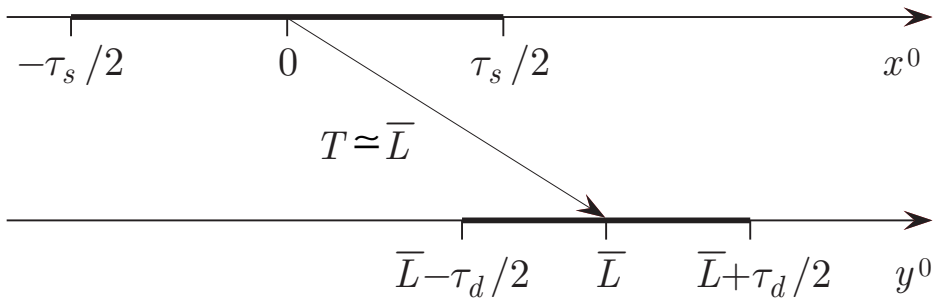

With certain technical simplifications, the factor (102) can be expressed through a real-valued function $S(t,t',b)$ of three dimensionless variables, namely:

$$S_{ij} = S\left(\mathfrak{D}\tau_s, \mathfrak{D}\tau_d, \mathscr{B}_{ij}\right),$$

$$2t'\,S(t,t',b) = \exp\left(-b^2\right)\mathrm{Re}\left[\mathsf{lerf}\left(t+t'+ib\right) - \mathsf{lerf}\left(t-t'+ib\right)\right].$$

7.18.1 Diagonal decoherence function.

$$S(t,t',0) = \frac{1}{2t'}\left[\mathsf{lerf}\left(t+t'\right) - \mathsf{lerf}\left(t-t'\right)\right] \equiv S_0(t,t'), \tag{112}$$

This function corresponds to the noninterference (neutrino mass independent) decoherence factors S_{ii}. The following inequalities can be proved:

$$0 < S_0(t,t') < 1, \quad S_0(t,t') < t/t' \ \text{ for } \ t' \geq t, \quad S_0(t+\delta t, t) > \mathsf{erf}(\delta t) \ \text{ for } \ \delta t > 0.$$

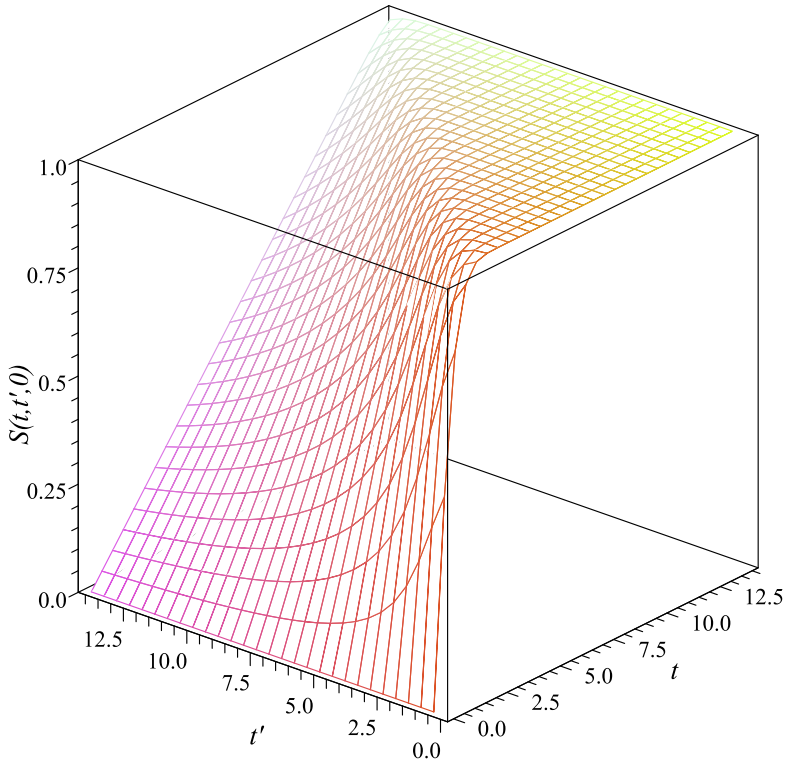

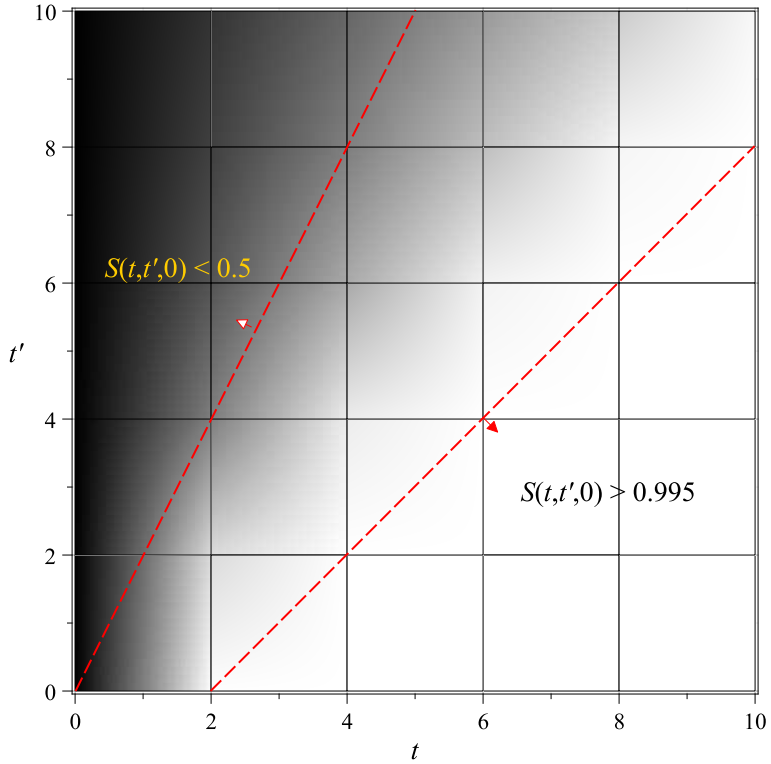

The strong dependence of the common suppression factor $S_0(t,t')$ on its arguments at $t \lesssim t'$ provides a potential possibility of an experimental estimation of the function $\mathfrak{D}$ (or, rather, of its mean values within the phase spaces), based on the measuring the count rate $dR_{\alpha\beta} = dN_{\alpha\beta}/\tau_d$ as a function of τ_d and τ_s (at fixed $\overline{L}$) and comparing the data with the results of Monte-Carlo simulations.

The optimal strategy of such an experiment should be a subject of a dedicated analysis.

For the important special case, $t' = t$ (representative, in particular, for the experiments with accelerator neutrino beams), we find

$$S_0(t,t) = \mathrm{erf}(2t) - \frac{1-e^{-4t^2}}{2\sqrt{\pi}t} \approx \begin{cases} \dfrac{2t}{\sqrt{\pi}}\left(1 - \dfrac{2t^2}{3} + \dfrac{8t^4}{15}\right) & \text{for } t \ll 1, \\ 1 - \dfrac{1}{2\sqrt{\pi}t} & \text{for } t \gg 1. \end{cases} \tag{113}$$

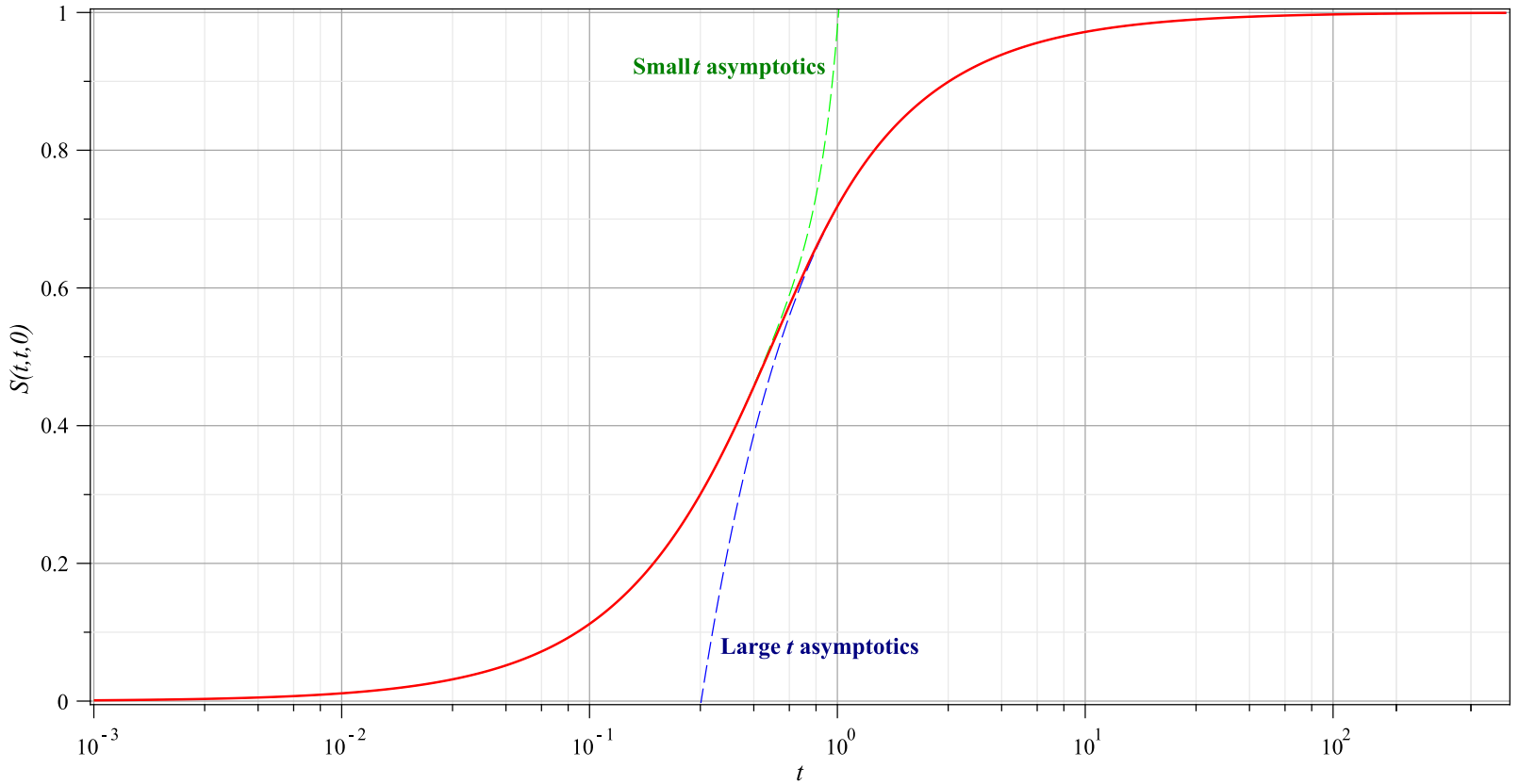

7.18.2 Nondiagonal decoherence function.

The decoherence function $S(t,t',b)$ at $b \neq 0$ is much more involved.

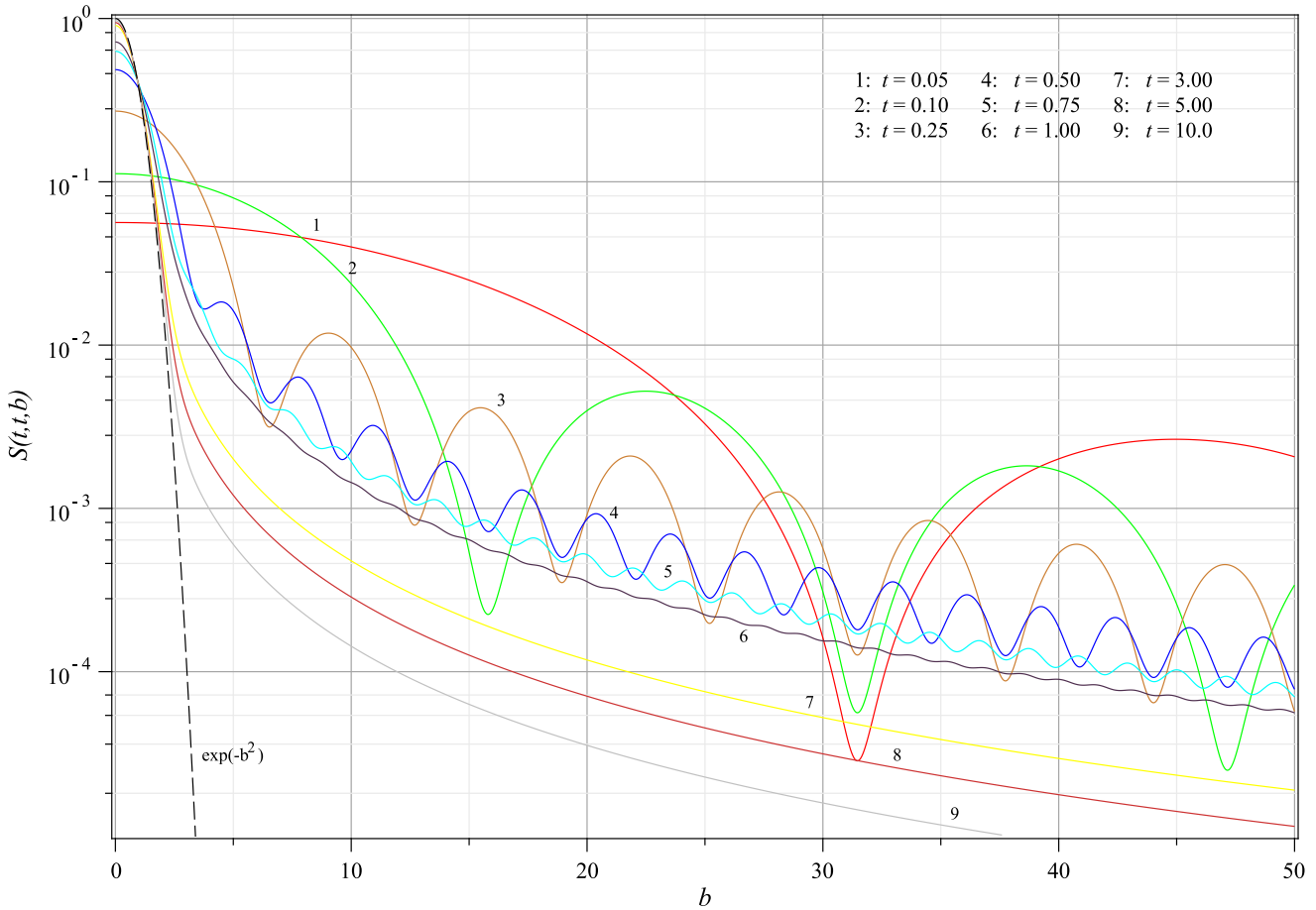

At very large t, the function $S(t,t,b)$ becomes nearly independent on t, slowly approaching the asymptotic behavior $S(t,t,b) \sim \exp(-b^2)$ $(t,t' \to \infty)$.

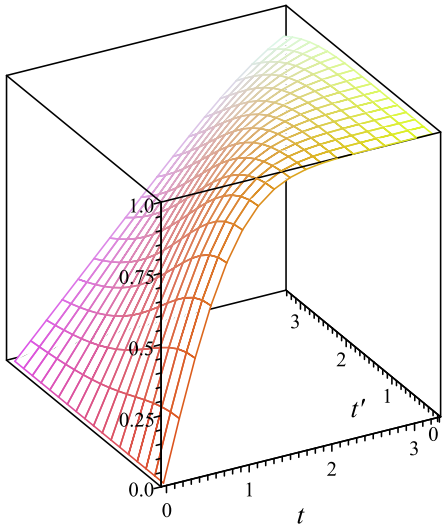

$S(t, t', 0.1)$.

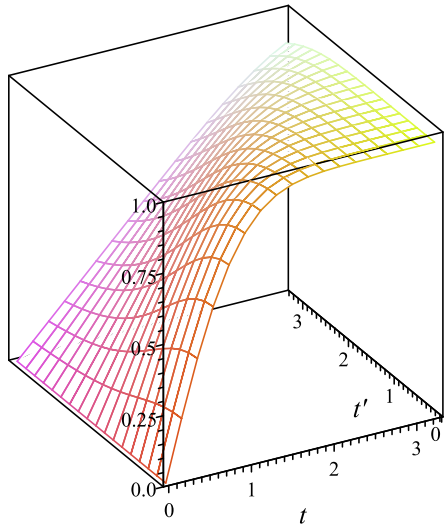

$S(t, t', 0.2)$.

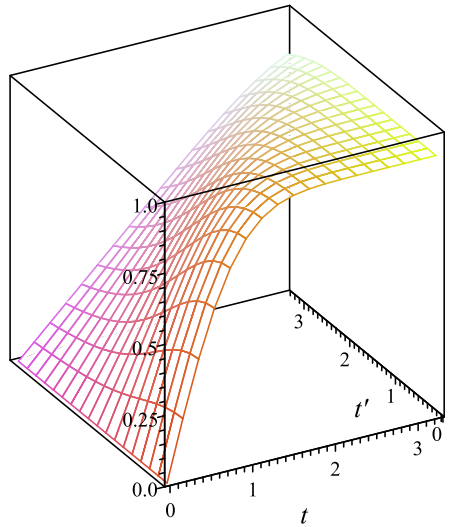

$S(t, t', 0.3)$.

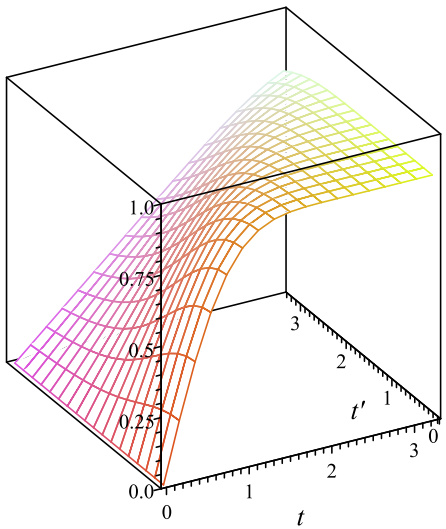

$S(t, t', 0.4)$.

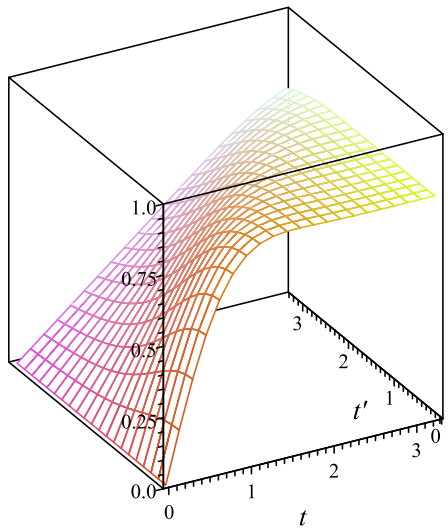

$S(t, t', 0.5)$.

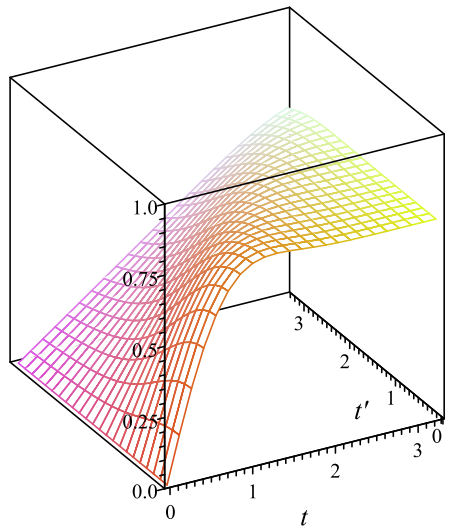

$S(t, t', 0.6)$.

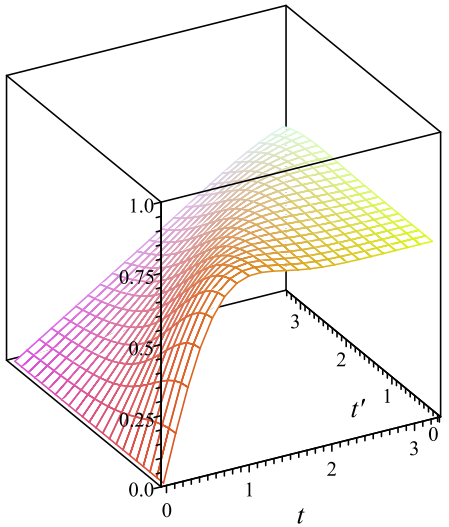

$S(t, t', 0.7)$.

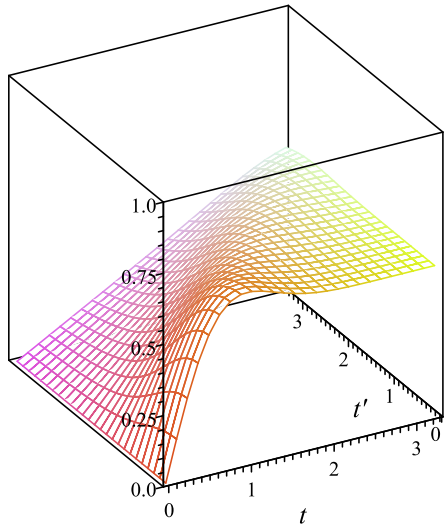

$S(t, t', 0.8)$.

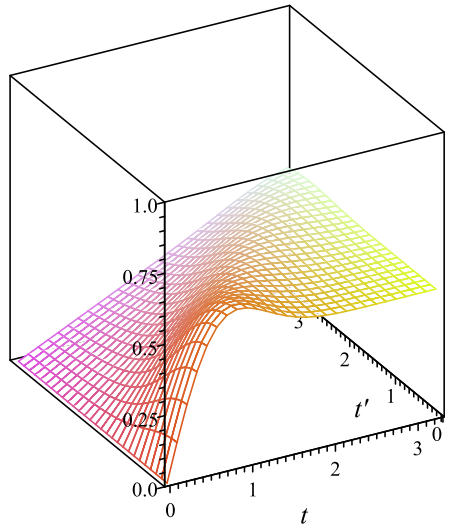

$S(t, t', 0.9)$.

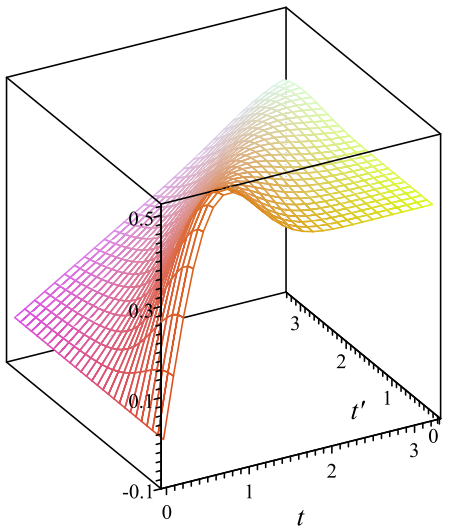

$S(t, t', 1.0)$.

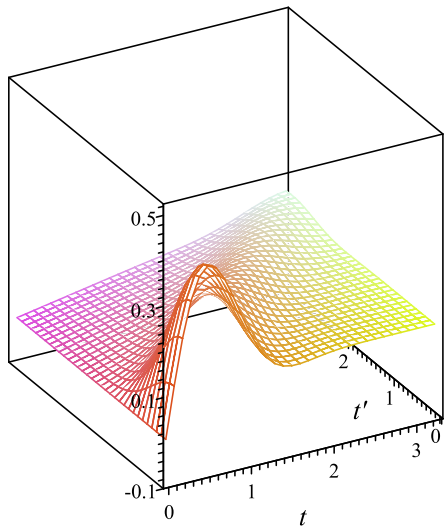

$S(t, t', 1.5)$.

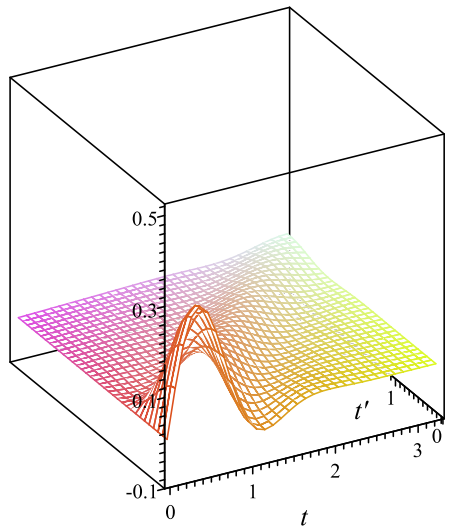

$S(t, t', 2.0)$.

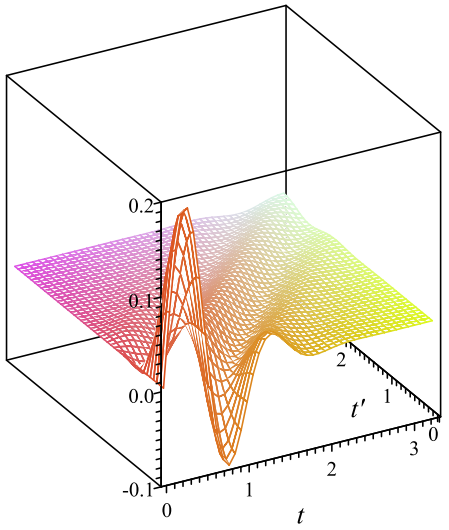

$S(t, t', 3.0)$.

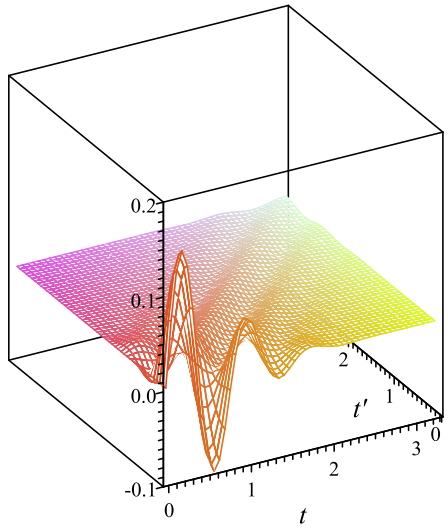

$S(t, t', 4.0)$.

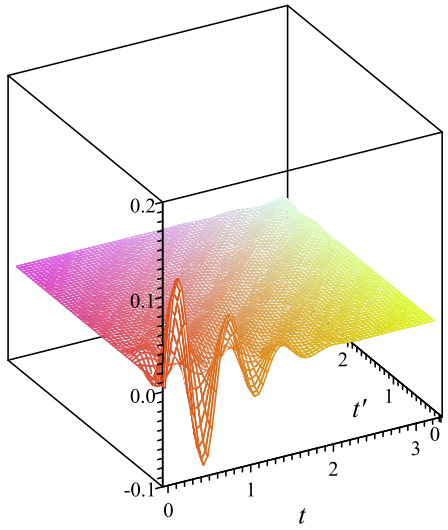

$S(t, t', 5.0)$.

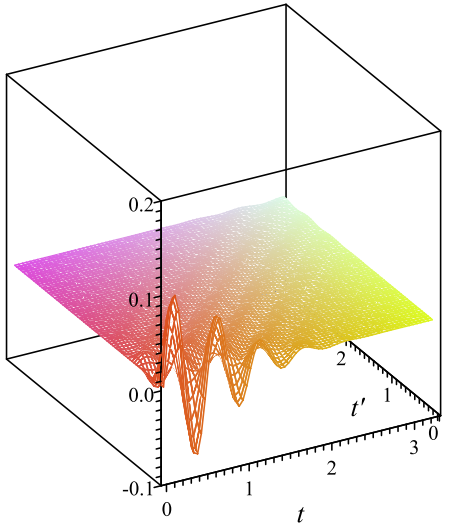

$S(t, t', 6.0)$.

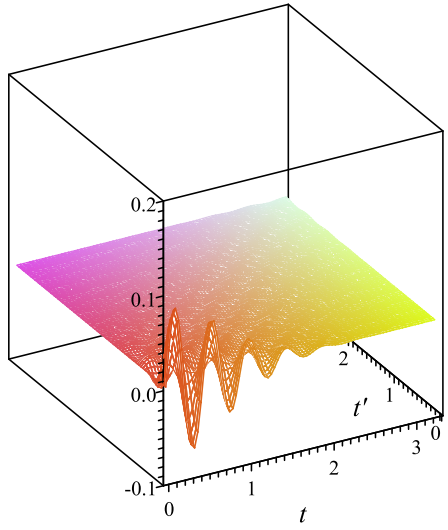

$S(t, t', 7.0)$.

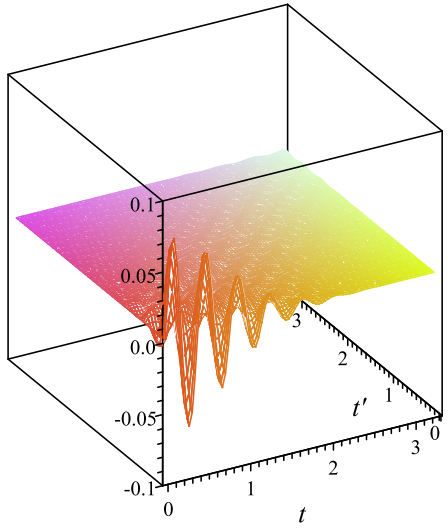

$S(t, t', 8.0)$.

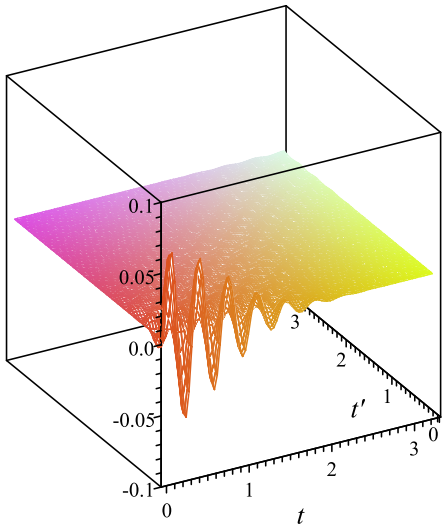

$S(t, t', 9.0)$.

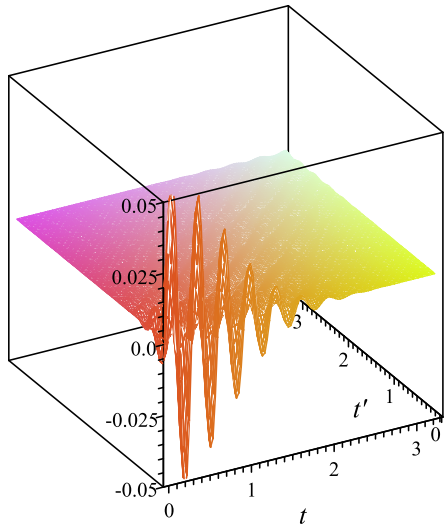

$S(t, t', 10.0)$.

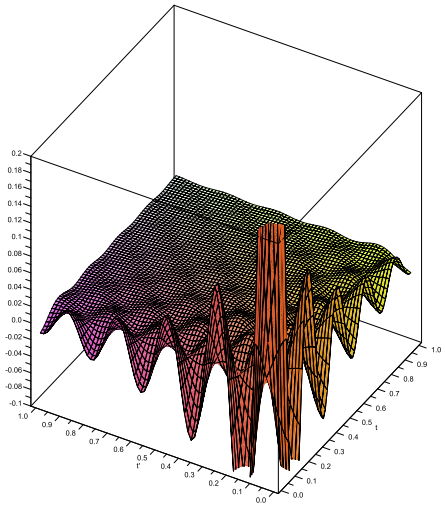

$S(t, t', 15.0)/S_0(t, t')$.

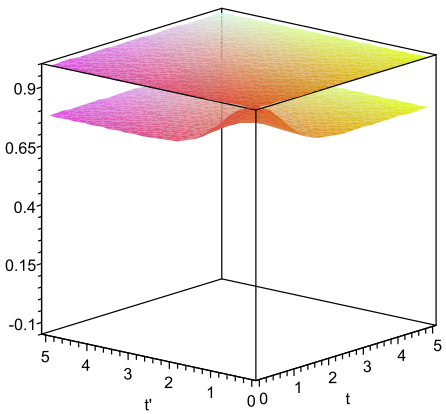

$S(t, t', 0.10)/S_0(t, t')$,
$S(t, t', 0.50)/S_0(t, t')$.

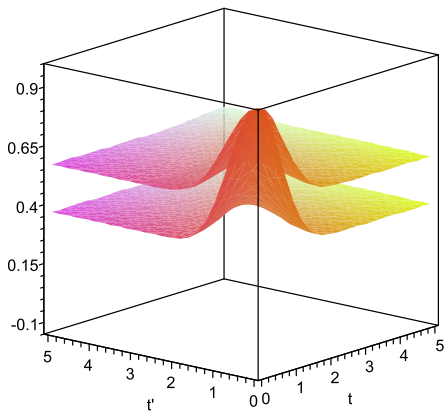

$S(t, t', 0.75)/S_0(t, t')$,
$S(t, t', 1.00)/S_0(t, t')$.

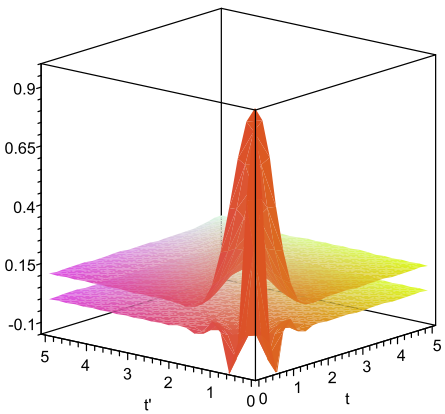

$S(t, t', 1.50)/S_0(t, t')$,
$S(t, t', 4.00)/S_0(t, t')$.

7.18.3 Flavor transitions in the asymptotic regime.

In the asymptotic regime,

$$S(t,t',b) \sim \exp(-b^2) \quad (t,t' \to \infty).$$

the probability factor (107) takes on the form already known from the literature,[a]

$$\mathcal{P}_{\alpha\beta}(E_\nu, \overline{L}) = \sum_{ij} V^*_{\alpha i} V_{\alpha j} V_{\beta i} V^*_{\beta j} \exp\left(i\varphi_{ij} - \mathscr{A}^2_{ij} - \mathscr{B}^2_{ij} - \Theta_{ij}\right), \tag{114}$$

but with the essential difference that the factors $\mathscr{A}_{ij}$, $\mathscr{B}_{ij}$ and Θ_{ij} do depend (through the functions $\mathfrak{D}$, $\mathfrak{n}$, and $\mathfrak{m}$) on the neutrino energy and momenta of the external WPs.

This dependence drastically affects the magnitude and shape of these factors if at least some of the WPs have relativistic momenta (that is always the case in the contemporary neutrino oscillation experiments). For sufficiently small and/or hierarchically different momentum spreads $\sigma_\varkappa$, the functions $\mathscr{A}_{ij}$ and $\mathscr{B}_{ij}$ may vary in many orders of magnitude through their multidimensional domain.

[a] See, e.g., C. Giunti C and C. W. Kim, *Fundamentals of Neutrino Physics and Astrophysics* (Oxford University Press Inc., New York, 2007); M. Beuthe, *Oscillations of neutrinos and mesons in quantum field theory*, Phys. Rept. **375** (2003) 105 (arXiv:hep-ph/0109119); M. Beuthe, *Towards a unique formula for neutrino oscillations in vacuum*, Phys. Rev. D **66** (2002) 013003 (arXiv:hep-ph/0202068).

7.18.4 Major properties of the transition "probability".

- The factors $\exp\left(-\mathscr{A}_{ij}^2\right)$ (with $i\neq j$) suppress the interference terms at the distances exceeding the "coherence length"

$$L_{ij}^{\rm coh}=\frac{1}{\Delta v_{ij}\mathfrak{D}}\gg|L_{ij}|\qquad(\Delta v_{ij}=|v_j-v_i|),$$

when the νWPs $\psi^i_{X_d}(\mathbf{p}_i,X_s-X_d)$ and $\psi^j_{X_d}(\mathbf{p}_j,X_s-X_d)$ are strongly separated in space and do not interfere anymore. Clearly $L_{ij}^{\rm coh}\to\infty$ in the plane-wave limit.

- The suppression factors $\exp\left(-\mathscr{B}_{ij}^2\right)$ ($i\neq j$) work in the opposite situation, when the external packets in $\mathcal{S}$ or $\mathcal{D}$ (or in both $\mathcal{S}$ and $\mathcal{D}$) are strongly delocalized

The gross dimension of the the neutrino production and absorption regions in $\mathcal{S}$ and $\mathcal{D}$ is of the order of $1/\mathfrak{D}$. The interference terms vanish if this scale is large compared to the "interference length"

$$L_{ij}^{\rm int}=\frac{1}{4\Delta E_{ij}}=\frac{2L_{ij}}{\pi\mathfrak{n}}.$$

In other words, the QFT approach predicts vanishing of neutrino oscillations in the plane-wave limit. In this limit, the flavor transition probability does not depend on $\overline{L}$, E_ν, and neutrino masses m_i and becomes

$$\mathcal{P}_{\alpha\beta}^{\rm PWL}=\sum_i|V_{\alpha i}|^2|V_{\beta i}|^2\leq 1.$$

Thereby, a nontrivial interference of the diagrams with the intermediate neutrinos of different masses is only possible if $\mathfrak{D}\neq 0$.

- Our detailed analysis of the generic subprocesses $1 \to 2$, $1 \to 3$, and $2 \to 2$ shows that $\mathfrak{D} \neq 0$ if in both vertices of the macrodiagram there are at least two interacting WPs $\varkappa$ (no matter in or out) with $\sigma_\varkappa \neq 0$.

- The same requirement unavoidably leads to the vanishing of the non-diagonal terms, when the mean distance between $\mathcal{S}$ and $\mathcal{D}$ becomes large enough in comparison with the coherence lengths L_{ij}^{coh}.

- As a result, the range of applicability of the standard QM formula for the neutrino oscillations probability is limited by rather restrictive conditions,

$$\left\langle \left(\frac{2\pi \mathfrak{D} L}{E_\nu L_{ij}} \right)^2 \right\rangle \ll 1, \quad \left\langle \left(\frac{\pi \mathfrak{n}}{2\mathfrak{D} L_{ij}} \right)^2 \right\rangle \ll 1, \quad \text{and} \quad \langle |\Theta_{ij}| \rangle \ll 1.$$

The angle brackets symbolize an averaging over the phase subspace of the process (42) which provides the main contribution into the measured count rate.

The obtained conditions were obtained under a number of assumptions and simplifications, which are not necessarily adequate to fully represent the real-life experimental conditions. Our consideration suggests that in the analysis and interpretation of real data one should take into account the operating times of the source and detector, their geometry and dimensions, explicit form of the distribution functions of in-packets, and other technical details.

7.19 Intermediary conclusions on the QFT approach.

- The standard QM ν-oscillation formula has rather limited range of applicability.
- The QFT modifications drastically depend upon:

  - ▷ momentum spreads of the external "in" and "out" wave packets;
  - ▷ reaction types in the neutrino production and absorption regions ["source" and "detector", respectively] and phase-space domains of these reactions;
  - ▷ time interval of steady-state operation of the source "machine " and detector exposure time;
  - ▷ dimensions of the source and detector and distance between them.

- Essentially all QFT effects are decoherent and thus lead to a "smoothing", distortion or vanishing of the interference (oscillating) terms and to a general suppression of the neutrino event rate in the detector.
- The effective neutrino energy uncertainty (or "fuzziness") $\mathfrak{D}$ and dispersion correction factors $\mathfrak{n}$ and $\mathfrak{m}$, responsible for the decoherent effects, are rather involved functions of the momenta $\mathbf{p}_\varkappa$ masses $m_\varkappa$ and momentum spreads $\sigma_\varkappa$ of the external packets $\varkappa$. However, these functions can be studied in special synchronized or desynchronized measurements.

Часть IV

Neutrino velocity measurements

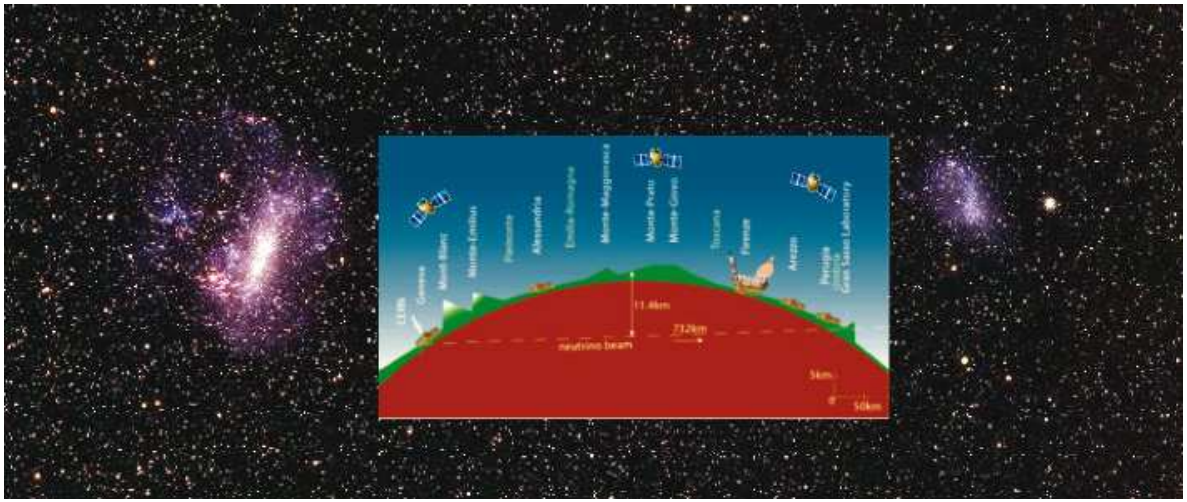

8 Tests of Lorentz invariance.

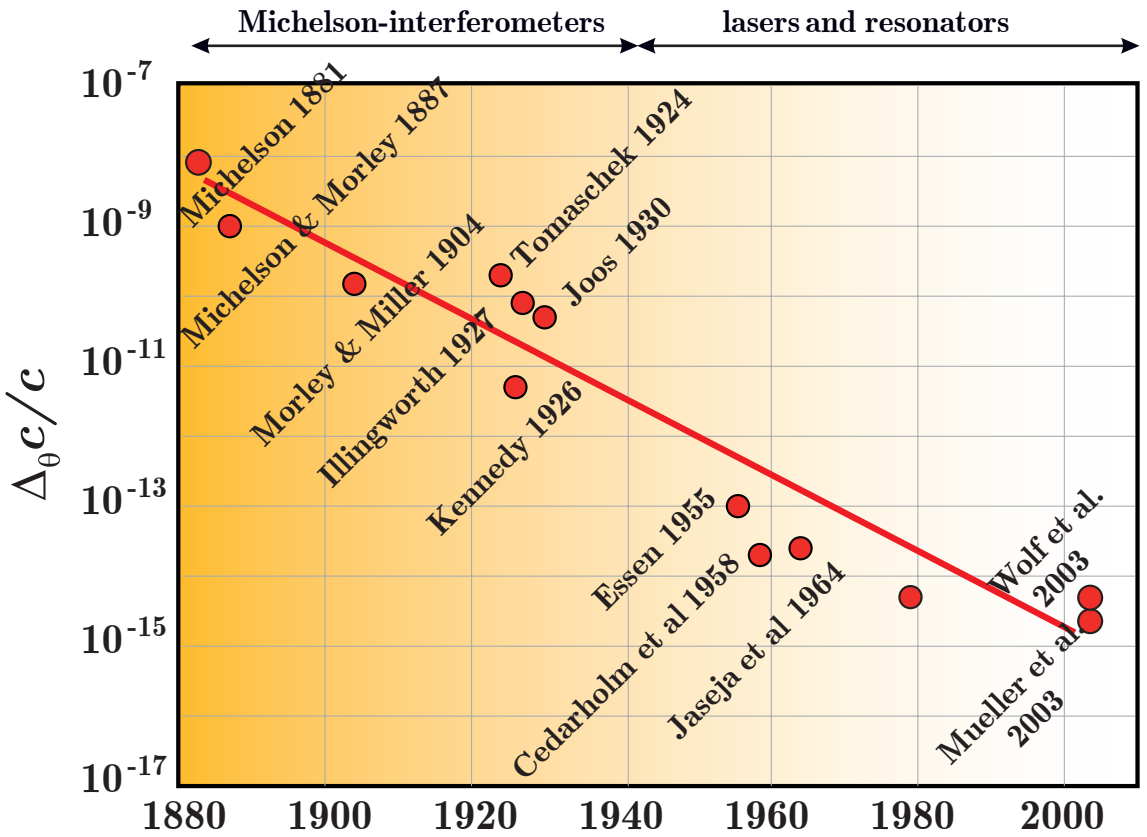

Improvements of the Michelson-Morley experiment since 1881.

[Figure is taken from S. Herrmann *et al.*, "Test of Lorentz invariance using a continuously rotating optical resonator", Lect. Notes Phys. **702** (2006) 385-400.]

The constancy of c, i.e. its independence on laboratory velocity and orientation has been verified experimentally at improved precision by numerous repetitions of the MM-experiment, providing a firm experimental basis for special relativity so far.

- The best current limit for a possible anisotropy of the speed of light is

$$\boxed{\Delta_\theta c/c < 10^{-17}.}$$

[Ch. Eisele *et al.*, Phys. Rev. Lett. **103** (2009) 090401; S. Herrmann *et al.*, Phys. Rev. D **100** (2009) 105011 (arXiv:1002.1284 [physics.class-ph]).]

The sensitivity of the next-generation Michelson-Morley type experiments to violation of the Lorentz invariance is expected to be in the 10^{-19} to 10^{-20} regime.

[M. Nagel *et al.*, arXiv:1112.3857 [physics.class-ph].]

- The relativistic relation

$$\boxed{v = p/\sqrt{p^2 + m^2}} \tag{115}$$

is confirmed in the accelerator experiments for $1 - v$ down to 2×10^{-7}.

The relation (115) has been tested in the SLAC accelerator by comparison of relative velocities of γ quanta with mean energies ~ 15 GeV and electrons with energies in the interval 15–20.5 GeV by using a time-of-flight technique with 1-psec sensitivity and a flight path of about 1 km. At such energies, the expected value of $v_\gamma - v_e = 1 - v_e$ was $(3.1 - 5.8) \times 10^{-10}$. No significant difference in v_γ and v_e was observed to within 2×10^{-7}.

[Z. G. T. Guiragossian *et al.*, Phys. Rev. Lett. **34** (1975) 335.]

The accuracy of the earlier experiments was order of magnitude lower.

9 Accelerator measurements of neutrino velocity.

In all ν experiments it is assumed that the relation (115) holds for muons, pions, and kaons.

- FNAL 1976 [345 m (decay pipe) + 550 m (shield), $\langle E_\nu^{(\pi)} \rangle = 25$ GeV, $\langle E_\nu^{(K)} \rangle = 75$ GeV]:

$$|v_\nu - v_\mu| < 4 \times 10^{-4} \ (99\% \text{ C.L.})$$

[J. Alspector *et al.*, Phys. Rev. Lett. **36** (1976) 837.]

- FNAL 1979 [345 m (decay pipe) + 550 m (shield), $E_\nu^{(\pi,K)} = 30$ to 200 GeV]:

$$|v_\nu - \overline{v}_\nu| < 7 \times 10^{-5}, \quad |v_\nu^{(K)} - v_\nu^{(\pi)}| < 5 \times 10^{-5}, \quad |v_{\nu,\overline{\nu}} - 1| < 4 \times 10^{-5} \ (95\% \text{ C.L.}).$$

[G. R. Kalbfleisch *et al.*, Phys. Rev. Lett. **43** (1979) 1361.]

- FNAL Tevatron – FMMF (1995) [Hadron & muon shield is located 542 m downstream of the neutrino target, the FMMF (E733) detector is located 1599 m downstream of the neutrino target; wide band neutrino beam]

  There were some time anomalies but there is no definite conclusions concerning v_ν. Seems to be in agreement with the FNAL 1979 limits.

  [E. Gallas *et al.*, (FMMF Collaboration) Phys. Rev. Lett. **52** (1995) 6; E. Gallas, PhD, Michigan State University, 1993; FERMILAB-THESIS-1993-36, UMI-94-06493.]

- FNAL-SOUDAN (MINOS experiment) 2007 [734 km, $\langle E_\nu \rangle \sim 3$ GeV, $E_\nu \lesssim 120$ GeV]:

$$\delta \mathrm{t} = (126 \pm 32_{\mathrm{stat}} \pm 64_{\mathrm{sys}}) \text{ ns } (68\% \text{ C.L.}),$$

$$\Downarrow (?)$$

$$(v_\nu - 1) = (5.1 \pm 2.8_{\mathrm{stat}} \pm 0.30_{\mathrm{sys}}) \times 10^{-5} \ (68\% \text{ C.L.}).$$

The measurement is consistent with the speed of light to less than 1.8σ.
The corresponding 99% confidence limit on the speed of the neutrino is

$$-2.4 \times 10^{-5} < (v_\nu - 1) < 12.6 \times 10^{-5} \ (99\% \text{ C.L.}).$$

This measurement has implicitly assumed that the m_2 and m_3 neutrino mass eigenstates that comprise the beam are traveling at the same velocity. This assumption is borne out in observing that the arrival times at the far detector match the expectation distribution. Indeed, if the two eigenstates were to travel at velocities differing by as little as $\delta v/v \gtrsim 4 \times 10^{-7}$, the short ~ 1 ns [~ 29.4 cm, VN] bunches would separate in transit and thus decohere, changing or destroying oscillation effects at the far detector.

[P. Adamson *et al.* (MINOS Collaboration) Phys. Rev. D **76** (2007) 072005.]

A few details:

⋆ MINOS measures the absolute transit time of an ensemble of neutrinos, to < 100 ns accuracy, by comparing ν arrival times at the near detector (ND) and far detector (FD). The distance between front face of the ND and the center of the FD is 734298.6 ± 0.7 m.

⋆ The beam flavor content: 93% ν_μ, 6% $\overline{\nu}_\mu$, 1% $\nu_e + \overline{\nu}_e$ at ND. After oscillating, the beam at FD is approximately 60% ν_μ.

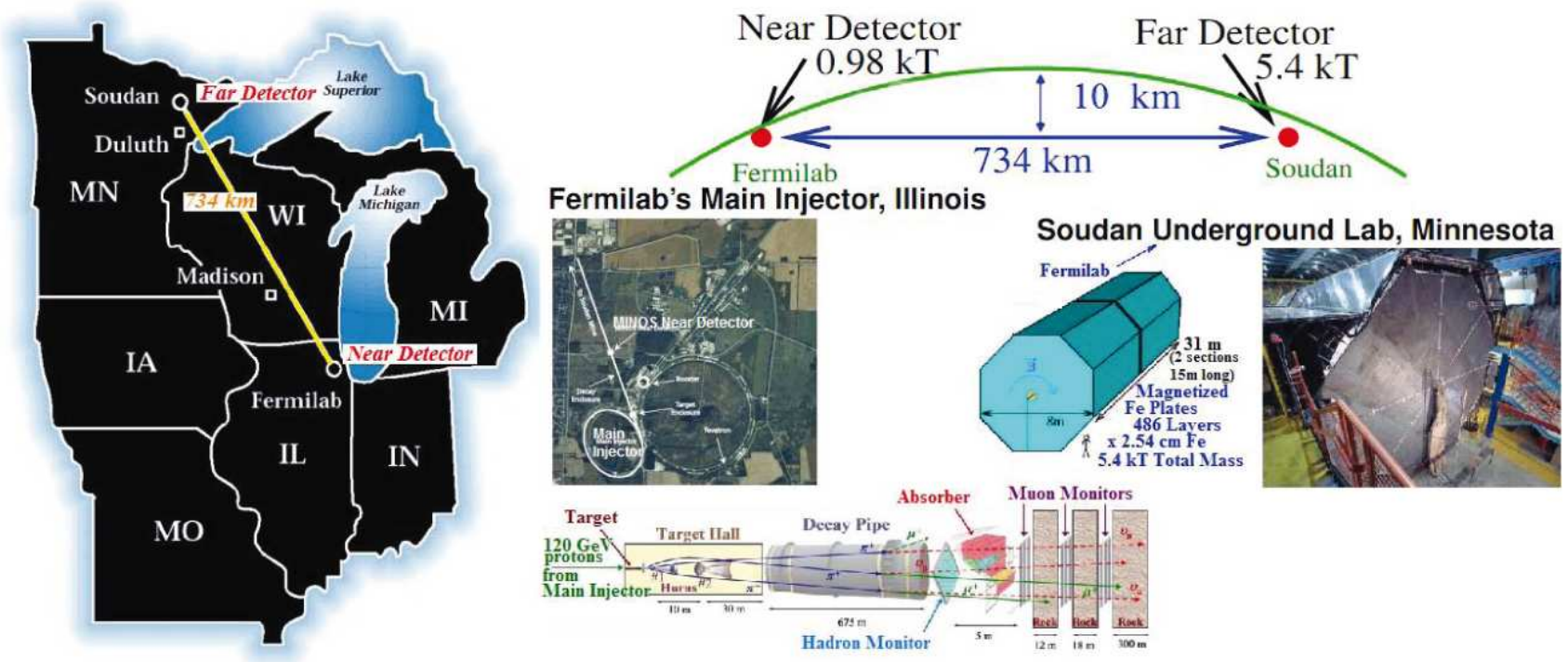

Schematic layout of the MINOS experiment.

[Borrowed from G. Brunetti, "Neutrino velocity measurement with the OPERA experiment in the CNGS beam," PhD thesis, in joint supervision of the Université Claude Bernard, Lyon-I and Universitá degli Studi di Bologna (May 2011), N° d'ordre 88-2011, LYCEN–T 2011-10; http://amsdottorato.cib.unibo.it/3917/, http://tel.archives-ouvertes.fr/tel-00633424.]

- CERN-LNGS (OPERA experiment) 2011 [730 km, $\langle E_\nu \rangle \sim 17$ GeV, $E_\nu \lesssim 350$ GeV]:

$$\delta \mathrm{t} = \left(57.8 \pm 7.8_{\mathrm{stat}}\ {}^{+8.3}_{-5.9}\,(\mathrm{syst})\right)\ \mathrm{ns},$$

$$\Downarrow\ (?)$$

$$(v_\nu - 1) = \left(2.37 \pm 0.32_{\mathrm{stat}}\ {}^{+0.34}_{-0.24}\,(\mathrm{syst})\right) \times 10^{-5}.$$

[T. Adam *et al.* (OPERA Collaboration) arXiv:1109.4897v2 [hep-ex] (November 17, 2011).]

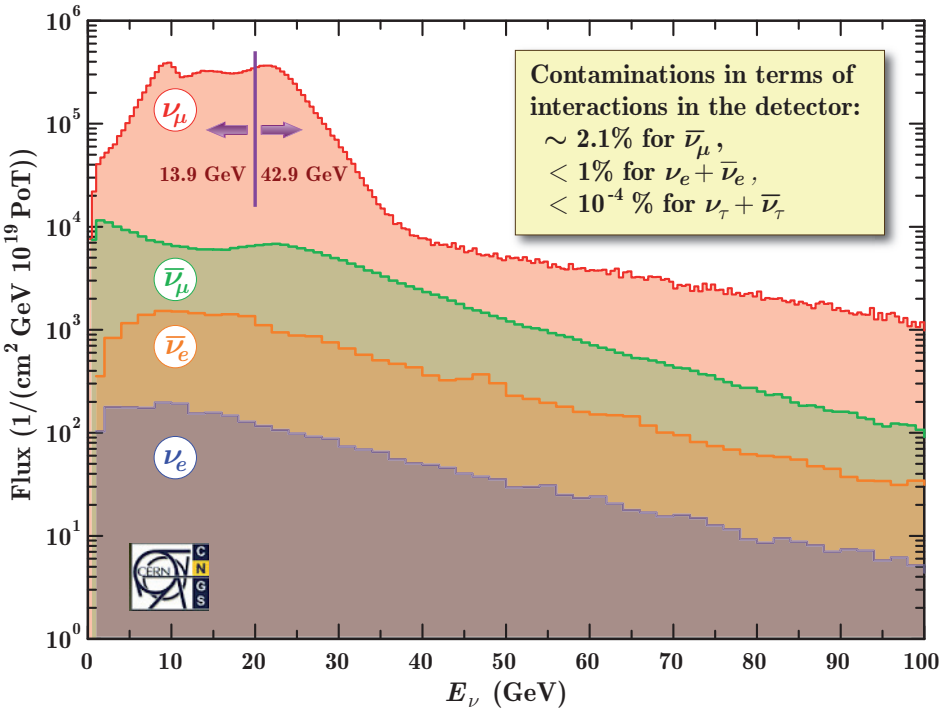

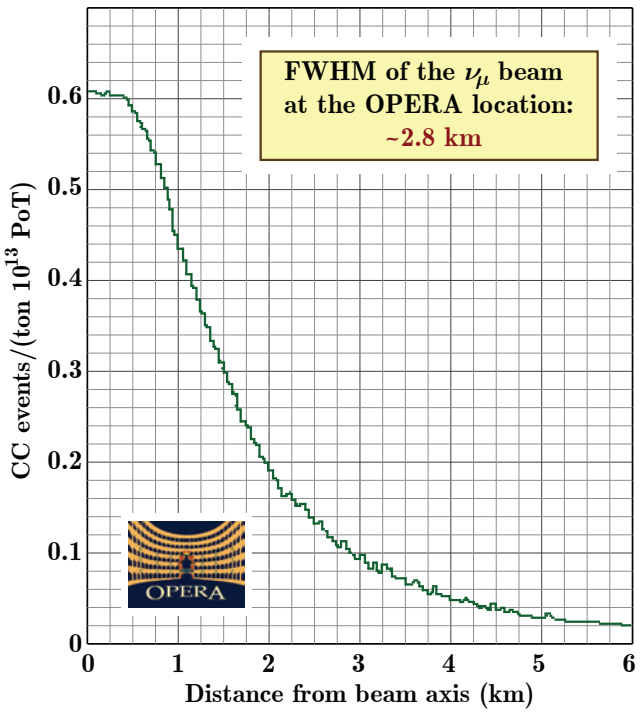

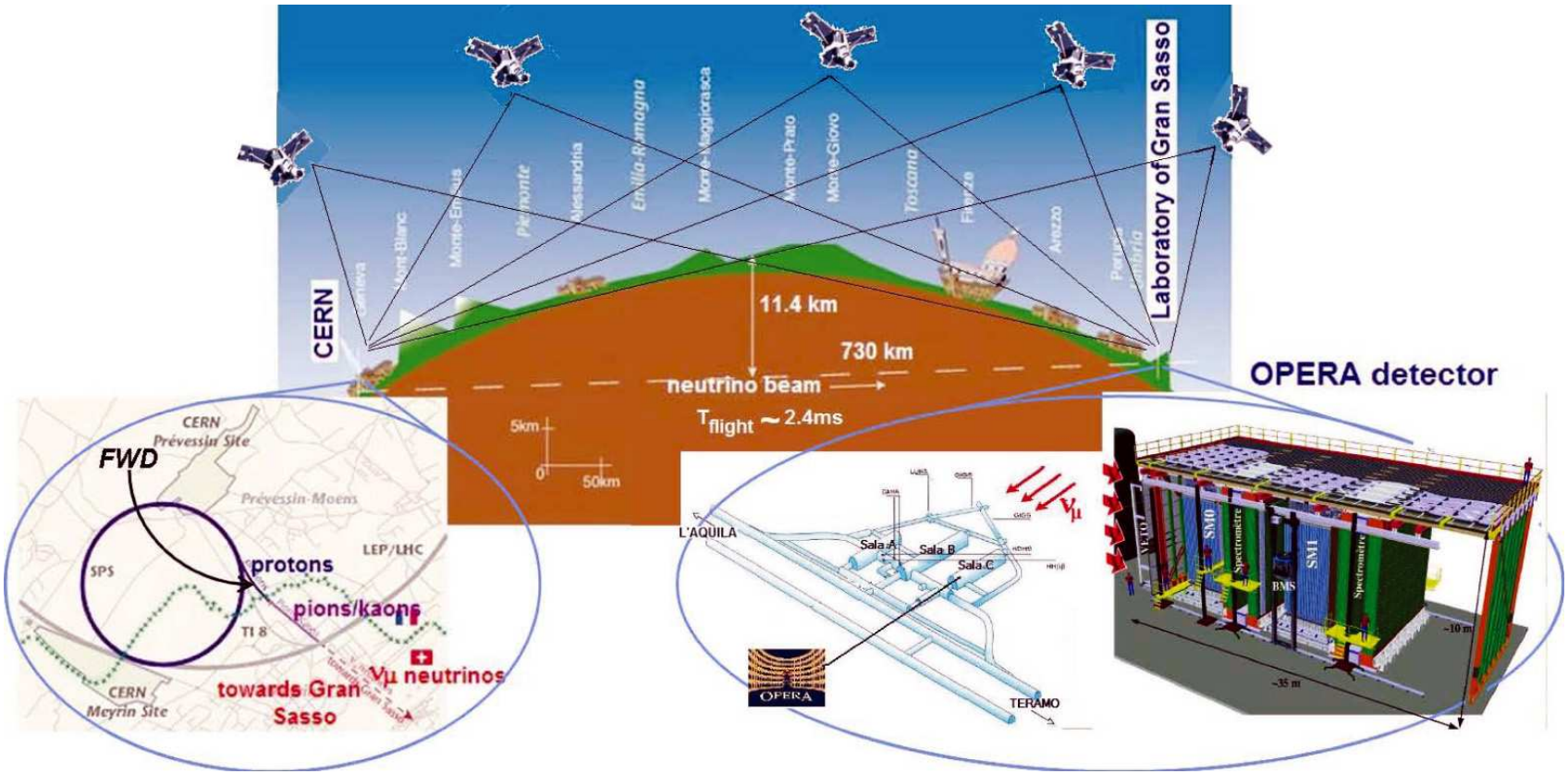

Schematic layout of the OPERA experiment.

[Borrowed from G. Brunetti, "Neutrino velocity measurement with the OPERA experiment in the CNGS beam," PhD thesis, in joint supervision of the Université Claude Bernard, Lyon-I and Universitá degli Studi di Bologna (May 2011), N° d'ordre 88-2011, LYCEN–T 2011-10; http://amsdottorato.cib.unibo.it/3917/, http://tel.archives-ouvertes.fr/tel-00633424.]

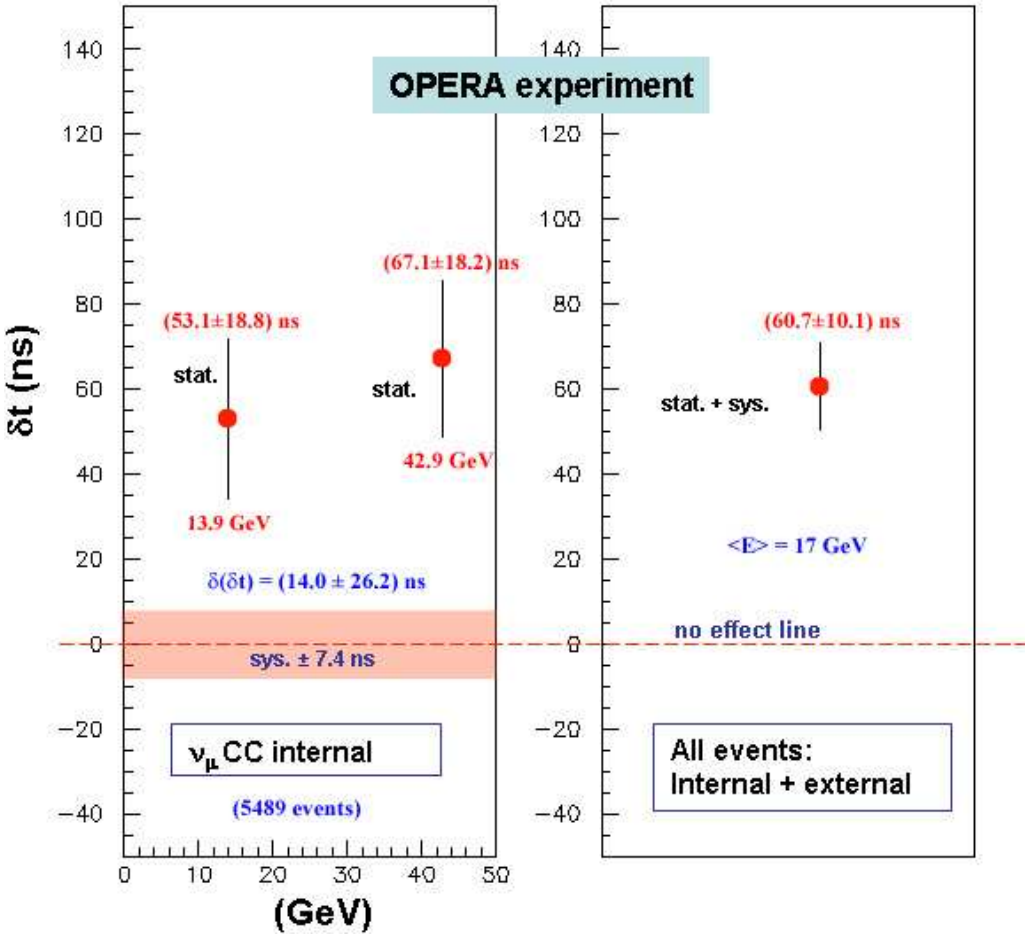

◁ Summary of the results for the measurement of δt.

The left plot shows δt vs. neutrino energy for ν_μ CC internal events. The errors attributed to the two points are just statistical in order to make their relative comparison easier since the systematic error (represented by a band around the no-effect line) cancels out.

The right plot shows the global result of the analysis including both internal and external events (for the latter the neutrino energy cannot be measured).

The error bar in the right plot includes statistical and systematic errors added in quadrature.

The result provides no clues on a possible energy dependence of δt in the domain explored by the OPERA, within the statistical accuracy of the measurement.

10 Astrophysical constraint.

ν burst from SN 1987A (Kamiokande-II, IMB, BUST) [≈ 51 kps, $\langle E_{\overline{\nu}} \rangle \sim 15$ MeV, $E_{\overline{\nu}} \lesssim 40$ MeV]:

$$|v_\nu - 1| < 2 \times 10^{-9}.$$

[K. Hirata *et al.* (Kamiokande- Collaboration) Phys. Rev. Lett. 58 (1987) 1490; R. M. Bionta *et al.* (IMB Collaboration) Phys. Rev. Lett. 58 (1987) 1494; E. N. Alekseev *et al.* J. Exp. Theor. Phys. Lett. 45 (1987) 589]

Arguments: [M. J. Longo Phys. Rev. D 36 (1987) 3276]

The arrival time of the antineutrinos is known to be within a few seconds of 7:35:40 UT on February 23, 1987. The arrival time of the first light from SN is less well known. The last confirmed evidence of no optical brightening was at approximately 2:20 UT[a]. The earliest observations of optical brightening were at 10:38 UT by Garrad and by McNaught[b].

Standard SN theory expects that the neutrinos and antineutrinos are emitted in the first few second of the collapse, while the optical outburst begins ~ 1 h later, when the cooler envelope is blown away.

Altogether this leads to an uncertainty of about 3 h. Hence

$$|v_\nu - 1|_{\max} \sim 3 \text{ h}/(1.6 \times 10^5 \times 365 \times 24\text{h}) \approx 2 \times 10^{-9}.$$

However Longo's limit is generally not robust.

[a] I. Shelton, IUA Circular No. 4330,1987.

[b] G. Garradd, IUA Circular No. 4316, 1987; R. H. McNaught, *ibid.*

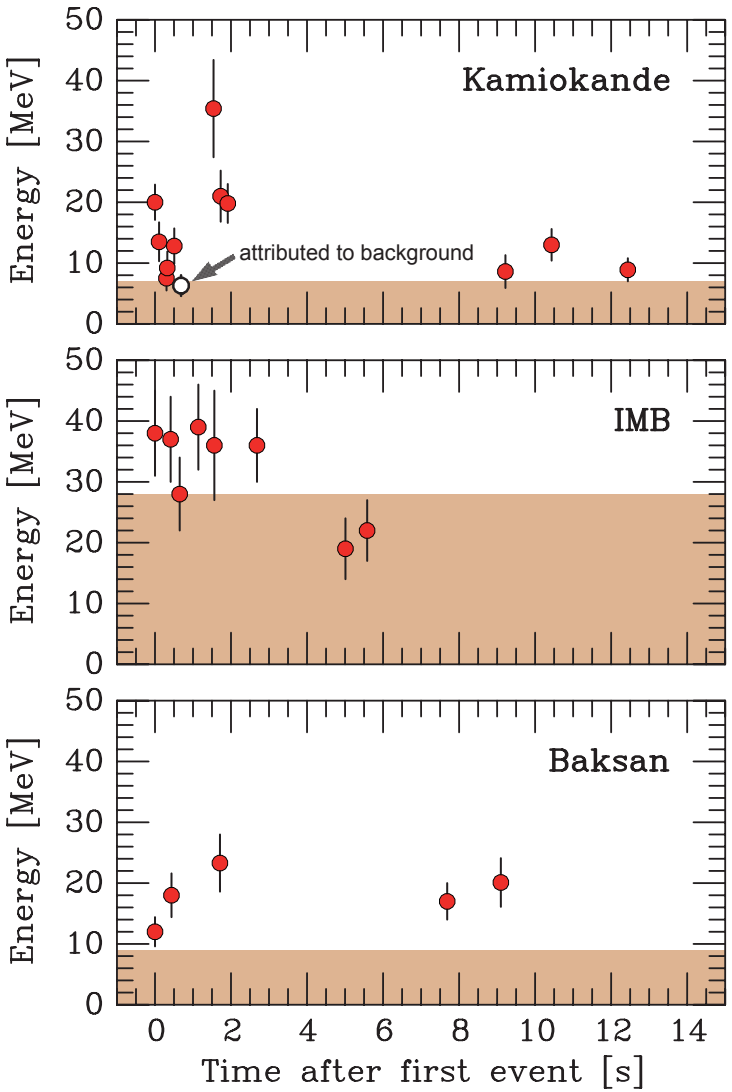

SN 1987A antineutrino observations at Kamiokande, IMB and Baksan detectors. The energies refer to the secondary positrons from the reaction $\overline{\nu}_e p \to n e^+$. In the shaded area the trigger efficiency is less than 30%. The clocks have unknown relative offsets; in each case the first event was shifted to $t = 0$.
The signal does show a number of "anomalies".

- The average $\overline{\nu}_e$ energies inferred from the IMB and Kamiokande observations are quite different.
- The large time gap of 7.3 s between the first 8 and the last 3 Kamiokande events looks worrisome.
- The distribution of the positrons should be isotropic, but is found to be significantly peaked away from the direction of the SN.

In the absence of other explanations, these features are blamed on statistical fluctuations in the sparse data.

[G. G. Raffelt, "Particle physics from stars," Ann. Rev. Nucl. Part. Sci. **49** (1999) 163–216 (hep-ph/9903472).]

Kamiokande II result

TABLE I. Measured properties of the twelve electron events detected in the neutrino burst. The electron angle in the last column is relative to the direction of SN1987A. The errors on electron energies and angles are one-standard-deviation Gaussian errors.

Event number	Event time (sec)	Number of PMT's (N_{hit})	Electron energy (MeV)	Electron angle (degrees)
1	0	58	20.0 ± 2.9	18 ± 18
2	0.107	36	13.5 ± 3.2	15 ± 27
3	0.303	25	7.5 ± 2.0	108 ± 32
4	0.324	26	9.2 ± 2.7	70 ± 30
5	0.507	39	12.8 ± 2.9	135 ± 23
6	0.686	16	6.3 ± 1.7	68 ± 77
7	1.541	83	35.4 ± 8.0	32 ± 16
8	1.728	54	21.0 ± 4.2	30 ± 18
9	1.915	51	19.8 ± 3.2	38 ± 22
10	9.219	21	8.6 ± 2.7	122 ± 30
11	10.433	37	13.0 ± 2.6	49 ± 26
12	12.439	24	8.9 ± 1.9	91 ± 39

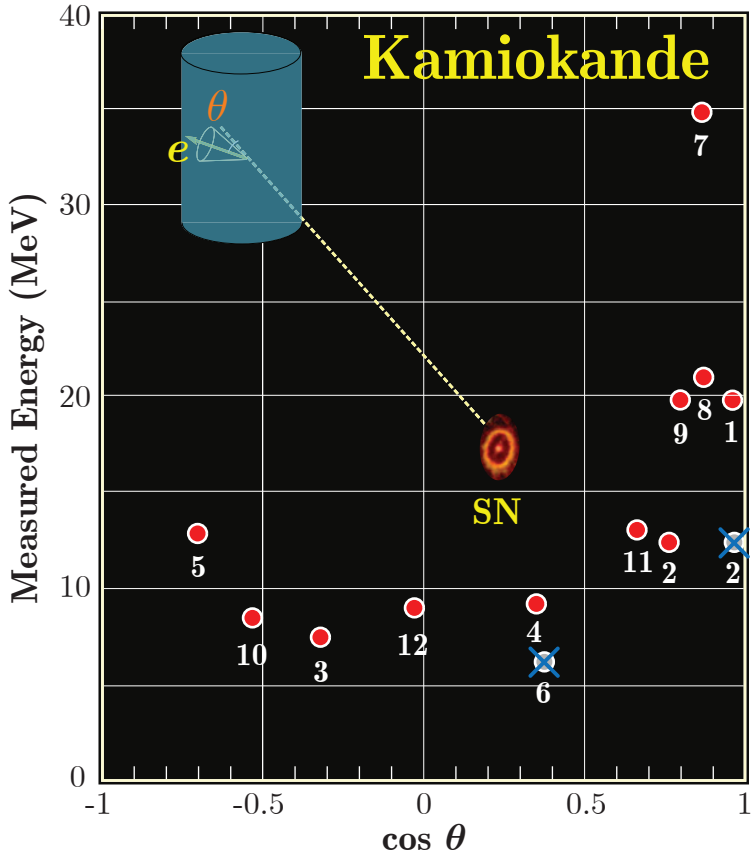

[K. Hirata *et al.* Phys. Rev. Lett. 58 (1987) 1490–1493; K. Hirata *et al.* Phys. Rev. D 38 (1998) (448–458).]

IMB result

TABLE III. Characteristics of the contained neutrino events recorded on 23 February.

Event No.[a]	Time (UT)	No. of PMT's	Energy[b] (MeV)	Angular distribution[c] (degrees)
33162	7:35:41.37	47	38	74
33164	7:35:41.79	61	37	52
33167	7:35:42.02	49	40	56
33168	7:35:42.52	60	35	63
33170	7:35:42.94	52	29	40
33173	7:35:44.06	61	37	52
33179	7:35:46.38	44	20	39
33184	7:35:46.96	45	24	102

[a]The event numbers are not sequential. Interspersed with the contained neutrino events are fifteen entering cosmic-ray muons.

[b]Error in energy determination is ±25% (systematic plus statistical).

[c]Individual track reconstruction uncertainty is 15°. Note that this angular distribution will be systematically biased toward the source because of the location of the inoperative PMT's.

[R. M. Bionta *et al.* Phys. Rev. Lett. 58 (1987) 1494–1496.]

TABLE I. Energies and angles of the eight events from supernova SN1987A. (a) Absolute UT is accurate to ±50 ms. Relative times are accurate to the nearest millisecond. (b) Additional systematic error in energy scale estimated to be ±10%. (c) Angle with respect to direction away from SN1987A. Angle errors include multiple scattering and event reconstruction. (d) assumes events are due to $\bar{\nu}+p \rightarrow e^{+}+n$ on free protons.

Event	(a) Time (UT) 23 Feb. 1987	(b) Measured energy (MeV)	(c) Polar angle (deg)	(d) Antineutrino energy (MeV)
1	7:35:41.374	38±7	80±10	41±7
2	7:35:41.786	37±7	44±15	39±7
3	7:35:42.024	28±6	56±20	30±6
4	7:35:42.515	39±7	65±20	42±7
5	7:35:42.936	36±9	33±15	38±9
6	7:35:44.058	36±6	52±10	38±6
7	7:35:46.384	19±5	42±20	21±5
8	7:35:46.956	22±5	104±20	24±5

[C. B. Bratton *et al.* Phys. Rev. D 37 (1988) 3361-3363; see]

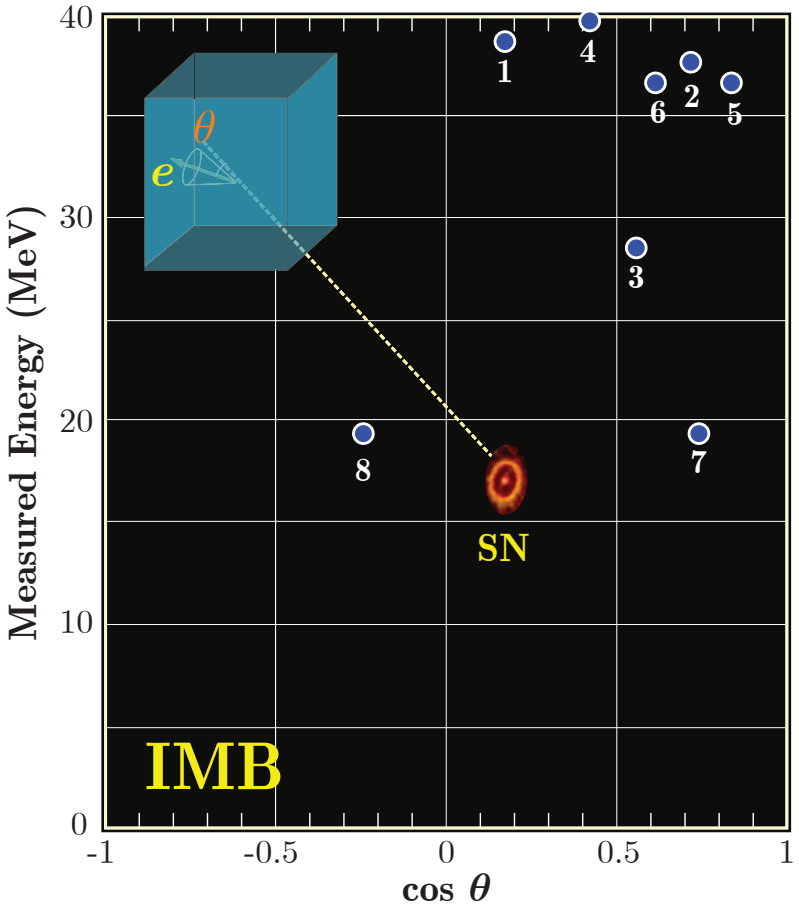

We have to remember about the first low-energy antineutrino pulse ($E_{\overline{\nu}} = 7 - 11$ MeV) detected by LSD[a] at 2:52:36 UT that is $4^{\mathrm{h}}44^{\mathrm{m}}$ earlier the second (Kamiokande-II-IMB-BUST) pulse. This fact is usually ignored by the community.

Naive estimations:
Assuming that δv is energy independent and $\delta \mathrm{t}_{L=730\,\mathrm{km}} \approx 60$ ns (OPERA) we obtain

$$\delta \mathrm{t}_{\mathrm{SN1987A}} \approx 4 \text{ yr}.$$

So it seems that any case there is a huge contradiction between the MINOS/OPERA result and astrophysics.

[a] V. L. Dadykin *et al.*, Pisma v Zh. Eksp. Teor. Fiz. **45** (1987) 464.

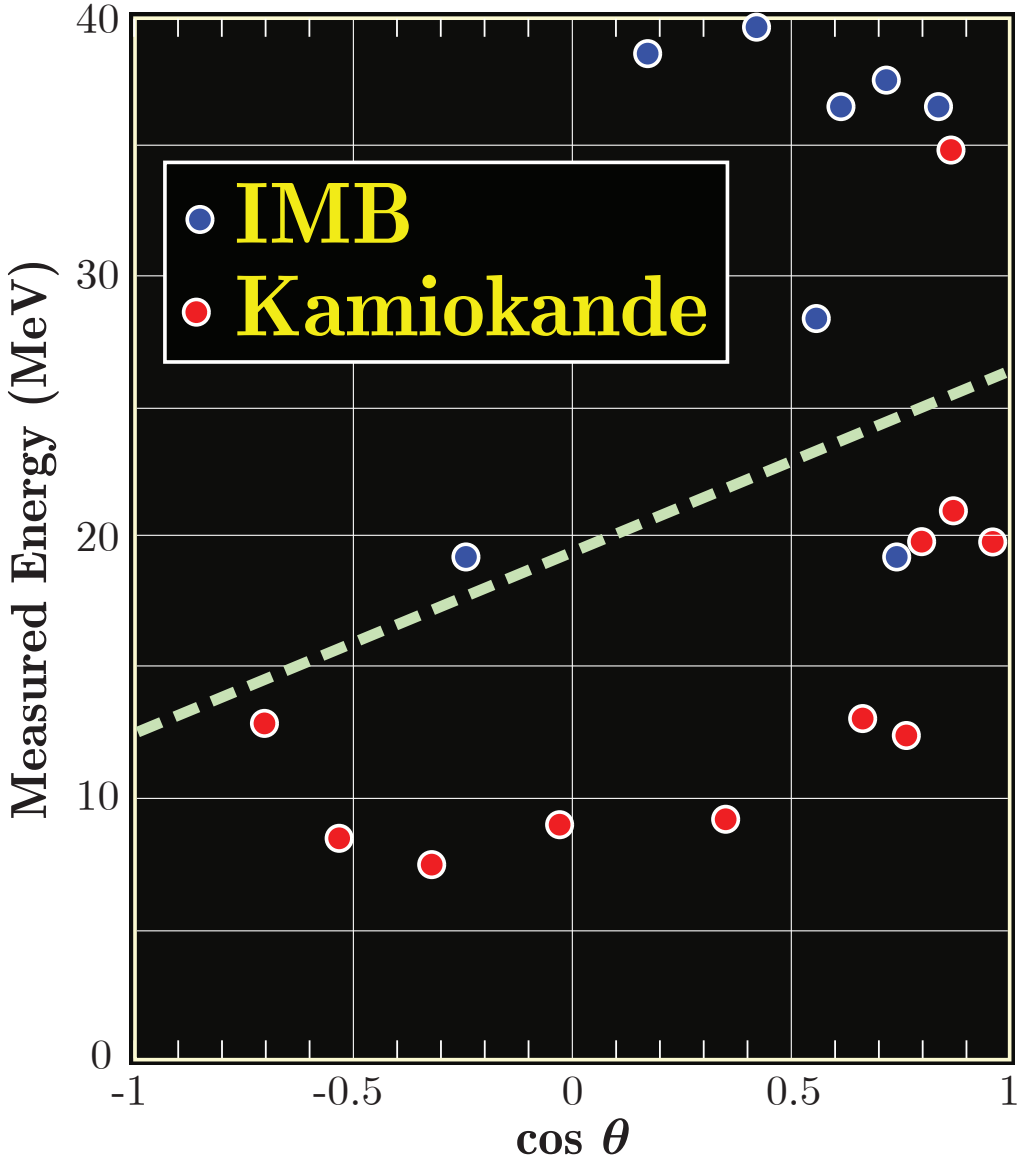

11 A possible explanation.

In the previous lectures we have developed a covariant QFT approach which operates with the relativistic wavepackets describing initial and final states of particles involved into the neutrino production and detection. The neutrino is described as a virtual mass eigenfield travelling between the macroscopically separated vertices of Feynman graphs. Thus we make no any assumption about its wavefunction. Instead, we compute it and prove that it is a wavepacket with spatial and momentum widths defined and functionally dependent on those of the external particles involved into the neutrino production and detection subprocesses.

Explicitly the effective neutrino spinor wavefunction reads

$$\begin{aligned}\psi^j_y(\mathbf{p}_j,x) &= \exp\left\{-i(p_jy)-\sigma_j^2\left[(p_jx)^2-m_j^2x^2\right]\right\}u_-(\mathbf{p}_j)\\ &= \exp\left[-iE_j\left(y_0-\mathbf{v}_j\mathbf{y}\right)-\sigma_j^2\Gamma_j^2\left(\mathbf{x}_\parallel-\mathbf{v}_jx_0\right)^2-\sigma_j^2\mathbf{x}_\perp^2\right]u_-(\mathbf{p}_j),\end{aligned}$$

where $y=(y_0,\mathbf{y})=X_d$ is the interaction point and $x=(x_0,\mathbf{x})$ ($\mathbf{x}=\mathbf{x}_\parallel+\mathbf{x}_\perp$) is the distance between the production and interaction (impact) points, $x=X_d-X_s$.

The main (but not the only) processes of ν_μ production in the MINOS and OPERA experiments are the $\pi_{\mu 2}$ and $K_{\mu 2}$ decays. It has been shown that the neutrino wavepackets from these decays appear as huge but superfine disks of microscopic (energy dependent) thickness in longitudinal direction, comparable with the thickness of a soap-bubble skin, and macroscopically large (energy independent) diameter in the transverse plane.

Summary of the previous results:

We can neglect the contributions into σ_j from the particles, interacting with neutrinos in the detector (reasonably assuming that their 4-momentum spreads are much larger than σ_π, σ_K, and σ_μ). With this simplification we have derived that

$$\sigma_j^2 \approx \frac{m_j^2}{2}\left(\frac{m_a^2}{\sigma_a^2}+\frac{m_\mu^2}{\sigma_\mu^2}\right)^{-1}, \quad a=\pi \text{ or } K.$$

Then from the above-mentioned conditions of stability for the meson and muon wavepackets it follows that σ_j must satisfy the following conditions:

$$\sigma_j^2 \ll \frac{m_j^2}{2}\left(\frac{m_\mu}{\Gamma_\mu}+\frac{m_a}{\Gamma_a}\right)^{-1},$$

where $\Gamma_a = 1/\tau_a$ and $\Gamma_\mu = 1/\tau_\mu$ are the full decay widths of the meson a and muon. Considering that for *any* know meson $\mathbf{m}_\mu/\Gamma_\mu \gg m_a/\Gamma_a$, we conclude that the neutrino momentum uncertainty is fantastically small:

$$\frac{\sigma_j^2}{m_j^2} \ll \frac{\Gamma_\mu}{2m_\mu} \approx 1.4\times 10^{-18}.$$

From this inequality one can immediately derive the lower bounds for the effective spatial dimensions of the neutrino wavepacket:

$$d_j^\perp \gg 2.5\left(\frac{0.1\text{ eV}}{m_j}\right)\text{ km} \quad \text{and} \quad d_j^\parallel = \frac{d_j^\perp}{\Gamma_j} \gg 2.5\times 10^{-5}\left(\frac{1\text{ GeV}}{E_\nu}\right)\left(\frac{0.1\text{ eV}}{m_j}\right)\text{ cm}.$$

This provides us with an idea of how to explain the MINOS-OPERA anomaly.

12 Qualitative estimations.

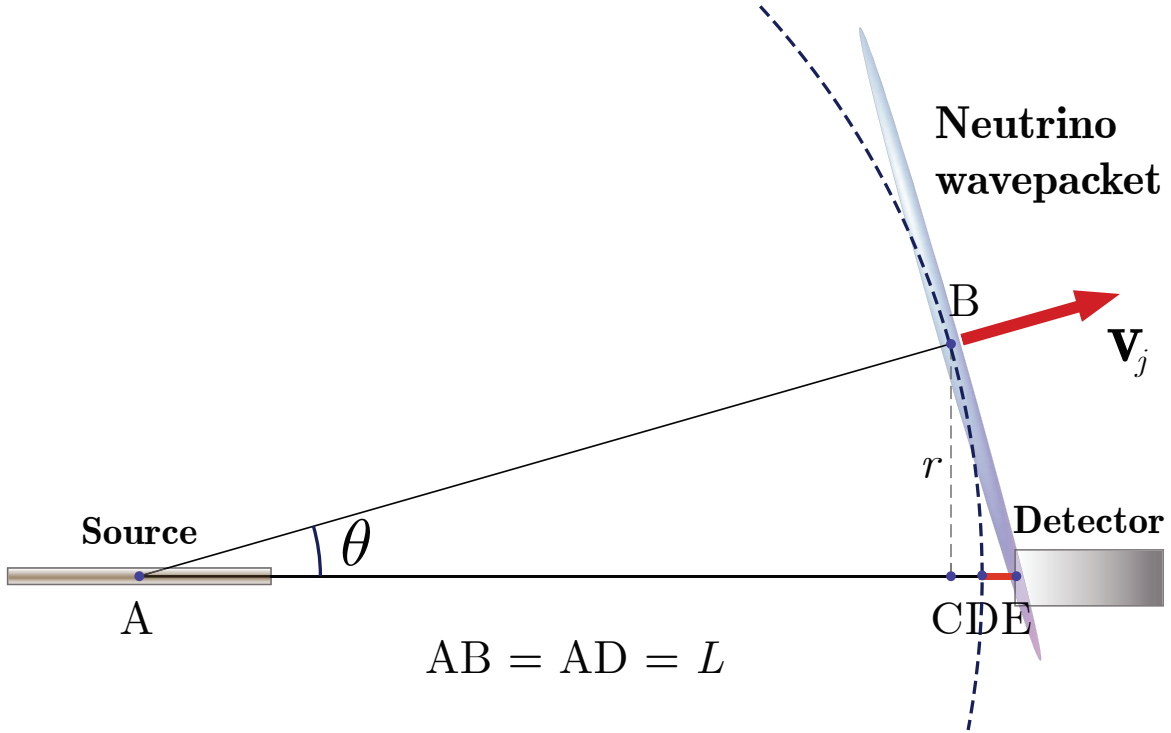

Рис. 36: Neutrinos are emitted from the "Source" and are registered in the "Detector". The centers of the neutrino wavepackets will arrive at the points B and D simultaneously, while the signal from the neutrino wavepacket (shown as an extremely oblate spheroid) which moves under the angle $\theta = \angle$BAC to the beam axis will arrive earlier since DE > 0. Neutrino velocity vector $\mathbf{v}_j$ lies in the plane of the figure. Proportions do not conform to reality.

The school-level planimetry suggests that the advancing time is given by

$$\delta t = L\,(1/\cos\theta - 1) \approx r^2/(2L). \tag{116}$$

Here we assume that

(i) $1 - v_\nu \lll 1$,

(ii) the neutrino wavepacket effective width is much larger than the detector dimensions, and

(iii) $\theta \ll 1$.

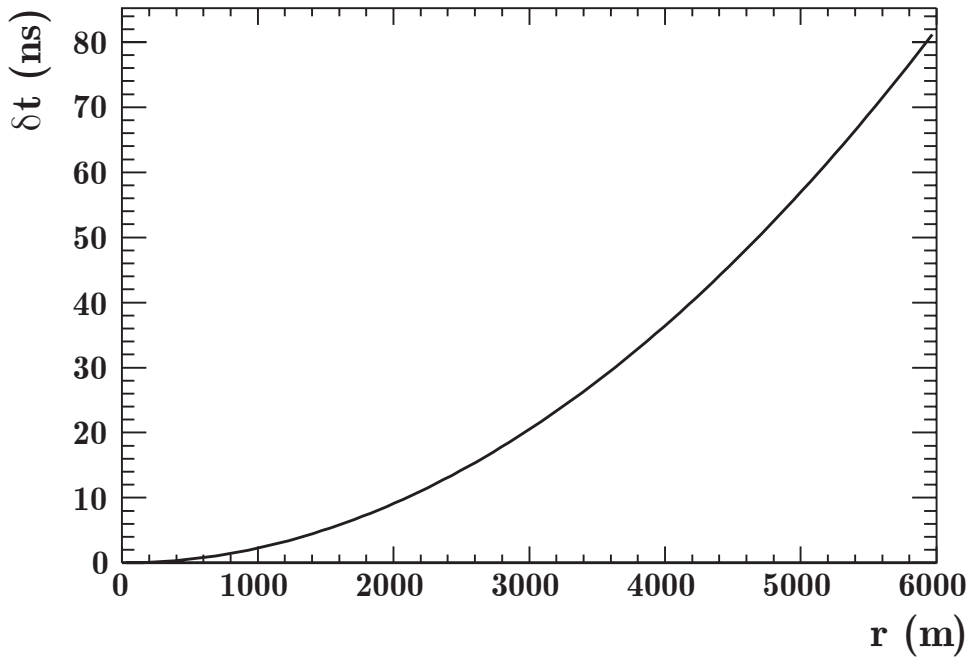

Рис. 37: Advance δt as a function of r.

A point particle a cannot affect the space-time point X.

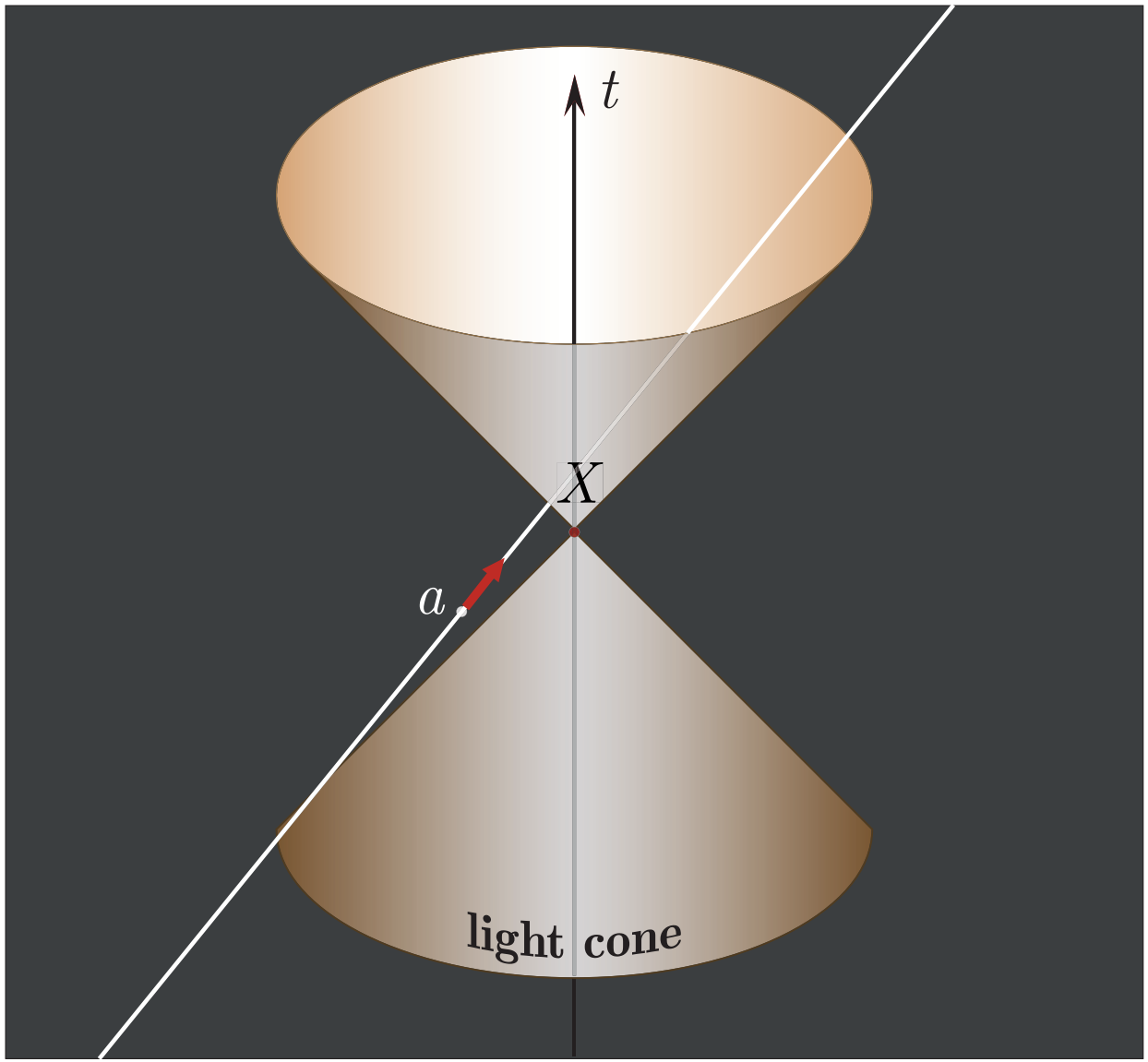

A finite size body a (or a wavepacket) whose center moves along the same world line as the particle a can affect the space-time‘point X.

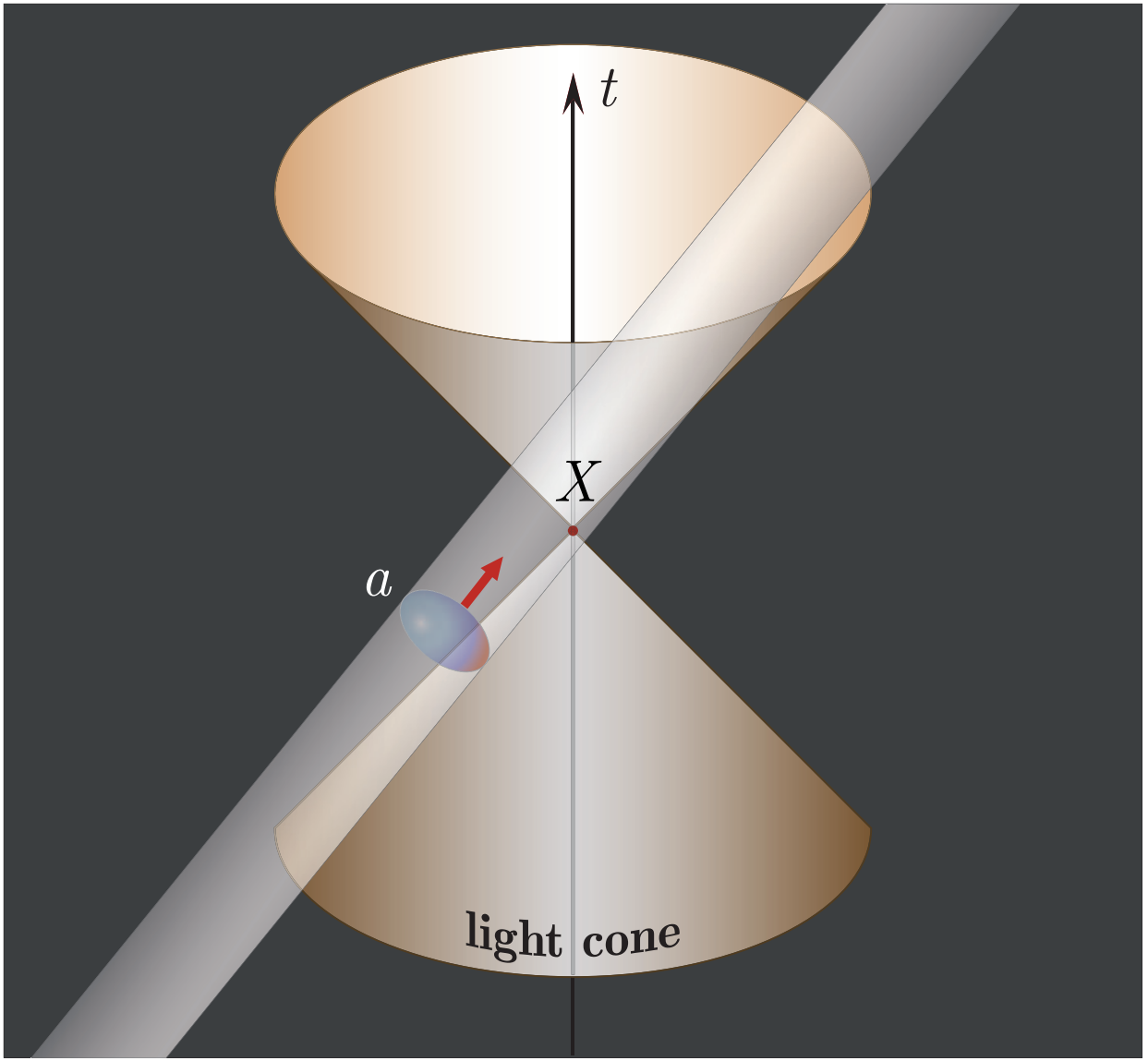

What is the probability to find a neutrino at a distance r from the beam axis? This could be estimated taking into account that neutrino production is dominated by two-particle decays of pions and kaons. The angular distribution of massless neutrinos from these decays is

$$\frac{dI}{d\Omega} = \frac{1 - v_a^2}{4\pi(1 - v_a \cos\theta)^2} \approx \frac{1}{\pi(1 + \Gamma_a^2\theta^2)^2}. \tag{117}$$

Here θ is the angle between the momenta of the meson a and neutrino ($0 \leq \theta \leq \pi$), v_a is the meson velocity, and $\Gamma_a = (1 - v_a^2)^{-1/2} = E_a/m_a$. The second approximate equality in Eq. (117) holds for small angles and relativistic meson energies ($\theta \ll 1$, $4\Gamma_a^2 \gg 1$). In the latter case, the main contribution to the neutrino event rate comes from the narrow cone $\theta \lesssim 1/\Gamma_a$. Considering that the mean neutrino energy, $\overline{E}_\nu$, from the muonic decay of a meson with energy E_a is $\overline{E}_\nu = \Gamma_a E_\nu^{(a)}$, where

$$E_\nu^{(a)} = (m_a^2 - m_\mu^2)/(2m_a)$$

is the neutrino energy in the rest frame of the particle a, the characteristic angle can be defined as

$$\theta_{(a)} = E_\nu^{(a)}/\overline{E}_\nu.$$

In the case of OPERA, one can (very) roughly estimate the characteristic angles for the "low-energy" (LE) range ($E_\nu < 20$ GeV, $\overline{E}_\nu \approx 13.9$ GeV) and "high-energy" (HE) range ($E_\nu > 20$ GeV, $\overline{E}_\nu \approx 42.9$ GeV), assuming that the main neutrino sources in these ranges are, respectively, $\pi_{\mu 2}$ and $K_{\mu 2}$ decays:

$$\theta_{\mathsf{LE}} \gtrsim \theta_{(\pi)} = 2.1 \times 10^{-3}, \quad \theta_{\mathsf{HE}} \lesssim \theta_{(K)} = 5.5 \times 10^{-3}.$$

This provides us with an order-of-magnitude estimate of the mean values of r and advancing times δt:

$$r_{\mathsf{LE}} \gtrsim 1.7 \text{ km}, \quad r_{\mathsf{HE}} \lesssim 11 \text{ km};$$
$$\delta t_{\mathsf{LE}} \gtrsim 5.6 \text{ ns}, \quad \delta t_{\mathsf{HE}} \lesssim 36.7 \text{ ns}.$$

Since the LE and HE ranges contribute almost equally to the CNGS ν_μ beam, there must be a definite trend towards earlier neutrino arrival to OPERA with approximately 21 ns mean time-shift and a "tail" or, better to say, "fore" of the same order coming from the "edges" of the CNGS beam.

Similar estimation for the low-energy NuMI beam at Fermilab producing neutrinos for the MINOS experiment can be done with a better accuracy, since the $\pi_{\mu 2}$ decay is here the dominant source of neutrinos and the radial distribution of the beam is expected to be very flat. So, by using $\overline{E}_\nu = 3$ GeV we obtain

$$r \approx 36.2 \text{ km}, \quad \delta t \approx 120.7 \text{ ns}. \tag{118}$$

The latter number is in surprisingly good agreement with the MINOS observation. Obviously, MINOS should observe at the average a much earlier arrival of neutrinos, in comparison with OPERA, because of the lower mean neutrino energy which corresponds to a wider transverse beam distribution and hence to a larger input from the misaligned neutrinos.

13 Numerical estimations.

Let us now reevaluate the rough estimations given above with a somewhat detailed but still simplified calculation. In particular, we could profit from the simulation of expected radial distribution of ν_μ charged current (CC) events performed by the OPERA Collaboration.
This distribution ($\rho_{CC}(r)$) which we digitalized for our purposes is displayed in Fig. 38. Being dominated by the $\pi_{\mu 2}$ and $K_{\mu 2}$ decays, the transverse beam size at Gran Sasso is of the order of kilometers and the full width at half maximum of the distribution is about 2.8 km.

[Figure is taken from <http://proj-cngs.web.cern.ch/proj-cngs/Beam~Performance/NeutrinoRadial.htm>.]

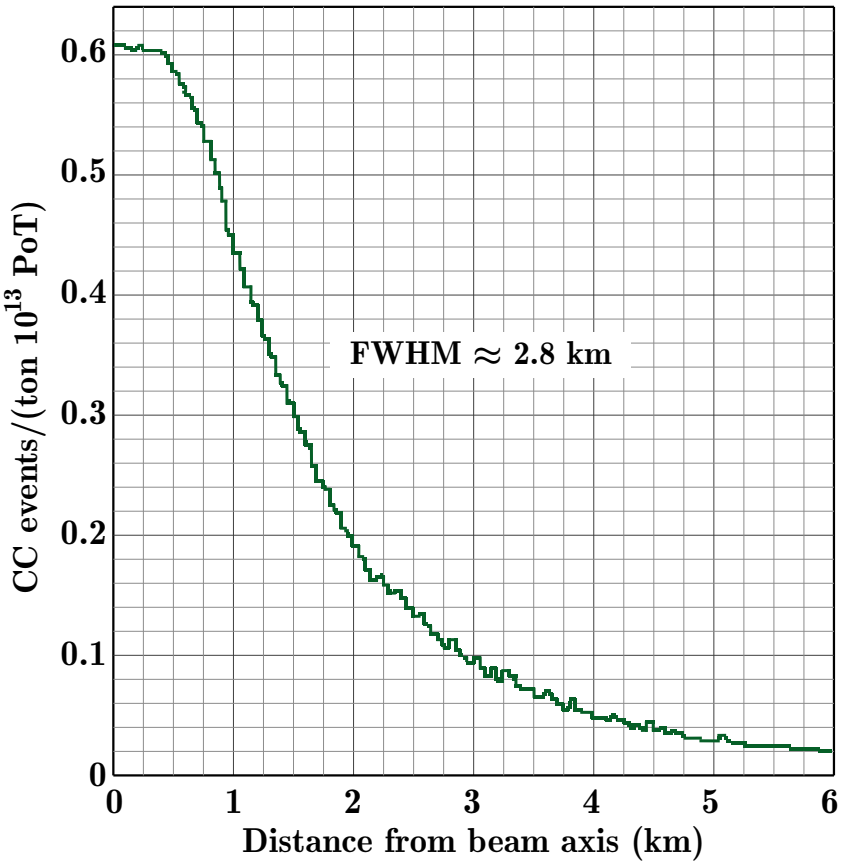

Рис. 38: Probability of neutrino charged current interactions expected in OPERA as a function of the distance from the beam axis r.

The distribution $\rho_{CC}(r)$ transformed (with help of Eq. (116)) into the δt distribution as

$$P_{CC}(\delta t) = \frac{r\rho_{CC}\left(r\left(\delta t\right)\right)}{\int_0^\infty drr\rho_{CC}(r)}$$

is shown in left panel of Fig. 39. Its average $\langle\delta t\rangle$ is about 20 ns with similar variance and with the tail extending up to about 100 ns.

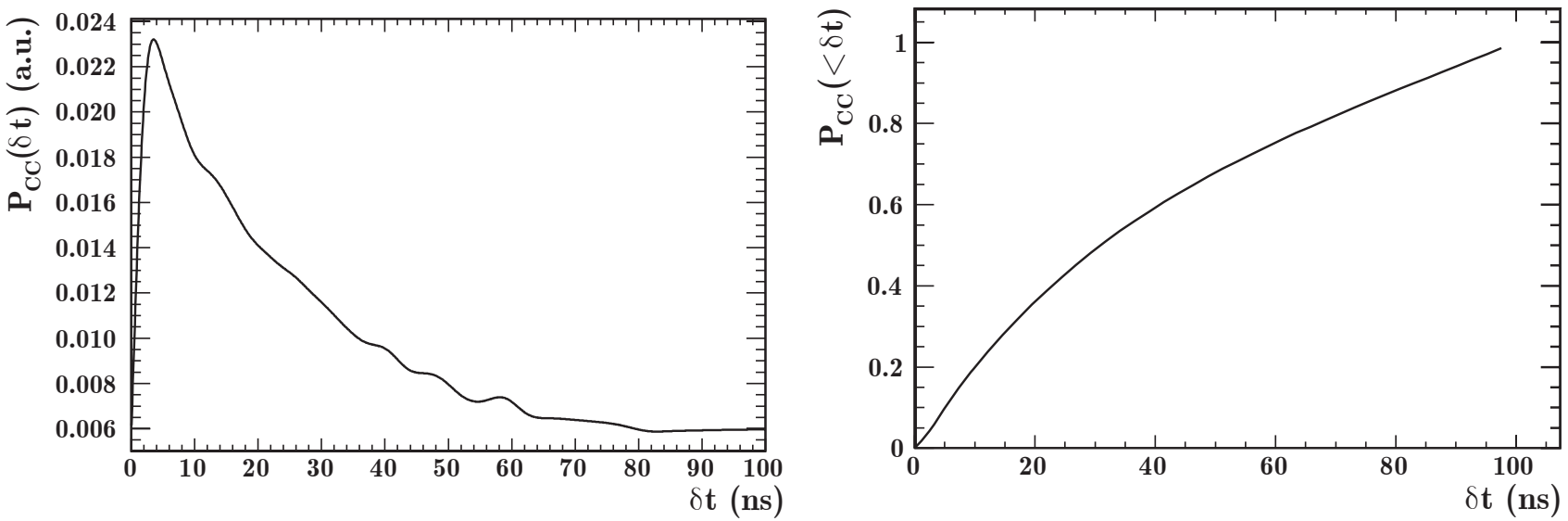

Рис. 39: *Left panel*: Advance δt distribution expected in OPERA. *Right panel*: $P_{CC}(<\delta t)$ distribution expected in OPERA.

Right panel of Fig. 39 shows the integral distribution

$$P_{\mathsf{CC}}\left(<\delta t\right)=\int_0^{\delta t} dt P_{\mathsf{CC}}(t).$$

Examination of this figure suggests that all CC events roughly equally populate the following intervals in δt:

$$(0,20)\ \text{ns}, \quad (20,45)\ \text{ns}, \quad \text{and} \quad (45,100)\ \text{ns}.$$

Finally, we compute the expected time distribution in OPERA, $g(t)$, as a convolution of the probability density function of arrival time $f(t)$ taking into account an earlier arrival of neutrino signal as follows:

$$g(t)=\frac{\int_0^{\infty} f\left(t+\delta t(r)\right)\rho_{\mathsf{CC}}(r) r dr}{\int_0^{\infty}\rho_{\mathsf{CC}}(r) r dr}. \tag{119}$$

The resulting curve $g(t)$ is displayed superimposed in Figs. 40 (for the first beam extraction) and 41 (for the second beam extraction) by dashed lines. On the average, time distribution is shifted to the left by about 20 ns. However, and this is even more important, the leading and trailing edges of the signal are shifted by two-three times larger amount as they accumulate the advance effect from the total $f(t)$ distribution, including long tails. In general, the impact of the misaligned neutrinos is predicted to be asymmetric in time.

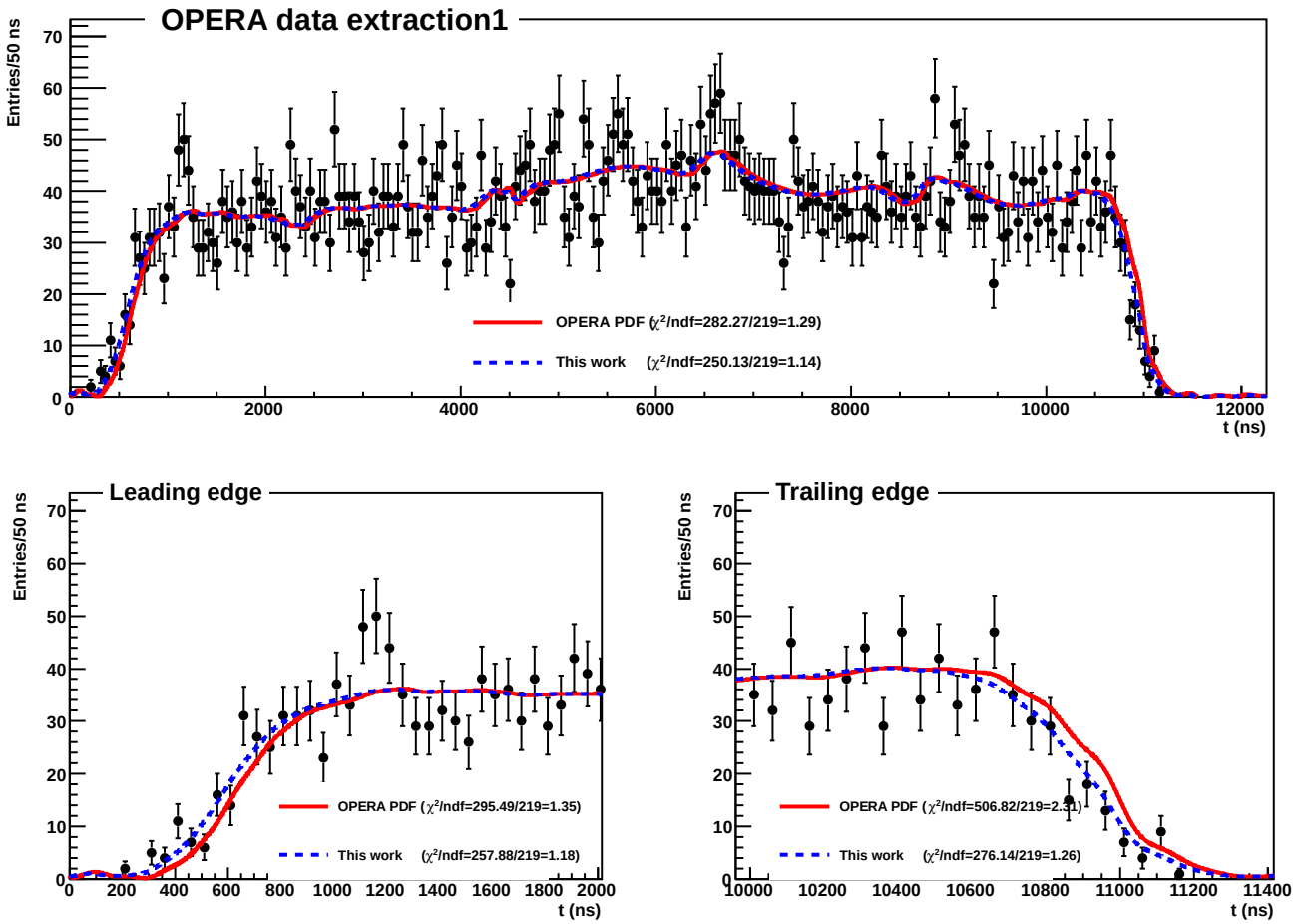

Рис. 40: *Top panel*: time probability density function for the first beam extraction, measured (points) and expected (solid curve) by the OPERA Collaboration after account of the systematic "instrumental" shift. Dashed curve is obtained according to Eq. (119). *Bottom left and right panels*: zooms of the top panel for the leading and trailing fronts of the signal, respectively.

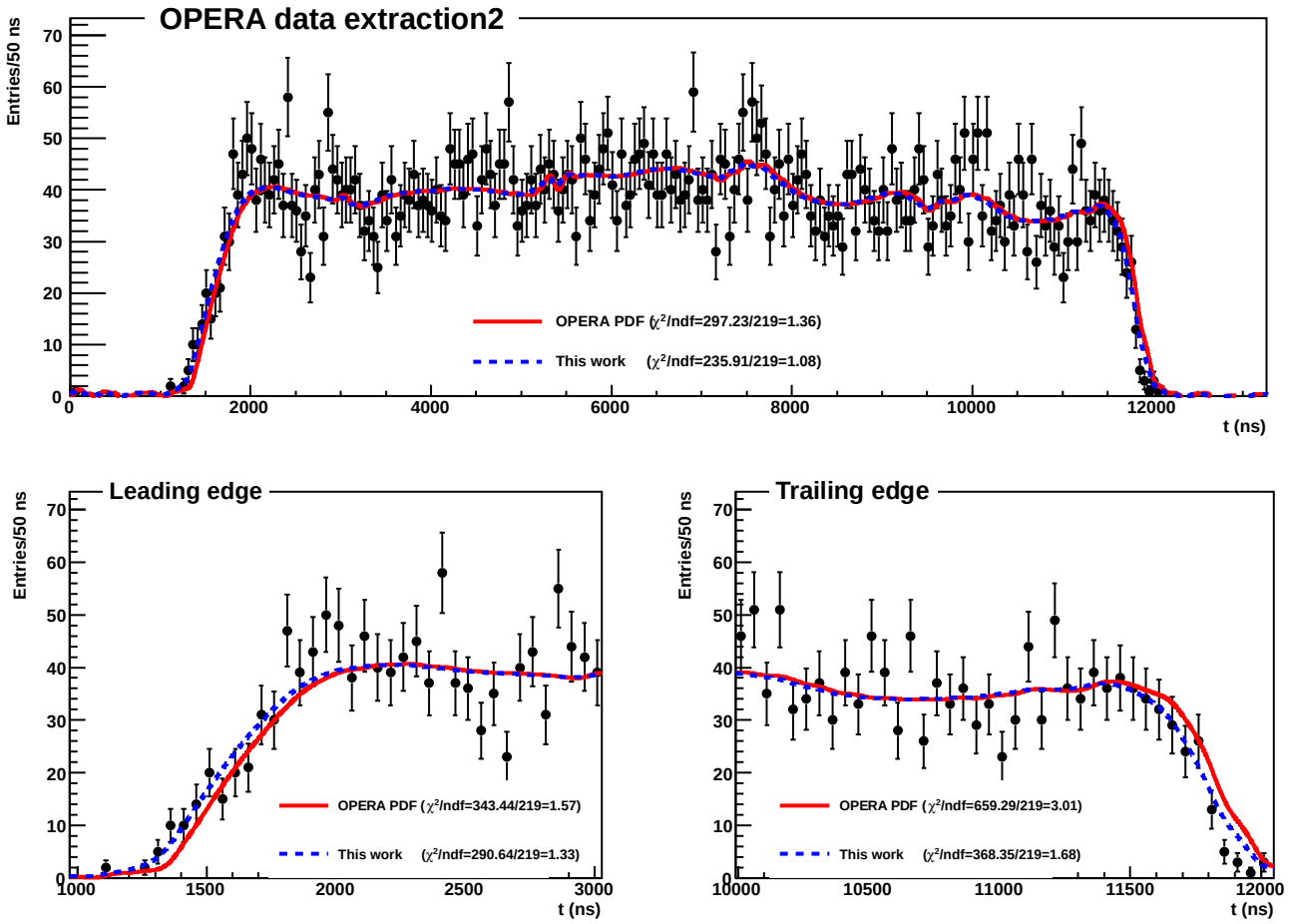

Рис. 41: The same as in Fig. 40 but for the second beam extraction.

14 Preliminary conclusions.

Large transverse size of the neutrino wavepacket and uncollimated beam of neutrinos seem to explain the earlier arrival of the neutrino signal in OPERA and MINOS. The neutrino signal is estimated to arrive in advance by about 20 ns in the mean (with a similar variance) for OPERA and by about 120 ns for MINOS. In the case of the OPERA experiment only this effect essentially reduces the statistical significance of its observation. Moreover, we have evaluated the expected time distribution of the neutrino arrival in OPERA and obtained that the left and right fronts are shifted to the left by about 40–50 ns. This probably explains the observed anomaly almost all-in-all without any exotic hypothesis, like Lorentz violation and so on.

Let us underline that in our calculations we do not use any adjustable parameter. In the case of the MINOS experiment there is also a surprisingly good agreement between our expectation (118) and experimental result. Therefore, we argue that observations of superluminal neutrinos by the OPERA and MINOS experiments can be (at least partially) treated as a manifestation of the huge transverse size of the neutrino wavefunction.

This kind of effects could be investigated in the future experiments (in particular, in the off-axis neutrino experiments) with more details in order to prove or disprove our explanation.

Let us note that one should not expect an increase in the number of neutrino induced events due to the misaligned neutrino interactions because this effect will be compensated by the corresponding decrease of the number of aligned neutrinos.

15 What about SN1987A?

Let us briefly discuss the situation with the observed (anti)neutrino signal from SN1987A. A proper treatment of these neutrinos should take care about the dispersion of the neutrino wavepackets at astronomical distances. Deliberately neglecting the dispersion, it appears that any terrestrial detector is sensitive only to the aligned neutrinos, since the misaligned neutrinos will have negligible impact due to the smallness of their wavepacket transverse size relative to the astrophysical scale of about 50 kps. Therefore, no advance signal should be expected. However this problem is not so simple and needs in a more detailed theoretical analysis.

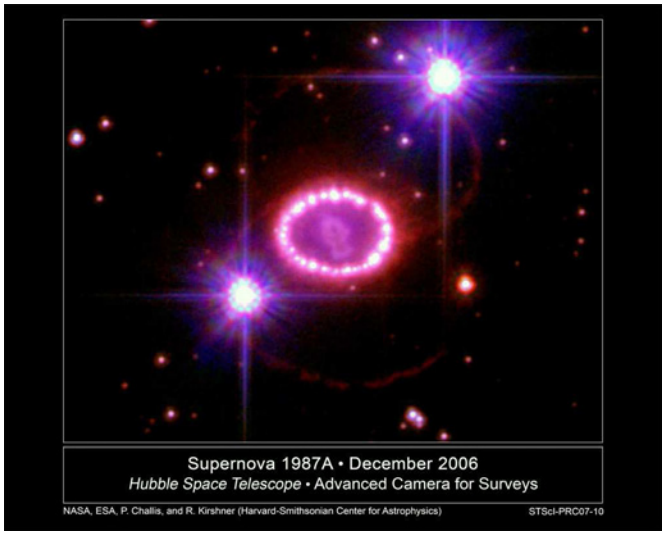

Часть V

APPENDICES

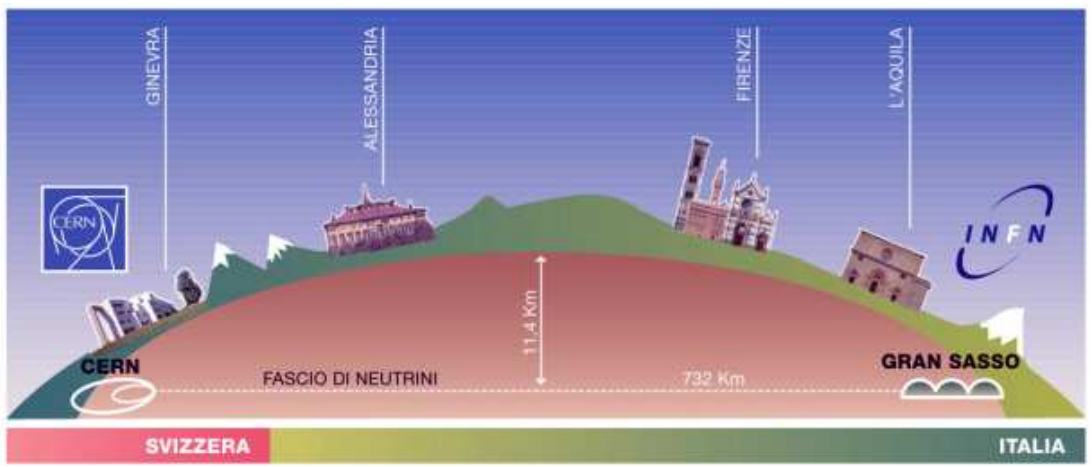

16 Multi-packet states.

- The multi-packet state can be written in two forms:

$$|\{\mathbf{p},s,x\}_n\rangle = \left(\prod_{i=1}^{n} 2E_{\mathbf{p}_i}\right)^{1/2} A^\dagger_{\mathbf{p}_1 s_1}(x_1)A^\dagger_{\mathbf{p}_2 s_2}(x_2)\cdots A^\dagger_{\mathbf{p}_n s_n}(x_n)|0\rangle \qquad (120a)$$

and

$$|\{\mathbf{p},s,x\}_n\rangle = (\pm 1)^{n(n-1)/2}\left(\prod_{i=1}^{n} 2E_{\mathbf{p}_i}\right)^{1/2} A^\dagger_{\mathbf{p}_n s_n}(x_n)\cdots A^\dagger_{\mathbf{p}_2 s_2}(x_2)A^\dagger_{\mathbf{p}_1 s_1}(x_1)|0\rangle, \qquad (120b)$$

where the sign "+" ("−") is for bosons (fermions). Let us check the equivalence of these definitions. It is evident for $n = 1, 2$. For $n \geq 2$ we obtain after n successive permutations:

$$|\{\mathbf{p},s,x\}_{n+1}\rangle = (\pm 1)^{n}\left(\prod_{i=1}^{n+1} 2E_{\mathbf{p}_i}\right)^{1/2} A^\dagger_{\mathbf{p}_{n+1} s_{n+1}}(x_{n+1})A^\dagger_{\mathbf{p}_1 s_1}(x_1)\cdots A^\dagger_{\mathbf{p}_n s_n}(x_n)|0\rangle.$$

Assuming validity of Eq. (120b), the right-hand part of the last equality can be written as

$$(\pm 1)^{n+n(n-1)/2}\left(\prod_{i=1}^{n+1} 2E_{\mathbf{p}_i}\right)^{1/2} A^\dagger_{\mathbf{p}_{n+1} s_{n+1}}(x_{n+1})A^\dagger_{\mathbf{p}_n s_n}(x_n)\cdots A^\dagger_{\mathbf{p}_1 s_1}(x_1)|0\rangle.$$

Since $(-1)^{n+n(n-1)/2} = (-1)^{-n+n(n-1)/2} = (-1)^{n(n+1)/2} = (-1)^{(n+1)[(n+1)-1]/2}$, the equality (120b) is proved by induction on n.

• Let us now prove Eq. (111). It is obviously satisfied for $n = 1$.

By direct calculation one checks that

$$\begin{aligned} M_2 &\equiv \langle \mathbf{q}_1, r_1, y_1; \mathbf{q}_2, r_2, y_2 | \mathbf{p}_1, s_1, x_1; \mathbf{p}_2, s_2, x_2 \rangle \\ &= \exp\left[i\left(q_1 y_1 + q_2 y_2 - p_1 x_1 - p_2 x_2\right)\right] \\ &\quad \times \left[\delta_{s_1 r_1}\delta_{s_2 r_2}\mathcal{D}(\mathbf{p}_1, \mathbf{q}_1; x_1 - y_1)\mathcal{D}(\mathbf{p}_2, \mathbf{q}_2; x_2 - y_2)\right. \\ &\quad \left. \pm\delta_{s_1 r_2}\delta_{s_2 r_1}\mathcal{D}(\mathbf{p}_1, \mathbf{q}_2; x_1 - y_2)\mathcal{D}(\mathbf{p}_2, \mathbf{q}_1; x_2 - y_1)\right] \\ &= \exp\left[i\sum_{i=1}^{2}\left(q_i y_i - p_i x_i\right)\right]|\mathbb{D}_2|, \end{aligned}$$

that is, Eq. (111) is satisfied also for $n = 2$. Now we calculate the matrix element $M_{n+1} \equiv \langle \{\mathbf{q}, r, y\}_{n+1} \,|\, \{\mathbf{p}, s, x\}_{n+1} \rangle$ for $n \geq 2$. According to Eq. (120b),

$$\begin{aligned} M_{n+1} &= \left(\prod_{i=1}^{n+1} 4E_{\mathbf{q}_i}E_{\mathbf{p}_i}\right)^{1/2} \langle 0|A_{\mathbf{q}_{n+1}r_{n+1}}(y_{n+1})\cdots A_{\mathbf{q}_2 r_2}(y_2)A_{\mathbf{q}_1 r_1}(y_1) \\ &\quad \times A^{\dagger}_{\mathbf{p}_1 s_1}(x_1)A^{\dagger}_{\mathbf{p}_2 s_2}(x_2)\cdots A^{\dagger}_{\mathbf{p}_{n+1}s_{n+1}}(x_{n+1})|0\rangle \\ &= \left(\prod_{i=1}^{n+1} 4E_{\mathbf{q}_i}E_{\mathbf{p}_i}\right)^{1/2} \langle 0|A_{\mathbf{q}_1 r_1}(y_1)\cdots A_{\mathbf{q}_n r_n}(y_n)A_{\mathbf{q}_{n+1}r_{n+1}}(y_{n+1}) \\ &\quad \times A^{\dagger}_{\mathbf{p}_{n+1}s_{n+1}}(x_{n+1})A^{\dagger}_{\mathbf{p}_n s_n}(x_n)\cdots A^{\dagger}_{\mathbf{p}_1 s_1}(x_1)|0\rangle. \end{aligned}$$

Then, after successive permutations of the operator $A^{\dagger}_{\mathbf{p}_{n+1}s_{n+1}}(x_{n+1})$ with the operators $A_{\mathbf{q}_n r_n}(y_n)$, ..., $A_{\mathbf{q}_1 r_1}(y_1)$, by applying Eq. (111) for the n-packet matrix elements, and taking into account the (anti)commutation relation (106), we obtain

$$
\begin{aligned}
M_{n+1} = & \left(\prod_{i=1}^{n+1} 4E_{\mathbf{q}_i} E_{\mathbf{p}_i} \right)^{1/2} \sum_{j=1}^{n+1} (\pm 1)^{n+j+1} \delta_{s_{n+1} r_j} \exp\left[i(q_j y_j - p_{n+1} x_{n+1}) \right] \\
& \times \left(4E_{\mathbf{q}_j} E_{\mathbf{p}_{n+1}} \right)^{-1/2} \mathcal{D}\left(\mathbf{p}_{n+1}, \mathbf{q}_j; x_{n+1} - y_j \right) \\
& \times \langle 0 | A_{\mathbf{q}_1 r_1}(y_1) \cdots A_{\mathbf{q}_{j-1} r_{j-1}}(y_{j-1}) A_{\mathbf{q}_{j+1} r_{j+1}}(y_{j+1}) \cdots \\
& \cdots A_{\mathbf{q}_n r_n}(y_n) A_{\mathbf{q}_{n+1} r_{n+1}}(y_{n+1}) A^{\dagger}_{\mathbf{p}_n s_n}(x_n) \cdots A^{\dagger}_{\mathbf{p}_1 s_1}(x_1) | 0 \rangle .
\end{aligned}
$$

The right-hand part of this relation can be rewritten in compact form as

$$
\exp\left[i \sum_{i=1}^{n+1} (q_i y_i - p_i x_i) \right] \sum_{j=1}^{n+1} (\pm 1)^{n+j+1} \delta_{s_{n+1} r_j} \mathcal{D}\left(\mathbf{p}_{n+1}, \mathbf{q}_j; x_{n+1} - y_j \right) |\mathbb{D}^{(j)}_{n+1}|,
$$

where $|\mathbb{D}^{(j)}_{n+1}|$ is the minor of order n of $|\mathbb{D}_{n+1}|$ obtained after deleting from the latter the $(n+1)$-th row and j-th column. The sum over j in the last expression just represents the minor expansion of $|\mathbb{D}_{n+1}|$ over the bottom [$(n+1)$-th] row, hence

$$
M_{n+1} = \exp\left[i \sum_{i=1}^{n+1} (q_i y_i - p_i x_i) \right] |\mathbb{D}_{n+1}|.
$$

This completes the proof by induction.

17 Gaussian integration in Minkowski spacetime

We are frequently dealing with the Gaussian integrals

$$\mathcal{G}(A,B) = \int dx \exp\left(-A_{\mu\nu}x^\mu x^\nu + B_\mu x^\mu\right), \tag{121}$$

where $A = ||A_{\mu\nu}||$ is a symmetric and positive-definite matrix and B_μ are some complex constants. While these integrals are well known we reconsider this issue here, because there is some confusion in the literature concerning the correct definition of the matrix inverse to A in Minkowski space. In our case $A_{\mu\nu}$ and B_μ form, respectively, a tensor and 4-vector, though this fact is not used below. Moreover, the main steps of the subsequent derivation are not affected by the space-time dimension and signature.

The matrix A can always be diagonalized by an orthogonal transformation $O = ||O_{\mu\nu}||$:

$$A_{\mu\nu} = \sum_\alpha a_\alpha O_{\mu\alpha}O_{\nu\alpha}, \quad \sum_\alpha O_{\mu\alpha}O_{\nu\alpha} = \delta_{\mu\nu}, \tag{122}$$

where $a_\alpha > 0$ are the eigenvalues of A. Taking this into account, the quadratic form in the integrand of Eq. (121) can be rewritten as

$$\begin{aligned} -A_{\mu\nu}x^\mu x^\nu + B_\mu x^\mu &= -\sum_\alpha a_\alpha \left(O_{\mu\alpha}x^\mu\right)\left(O_{\nu\alpha}x^\nu\right) + B_\mu x^\mu \\ &= \sum_\alpha \left(-a_\alpha y_\alpha^2 + \sum_\mu B_\mu O_{\mu\alpha} y_\alpha\right), \end{aligned} \tag{123}$$

where $y_\alpha = O_{\mu\alpha} x^\mu$ (and thus $x^\mu = \sum_\alpha O_{\mu\alpha} y_\alpha$). The Jacobian of this transformation is $|O| = 1$, hence $dx = dy$. Substituting Eq. (123) into (121) reduces it to the standard Gaussian quadratures:

$$\mathcal{G}(A,B) = \prod_\alpha \sqrt{\frac{\pi}{a_\alpha}} \exp\left[\frac{1}{4a_\alpha}\left(\sum_\mu B_\mu O_{\mu\alpha}\right)^2\right].$$

According to Eq. (122)

$$\sum_\alpha a_\alpha^{-1} O_{\mu\alpha} O_{\nu\alpha} = \left(A^{-1}\right)_{\mu\nu} \stackrel{\text{def}}{=} \widetilde{A}^{\mu\nu} \quad \text{and} \quad \prod_\alpha a_\alpha = |A|.$$

Therefore, for the 4D Minkowski space-time

$$\mathcal{G}(A,B) = \frac{\pi^2}{\sqrt{|A|}} \exp\left[\frac{1}{4}\sum_{\mu\nu}\left(A^{-1}\right)_{\mu\nu} B_\mu B_\nu\right] = \frac{\pi^2}{\sqrt{|A|}} \exp\left(\frac{1}{4}\widetilde{A}^{\mu\nu} B_\mu B_\nu\right). \qquad (124)$$

Note that $\widetilde{A} = g A^{-1} g$ and thus $|\widetilde{A}| = 1/|A| = \prod_\alpha a_\alpha^{-1}$. Therefore the matrix $\widetilde{A}$ is positive-definite and of course symmetric.

18 Stationary point: general case.

Приведем здесь метод решения уравнения (52) в общем случае, т.е. для произвольной конфигурации внешних импульсов. Общее решение представляет интерес как с методической точки зрения, так и для практического суммирования диаграмм с тяжелыми и легкими нейтрино в промежуточных состояниях. Хотя предлагаемый алгоритм довольно громоздок, он легко может быть реализован в виде компьютерной программы на удобном языке программирования и поэтому полезен прежде всего при численном анализе.

Удобно работать с уравнением (52), записанным в виде (130), в котором неизвестной величиной является скорость виртуального нейтрино. Возводя обе части (130) в квадрат, приходим к алгебраическому уравнению четвертого порядка

$$v^4 + c_3 v^3 + c_2 v^2 + c_1 v + c_0 = 0, \tag{125}$$

коэффициенты которого имеют вид

$$c_0 = \frac{(\mathbf{Rl})^2 - (\boldsymbol{\eta}\mathbf{l})^2}{(\mathbf{Rl})^2 + \eta_0^2}, \qquad c_1 = -2\frac{R(\mathbf{Rl}) + 2(\mathbf{Rl})^2 - \eta_0(\boldsymbol{\eta}\mathbf{l})}{(\mathbf{Rl})^2 + \eta_0^2},$$

$$c_2 = \frac{R^2 + 6(\mathbf{Rl})^2 + 4R(\mathbf{Rl}) + (\boldsymbol{\eta}\mathbf{l})^2 - \eta_0^2}{(\mathbf{Rl})^2 + \eta_0^2}, \qquad c_3 = -2\frac{R(\mathbf{Rl}) + 2(\mathbf{Rl})^2 + \eta_0(\boldsymbol{\eta}\mathbf{l})}{(\mathbf{Rl})^2 + \eta_0^2}.$$

Здесь $\eta_\mu = Y_\mu/m_j$; всюду далее предполагается, что $m_j > 0$ (случай безмассового нейтрино тривиален), а индекс «j», нумерующий нейтрино, не пишется. Все остальные обозначения такие же, как и в основном тексте.

Решение уравнения (125) может быть найдено методом Декарта-Эйлера. Согласно этому методу, запишем уравнение (125) в «неполном» виде

$$\left(v+\frac{c_3}{4}\right)^4+\widetilde{c}_2\left(v+\frac{c_3}{4}\right)^2+\widetilde{c}_1\left(v+\frac{c_3}{4}\right)+\widetilde{c}_0=0. \tag{126}$$

Решения этого уравнения строятся из корней кубического уравнения

$$z^3+a_2z^2+a_1z+a_0=0, \tag{127}$$

в котором

$$a_0=-\frac{\widetilde{c}_1^2}{64},\quad a_1=\frac{\widetilde{c}_2^2-4\widetilde{c}_0}{16},\quad a_2=\frac{\widetilde{c}_2}{2}.$$

Уравнение (127) также может быть тождественно преобразовано к «неполной» форме (форме Кардано):

$$\left(z+\frac{a_2}{3}\right)^3+\mathfrak{p}\left(z+\frac{a_2}{3}\right)+\mathfrak{q}=0.$$

Здесь использованы следующие обозначения:

$$\mathfrak{p}=a_1-\frac{a_2^2}{3}=-\frac{\left[R^2+4R(\mathbf{Rl})-\eta_0^2+(\boldsymbol{\eta}\mathbf{l})^2\right]^2}{48\left[(\mathbf{Rl})^2+\eta_0^2\right]^2},$$

$$\mathfrak{q}=a_0-\frac{a_1a_2}{3}+2\left(\frac{a_2}{3}\right)^3=-\frac{A}{864\left[(\mathbf{Rl})^2+\eta_0^2\right]^3},$$

$$A=A_0+A_1(\mathbf{Rl})+A_2(\mathbf{Rl})^2+A_3(\mathbf{Rl})^3,$$

$$A_0 = R^6 - 3\left[\eta_0^2 - (\boldsymbol{\eta}\mathbf{l})^2\right]R^4 + 3\left[\eta_0^4 + 16\eta_0^2(\boldsymbol{\eta}\mathbf{l})^2 + (\boldsymbol{\eta}\mathbf{l})^4\right]R^2 - \left[\eta_0^2 - (\boldsymbol{\eta}\mathbf{l})^2\right]^3,$$
$$A_1 = 12R\left\{R^4 - 2\left[\eta_0^2 - (\boldsymbol{\eta}\mathbf{l})^2\right]R^2 + \left[\eta_0^2 - 7\eta_0(\boldsymbol{\eta}\mathbf{l}) + (\boldsymbol{\eta}\mathbf{l})^2\right](\eta l)^2\right\},$$
$$A_2 = 48R^2\left[R^2 - \eta_0^2 + (\boldsymbol{\eta}\mathbf{l})^2\right] + 54(\eta l)^4,$$
$$A_3 = 64R^3.$$

Число вещественных корней определяется знаком функции

$$\mathfrak{B} = \frac{\mathfrak{q}^2}{4} + \frac{\mathfrak{p}^3}{27} = \frac{\left[\eta_0(\boldsymbol{\eta}\mathbf{l})R - (\eta l)^2(\mathbf{R}\mathbf{l})\right]^2 B}{27648\left[(\mathbf{R}\mathbf{l})^2 + \eta_0^2\right]^6},$$

совпадающим со знаком полинома $B = B_0 + B_1(\mathbf{R}\mathbf{l}) + B_2(\mathbf{R}\mathbf{l})^2 + B_3(\mathbf{R}\mathbf{l})^3$, коэффициенты которого имеют вид

$$B_0 = R^6 - 3\left[\eta_0^2 - (\boldsymbol{\eta}\mathbf{l})^2\right]R^4 + 3\left[\eta_0^4 + 7\eta_0^2(\boldsymbol{\eta}\mathbf{l})^2 + (\boldsymbol{\eta}\mathbf{l})^4\right]R^2 - \left[\eta_0^2 - (\boldsymbol{\eta}\mathbf{l})^2\right]^3,$$
$$B_1 = 6R\left\{2R^4 - 4\left[\eta_0^2 - (\boldsymbol{\eta}\mathbf{l})^2\right]R^2 + \left[2\eta_0 - (\boldsymbol{\eta}\mathbf{l})\right]\left[\eta_0 - 2(\boldsymbol{\eta}\mathbf{l})\right](\eta l)^2\right\},$$
$$B_2 = 48R^2\left[R^2 - \eta_0^2 + (\boldsymbol{\eta}\mathbf{l})^2\right] + 27(\eta l)^4,$$
$$B_3 = 64R^3.$$

При $B < 0$ имеется три различных вещественных корня, при $B > 0$ – один вещественный и пара взаимно сопряженных комплексных корней, при $B = 0$ два или все три вещественных корня могут совпадать. Можно доказать следующее полезное тождество:

$$A = B + 27\left[\eta_0(\boldsymbol{\eta}\mathbf{l})R - (\eta l)^2(\mathbf{R}\mathbf{l})\right]^2. \qquad (128)$$

Решение Ферро-Тарталья-Кардано в радикалах.

Корни «неполного» кубического уравнения (127) равны

$$z_0 = a + (A_+ + A_-), \quad z_\pm = a - \frac{1}{2}(A_+ + A_-) \pm i\frac{\sqrt{3}}{2}(A_+ - A_-),$$

где

$$a = \frac{a_2}{3} = -\frac{C_0 + C_1(\mathbf{Rl}) + C_2(\mathbf{Rl})^2 + C_3(\mathbf{Rl})^3}{12\left[(\mathbf{Rl})^2 + \eta_0^2\right]^2},$$

$$A_\pm^3 = -\frac{\mathfrak{q}}{2} \pm \sqrt{\mathfrak{B}} = \frac{\frac{A}{18} \pm i^\delta \left|\eta_0(\boldsymbol{\eta}\mathbf{l})R - (\eta l)^2(\mathbf{Rl})\right| \sqrt{\frac{|B|}{3}}}{96\left[(\mathbf{Rl})^2 + \eta_0^2\right]^3};$$

$$C_0 = -\eta_0^2\left[2R^2 - 2\eta_0^2 - (\boldsymbol{\eta}\mathbf{l})^2\right], \qquad C_1 = -2\eta_0\left[4\eta_0 - 3(\boldsymbol{\eta}\mathbf{l})\right]R,$$

$$C_2 = R^2 - 2(\eta l)\left[5\eta_0 - (\boldsymbol{\eta}\mathbf{l})\right], \qquad C_3 = 4R;$$

$\delta = 0$ при $B \geq 0$ и $\delta = 1$ при $B < 0$. Выражение для $A_\pm$ упрощается, если учесть тождество (128):

$$A_\pm = \frac{\left[3\sqrt{3}\left|\eta_0(\boldsymbol{\eta}\mathbf{l})R - (\eta l)^2(\mathbf{Rl})\right| \pm i^\delta\sqrt{|B|}\right]^{2/3}}{12\left[(\mathbf{Rl})^2 + \eta_0^2\right]}.$$

Решение в тригонометрической форме Виета.

Для полноты приведем также более компактную тригонометрическую форму решения (форму Виета), которая может оказаться более удобной при численных рачетах и во всяком случае полезна для контроля точности вычислений путем сравнения с каноническим решением. Явный вид тригонометрического решения зависит от знака функции B.

Случай $B < 0$. Как уже отмечалось, в этом случае (иногда называемом «неприводимым»), уравнение (127) имеет три вещественных корня:

$$z_0 = a + \zeta_0 \cos\frac{\alpha}{3}, \quad z_\pm = a - \zeta_0 \cos\left(\frac{\alpha \pm \pi}{3}\right),$$

где

$$\zeta_0 = \frac{\left|R^2 + 4R(\mathbf{Rl}) - \eta_0^2 + (\boldsymbol{\eta}\mathbf{l})^2\right|}{6\left[(\mathbf{Rl})^2 + \eta_0^2\right]}, \quad \cos\alpha = -\frac{A}{\left|R^2 + 4R(\mathbf{Rl}) - \eta_0^2 + (\boldsymbol{\eta}\mathbf{l})^2\right|^3}.$$

Случай $B \geq 0$. В этом случае уравнение (127) имеет один вещественный и два комплексных корня. Введем обозначения:

$$\tan\alpha' = \sqrt[3]{\tan\frac{\beta}{2}}, \quad \sin\beta = -\frac{4}{\cos\alpha} = \frac{4}{A}\left|R^2 + 4R(\mathbf{Rl}) - \eta_0^2 + (\boldsymbol{\eta}\mathbf{l})^2\right|^3, \quad |\beta| \leq \frac{\pi}{2}$$

(во всех случаях берется реальное значение кубического корня). Тогда корни равны

$$z_0 = a - \zeta_0 \operatorname{cosec} 2\alpha', \quad z_\pm = a + \frac{\zeta_0}{2}\left(\operatorname{cosec} 2\alpha' \pm i\sqrt{3}\cot 2\alpha'\right), \quad |\alpha'| \leq \frac{\pi}{4}.$$

Корни уравнения (125).

Корни «неполного» уравнения четвертой степени (126) даются комбинациями

$$\Xi_n = \pm\sqrt{z_-} \pm \sqrt{z_0} \pm \sqrt{z_+},$$

в которых четыре из восьми возможных сочетаний знаков выбираются так, чтобы выполнялось условие

$$-\sqrt{z_-}\sqrt{z_0}\sqrt{z_+} = \frac{\widetilde{c}_1}{8} = \frac{D_0 + D_1(\mathbf{Rl}) + D_2(\mathbf{Rl})^2 + D_3(\mathbf{Rl})^3 + D_4(\mathbf{Rl})^4}{8\left[(\mathbf{Rl})^2 + \eta_0^2\right]^3}.$$

Здесь использованы обозначения:

$$\begin{aligned}
D_0 &= \eta_0^3(\boldsymbol{\eta}\mathbf{l})\left(R^2 + \eta_0^2\right), \\
D_1 &= \eta_0^2\left[R^2 - 3\eta_0^2 + 4\eta_0(\boldsymbol{\eta}\mathbf{l}) - 2(\boldsymbol{\eta}\mathbf{l})^2\right] R, \\
D_2 &= \eta_0\left\{2\left[3\eta_0 - (\boldsymbol{\eta}\mathbf{l})\right] R^2 - (\eta l)\left[6\eta_0^2 - 3\eta_0(\boldsymbol{\eta}\mathbf{l}) + (\boldsymbol{\eta}\mathbf{l})^2\right]\right\}, \\
D_3 &= \left[9\eta_0^2 - 8\eta_0(\boldsymbol{\eta}\mathbf{l}) + (\boldsymbol{\eta}\mathbf{l})^2\right] R, \\
D_4 &= 2(\eta l)^2.
\end{aligned}$$

Все четыре корня уравнения (125) могут быть теперь найдены по формуле

$$v_n = \Xi_n - c_3/4 \quad (n = 1, 2, 3, 4).$$

Единственный интересующий нас вещественный неотрицательный корень, соответствующий стационарной точке, должен удовлетворять условию положительности второй производной (54).

Найденные в основном тексте решения для двух противоположных предельных случаев ($1 - v \ll 1$ и $v \sim 1$) могут служить дополнительными критериями единственности решения общего вида, основанного на описанном здесь алгоритме, поскольку они должны гладко «сшиваться» с правильным численным решением при соответствующих вариациях импульсов внешних волновых пакетов и дискретных параметров, определяющих величину эффективной скорости виртуального нейтрино.

19 Stationary point: nonrelativistic case.

Здесь мы изучим частный случай, отвечающий следующей конфигурации внешних импульсов:

$$q_s^0 \sim -q_d^0 \sim m_j \gg |\mathbf{q}_s| \sim |\mathbf{q}_d|. \tag{129}$$

Этот случай представляет потенциальный интерес для экспериментов по поиску (пока гипотетических) тяжелых нейтрино. Удобно переписать (52) в терминах скорости виртуального нейтрино $v_j = |\mathbf{q}_j|/q_0$:

$$\frac{m_j}{\sqrt{1-v_j^2}}\left[R - (\mathbf{Rl})\frac{(1-v_j)^2}{v_j}\right] = Y_0 - \frac{(\mathbf{Yl})}{v_j}, \tag{130}$$

Введем безразмерный 4-вектор $\varrho_j = (\varrho_j^0, \boldsymbol{\varrho}_j)$ с компонентами

$$\varrho_j^\mu = \frac{1}{\mathscr{R}}\left(R_0^\mu - \frac{1}{m_j}Y^\mu\right) \tag{131}$$

Нетрудно видеть, что при выполнении условий (129) эти компоненты малы по абсолютной величине. В самом деле, подставив в определение (131) выражение для 4-вектора Y, которое в покомпонентной записи имеет вид

$$Y^\mu = \widetilde{\Re}_s^{\mu 0} q_s^0 - \widetilde{\Re}_d^{\mu 0} q_d^0 + \widetilde{\Re}_s^{\mu k} q_s^k - \widetilde{\Re}_d^{\mu k} q_d^k,$$

найдем

$$\varrho_j^\mu = \frac{1}{m_j \mathscr{R}} \left[\widetilde{\Re}_s^{\mu 0} \left(m_j - q_s^0 \right) + \widetilde{\Re}_d^{\mu 0} \left(m_j + q_d^0 \right) - \widetilde{\Re}_s^{\mu k} q_s^k + \widetilde{\Re}_d^{\mu k} q_d^k \right]. \tag{132}$$

Поскольку все слагаемые в (132) содержат малые множители ($1 - q_s^0/m_j$, q_s^k/m_j, и т.д.), можно заключить, что $|\varrho_{j\mu}| \ll 1$. Учитывая это, будем искать решение уравнения (130) в виде двойного степенного ряда

$$v_j = \bar{v}_j \left[1 + \sum_{n=1}^{\infty} \sum_{m=0}^{\infty} C_{nm}^{(v)} (\boldsymbol{\varrho}_j \mathbf{l})^n \varrho_{j0}^m \right], \quad \bar{v}_j = \frac{(\boldsymbol{\varrho}_j \mathbf{l})}{1 + \varrho_{j0}}. \tag{133}$$

Выпишем первые шесть безразмерных коэффициентных функций $C_{nm}^{(v)}$:

$$\begin{aligned}
C_{10}^{(v)} &= -\frac{1}{2} C_{11}^{(v)} = 3 C_{12}^{(v)} = \frac{3(\mathbf{Rl})}{2\mathscr{R}}, \\
C_{20}^{(v)} &= \frac{9(\mathbf{Rl})^2}{2\mathscr{R}^2} - \frac{R_{00}}{2\mathscr{R}} + \frac{1}{2}, \\
C_{21}^{(v)} &= -\frac{18(\mathbf{Rl})^2}{\mathscr{R}^2} + \frac{3R_{00}}{2\mathscr{R}} + \frac{3}{2}, \\
C_{30}^{(v)} &= \frac{3(\mathbf{Rl})}{8\mathscr{R}} \left[\frac{45(\mathbf{Rl})^2}{\mathscr{R}^2} - \frac{10R_{00}}{\mathscr{R}} - \frac{23}{3} \right].
\end{aligned} \tag{134}$$

Из (133) и (134) получаем

$$E_j = m_j + \frac{m_j v_j^2}{2} \left(1 + \frac{3}{4} \delta_j + \ldots \right), \quad P_j = m_j v_j \left(1 + \frac{1}{2} \delta_j + \ldots \right). \tag{135}$$

Здесь функция

$$\delta_j = (\boldsymbol{\varrho}_j \mathbf{l})^2 \left[1 + \frac{3(\mathbf{R}\mathbf{l})}{\mathscr{R}} (\boldsymbol{\varrho}_j \mathbf{l}) - \varrho_{j0} \right]$$

определяет величину главных релятивистских поправок, а точками обозначены поправки высших порядков по $(\boldsymbol{\varrho}_j \mathbf{l})$ и ϱ_{j0}. Как видим, нерелятивистское соотношение между эффективными скоростью, энергией и импульсом остаются справедливыми вплоть до второго порядка по $(\boldsymbol{\varrho}_j \mathbf{l})$ и что релятивистские поправки к E_j и P_j положительны.

Ниже будет доказано, что функция $\mathscr{R}$ положительна. Учитывая этот факт нетрудно видеть, что вторая производная (54б) положительна в стационарной точке. Действительно, подставив (133) и (134) в (54б) получим

$$\left. \frac{d^2 F_j(q_0)}{dq_0^2} \right|_{q_0 = E_j} = 2R + \frac{2\mathscr{R}}{\bar{v}_j^2} \left[1 - \frac{6(\mathbf{R}\mathbf{l})}{\mathscr{R}} (\boldsymbol{\varrho}_j \mathbf{l}) + \varrho_{j0} + \ldots \right] > 0. \qquad (136)$$

Возникающая здесь особенность при $\bar{v}_j = 0$ не должна вызывать недоумения, поскольку она лишь подтверждает интуитивное ожидание того, что амплитуда процесса с «покоящимся» нейтрино в промежуточном состоянии должна равняться нулю. Тем не менее, этот случай требует более детального изучения условий применимости метода перевала и теоремы ГС. Эти вопросы будут обсуждаться в отдельной работе.

Обратимся к специальному случаю точного баланса передачи энергии-импульса в вершинах макродиаграммы. Будем использовать следующие обозначения

$$q_s^0 = -q_d^0 \equiv \mathcal{E} > 0, \quad \mathbf{q}_s = -\mathbf{q}_d \equiv \mathcal{P}\mathbf{l}, \quad \mathcal{P} > 0/ \qquad (137)$$

В соответствии с условием (129), примем, что

$$0 \le \mathcal{E}/m_j - 1 \ll 1 \quad \text{и} \quad 0 \le \mathcal{P}/m_j \ll 1.$$

Имеем

$$\varrho_j^\mu = \frac{1}{\mathscr{R}} \left[R_k^\mu l_k \frac{\mathcal{P}}{m_j} - R_0^\mu \left(\frac{\mathcal{E}}{m_j} - 1 \right) \right]$$

и, следовательно,

$$\varrho_{j0} = \frac{(\mathbf{Rl})}{\mathscr{R}} \frac{\mathcal{P}}{m_j} - \frac{R_{00}}{\mathscr{R}} \left(\frac{\mathcal{E}}{m_j} - 1 \right), \quad (\boldsymbol{\varrho}_j \mathbf{l}) = \frac{\mathcal{P}}{m_j} - \frac{(\mathbf{Rl})}{\mathscr{R}} \left(\frac{\mathcal{E}}{m_j} - 1 \right).$$

Подставив найденные соотношения в (133), учитывая (134) и переразложив полученное выражение по степеням двух малых независимых параметров $\mathcal{P}/m_j$ и $\mathcal{E}/m_j - 1$, приходим к следующему выражению для эффективной скорости виртуального нейтрино:

$$v_j = \bar{v}_j \left\{ 1 + \frac{(\mathbf{Rl})}{2\mathscr{R}} \frac{\mathcal{P}}{m_j} + \left[\frac{R_{00}}{\mathscr{R}} - \frac{3(\mathbf{Rl})^2}{2\mathscr{R}^2} \right] \left(\frac{\mathcal{E}}{m_j} - 1 \right) + \dots \right\}, \quad \bar{v}_j = (\boldsymbol{\varrho}_j \mathbf{l}). \tag{138}$$

Из (138) находим эффективную энергию и импульс виртуального нейтрино в лидирующем порядке по $\mathcal{P}/m_j$ и $\mathcal{E}/m_j - 1$:

$$E_j \approx m_j + m_j \bar{v}_j^2/2, \quad P_j \approx m_j \bar{v}_j.$$

Эти простые формулы полностью отвечают интуитивным ожиданиями лишь при $|\mathcal{E}/m_j - 1| \lesssim \mathcal{P}^2/m_j^2$. В этом (и только в этом) частном случае

$$\bar{v}_j \approx \mathcal{P}/m_j, \quad E_j \approx m_j + \mathcal{P}^2/(2m_j) \quad \text{и} \quad P_j \approx \mathcal{P}.$$

20 Stationary point: ultrarelativistic case.

Для иллюстрации общих результатов, полученных в ультрарелятивистском случае, рассмотрим специальную конфигурацию внешних импульсов

$$q_s^0 = -q_d^0 \equiv \mathcal{E} > 0, \quad \mathbf{q}_s = -\mathbf{q}_d \equiv \mathcal{P}\mathbf{l}, \quad \mathcal{P} > 0, \tag{139}$$

отвечающую точному сохранению энергии и импульса, «перетекающих» из S в D.
Будем называть величину $\mathcal{Q}^2 = \mathcal{E}^2 - \mathcal{P}^2$ виртуальностью нейтрино.
Ультрарелятивистский случай определяется условиями $|\mathcal{Q}^2| \ll \mathcal{E}^2$ и $m_j^2 \ll \mathcal{E}^2$, но виртуальность, конечно, не обязана совпадать с m_j^2 даже по порядку величины.
Нетрудно показать, что для конфигурации (139)

$$E_\nu = \mathcal{E}\left[1 + \mathfrak{n}_0\left(1 - \frac{\mathcal{P}}{\mathcal{E}}\right)\right], \quad \mathfrak{n} = \mathfrak{n}_0 - \left(1 - \frac{\mathcal{P}}{\mathcal{E}}\right)\left(\mathfrak{n}_0^2 - \frac{\mathscr{R}}{R}\right)\left[1 + \mathfrak{n}_0\left(1 - \frac{\mathcal{P}}{\mathcal{E}}\right)\right]^{-1},$$

где

$$\mathfrak{n}_0 = \frac{(\mathbf{Rl}) - \mathscr{R}}{R} = \mathfrak{m} - \frac{\mathscr{R}}{R}; \tag{140}$$

Разложив E_ν и $\mathfrak{n}$ по малому параметру $\mathcal{Q}^2/\mathcal{E}^2$, получим:

$$E_\nu = \mathcal{E}\left[1 + \mathfrak{n}_0\frac{\mathcal{Q}^2}{2\mathcal{E}^2}\left(1 + \frac{\mathcal{Q}^2}{2\mathcal{E}^2} + \frac{\mathcal{Q}^4}{8\mathcal{E}^4} + \dots\right)\right],$$

$$\mathfrak{n} = \mathfrak{n}_0 + \left(\mathfrak{m} - \mathfrak{n}_0 - \mathfrak{n}_0^2\right)\frac{\mathcal{Q}^2}{2\mathcal{E}^2}\left[1 - (2\mathfrak{n}_0 - 1)\frac{\mathcal{Q}^2}{4\mathcal{E}^2} + \left(2\mathfrak{n}_0^2 - 2\mathfrak{n}_0 + 1\right)\frac{\mathcal{Q}^4}{8\mathcal{E}^4} + \dots\right],$$

где, как обычно, точками обозначены поправки высших порядков. Т.о. $E_\nu \to \mathcal{E}$ и $\mathfrak{n} \to \mathfrak{n}_0$ при $\mathcal{Q}^2 \to 0$. Переразлагая полученные выше выражения для E_j и P_j по двум малым (независимым) параметрам $\mathcal{Q}^2/\mathcal{E}^2$ и $m_j^2/\mathcal{E}^2$ найдем:

$$E_j = \mathcal{E} + \frac{\mathcal{Q}^2 - m_j^2}{2\mathcal{E}} \left[\mathfrak{n}_0 \left(1 + \frac{\mathcal{Q}^2}{4\mathcal{E}^2} \right) + \left(4\mathfrak{n}_0^2 + 3\mathfrak{n}_0 - 2\mathfrak{m} \right) \frac{m_j^2}{4\mathcal{E}^2} + \ldots \right],$$

$$P_j = \mathcal{P} + \frac{\mathcal{Q}^2 - m_j^2}{2\mathcal{E}} \left[(\mathfrak{n}_0 + 1) \left(1 + \frac{\mathcal{Q}^2}{4\mathcal{E}^2} \right) + \left(4\mathfrak{n}_0^2 + 5\mathfrak{n}_0 - 2\mathfrak{m} + 1 \right) \frac{m_j^2}{4\mathcal{E}^2} + \ldots \right].$$

Отсюда видно, в частности, что эффективная энергия (импульс) нейтрино может быть как меньше, так и больше переданной энергии $\mathcal{E}$ (переданного импульса $\mathcal{P}$); естественно, $E_j = \mathcal{E}$ и $P_j = \mathcal{P}$ при $\mathcal{Q}^2 = m_j^2$ (и только в этом случае). Другими словами, даже при точном балансе переданных 4-импульсов в вершинах диаграммы, эффективный 4-импульс виртуального нейтрино $(E_j, P_j \mathbf{l})$ вообще говоря не совпадает с $(\mathcal{E}, \mathcal{P}\mathbf{l})$. Разложение для эффективной скорости нейтрино имеет вид

$$v_j = 1 - \frac{m_j^2}{2\mathcal{E}^2} \left[1 - \mathfrak{n}_0 \frac{\mathcal{Q}^2}{\mathcal{E}^2} + (4\mathfrak{n}_0 + 1) \frac{m_j^2}{4\mathcal{E}^2} + \ldots \right],$$

так что главная поправка к ультрарелятивистскому пределу $v_j = 1$ не зависит от виртуальности нейтрино.

21 The amplitude: More details.

Выше было доказано, что как в ультрарелятивистском, так и в нерелятивистском случае функция $F_j(q_0)$ имеет *абсолютный минимум* при $q_0 = E_j$; в окрестности минимума она может быть аппроксимирована параболой:

$$F_j(q_0) \simeq F_j(E_j) + \frac{(q_0 - E_j)^2}{2\mathfrak{D}_j^2}. \tag{141}$$

Здесь введена положительно определенная функция

$$\mathfrak{D}_j = \left\{ \left[d^2 F_j(q_0)/dq_0^2 \right]_{q_0 = E_j} \right\}^{-1/2}. \tag{142}$$

В ультрарелятивистском случае, рассмотрением которого мы ограничимся в дальнейшем,

$$\mathfrak{D}_j \simeq \frac{E_\nu}{E_j\sqrt{2R}} \simeq \frac{E_\nu}{\sqrt{2\mathfrak{F}}} \equiv \mathfrak{D}. \tag{143}$$

В рамках сделанных нами приближений эта величина не зависит от j (т.е. универсальна для всех нейтрино) и мала по сравнению с репрезентативной энергией нейтрино ($\mathfrak{D} \ll E_\nu$). Примем теперь во внимание, что в окрестности стационарной точки E_j все множители подынтегрального выражения в правой части (49), за исключением экспоненты

$$\exp\left[-\frac{1}{4} F_j(q_0) - i\left(q_0 T - \sqrt{q_0^2 - m_j^2}\, L \right) \right],$$

являются слабо меняющимися функциями переменной интегрирования q_0 и могут быть поэтому вынесены из под интеграла в точке $q_0 = E_j$. Используя (141) и разложение

$$\sqrt{q_0^2 - m_j^2} = P_j + \frac{1}{v_j}(q_0 - E_j) - \frac{m_j^2}{2P_j^3}(q_0 - E_j)^2 + \ldots$$

мы приходим к следующему простому интегралу:

$$I_j = \int_{-\infty}^{\infty} dq_0 \exp\left[-i\left(E_j T - P_j L\right) + i\left(\frac{L}{v_j} - T\right)(q_0 - E_j) - \right.$$
$$\left. -\frac{1}{4}F_j(E_j) - \left(\frac{1}{8\mathfrak{D}_j^2} + \frac{im_j^2 L}{2P_j^3}\right)(q_0 - E_j)^2\right].$$

Вводя комплекснозначную фазовую функцию

$$\Omega_j(T, L) = i\left(E_j T - P_j L\right) + 2\widetilde{\mathfrak{D}}_j^2\left(\frac{L}{v_j} - T\right)^2, \tag{144}$$

в которой

$$\widetilde{\mathfrak{D}}_j^2 = \frac{\mathfrak{D}_j^2}{1 + i\mathfrak{r}_j} \simeq \frac{\mathfrak{D}^2}{1 + i\mathfrak{r}_j}, \quad \mathfrak{r}_j = \frac{4m_j^2\mathfrak{D}_j^2 L}{P_j^3} \simeq \frac{4m_j^2\mathfrak{D}^2 L}{E_\nu^3}, \tag{145}$$

получаем:

$$I_j = 2\sqrt{2\pi}\widetilde{\mathfrak{D}}_j \exp\left[-\frac{1}{4}F_j(E_j) - \Omega_j(T, L)\right].$$

Комплексная “дисперсия” $\widetilde{\mathfrak{D}}_j$ зависит от эффективной энергии нейтрино и от пространственного расстояния L между прицельными точками в источнике и детекторе;

ее модуль и аргумент даются следующими формулами:

$$|\widetilde{\mathfrak{D}}_j| \simeq \mathfrak{D}\left(1+\mathfrak{r}_j^2\right)^{-1/4}, \quad \arg(\widetilde{\mathfrak{D}}_j) \simeq \frac{1}{2}\arctan\left(\mathfrak{r}_j\right).$$

Собрав все множители, мы получаем следующее окончательное выражение для функции (49):

$$\mathbb{G}^j_{\nu\nu'\mu'\mu}\left(\{\mathbf{p}_\varkappa, x_\varkappa\}\right) = \Delta_{\nu\nu'}(p_j - p_\beta)\hat{p}_j\Delta_{\mu'\mu}(p_j + p_\alpha)|\mathbb{V}_d(p_j)\mathbb{V}_s(p_j)|\frac{\widetilde{\mathfrak{D}}_j e^{-\Omega_j - i\Theta}}{i(2\pi)^{3/2}L}. \qquad (146)$$

Здесь введен 4-вектор $p_j = (E_j, P_j\mathbf{l})$ и опущен вклад, пропорциональный m_j (см. примечание а). Фазовый фактор $-ie^{-i\Theta}$ в (146) несуществен, поскольку он исчезает в квадрате модуля амплитуды.

Благодаря наличию "размазанных" δ-функций $\widetilde{\delta}_s\left(p_j - q_s\right)$ и $\widetilde{\delta}_d\left(p_j + q_d\right)$, входящих в выражения для интегралов перекрытия $\mathbb{V}_s(p_j)$ и $\mathbb{V}_d(p_j)$ и ответственных за приближенное сохранение энергии-импульса $\left(p_j \approx q_s \approx -q_d\right)$, а также предполагаемой малости масс нейтрино по сравнению с репрезентативной энергией E_ν, мы можем положить $m_j = 0$ во всем предэкспоненциальном факторе в правой части (146). Применим теперь тождество

$$P_-\hat{p}_\nu P_+ = P_- u_-(\mathbf{p}_\nu)\overline{u}_-(\mathbf{p}_\nu)P_+$$

(в котором $P_\pm = \frac{1}{2}(1 \pm \gamma_5)$, $\mathbf{p}_\nu = E_\nu\mathbf{l}$, и $u_-(\mathbf{p}_\nu)$ – обычный дираковский биспинор для свободного безмассового лево-спирального нейтрино ν) и определим с его помощью

матричные элементы

$$M_s = \frac{g^2}{8}\overline{u}_-(\mathbf{p}_\nu)\mathcal{J}_s^\mu \Delta_{\mu\mu'}(p_\nu + p_\alpha)O^{\mu'}u(\mathbf{p}_\alpha),$$
$$M_d^* = \frac{g^2}{8}\overline{v}(\mathbf{p}_\beta)O^{\mu'}\Delta_{\mu'\mu}(p_\nu - p_\beta)\mathcal{J}_d^{*\mu}u_-(\mathbf{p}_\nu), \tag{147}$$

описывающие рождение и поглощение *реального* безмассового нейтрино в реакциях $I_s \to F_s'\ell_\alpha^+\nu$ и $\nu I_d \to F_d'\ell_\beta^-$ соответственно[a]. Тогда, с учетом вышеприведенных результатов, мы получаем окончательное выражение для амплитуды (44):

$$\mathcal{A}_{\beta\alpha} = \sum_j \frac{|\mathbb{V}_s(p_j)\mathbb{V}_d(p_j)|M_s M_d^*}{i(2\pi)^{3/2}\mathcal{N}L} V_{\alpha j}^* \widetilde{\mathfrak{D}}_j V_{\beta j}\, e^{-\Omega_j - i\Theta}. \tag{148}$$

Полезно выделить в этой формуле независящий от j общий множитель, ответственный за приближенное сохранение энергии-импульса в вершинах. Для этого, используя явный

[a] При дополнительных условиях $|(p_\nu + p_\alpha)^2| \ll m_W^2$ и $|(p_\nu - p_\beta)^2| \ll m_W^2$, пропагатор W-бозона можно приближенно записать как $-ig_{\mu\nu}/m_W^2$, что соответствует четырехфермионной теории слабого взаимодействия. Тогда, воспользовавшись известным тождеством СМ $g^2/8 = G_F m_W^2/\sqrt{2}$, можно переписать матричные элементы (147) в виде

$$M_s \approx -i\frac{G_F}{\sqrt{2}}\,\overline{u}_-(\mathbf{p}_\nu)\mathcal{J}_s^\mu O_\mu v(\mathbf{p}_\alpha), \quad M_d^* \approx -i\frac{G_F}{\sqrt{2}}\,\overline{u}(\mathbf{p}_\beta)\mathcal{J}_d^{*\mu}O_\mu u_-(\mathbf{p}_\nu).$$

Однако это несколько ограничительное упрощение (неприменимое, в частности, при сверхвысоких энергиях) не является необходимым и не будет использоваться в дальнейшем анализе.

вид “размазанных” δ-функций, запишем

$$\widetilde{\delta}_s(p_j - q_s)\widetilde{\delta}_d(p_j + q_d) = \widetilde{\delta}_s(p_\nu - q_s)\widetilde{\delta}_d(p_\nu + q_d)e^{-\Theta_j},$$

где

$$\begin{aligned}\Theta_j &= \frac{1}{4}\left[2\left(Y_\mu - R_{\mu\mu'}p_\nu^{\mu'}\right) + R_{\mu\mu'}\left(p_\nu - p_j\right)^{\mu'}\right]\left(p_\nu - p_j\right)^{\mu} = \\ &= \frac{1}{2}\left\{E_\nu\left[(\mathbf{Rl}) - R_{00}\right] + Y_0\right\}\left(E_\nu - E_j\right) + \frac{1}{2}\left\{E_\nu\left[(\mathbf{Rl}) - \mathscr{R}\right] - (\mathbf{Yl})\right\}\left(E_\nu - P_j\right) + \\ &\quad + \frac{1}{4}\left[R_{00}\left(E_\nu - E_j\right)^2 - 2(\mathbf{Rl})\left(E_\nu - E_j\right)\left(E_\nu - P_j\right) + \mathscr{R}\left(E_\nu - P_j\right)^2\right].\end{aligned}$$

Тогда амплитуду (148) можно представить в следующем виде:

$$\mathcal{A}_{\beta\alpha} = \frac{|\mathbb{V}_s(p_\nu)\mathbb{V}_d(p_\nu)|M_sM_d^*}{i(2\pi)^{3/2}\mathcal{N}L}\sum_j V_{\alpha j}^*\widetilde{\mathfrak{D}}_j V_{\beta j}\, e^{-\Omega_j - \Theta_j - i\Theta}. \qquad (149)$$

Используя (59) можно представить функцию Θ_j в виде разложения по r_j:

$$\Theta_j = m_j^2 R\left[(\mathfrak{n}_0 - \mathfrak{n}) + \frac{1}{2}\left(\mathfrak{m} - \mathfrak{n} - \mathfrak{n}^2\right)r_j + \left(\mathfrak{n} + \frac{1}{2}\right)\left(\mathfrak{m} - \mathfrak{n} - \mathfrak{n}^2\right)r_j^2 + \mathcal{O}(r_j^3)\right].$$

Напомним, что функция $\mathfrak{n}_0$ определяется согласно (140) и совпадает с $\mathfrak{n}$ в случае точного сохранения энергии-импульса в вершинах (см. раздел 7.12.2). При выполнении принятых нами условий (66) можно написать приближенно:

$$\Theta_j \approx m_j^2 R\left[(\mathfrak{n}_0 - \mathfrak{n}) + \frac{1}{2}\left(\mathfrak{m} - \mathfrak{n} - \mathfrak{n}^2\right)r_j\right],$$

а в окрестности максимума произведения $\widetilde{\delta}_s(p_\nu - q_s)\widetilde{\delta}_d(p_\nu + q_d)$ (т.е. при $q_s \approx -q_d \approx p_\nu$) можно пренебречь и знаконеопределенной разностью $\mathfrak{n}_0 - \mathfrak{n}$. Тогда

$$\Theta_j \approx \frac{m_j^4 R\left(\mathfrak{m} - \mathfrak{n}_0 - \mathfrak{n}_0^2\right)}{4E_\nu^2} = \frac{m_j^4\left[R_{00}\mathscr{R} - (\mathbf{Rl})^2\right]}{4RE_\nu^2}. \tag{150}$$

Ниже мы докажем, что эта величина положительна.

Из вывода формулы (149) и ее структуры видно, что она справедлива не только для рассмотренного класса процессов, но, при соответствующем переопределении матричных элементов (147), и для любых других процессов, идущих за счет обмена виртуальными нейтрино между вершинами макродиаграммы. Нетрудно обобщить формулу (148) и на случай реакций с обменом антинейтрино, для чего следует сделать в ней замену $\mathbf{V} \longmapsto \mathbf{V}^\dagger$ (т.е., $V_{\alpha j}^* \longmapsto V_{\alpha j}$, $V_{\beta j} \longmapsto V_{\beta j}^*$) и должным образом модифицировать матричные элементы (147).

Overlap volumes.

При анализе измеряемых характеристик (таких, например, как скорость счета нейтринных событий в установке) полезно использовать представление для величин $|\mathbb{V}_s(q)|^2$ и $|\mathbb{V}_d(q)|^2$, несколько отличающиеся от того, которое может быть получено в результате непосредственного применения явной формулы для интегралов перекрытия. Удобнее возвратиться к определению этих интегралов и записать $|\mathbb{V}_{s,d}(q)|^2$ в следующем виде:

$$|\mathbb{V}_{s,d}(q)|^2 = \int dx \int dy \, \exp\left[i\left(q_{s,d} \pm q\right)(x-y) - \Upsilon_{s,d}(x) - \Upsilon_{s,d}(y)\right],$$

где

$$\Upsilon_{s,d}(x) = \sum_{\varkappa \in S,D} T_{\varkappa}^{\mu\nu} \left(x_{\varkappa} - x\right)_{\mu} \left(x_{\varkappa} - x\right)_{\nu}, \quad S = I_s \oplus F_s, \quad D = I_d \oplus F_d.$$

После замены переменных интегрирования

$$x = x' + y'/2 \quad \text{и} \quad y = x' - y'/2$$

(с единичным якобианом) последний интеграл можно переписать как

$$|\mathbb{V}_{s,d}(q)|^2 = \int dy' \exp\left[i\left(q_{s,d} \pm q\right)y' - \frac{1}{2}\Re_{s,d}^{\mu\nu} y'_{\mu} y'_{\nu}\right] \int dx' \exp\left[-2\Upsilon_{s,d}(x')\right]. \qquad (151)$$

Вводя обозначения

$$\delta_{s,d}(K) = \int \frac{dx}{(2\pi)^4} \exp\left(iKx - \frac{1}{2}\Re^{\mu\nu}_{s,d} x_\mu x_\nu\right) = \frac{\exp\left(-\frac{1}{2}\widetilde{\Re}^{\mu\nu}_{s,d} K_\mu K_\nu\right)}{(2\pi)^2\sqrt{|\Re_{s,d}|}}, \tag{152}$$

$$\mathrm{V}_{s,d} = \int dx \prod_{\varkappa\in S,D} |\psi_\varkappa(\mathbf{p}_\varkappa, x_\varkappa - x)|^2 = \frac{\pi^2 \exp(-2\mathfrak{S}_{s,d})}{4\sqrt{|\Re_{s,d}|}}, \tag{153}$$

представим (151) в следующей компактной форме:

$$\boxed{|\mathbb{V}_{s,d}(q)|^2 = (2\pi)^4 \delta_{s,d}(q \mp q_{s,d})\,\mathrm{V}_{s,d}.} \tag{154}$$

Функции $\delta_s(K)$ и $\delta_d(K)$ конечно не совпадают с использовавшимися ранее функциями $\widetilde{\delta}_s(K)$ и $\widetilde{\delta}_d(K)$, но имеют тот же самый плосковолновой предел (т.е. $\delta_{s,d}(K) \to \delta(K)$) и подобные же свойства. Физический смысл и свойства симметрии функций (153) очевидны из предыдущего рассмотрения, а их интегральное представление подсказывает, что величины V_s и V_d можно трактовать как 4-мерные объемы перекрытия in- и out-пакетов в источнике и детекторе. Из явного вида этих функций следует, что они принимают максимальные значения,

$$\mathrm{V}^0_{s,d} = \frac{\pi^2}{4\sqrt{|\Re_{s,d}|}},$$

когда классические мировые линии пакетов пересекаются в прицельных точках, что отвечает упоминавшейся выше наглядной картине сталкивающихся (для in-пакетов) или разлетающихся (для out-пакетов) взаимопроникающих облачков.

Microscopic probability.

Теперь, с помощью (148) и формул для четырехмерных объемов перекрытия $\mathrm{V}_{s,d}$ мы получаем выражение для микроскопической вероятности процесса (42)

$$|\mathcal{A}_{\beta\alpha}|^2 = \frac{(2\pi)^4\delta_s(p_\nu - q_s)\mathrm{V}_s|M_s|^2}{\prod_{\varkappa\in S} 2E_\varkappa \mathrm{V}_\varkappa}\ \frac{(2\pi)^4\delta_d(p_\nu + q_d)\mathrm{V}_d|M_d|^2}{\prod_{\varkappa\in D} 2E_\varkappa \mathrm{V}_\varkappa}$$
$$\times \frac{\mathfrak{D}^2}{(2\pi)^3 L^2}\Big|\sum_j V^*_{\alpha j}V_{\beta j}\, e^{-\Omega_j - \Theta_j}\Big|^2, \qquad (155)$$

Это выражение зависит от координат $x_\varkappa$ и средних импульсов $\mathbf{p}_\varkappa$ всех участвующих в реакции волновых пакетов, а также от параметров $\sigma_\varkappa$. Вероятность (155) исчезающе мала, если мало произведение объемов перекрытия

$$\mathrm{V}_s\mathrm{V}_d = \left(\frac{\pi}{2}\right)^4 (|\Re_s||\Re_d|)^{-1/2} \exp\left[-2\left(\mathfrak{S}_s + \mathfrak{S}_d\right)\right],$$

т.е., если in- и out-пакеты в источнике и детекторе не пересекаются в пространственно-временных областях, окружающих прицельные точки X_s и X_d.

Отметим, что и 4-вектор p_ν является функцией $p_\varkappa$ и $\sigma_\varkappa$, причем $p_\nu = q_s = -q_d$ в пределе $\sigma_\varkappa = 0$, $\forall\varkappa$. Поэтому при достаточно малых $\sigma_\varkappa$

$$\delta_s(p_\nu - q_s)\delta_d(p_\nu + q_d) \approx \delta_s(0)\delta_d(0) = (2\pi)^{-4}(|\Re_s||\Re_d|)^{-1/2}.$$

А чем же определяется приближенное равенство q_s и q_d?

Для ответа на этот вопрос преобразуем выражение (155) способом, предложенным Кардаллом[a]. Используя явный вид функций $\delta_{s,d}$ и $\mathfrak{D}$, нетрудно вывести следующее приближенное соотношение

$$2\sqrt{\pi}\mathfrak{D}\delta_s\left(p_\nu - q_s\right)\delta_d\left(p_\nu + q_d\right)F(p_\nu) = \int dE'_\nu \delta_s\left(p'_\nu - q_s\right)\delta_d\left(p'_\nu + q_d\right)F(p'_\nu), \qquad (156)$$

в котором $F(p_\nu)$ – произвольная медленно меняющаяся функция p_ν, а $p'_\nu = (E'_\nu, \mathbf{p}'_\nu) = E'_\nu l$.

Соотношение (156) справедливо с той же точностью, с какой была получена формула (148) для амплитуды, а именно, – с точностью использованного при выводе метода перевала.

С помощью (156) получаем

$$|\mathcal{A}_{\beta\alpha}|^2 = \int dE_\nu \frac{(2\pi)^4\delta_s(p_\nu - q_s)\mathrm{V}_s|M_s|^2}{\prod_{\varkappa\in S}2E_\varkappa \mathrm{V}_\varkappa}\frac{(2\pi)^4\delta_d(p_\nu + q_d)\mathrm{V}_d|M_d|^2}{\prod_{\varkappa\in D}2E_\varkappa \mathrm{V}_\varkappa} \times\frac{\mathfrak{D}}{2\sqrt{\pi}(2\pi)^3L^2}\left|\sum_j V^*_{\alpha j}V_{\beta j}\,e^{-\Omega_j-\Theta_j}\right|^2, \qquad (157)$$

где штрих у "немой" переменной интегрирования E_ν опущен, но теперь она (как и вектор $\mathbf{p}_\nu = E_\nu\mathbf{l}$) уже никак не связана с параметрами внешних пакетов.

[a] C. Y. Cardall, "Coherence of neutrino flavor mixing in quantum field theory," Phys. Rev. D **61** (2000) 073006 [arXiv:hep-ph/9909332].

В рамках сделанных приближений формулы (155) и (157) эквивалентны, но из (157) видно, что закон сохранения энергии-импульса регулируется подынтегральными факторами $\delta_s(p_\nu - q_s)$ и $\delta_d(p_\nu + q_d)$, которые, при достаточно малых $\sigma_\varkappa$, можно заменить обычными δ-функциями.

22 Formulas for the processes $2 \to 2$ and $1 \to 3$.

В этом дополнении мы приведем некоторые громоздкие формулы и технические подробности, полезные для практических расчетов амплитуды макропроцесса, включающего квазиупругое рассеяние виртуального нейтрино в детекторе.

Коэффициенты A_{kl}, B_{kl} и C_{kl}.

Отличные от нуля коэффициенты A_{kl}, B_{kl} $(0 \le k, l \le 2)$ и C_{kl} $(0 \le k, l \le 3)$ фигурирующие в выражениях для функций $|\Re_d|$, $\mathfrak{F}_d(s, Q^2)$ и $\mathfrak{n}_d(s, Q^2)$, относящихся к

рассеянию $2 \to 2$ в детекторе имеют вид

$$
\begin{aligned}
A_{00} &= \sigma_b^2 m_a^2 m_\ell^2 \left[\sigma_a^2\left(\sigma_a^2+\sigma_b^2\right)\left(m_a^2-2m_b^2\right)+\sigma_\ell^2\left(\sigma_b^2+\sigma_\ell^2\right)\left(m_\ell^2-2m_b^2\right)-3\sigma_a^2\sigma_\ell^2 m_b^2\right]+\\
&\quad+\sigma_3^2 m_b^2\left[\sigma_b^2 m_b^2\left(\sigma_a^2 m_\ell^2+\sigma_\ell^2 m_a^2\right)+\sigma_a^2\sigma_\ell^2\left(m_b^4-4m_a^2 m_\ell^2\right)\right],\\
A_{01} &= \sigma_a^2\left\{\sigma_b^2\left[2\sigma_a^2 m_\ell^2\left(m_a^2+m_b^2\right)+\sigma_\ell^2\left(m_b^2+m_\ell^2\right)\left(m_a^2+2m_b^2\right)\right]+\right.\\
&\quad\left.+2\left[\sigma_b^4 m_\ell^2\left(m_a^2+m_b^2\right)+\sigma_\ell^2 m_b^4\left(\sigma_a^2+\sigma_\ell^2\right)\right]\right\},\\
A_{02} &= \sigma_3^2\sigma_a^2\left(\sigma_b^2 m_\ell^2+\sigma_\ell^2 m_b^2\right),\\
A_{10} &= -\sigma_\ell^2\left\{\sigma_b^2\left[\sigma_a^2\left(m_a^2+m_b^2\right)\left(2m_b^2+m_\ell^2\right)+2\sigma_\ell^2 m_a^2\left(m_b^2+m_\ell^2\right)\right]+\right.\\
&\quad\left.+2\left[\sigma_b^4 m_a^2\left(m_b^2+m_\ell^2\right)+\sigma_a^2 m_b^4\left(\sigma_a^2+\sigma_\ell^2\right)\right]\right\},\\
A_{11} &= -\sigma_a^2\sigma_\ell^2\left[\sigma_b^2\left(m_a^2+m_b^2+m_\ell^2\right)+2\sigma_3^2 m_b^2\right],\\
A_{12} &= -\sigma_a^2\sigma_b^2\sigma_\ell^2,\\
A_{20} &= \sigma_3^2\sigma_\ell^2\left(\sigma_a^2 m_b^2+\sigma_b^2 m_a^2\right),\\
A_{21} &= \sigma_a^2\sigma_b^2\sigma_\ell^2;\\
B_{00} &= m_a^2 m_\ell^2\left\{\sigma_b^2\left(m_a^2+m_\ell^2\right)\left[\sigma_a^2\left(m_a^2+m_b^2\right)+\sigma_b^2\left(m_a^2+m_\ell^2\right)+\right.\right.\\
&\quad\left.\left.+\sigma_\ell^2\left(m_b^2+m_\ell^2\right)\right]+m_b^2\left(\sigma_a^4 m_a^2+\sigma_\ell^4 m_\ell^2+\sigma_a^2\sigma_\ell^2 m_b^2\right)\right\},\\
B_{01} &= m_a^2\left\{2\sigma_\ell^4 m_b^2 m_\ell^2+\sigma_\ell^2\left(m_b^2+m_\ell^2\right)\left[\sigma_b^2\left(m_a^2+2m_\ell^2\right)+\sigma_a^2 m_b^2\right]+\right.\\
&\quad\left.+\sigma_b^2 m_\ell^2\left[\sigma_a^2\left(2m_a^2+m_b^2+m_\ell^2\right)+2\sigma_b^2\left(m_\ell^2+m_a^2\right)\right]\right\},\\
B_{02} &= \sigma_3^2 m_a^2\left(\sigma_b^2 m_\ell^2+\sigma_\ell^2 m_b^2\right),\\
B_{10} &= -m_\ell^2\left\{\sigma_\ell^2\left[\sigma_b^2 m_a^2\left(m_a^2+m_b^2+2m_\ell^2\right)+\sigma_a^2 m_b^2\left(m_a^2+m_b^2\right)\right]+\right.\\
&\quad\left.+\sigma_a^2\sigma_b^2\left(m_a^2+m_b^2\right)\left(m_\ell^2+2m_a^2\right)+2m_a^2\left[\sigma_a^4 m_b^2+\sigma_b^4\left(m_\ell^2+m_a^2\right)\right]\right\},
\end{aligned}
$$

Низкоэнергетические пределы функций $\mathfrak{F}_d$ и $\mathfrak{n}_d$.

Пределы функций $\mathfrak{F}_d$ и $\mathfrak{n}_d$ на кинематическом пороге квазиупругой реакции $\nu + b \to b + \ell$ в детекторе имеют следующий вид[a]:

$$\mathfrak{F}_d(s_{\mathsf{th}}, Q^2_{\mathsf{th}}) = \frac{(m_b + m_\ell)^2}{\sigma_b^2 + \sigma_\ell^2} + \frac{m_a^2}{\sigma_a^2}, \quad \mathfrak{n}_d(s_{\mathsf{th}}, Q^2_{\mathsf{th}}) = -\frac{\left(\sigma_b^2 + \sigma_\ell^2\right)\left[(m_b + m_\ell)^2 - m_a^2\right]}{2\left[\sigma_a^2 (m_b + m_\ell)^2 + \sigma_b^2 m_a^2 + \sigma_\ell^2 m_a^2\right]}.$$

Здесь предполагается, что $m_a < m_b + m_\ell$. Пороговые значения величин s и Q^2 равны при этом

$$s_{\mathsf{th}} = (m_b + m_\ell)^2 \quad \text{и} \quad Q^2_{\mathsf{th}} = m_\ell \left(m_b - \frac{m_a^2}{m_b + m_\ell} \right).$$

Для беспороговой реакции ($m_a > m_b + m_\ell$, $s_{\mathsf{th}} = m_a^2$, $Q^2_{\mathsf{th}} = -m_\ell^2$) находим:

$$\mathfrak{F}_d(s_{\mathsf{th}}, Q^2_{\mathsf{th}}) = 0, \quad \mathfrak{n}_d(s_{\mathsf{th}}, Q^2_{\mathsf{th}}) = 1 - \frac{\sigma_3^2\left[2\sigma_a^2 m_b^2 + \sigma_b^2\left(m_a^2 + m_b^2 - m_\ell^2\right)\right]}{2\left[\sigma_a^2\sigma_b^2\left(m_a^2 + m_b^2 - m_\ell^2\right) + \sigma_a^4 m_b^2 + \sigma_b^4 m_a^2\right]}.$$

Таким образом, точное обращение функции $\mathfrak{F}_d$ в нуль возможно только для беспороговой реакции (например, $\nu n \to pe$) при $E_\nu = 0$. Разумеется, этот формальный предел выходит далеко за рамки ультрарелятивистского приближения $E_\nu^2 \gg \max(m_j^2)$, использованного при выводе формул для функций $\mathfrak{F}_d$ и $\mathfrak{n}_d$ и практического значения не имеет, поскольку все современные нейтринные эксперименты работают исключительно с

[a] Все формулы написаны в «ПВ$_0$-пределе», предполагающем точный закон сохранения энергии-импульса в реакции $2 \to 2$ плюс $m_j = 0$, $\forall j$. Кроме того предполагается, если не оговорено противного, что все параметры $\sigma_\varkappa$ отличны от нуля.

пучками ультрарелятивистских нейтрино и антинейтрино[b]. Интересно отметить при этом, что предел $\mathfrak{F}_d$ при $E_\nu = \max(m_j) \equiv m_\nu$ и $Q^2 = -m_\ell^2$ (для беспороговой реакции), который дается выражением

$$\frac{4m_a^2 m_\ell^2 m_\nu^2}{\sigma_3^2 \sigma_a^2 \sigma_b^2 \sigma_\ell^2} \left[\frac{\sigma_a^2 \sigma_b^2 \left(m_a^2 + m_b^2 - m_\ell^2\right) + \sigma_b^4 m_a^2 + \sigma_a^4 m_b^2}{\left(m_a^2 - m_b^2\right)^2 - 2m_\ell^2 \left(m_a^2 + m_b^2\right)^2 + m_\ell^4} \right] \left(\frac{m_a^2}{\sigma_a^2} + \frac{m_b^2}{\sigma_b^2} + \frac{m_\ell^2}{\sigma_\ell^2} \right)^{-1},$$

все еще может быть большим по величине, если по крайней мере два из трех параметров σ_a, σ_b и σ_ℓ малы по сравнению с m_ν.

Высокоэнергетические асимптотики функций $\mathfrak{F}_d$ и $\mathfrak{n}_d$.

В предположении, что $\sigma_{a,b,\ell} \neq 0$ и $Q^2 < \infty$, асимптотическое поведение функций $\mathfrak{F}_d(s, Q^2)$ и $\mathfrak{n}_d(s, Q^2)/s$ при высоких энергиях не зависит от переменной s, а именно:

$$\mathfrak{F}_d(s, Q^2) \underset{s\to\infty}{\sim} \frac{m_a^2}{\sigma_a^2} + \frac{m_b^2}{\sigma_b^2} + \frac{m_\ell^2}{\sigma_\ell^2} - \left(\frac{m_a^2}{\sigma_a^2} + \frac{m_b^2}{\sigma_b^2} \right)^2 \left(\frac{Q^2}{\sigma_3^2} + \frac{m_a^2}{\sigma_a^2} + \frac{m_b^2}{\sigma_b^2} \right)^{-1},$$

$$\mathfrak{n}_d(s, Q^2) \underset{s\to\infty}{\sim} \frac{s}{2\sigma_a^2} \left[\frac{m_a^2}{\sigma_a^2} + \frac{m_b^2}{\sigma_b^2} + \frac{m_\ell^2}{\sigma_\ell^2} + \frac{\sigma_3^2 m_\ell^2}{\sigma_\ell^2 Q^2} \left(\frac{m_a^2}{\sigma_a^2} + \frac{m_b^2}{\sigma_b^2} \right) \right]^{-1}.$$

[b] Здесь уместно напомнить, что более общий анализ, охватывающий нерелятивистский случай представляет потенциальный интерес в контексте изучения возможности детектирования реликтовых нейтрино, а так же для ускорительных и астрофизических экспериментов по поиску гипотетических сверхтяжелых нейтрино и «кэВных» стерильных нейтрино.

Эти асимптотики удовлетворяют следующим неравенствам:

$$\frac{m_\ell^2}{\sigma_\ell^2} < \mathfrak{F}_d(s,Q^2) < \frac{m_a^2}{\sigma_a^2} + \frac{m_b^2}{\sigma_b^2} + \frac{m_\ell^2}{\sigma_\ell^2},$$

$$\frac{\sigma_b^2\sigma_l^2\left(m_b^2 - m_a^2\right)}{2\sigma_3^2\left(\sigma_a^2 m_b^2 + \sigma_b^2 m_a^2\right)} < \mathfrak{n}_d(s,Q^2) < \frac{s}{2m_a^2}\left[1 + \frac{\sigma_a^2}{m_a^2}\left(\frac{m_b^2}{\sigma_b^2} + \frac{m_\ell^2}{\sigma_\ell^2}\right)\right]^{-1},$$

($s \to \infty$, $Q^2 < \infty$), а их предельные значения на кинематических границах таковы:

$$\lim_{s\to\infty} \mathfrak{F}_d(s,Q_-^2) = \frac{m_\ell^2}{\sigma_\ell^2}, \qquad \lim_{s\to\infty} \mathfrak{n}_d(s,Q_-^2) = \frac{\sigma_b^2\left(m_a^2 - m_b^2\right) - \sigma_\ell^2 m_b^2}{2\left(\sigma_a^2 m_b^2 + \sigma_b^2 m_a^2\right)},$$

$$\lim_{s\to\infty} \mathfrak{F}_d(s,Q_+^2) = \frac{m_b^2}{\sigma_b^2}, \qquad \lim_{s\to\infty} \mathfrak{n}_d(s,Q_+^2) = \frac{\sigma_\ell^2\left(m_a^2 - m_\ell^2\right) - \sigma_b^2 m_\ell^2}{2\left(\sigma_a^2 m_\ell^2 + \sigma_\ell^2 m_a^2\right)}.$$

Эти величины, как видим, симметричны по отношению к замене индексов $b \longleftrightarrow \ell$. Пороговые значения $\mathfrak{n}_d(s,Q_\pm^2)$ обращаются в нуль при специфических соотношениях между параметрами $\sigma_\varkappa$ и массами. В этих экзотических случаях нужно учесть следующие ($\sim 1/s$) поправки.

В частном случае, когда частица-мишень a есть нуклон, из динамических соображений следует, что при высокой энергии нейтрино средний угол рассеяния в с.ц.м., $\langle\theta_*\rangle$, равен по порядку величины обратному лоренцевскому фактору лептона $\Gamma_\ell^* = E_\ell^*/m_\ell$. Поэтому $\langle Q^2\rangle \sim m_\ell^2$ и $\langle\theta\rangle \sim m_\ell/\sqrt{s}$, где θ есть угол рассеяния лептона в л.с. (совпадающей с с.с.о. нуклона). Можно показать, что соответствующие асимптотики функций $\mathfrak{F}_d$ и $\mathfrak{n}_d$

имеют вид

$$\mathfrak{F}_d\left(s,m_\ell^2\right) \underset{s\to\infty}{\sim} \frac{m_\ell^2}{\sigma_\ell^2}\left[1+\frac{\sigma_\ell^2}{\sigma_3^2}\left(\frac{m_a^2}{\sigma_a^2}+\frac{m_b^2}{\sigma_b^2}\right)\left(\frac{m_a^2}{\sigma_a^2}+\frac{m_b^2}{\sigma_b^2}+\frac{m_\ell^2}{\sigma_3^2}\right)^{-1}\right] < 2\frac{m_\ell^2}{\sigma_\ell^2},$$

$$\mathfrak{n}_d\left(s,m_\ell^2\right) \underset{s\to\infty}{\sim} \frac{\sigma_b^2\sigma_\ell^2 s}{2\left[\left(\sigma_b^2 m_a^2+\sigma_a^2 m_b^2\right)\left(\sigma_a^2+\sigma_b^2+2\sigma_\ell^2\right)+\sigma_a^2\sigma_b^2 m_\ell^2\right]} < \frac{E_\nu}{2m_a}.$$

Поскольку при высоких энергиях существенный вклад в скорость счета квазиупругих событий дает лишь узкая область углов, близких к $\theta = \langle\theta\rangle$, можно заключить, что эффективное асимптотическое значение $\mathfrak{F}_d$ является практически константой, которая определяется в основном величиной дисперсии импульса лептонного волнового пакета, σ_ℓ. При этом произвольные[c] вариации параметров σ_a и σ_b могут изменить асимптотику лишь в пределах фактора 2.

Асимптотическое поведение $\mathfrak{F}_d(s,Q^2)$ резко изменяется, если один (и только один) из параметров $\sigma_{\varkappa}$ обращается в нуль. При этом, в случае $\sigma_a = 0$ или $\sigma_b = 0$ асимптотика не зависит от s:

$$\mathfrak{F}_d(s,Q^2) \underset{s\to\infty}{\longrightarrow} \begin{cases} \dfrac{Q^2}{\sigma_b^2+\sigma_\ell^2}+\dfrac{m_\ell^2}{\sigma_\ell^2}, & \text{при } \sigma_a = 0, \\ \dfrac{Q^2}{\sigma_a^2+\sigma_\ell^2}+\dfrac{m_\ell^2}{\sigma_\ell^2}, & \text{при } \sigma_b = 0, \end{cases}$$

[c] Не нарушающие, разумеется, условия применимости модели СРГП.

а при $\sigma_\ell = 0$ квадратично растет с s:

$$\mathfrak{F}_d(s, Q^2) \underset{s\to\infty}{\sim} \frac{\left(\dfrac{Q^2}{\sigma_a^2+\sigma_b^2} + \dfrac{m_a^2}{\sigma_a^2} + \dfrac{m_b^2}{\sigma_b^2}\right) s^2}{\left(Q^2 + m_a^2 + m_b^2\right)^2 - 4m_a^2 m_b^2}, \quad \text{при } \sigma_\ell = 0.$$

Некоторые свойства функции $\mathfrak{F}_d$ становятся более прозрачными если записать ее в терминах переменных E_ν и θ_*. Рассмотрим асимптотическое разложение $\mathfrak{F}_d$ при $E_\nu \to \infty$ и фиксированном значении угла θ_*. Для не слишком малых значений $\sin\theta_*$ она может быть записана как

$$\begin{aligned}\mathfrak{F}_d(E_\nu, \theta_*) = \frac{m_a^2}{\sigma_a^2} + \frac{m_b^2}{\sigma_b^2} + \frac{m_\ell^2}{\sigma_\ell^2} - \frac{a_1\sigma_3^2}{2m_a E_\nu \sin^2\theta_*} \Bigg\{ \Bigg[\left(\frac{m_b^2}{\sigma_b^2} + \frac{m_\ell^2}{\sigma_\ell^2}\right)\cos\theta_* \; + \\ + \left(\frac{m_b^2\sigma_\ell^2 - m_\ell^2\sigma_b^2}{m_\ell^2\sigma_b^2 + m_b^2\sigma_\ell^2}\right)\left(\frac{2m_a^2}{\sigma_a^2} + \frac{m_b^2}{\sigma_b^2} + \frac{m_\ell^2}{\sigma_\ell^2}\right)\Bigg]^2 + \\ + \left(\frac{4m_a m_b m_\ell}{\sigma_a\sigma_b\sigma_\ell}\right)^2 \left(\frac{m_b^2}{\sigma_b^2} + \frac{m_\ell^2}{\sigma_\ell^2}\right)^{-2} \left(\frac{m_a^2}{\sigma_a^2} + \frac{m_b^2}{\sigma_b^2} + \frac{m_\ell^2}{\sigma_\ell^2}\right)\Bigg\} + \frac{1}{\sin^4\theta_*}\cdot\mathcal{O}\left(\frac{m_a^2}{E_\nu^2}\right).\end{aligned}$$

При $\sin\theta_* = 0$ получаем:

$$\mathfrak{F}_d(E_\nu, 0) = \frac{m_\ell^2}{\sigma_\ell^2}\left[1 - \frac{m_a^2 - m_b^2}{m_a E_\nu} + \mathcal{O}\left(\frac{m_a^2}{E_\nu^2}\right)\right],$$

$$\mathfrak{F}_d(E_\nu, \pi) = \frac{m_b^2}{\sigma_b^2}\left[1 - \frac{m_a^2 - m_\ell^2}{m_a E_\nu} + \mathcal{O}\left(\frac{m_a^2}{E_\nu^2}\right)\right].$$

Как отмечалось выше, при высоких энергиях $\langle\theta_*\rangle \sim \Gamma_\ell^* = E_\ell^*/m_\ell$. Можно показать, что соответствующее асимптотическое разложение имеет вид

$$\mathfrak{F}_d(E_\nu, \theta_* = 1/\Gamma_\ell^*) = \frac{m_\ell^2}{\sigma_\ell^2}\left[b_0 - \frac{b_1\sigma_3^2}{m_a(b_0-1)^2E_\nu} + \mathcal{O}\left(\frac{m_a^2}{E_\nu^2}\right)\right],$$

где

$$b_0 = 1 + \frac{\sigma_\ell^2\left(m_b^2\sigma_a^2 + m_a^2\sigma_b^2\right)}{\sigma_3^2\left(m_b^2\sigma_a^2 + m_a^2\sigma_b^2\right) + m_\ell^2\sigma_a^2\sigma_b^2},$$

$$\begin{aligned} b_1 = {} & 8\sigma_\ell^2\left(m_b^2\sigma_a^2 + m_a^2\sigma_b^2\right)^3\left[m_b^2\left(m_a^2 - m_b^2 + \frac{1}{3}m_\ell^2\right)\sigma_a^2 + m_a^2\left(m_a^2 - m_b^2 + \frac{4}{3}m_\ell^2\right)\sigma_b^2\right] + \\ & + 2\sigma_\ell^2\left(m_b^2\sigma_a^2 + m_a^2\sigma_b^2\right)\left[m_b^2\sigma_a^4 + \left(m_a^2 + m_b^2 + m_\ell^2\right)\sigma_a^2\sigma_b^2 + m_a^2\sigma_b^4\right] \times \\ & \times \left[m_b^2\left(m_a^2 - m_b^2 - m_\ell^2\right)\sigma_a^2 + m_a^2\left(m_a^2 - m_b^2 + m_\ell^2\right)\sigma_b^2\right]. \end{aligned}$$

Отсюда видно, что эффективное асимптотическое значение $\mathfrak{F}_d(E_\nu, \theta_*)$ практически постоянно и, учитывая что $1 < b_0 < 2$, его величина определяется в основном дисперсией импульса лептонного пакета.

Случай сильной иерархии.

Функция $\mathfrak{F}_d(s, Q^2)$ значительно упрощается в случае сильной иерархии между величинами параметров σ_a, σ_b и σ_ℓ. Вычисляя соответствующие последовательные

пределы, находим:

$$\mathfrak{F}_d(s,Q^2) \approx \begin{cases} \dfrac{\left(Q^2+m_\ell^2\right)^2}{\left(s-Q^2-m_b^2\right)^2-4m_a^2m_\ell^2}\left(\dfrac{m_a}{\sigma_a}\right)^2, & \text{при } \sigma_\ell \gg \sigma_a \gg \sigma_b, \\ \dfrac{\left(Q^2+m_\ell^2\right)^2}{\left(s-m_b^2-m_\ell^2\right)^2-4m_b^2m_\ell^2}\left(\dfrac{m_b}{\sigma_b}\right)^2, & \text{при } \sigma_\ell \gg \sigma_b \gg \sigma_a, \\ \dfrac{\left(s-m_a^2\right)^2}{\left(Q^2+m_a^2+m_b^2\right)^2-4m_a^2m_b^2}\left(\dfrac{m_b}{\sigma_b}\right)^2, & \text{при } \sigma_a \gg \sigma_b \gg \sigma_\ell, \\ \dfrac{\left(s-m_a^2\right)^2}{\left(s-Q^2-m_b^2\right)^2-4m_a^2m_\ell^2}\left(\dfrac{m_\ell}{\sigma_\ell}\right)^2, & \text{при } \sigma_a \gg \sigma_\ell \gg \sigma_b, \\ \dfrac{\left(s-Q^2-m_a^2-m_\ell^2\right)^2}{\left(s-m_b^2-m_\ell^2\right)^2-4m_b^2m_\ell^2}\left(\dfrac{m_\ell}{\sigma_\ell}\right)^2, & \text{при } \sigma_b \gg \sigma_\ell \gg \sigma_a, \\ \dfrac{\left(s-Q^2-m_a^2-m_\ell^2\right)^2}{\left(Q^2+m_a^2+m_b^2\right)^2-4m_a^2m_b^2}\left(\dfrac{m_a}{\sigma_a}\right)^2, & \text{при } \sigma_b \gg \sigma_a \gg \sigma_\ell. \end{cases}$$

Отсюда видно, в частности, что ни наибольший, ни наименьший из трех параметров $\sigma_\varkappa$ не влияет на форму и величину функции $\mathfrak{F}_d(s,Q^2)$. Это нетривиальное свойство можно обобщить на случай процессов с произвольным числом частиц в конечном состоянии. При этом, в случае сильной иерархии дисперсий $\sigma_\varkappa$, единственным существенным параметром является вторая по величине дисперсия после наибольшей из них. Этот факт очень полезен при анализе многочастичных процессов (с числом внешних пакетов

> 2), поскольку позволяет рассматривать пакеты с очень малыми (по сравнению с остальными) $\sigma_{\varkappa}$ как плоские волны. В частности, значительно упрощается расчет радиационных поправок с плосковолновыми фотонами во внешних линиях фейнмановских диаграмм, поскольку он может проводиться с использованием стандартных методов КТП. Напомним, что учет петлевых электрослабых поправок не приводит к дополнительным вычислительным усложнениям, связанным с пакетным формализмом, поскольку все они формально включены в соответствующие матричные элементы и никак не связаны с характеристиками внешних in- и out-состояний. По соглашению калибровочные бозоны так же не могут фигурировать в качестве внешних линий диаграмм.

Коэффициенты A'_{kl}, B'_{kl} и C'_{kl}.

Отличные от нуля коэффициенты A'_{kl} и B'_{kl} $(0 \le k,l \le 2)$, фигурирующие в выражениях для функций $|\Re_s|$ и $\mathfrak{F}_s(s,Q^2)$ для 3-частичного распада имеют вид

$$
\begin{aligned}
A'_{00} &= \sigma_\ell^2 \left[\sigma_a^2 m_b^2 \left(\sigma_a^2+\sigma_\ell^2\right)\left(m_a^2-m_\ell^2\right)^2 + \sigma_b^2 m_a^2 \left(\sigma_b^2+\sigma_\ell^2\right)\left(m_b^2-m_\ell^2\right)^2\right] + \\
&\quad + \sigma_a^2\sigma_b^2 m_\ell^2 \left\{\sigma_\ell^2\left[m_\ell^2\left(m_a^2+m_b^2+m_\ell^2\right) - 7m_a^2m_b^2\right] + \left(\sigma_a^2+\sigma_b^2\right)\left(m_\ell^4-4m_a^2m_b^2\right)\right\}, \\
A'_{01} &= -\sigma_a^2\left\{\sigma_b^2\left[\sigma_\ell^2\left(m_b^2+m_\ell^2\right)\left(m_a^2+2m_\ell^2\right) + 2m_\ell^4\left(\sigma_a^2+\sigma_b^2\right)\right] + \right. \\
&\quad \left. + 2\sigma_\ell^2 m_b^2\left(m_\ell^2+m_a^2\right)\left(\sigma_a^2+\sigma_\ell^2\right)\right\}, \\
A'_{02} &= \sigma_3^2\sigma_a^2\left(\sigma_b^2 m_\ell^2 + \sigma_\ell^2 m_b^2\right), \\
A'_{10} &= -\sigma_b^2\left\{\sigma_a^2\left[\sigma_\ell^2\left(m_\ell^2+m_a^2\right)\left(2m_\ell^2+m_b^2\right) + 2m_\ell^4\left(\sigma_a^2+\sigma_b^2\right)\right] + \right. \\
&\quad \left. + 2\sigma_\ell^2 m_a^2\left(\sigma_b^2+\sigma_\ell^2\right)\left(m_\ell^2+m_b^2\right)\right\}, \\
A'_{11} &= \sigma_a^2\sigma_b^2\left[\sigma_\ell^2\left(m_a^2+m_b^2+m_\ell^2\right) + 2\sigma_3^2 m_\ell^2\right], \\
A'_{12} &= -\sigma_a^2\sigma_b^2\sigma_\ell^2, \\
A'_{20} &= \sigma_3^2\sigma_b^2\left(\sigma_a^2 m_\ell^2 + \sigma_\ell^2 m_a^2\right), \\
A'_{21} &= -\sigma_a^2\sigma_b^2\sigma_\ell^2; \\
B'_{00} &= m_a^2 m_b^2\left\{\sigma_\ell^2\left(m_a^2+m_b^2\right)\left[\sigma_a^2\left(m_a^2+m_\ell^2\right) + \sigma_b^2\left(m_b^2+m_\ell^2\right) + \sigma_\ell^2\left(m_a^2+m_b^2\right)\right] + \right. \\
&\quad \left. + m_\ell^2\left(\sigma_a^4 m_a^2 + \sigma_b^4 m_b^2 + \sigma_a^2\sigma_b^2 m_b^2\right)\right\}, \\
B'_{01} &= -m_a^2\left\{\sigma_a^2\left[\sigma_b^2 m_\ell^2\left(m_b^2+m_\ell^2\right) + \sigma_\ell^2 m_b^2\left(2m_a^2+m_b^2+m_\ell^2\right)\right] + \right. \\
&\quad \left. + 2m_b^2\left[\sigma_b^4 m_\ell^2 + \sigma_\ell^4\left(m_a^2+m_b^2\right)\right] + \sigma_b^2\sigma_\ell^2\left(m_b^2+m_\ell^2\right)\left(m_a^2+2m_b^2\right)\right\}, \\
B'_{02} &= \sigma_a^2 m_b^2\left(\sigma_b^2 m_\ell^2 + \sigma_\ell^2 m_b^2\right),
\end{aligned}
$$

Случай сильной иерархии.

Подобно случаю рассеяния $2 \to 2$, функция $\mathfrak{F}_s(s_1, s_2)$ становится особенно простой при сильной иерархии между параметрами σ_a, σ_b и σ_ℓ:

$$\mathfrak{F}_s(s_1,s_2) \approx \begin{cases} \dfrac{\left(s_1+s_2-m_a^2-m_b^2\right)^2}{\left(s_2-m_a^2-m_\ell^2\right)^2-4m_a^2m_\ell^2}\left(\dfrac{m_a}{\sigma_a}\right)^2, & \text{при } \sigma_\ell \gg \sigma_a \gg \sigma_b, \\ \dfrac{\left(s_1+s_2-m_a^2-m_b^2\right)^2}{\left(s_1-m_b^2-m_\ell^2\right)^2-4m_b^2m_\ell^2}\left(\dfrac{m_b}{\sigma_b}\right)^2, & \text{при } \sigma_\ell \gg \sigma_b \gg \sigma_a, \\ \dfrac{\left(s_1-m_a^2\right)^2}{\left(s_1+s_2-m_\ell^2\right)^2-4m_a^2m_b^2}\left(\dfrac{m_b}{\sigma_b}\right)^2, & \text{при } \sigma_a \gg \sigma_b \gg \sigma_\ell, \\ \dfrac{\left(s_1-m_a^2\right)^2}{\left(s_2-m_a^2-m_\ell^2\right)^2-4m_a^2m_\ell^2}\left(\dfrac{m_\ell}{\sigma_\ell}\right)^2, & \text{при } \sigma_a \gg \sigma_\ell \gg \sigma_b, \\ \dfrac{\left(s_2-m_b^2\right)^2}{\left(s_1-m_b^2-m_\ell^2\right)^2-4m_b^2m_\ell^2}\left(\dfrac{m_\ell}{\sigma_\ell}\right)^2, & \text{при } \sigma_b \gg \sigma_\ell \gg \sigma_a, \\ \dfrac{\left(s_2-m_b^2\right)^2}{\left(s_1+s_2-m_\ell^2\right)^2-4m_a^2m_b^2}\left(\dfrac{m_a}{\sigma_a}\right)^2, & \text{при } \sigma_b \gg \sigma_a \gg \sigma_\ell. \end{cases}$$

Из этих формул видно, что ни наибольший, ни наименьший из параметров не влияют на величину и форму функции $\mathfrak{F}_s(s_1, s_2)$.

23 Complex error function and related formulas.

The error and complementary error functions of complex argument were studied in a number of works. Here we reproduce the well-known series expansions and asymptotic expansion:

$$\mathrm{erf}(z) = \frac{2}{\sqrt{\pi}} \sum_{n=0}^{\infty} \frac{(-1)^n z^{2n+1}}{(2n+1)n!} = \frac{2}{\sqrt{\pi}} e^{-z^2} \sum_{n=0}^{\infty} \frac{2^n z^{2n+1}}{(2n+1)!!}, \tag{158}$$

$$\mathrm{erfc}(z) \sim \frac{e^{-z^2}}{\sqrt{\pi} z} \left[1 + \sum_{n=1}^{\infty} \frac{(-1)^n (2n-1)!!}{(2z^2)^n} \right] \quad \left(z \to \infty, \ \ |\arg z| < \frac{3\pi}{4} \right). \tag{159}$$

Using these formulas, one obtains the expansions

$$\mathrm{ierf}(z) = \frac{1}{\sqrt{\pi}} \left[1 + z^2 - \frac{z^4}{6} + \frac{z^6}{30} - \frac{z^8}{168} + \mathcal{O}\left(z^{10}\right) \right], \tag{160a}$$

$$= \frac{e^{-z^2}}{\sqrt{\pi}} \left[1 + 2z^2 + \frac{4z^4}{3} + \frac{8z^6}{15} + \frac{16z^8}{105} + \mathcal{O}\left(z^{10}\right) \right], \tag{160b}$$

which are useful for, respectively, small and intermediate $|z|$.[a] To obtain the asymptotics of $\mathrm{erfc}(z)$ [and thus of $\mathrm{ierf}(z)$] at large $|z|$ and $|\arg z| > 3\pi/4$, one has to apply Eq. (159) to $\mathrm{erfc}(-z)$ and then use the rule $\mathrm{erfc}(z) = 2 - \mathrm{erfc}(-z)$. As a result, we find:

$$\mathrm{ierf}(z) \sim \pm z + \frac{e^{-z^2}}{2\sqrt{\pi} z^2} \left[1 - \frac{3}{2z^2} + \frac{15}{4z^4} - \frac{105}{8z^6} + \mathcal{O}\left(\frac{1}{z^8}\right) \right] \quad (z \to \infty), \tag{161}$$

[a] In practice, Eqs. (160a) and (160b) are fruitful for $|z| \lesssim 1$ and $1 \lesssim |z| \lesssim 4.5$, respectively.

where the upper (lower) sign must be taken for $|\arg z| < 3\pi/4$ ($|\arg z| > 3\pi/4$).

The subsequent formulas can be used for numerical evaluation of the error function with high accuracy. They are based on the following integral representation of $\mathrm{erfc}(z)$:

$$\mathrm{erfc}(z) = \frac{2z}{\pi}\int_0^\infty \frac{dt\, e^{-t^2}}{t^2+z^2} = \frac{z}{\pi}\int_{-\infty}^\infty \frac{dt\, e^{-t^2}}{t^2+z^2}.$$

From this equation one obtains

$$\begin{aligned}\mathrm{Re}\left[\mathrm{erfc}(a+ib)\right] = {} & \frac{r}{\pi}\exp\left[-r^2\cos(2\omega)\right]\left[r^2\cos(2ab+\omega)\mathscr{I}_0(a,b)\right. \\ & \left.+\cos(2ab-\omega)\mathscr{I}_2(a,b)\right], \qquad (162a)\\ \mathrm{Im}\left[\mathrm{erfc}(a+ib)\right] = {} & -\frac{r}{\pi}\exp\left[-r^2\cos(2\omega)\right]\left[r^2\sin(2ab+\omega)\mathscr{I}_0(a,b)\right. \\ & \left.+\sin(2ab-\omega)\mathscr{I}_2(a,b)\right], \qquad (162b)\end{aligned}$$

where

$$\mathscr{I}_n(a,b) = \int_{-\infty}^\infty \frac{dt\, t^n e^{-t^2}}{(t^2+a^2-b^2)^2+4a^2b^2} = \int_{-\infty}^\infty \frac{dt\, t^n e^{-t^2}}{\left[t^2+r^2\cos(2\omega)\right]^2+r^2\sin(2\omega)}, \qquad (163)$$

$$r = \sqrt{a^2+b^2},\ \ \cos\omega = a/r,\ \ \sin\omega = b/r;$$

all the quantities now being real. Note that the integrands in Eqs. (163) are positive and nonsingular (except for the trivial case $r = 0$), and quickly decay for large value of $|t|$. These properties allow accurate numerical integration based on standard quadrature rules.

24 Spatial integration.

The integration over $\mathbf{x}$ and $\mathbf{y}$ in the event rate integral is performed over the explored volume of the source and over the detector fiducial volume, respectively. Here we restrict ourselves to the simplest (while not very realistic) example of homogeneous source and detector. It implies that the density functions $\overline{f}_a(\mathbf{p}_a, s_a; \mathbf{x})$ do not depend of $\mathbf{x}$ within the source and detector volumes (and vanish outside these volumes). Thus our concern is only with the L-dependent factor $e^{\Phi_{ij}}/L^2$. Below we will also assume that the detector dimensions are negligibly small in comparison with these of the source, which are in turn small in comparison with the mean distance between the source and detector.

We place the origin of the coordinate system at an internal point of the detector (point O_d in Figure) and direct the z-axis along the unit vector $-\mathbf{l}$ that is to the interior of the source. Then $\mathbf{x} = L\mathbf{l}$, $L = O_sO_d$, and the source volume integral we are interested in can be written as

$$\mathcal{J}_{ij} \equiv \int_{\mathrm{V}_s} \frac{d\mathbf{x}}{L^2}\, e^{\Phi_{ij}(L)} = \int_{\Omega_s} d\mathbf{\Omega} \int_{L^N_{\mathbf{\Omega}}}^{L^F_{\mathbf{\Omega}}} dL\, e^{\Phi_{ij}(L)}.$$

Here V_s is the explored volume of the source, Ω_s is the solid angle under which this volume is seen from the origin O_d, $L^N_{\mathbf{\Omega}}$ and $L^F_{\mathbf{\Omega}}$ are, respectively, the distances from O_d to the near and far boundaries of the source for the given direction $\mathbf{\Omega} = (\sin\phi\sin\theta, \cos\phi\sin\theta, \cos\theta)$.

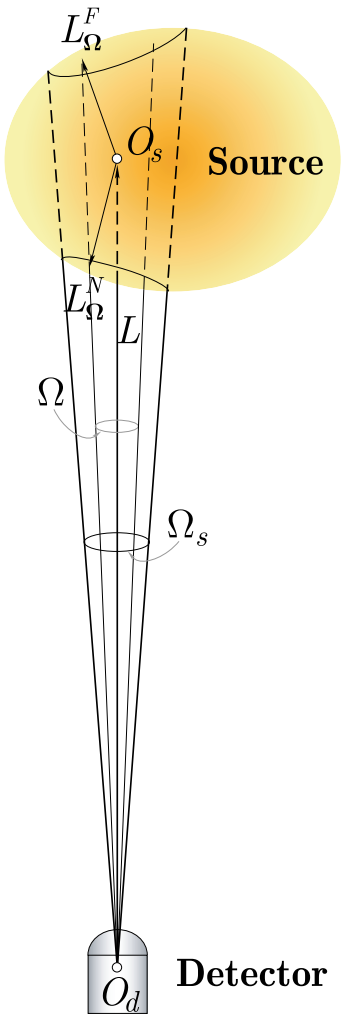

We may define the conventional distance between the source and detector as

$$\overline{L} = \frac{1}{2\Omega_s} \int_{\Omega_s} d\mathbf{\Omega} \left(L^F_{\mathbf{\Omega}} + L^N_{\mathbf{\Omega}} \right).$$

By way of avoiding misapprehension, we remark that, depending on the angular resolution of the detector, the solid angle Ω_s can be either smaller than or equal to the overall solid angle of the whole source machine; for instance, only a segment of the sun or atmosphere could be considered as the neutrino source. [Figure schematically illustrates the first possibility while the above equation for $\mathcal{J}_{ij}$ is valid in both cases.] Next, the smallness of Ω_s does not yet ensure the smallness of the source itself; a collimated accelerator beam provides a good counter-example.

The elementary integration over L yields

$$\mathcal{J}_{ij} = \frac{E_\nu L_{ij}}{4\sqrt{\pi} D} \int_{\Omega_s} d\mathbf{\Omega} \left[\mathrm{erf} \left(\frac{2\pi D L^F_{\mathbf{\Omega}}}{E_\nu L_{ij}} - \frac{i E_\nu}{2D} \right) - \mathrm{erf} \left(\frac{2\pi D L^N_{\mathbf{\Omega}}}{E_\nu L_{ij}} - \frac{i E_\nu}{2D} \right) \right] \times \exp \left[- \frac{2E_\nu^2 + (\Delta E_{ij})^2}{8D^2} \right] \quad (i \neq j), \tag{164a}$$

$$\mathcal{J}_{jj} = \int_{\mathrm{V}_s} \frac{d\mathbf{x}}{L^2} = \int_{\Omega_s} d\mathbf{\Omega} \left(L^F_{\mathbf{\Omega}} - L^N_{\mathbf{\Omega}} \right). \tag{164b}$$

These formulas may be of some utility in processing the data from "short baseline" neutrino experiments, in which the distance from the source (e.g., the pion decay channel of a neutrino factory) to detector is comparable in magnitude with the longitudinal dimension of the source.

In case of an "ideal" experiment, for which we accept that

$$r_N = \max_{\mathbf{\Omega}\in\Omega_s}\left(\overline{L} - L^N_{\mathbf{\Omega}}\right) \ll \overline{L} \quad \text{and} \quad r_F = \max_{\mathbf{\Omega}\in\Omega_s}\left(L^F_{\mathbf{\Omega}} - \overline{L}\right) \ll \overline{L}, \tag{165}$$

we can try to apply the following expansion of the probability integral:

$$\mathrm{erf}(z+\delta) \approx \mathrm{erf}(z) + \frac{2\delta}{\sqrt{\pi}} e^{-z^2}[1 - z\delta + \frac{2}{3}(2z^2-1)\delta^2 + \ldots]. \tag{166}$$

The $\mathcal{O}(\delta^2)$ and $\mathcal{O}(z^2\delta^2)$ terms of this expansion can be neglected by assuming that $|\delta| \ll 1$ and $|z\delta| \ll 1$. In our case, the first condition reads

$$\frac{2\pi D r_{N,F}}{E_\nu L_{ij}} \ll 1, \tag{167}$$

while the second one is found to be unnecessary owing to an approximate cancellation of the second-order terms. Indeed, by applying Eq. (166) we obtain

$$\mathcal{J}_{ij} \approx \int_{\Omega_s} d\mathbf{\Omega}\left(L^F_{\mathbf{\Omega}} - L^N_{\mathbf{\Omega}}\right) e^{\Phi_{ij}(\overline{L})}\left\{1 - \Delta_{\mathbf{\Omega}}\left[\frac{2i\pi\overline{L}}{L_{ij}} - \left(\frac{2\pi D\overline{L}}{E_\nu L_{ij}}\right)^2\right]\right\},$$

$$\Delta_{\mathbf{\Omega}} = 2\left(1 - \frac{L^N_{\mathbf{\Omega}} + L^F_{\mathbf{\Omega}}}{2\overline{L}}\right) = \frac{L^F_{\mathbf{\Omega}} - \overline{L}}{\overline{L}} - \frac{\overline{L} - L^N_{\mathbf{\Omega}}}{\overline{L}}.$$

Evidently $|\Delta_{\mathbf{\Omega}}| \ll 1$. Then by assuming that

$$\max_{\mathbf{\Omega}\in\Omega_s} \Delta_{\mathbf{\Omega}}\left[\left(\frac{2\pi D\overline{L}}{E_\nu L_{ij}}\right)^4 + \left(\frac{2\pi\overline{L}}{L_{ij}}\right)^2\right]^{1/2} \ll 1, \tag{168}$$

we arrive at the result (already valid for any i and j)

$$\mathcal{J}_{ij} \approx e^{\Phi_{ij}(\overline{L})} \int_{\Omega_s} d\mathbf{\Omega} \left(L^F_{\mathbf{\Omega}} - L^N_{\mathbf{\Omega}} \right) \approx \mathrm{V}_s \frac{e^{\Phi_{ij}(\overline{L})}}{\overline{L}^2}, \tag{169}$$

suspected from the mean-value theorem however supplemented with the nontrivial sufficient conditions for its validity (165), (167), and (168). The volume V_s in Eq. (169) has been estimated (with the same accuracy) to be

$$\mathrm{V}_s = \int_{\mathrm{V}_s} d\mathbf{x} = \frac{1}{3} \int_{\Omega_s} d\mathbf{\Omega} \left[\left(L^F_{\mathbf{\Omega}} \right)^3 - \left(L^N_{\mathbf{\Omega}} \right)^3 \right] \approx \overline{L}^2 \int_{\Omega_s} d\mathbf{\Omega} \left(L^F_{\mathbf{\Omega}} - L^N_{\mathbf{\Omega}} \right).$$

Now, supposing that the fiducial volume of the detector V_d is small enough in comparison with V_s (that is usually the case) and the geometry of the detector is not too bizarre, the integration over $\mathbf{y}$ trivially yields

$$\int_{\mathrm{V}_d} d\mathbf{y} \int_{\mathrm{V}_s} d\mathbf{x} \, \frac{e^{\Phi_{ij}(L)}}{L^2} \approx \mathrm{V}_s \mathrm{V}_d \, \frac{e^{\Phi_{ij}(\overline{L})}}{\overline{L}^2}, \tag{170}$$

where $\overline{L}$ still has a meaning of the conventional distance between the source and detector.

To illustrate significance of the conditions (165), (167), and (168), let us consider the simple case of a spheroidal source of radius r, those angular dimension θ_s is no larger than the angular resolution of the detector. Simple geometric consideration suggests that $\Delta_{\mathbf{\Omega}} = 2(1 - \cos\theta)$ and, of course, $r_N = r_F = r$. Hence

$$\max_{\mathbf{\Omega} \in \Omega_s} \Delta_{\mathbf{\Omega}} = \Delta_{\mathbf{\Omega}_s} = 2\left(1 - \cos\theta_s\right) \approx \theta_s^2 \approx \left(r/\overline{L} \right)^2. \tag{171}$$

To simplify further, we suppose that $2\pi\overline{L} \gg |L_{ij}|$ (which is always true for the solar and astrophysical neutrinos detected at earth) and $2\pi\overline{L} \lesssim |L_{ij}|E_\nu/D$ (which may be doubtful for the distant astrophysical neutrino sources but acceptable for sun). Then the condition (167) is automatically fulfilled while (168) is transformed to

$$\frac{2\pi r^2}{\overline{L}|L_{ij}|} \ll 1. \tag{172}$$

The latter is certainly not satisfied for sun with the currently accepted value of Δm^2_{12}. Indeed, the regions of effective neutrino production in the solar interior are the relatively narrow concentric spherical layers with typical radius from about $0.1R_\odot$ for ^{8}B, ^{7}Be, and CNO neutrinos to about $0.3R_\odot$ for pp, pep, and hep neutrinos (here $R_\odot$ is the solar radius). So the left part of the inequality (172) can roughly be estimated as

$$\frac{2\pi r^2}{\overline{L}|L_{12}|} \approx 26 \left(\frac{r}{0.2R_\odot}\right)^2 \left(\frac{|\Delta m^2_{12}|}{8\times 10^{-5}\ \text{eV}^2}\right)\left(\frac{1\ \text{MeV}}{E_\nu}\right).$$

Consequently (that is not a novelty) the approximation (170) is fully inapplicable to the solar neutrino oscillation studies.

To summarize: although our consideration is highly simplified in several respects,[a] it demonstrates that the integration over the source volume must be under careful control even in the long baseline neutrino oscillation experiments.

[a] A more sophisticated analysis must take into account the spatial distribution of colliding and/or decaying particles in the source and, what is very important for astrophysical applications (in particular, for the solar neutrino experiments), the background matter effects caused by the virtual neutrino forward scattering in the source.

25 Pion decay.

Assume that $\nu = \nu_i$ $(i = 1, 2, 3)$. Then in the pion rest frame $(\mathbf{p}^\star_\mu + \mathbf{p}^\star_\nu = 0)$

$$E^\star_\mu = \frac{m^2_\pi - m^2_\mu + m^2_i}{2m^2_\pi} \quad \text{and} \quad E^\star_\nu = \frac{m^2_\pi + m^2_\mu - m^2_i}{2m^2_\pi}.$$

$\Longrightarrow$ The final states are different for the pion decay modes with different ν-species.
$\Longrightarrow$ The full pion decay width is

$$\Gamma_\pi = \sum_i \Gamma\left(\pi \to \mu + \nu_i\right) \propto \sum_i \left|\langle \mu, \nu_i | \pi \rangle\right|^2.$$

In the Standard Model (somehow extended by a Dirac or Majorana neutrino mass term)

$$\langle \mu, \nu_i | \pi \rangle = V^*_{\mu i}\, M_i,$$

where $M_i = \text{const}$ in the pion rest frame. Since $m_i \lll m_{\mu,\pi}$, it can be approximated (with veeery good precision) as

$$M_i \approx \langle \mu, \nu_0 | \pi \rangle,$$

where ν_0 is a **fictitious massless** neutrino. So, due to unitarity of $\mathbf{V}$,

$$\Gamma_\pi \approx \sum_i |V^2_{\mu i}|\, \left|\langle \mu, \nu_0 | \pi \rangle\right|^2 = \left|\langle \mu, \nu_0 | \pi \rangle\right|^2,$$

$$\Downarrow$$

$$\boxed{\Gamma_\pi \approx \Gamma\left(\pi \to \mu + \nu_0\right).}$$

This result is almost model-independent and practically exact.